AFRL-HE-WP-TR-1998-0130

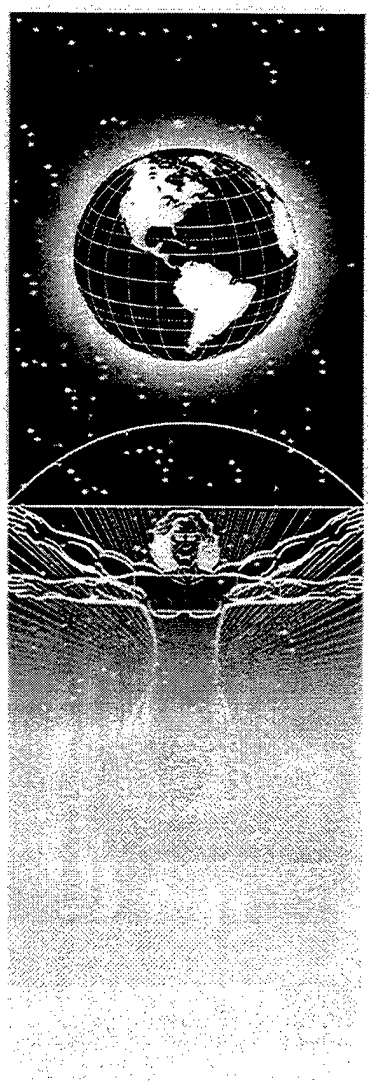

UNITED STATES AIR FORCE RESEARCH LABORATORY

4TH Generation Escape System Technologies Demonstration Phase II

A. Blair McDonald

BOEING
P.O. Box 516
St. Louis MO 63166-0516

July 1998

Final Report for the Period July 1995 to February 1998

Human Effectiveness Directorate
Biodynamics and Protection Division
Biodynamics and Acceleration Branch
BLDG 824 RM 206 2800 Q Street
Wright-Patterson AFB OH 45433-7947

NOTICES

When US Government drawings, specifications of other data are used for any purpose other than a definitely related Government procurement operation, the Government thereby incurs no responsibility nor any obligation whatsoever, and the fact that the Government may have formulated, furnished, or in any way supplied the said drawings, specifications or other data, is not to be regarded by implication or otherwise, as in any manner licensing the holder or any other person or corporation, or conveying any rights or permission to manufacture, use, or sell any patented invention that may in any way be related thereto.

Please do not request copies of this report from the Air Force Research Laboratory. Additional copies may be purchased from:

National Technical Information Services
5285 Port Royal Road
Springfield, Virginia 22161

Federal Government agencies registered with the Defense Technical Information Center should direct requests for copies of this report to:

Defense Technical Information Center
8725 John J. Kingman Rd STE 0944
Ft. Belvoir, VA 22060-6218

TECHNICAL REVIEW AND APPROVAL

AFRL-HE-WP-TR-1998-0130

DISCLAIMER

This Technical Report is published as received and has not been edited by the technical editing staff of the Air Force Research Laboratory.

This report has been reviewed by the Office of Public Affairs (PA) and is releasable to the National Technical Information Service (NTIS). At NTIS, it will be available to the general public, including foreign nations.

This technical report has been reviewed and is approved for publication.

FOR THE DIRECTOR

Roger L. Stork

ROGER L. STORK, Colonel, USAF, BSC
Chief Biodynamics and Protection Division
Human Effectiveness Directorate
Air Force Research Laboratory

REPORT DOCUMENTATION PAGE

Form Approved
OMB No. 0704-0188

1. AGENCY USE ONLY (Leave Blank)	2. REPORT DATE	3. REPORT TYPE AND DATES COVERED
	27 July 1998	Final – July 1995 to February 1998

4. TITLE AND SUBTITLE
4TH Generation Escape System Technologies Demonstration Phase II Final Report

5. FUNDING NUMBERS
Contract: F33615-92-C-2290
PE: 63231F
PR: orig. 2868 (currently 2830)
TA: 283068
WU: 28306835

6. AUTHOR(S)
A. Blair McDonald

7. PERFORMING ORGANIZATION NAME(S) AND ADDRESS(ES)
The Boeing Company
P.O. Box 516
St. Louis MO 63166-0516

8. PERFORMING ORGANIZATION REPORT NUMBER
MDC97K0154

9. SPONSORING/MONITORING AGENCY NAME(S) AND ADDRESS(ES)
Human Effectiveness Directorate
Biodynamics and Protection Division
Acceleration Effects and Escape Branch
BLDG 824 RM 206
2800 Q ST
Wright-Patterson AFB OH 45433-7947

10. SPONSORING/MONITORING AGENCY REPORT NUMBER
AFRL-HE-WP-TR-1998-0130

11. SUPPLEMENTARY NOTES

12a. DISTRIBUTION/AVAILABILITY STATEMENT
Approved for public release; distribution is unlimited

12b. DISTRIBUTION CODE
A

13. ABSTRACT (Maximum 200 words)
The Fourth Generation Escape System Technologies Demonstration Program was conducted to develop and demonstrate technologies that will enable the expansion of the escape envelope beyond that of current, third generation escape systems. The areas of the escape envelope in which expansion was demonstrated were escape under low-altitude, adverse-attitude conditions and escape at extremely high speed. The primary technologies that were developed for demonstration were: controllable propulsion, digital flight controls, and devices for crewmember protection at high speed. The program was a two-phase program. In Phase I, two competing controllable propulsion subsystems were designed, developed, and demonstrated. A trade study was used to select the propulsion system, the digital flight control system, and the high-speed protection devices to demonstrate in Phase II. In Phase II, the new technology systems were integrated into an ejection seat test vehicle and a series of ten ejection tests were conducted at a high-speed test track. The tests successfully demonstrated safe escape at speeds up to 700 knots equivalent airspeed and at adverse conditions as severe as 20 degrees of yaw at 450 knots equivalent airspeed. The system also successfully demonstrated an upward-seeking trajectory resulting in a ground avoidance capability.

14. SUBJECT TERMS
Ejection seat, escape system, pintle-controlled propulsion, controllable propulsion, life protection, windblast, limb restraint

15. NUMBER OF PAGES
222

16. PRICE CODE

17. SECURITY CLASSIFICATION OF REPORT	18. SECURITY CLASSIFICATION OF THIS PAGE	19. SECURITY CLASSIFICATION OF ABSTRACT	10. LIMITATION OF ABSTRACT
Unclassified	**Unclassified**	**Unclassified**	**UL**

(THIS PAGE INTENTIONALLY BLANK)

PREFACE

This report was prepared by the McDonnell Douglas Corporation (MDC), a wholly-owned subsidiary of the Boeing Company, to document work that was carried out in Phase II of the Fourth Generation Escape System Technologies Demonstration Program, USAF Contract No. F33615-C-2290. The work was carried out between July 1995 and February 1998 and was funded jointly by the United States Air Force and Navy. The program was managed by the Crew Escape Technologies (CREST) Office of the Biodynamics and Biocommunications Division of the Crew Systems Directorate, Armstrong Laboratory, Wright-Patterson AFB, Ohio. At the beginning of the work, the program was managed by the Acting CREST Program Manager, Mr. Roy R. Rasmussen, who was succeeded by the CREST Program Manager, Lt. Col. James M. Bates. Maj. Timothy D. Wieck replaced Lt. Col. Bates as the CREST Program Manager and concluded the program. Mr. Lawerence Specker of the CREST office was the Technical Director for the program. The Lead Engineer for the program was Mr. John Quartuccio, Naval Air Warfare Center - Aircraft Division, Patuxent River, Maryland, who was assisted by Mr. Craig Wheeler, Indian Head Division, Naval Surface Warfare Center, Indian Head, Maryland. The primary test work was carried out at Holloman AFB, New Mexico, where the Test Managers for the program were Mr. Dave Lacey and Mr. Tim Wolfe of the 846th Test Squadron. The MDC Technical Director was Mr. Jim Schoen, McDonnell Douglas Aerospace (MDA), Long Beach, California.

In the conduct of this program MDC was supported by major subcontractors; Gencorp Aerojet, Sacramento, California, and F&L Enterprises, Tehachapi, California and by USAF subcontractor, Systems Research Laboratories (SRL), Dayton, Ohio.

Important contributors to the technical conduct of the program included John Plaga and Thao Nguyen from the CREST office; Jeff Nichols, Tom Blachowski, Justin Hall, Donny Legget and Paul Johnsen from the Navy; Delane Bullman from SRL; Mike Galfano and Steve Burkham from Holloman AFB; Joe Morris, Paul Niedzielski, Kevin Peterson and Ruben Placencia from Aerojet; and Fred Rinke from F&L Enterprises. The MDA team included Jim Brooks, Buck Jackson, Will Burgener, Tom Frey, Brad Mastrolia, Joe D'Allura, Fred Duskin, Ty Wilson and Blair McDonald.

Senior USAF and Navy personnel guiding the program were Mr. Jim Brinkley and Mr. Terry Thomasson.

(THIS PAGE INTENTIONALLY BLANK)

Table of Contents

List of Figures

List of Tables

1.0 SUMMARY

The Fourth Generation Escape System Technologies Demonstration Program, USAF contract F33615-92-C-2290, was conducted to develop and demonstrate technologies which will enable the expansion of the aircrew escape envelope beyond that of current, or third, generation escape systems. The areas of the escape envelope in which expansion was to be demonstrated were for escape under low altitude, adverse attitude conditions and for escape at extremely high speed. The primary technologies which were developed for demonstration were:

- Controllable propulsion
- Digital flight controls
- Devices for crewmember protection at high speed

The program was a two phase program. In Phase I, two competing controllable propulsion subsystems were designed, developed and demonstrated. A trade study was conducted and a system developed by Aerojet was selected for escape system demonstration testing in Phase II. Trade studies were also conducted to select the digital flight control system and the high speed protection devices. The initial design of these systems and of the demonstration system was also completed in Phase I. The Phase I activities are documented in Reference #1.

In Phase II, the design of the flight control system and high speed protection devices was completed and tests were conducted on these and other components and subsystems to obtain data and to achieve operational verification. The new technology systems were integrated into an ACES II ejection seat test vehicle and the operation of the system was demonstrated in a series of ten system ejection tests from an F-16 forebody sled on the high speed test track at Holloman AFB. The Phase II objectives were to demonstrate flight control in ejections with adverse attitudes at speeds up to 450 KEAS and to demonstrate "safe escape" at speeds up to 700 KEAS. These objectives were met. The system successfully performed "upward seeking" trajectories from initial roll and yaw attitudes and successfully controlled the attitude and trajectory of the seat in ejections at 600 and 700 KEAS. The Multiaxial Dynamic Response Criteria (MDRC) is the evaluation criteria used to judge the severity of the forces imposed on the seat occupant and the successful operation of the demonstration system is reflected in the fact that the highest value of MDRC, which was recorded in the 700 KEAS test, was 1.03 using the medium risk criteria. The most serious problem encountered in the test program was mechanical failure of the avionics due to the dynamic mechanical environment of the seat. Once this problem was understood and resolved, the system performed with excellent reliability. This is particularly applicable to the final four tests, which represented increasingly stressful and demanding conditions. In these four successive successful tests, the ejection

sequences fully demonstrated the ability of the system to simultaneously control the attitude of the seat, control the trajectory of the seat and control the level of the loads applied to the seat occupant.

This report documents the Phase II effort and is submitted in accordance with Data Item A009 of the contract.

2.0 INTRODUCTION

The Fourth Generation Escape System Demonstration program is a five year program that was initiated in February 1992. The objective of the program was to demonstrate new escape system technologies which were considered to be critical to the development of a next, or fourth, generation escape system. For a fourth generation system, the requirement is to expand the safe escape envelope relative to that of current seats. The specific areas of the escape envelope in which increased capability is required are for escape under low altitude, adverse attitude conditions and for escape at extremely high speed. In order to achieve the required expansion of the escape envelope, the approach was to design and develop technologies which would achieve control of the flight path for ground avoidance in the low altitude, adverse attitude conditions and which would achieve stable flight and crewmember protection in escape at high speed. The technologies which were designed, developed and demonstrated in the program were: controllable propulsion, digital flight control and high speed protection devices.

Of the new technologies, the successful development of a controllable propulsion system was considered to be the most technically challenging element of the program. Therefore, to minimize risk, the program was structured to be conducted in two phases, with the controllable propulsion being demonstrated in the first phase and the complete escape system being demonstrated in the second phase. Two competing controllable propulsion systems were successfully demonstrated in Phase I. One was a gel-propellant system developed by TRW and the other was a solid-propellant, pintle-controlled system developed by Aerojet. A comprehensive trade-study was conducted and the Aerojet system was selected for the demonstration ejection tests in Phase II. Trade studies were also conducted to select the control system and the high speed protection devices.

In Phase II, the controllable propulsion system was integrated with the digital flight controls and this "flight control system", together with the selected high-speed protection devices, were installed on an ejection seat for system ejection demonstration testing. In addition, Phase II included a series of initial tests to obtain data and to verify the operation of the components and subsystems.

3.0 PROGRAM SCOPE

The elements of the Fourth Generation program are shown in the program schedule in Figure 3-1. Phase I was concerned primarily with the demonstration of the propulsion system and with the conduct of long-lead tasks which were necessary to support Phase II. This included the initial design of the control system and the high speed protection devices. In Phase II, the system design was finalized and hardware was procured and fabricated for test. As indicated in the program schedule, Phase II included the conduct of initial tests and system demonstration ejection tests.

The Phase II initial tests consisted of a variety of laboratory and wind tunnel tests which were carried out to provide the aerodynamic data and hardware operational data needed to support the ejection test program.

The system demonstration tests consisted of a series of ten ejection tests which were conducted on the high speed test track at Holloman AFB, using the Multi-Axis Seat Ejection (MASE) sled fitted with an F-16 forebody. The ejection tests were conducted with a range of initial conditions, which included adverse attitudes and a speed range from 0 to 700 KEAS.

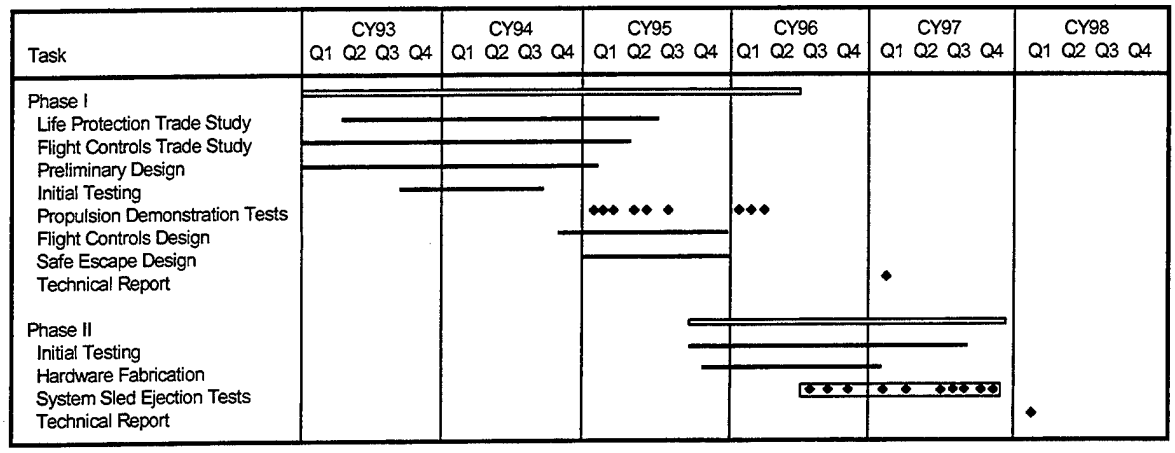

Figure 3-1 Program Schedule

4.0 SYSTEM DESCRIPTION AND OPERATION

The fourth generation demonstration system consists of a set of advanced technology systems: controllable propulsion, digital flight control and high speed protection devices, installed on a modified ACES II ejection seat. The capabilities introduced by the new technologies are:

- In ejections under low-altitude adverse-attitude conditions, the system will control the flight of the seat to provide a trajectory which will maneuver the seat and occupant and propel them away from the ground.

- In ejections at very high speed, the system will protect the crewmember by stabilizing the seat, by restraining and supporting the crewmember against windblast and by providing devices which will control the magnitude of the forces imposed on the crew member.

The ability to control the flight of the seat and to provide stability at very high speeds, is achieved by the flight control system which monitors the dynamic motion and accelerations of the seat and commands propulsion thrust and moments to control the seat attitude and trajectory. The application of controlling moments by the propulsion system is achieved by four controllable nozzles which are located at the aft corners of the seat. The nozzles are angled such that manipulation of the thrust distribution between the nozzles allows the motion of the seat to be controlled in yaw, pitch and roll. This is illustrated in Figure 4-1. For protection at high speed, the system includes restraint systems for the torso, arms and legs. Additional high speed protection measures consist of raising the legs and a system to protect the head. The head protection system consists of straps to limit lateral motion and a seat-mounted brim device to deflect the airflow over the head and reduce the force due to lift.

In an ejection with the fourth generation demonstration system, the sequence of events is controlled in real time and is determined by the initial conditions together with a range of variables associated with the operation of the system and the operation of the flight control system. The system has three basic operating modes, depending on the speed and altitude conditions. One mode covers the low speed, low altitude portion of the envelope. Another mode covers the high speed, low altitude portion and the third mode covers ejections at high altitude, typically above 15,000 feet. The primary operational difference between the low speed, low altitude mode and the other modes is that, in the low speed, low altitude mode the propulsion phase is followed by deployment of the recovery parachute whereas, in the other modes, the propulsion phase is followed by deployment of a drogue parachute. In a high

speed low altitude ejection, the drogue stabilizes the seat until it slows down to a safe speed for deployment of the recovery parachute. In a high altitude ejection, the seat descends on the drogue until the altitude for recovery parachute deployment is reached. The decision on whether to deploy the drogue or the recovery parachute after the propulsion phase is made based on the velocity which is calculated by the Inertial Measurement Unit (IMU) when the propulsion system is approaching burn-out.

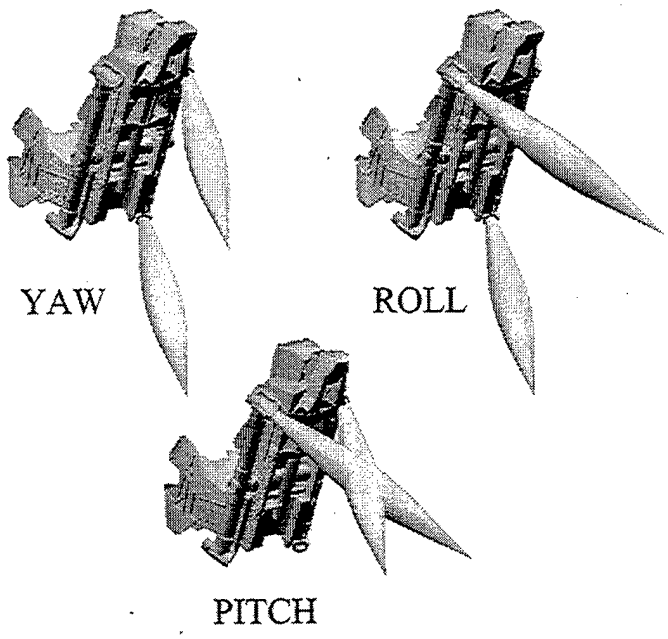

Figure 4-1 Thruster Geometry

The demonstration system consists basically of the new technologies with the ACES II ejection seat being used as a test vehicle. This approach was adopted so that the program effort could be focused on the new technologies and effort would not be expended on the design and development of new configurations of components and sub-systems, such as the recovery parachute, which were already qualified and whose operation was not involved with the demonstration of the new technologies. With this approach, the H-shaped propulsion system was installed on the seat with the two main legs and the four motors external to the seat structure. This general configuration would probably not be suitable for an aircraft installation, however the objective was to demonstrate the controllable propulsion technology and not to qualify a specific configuration. Similarly, several features of the demonstration system

were representative of operational systems but were not fully operational. For example, an element of the leg protection strategy is to raise the legs. In the demonstration seat, the seat pan is fixed in the raised position and a raising mechanism is not provided. This approach was justified on the basis that the technology involved in a leg raising mechanism is not new and therefore there was no technology requirement to support the cost and technical risk associated with developing a leg raising mechanism for an ACES II test vehicle. Other features which were representative rather than being fully operational, were the restraint systems for the torso, arms and legs which were all cinched-up prior to ejection. In an operational system, the head-protection "brim" would probably be deployed during ejection and would be retracted for seat-man separation. For the demonstration system, the brim was installed in the deployed position but was retracted when the recovery parachute was fired so that it would not interfere with the manikin as it separated from the seat.

The elements of the demonstration system are:

- ACES II test vehicle
- Controllable propulsion
- Avionics system
- Life protection devices
  - -Torso restraint harness
  - - Arm restraint (based on ACES II in the F-22 aircraft)
  - - Leg protection
  - - Head protection

The general arrangement of the demonstration seat assembly is illustrated in Figure 4-2. Photographs of the seat with the manikin and restraint harness are shown in Figures 4-3, 4-4 and 4-5.

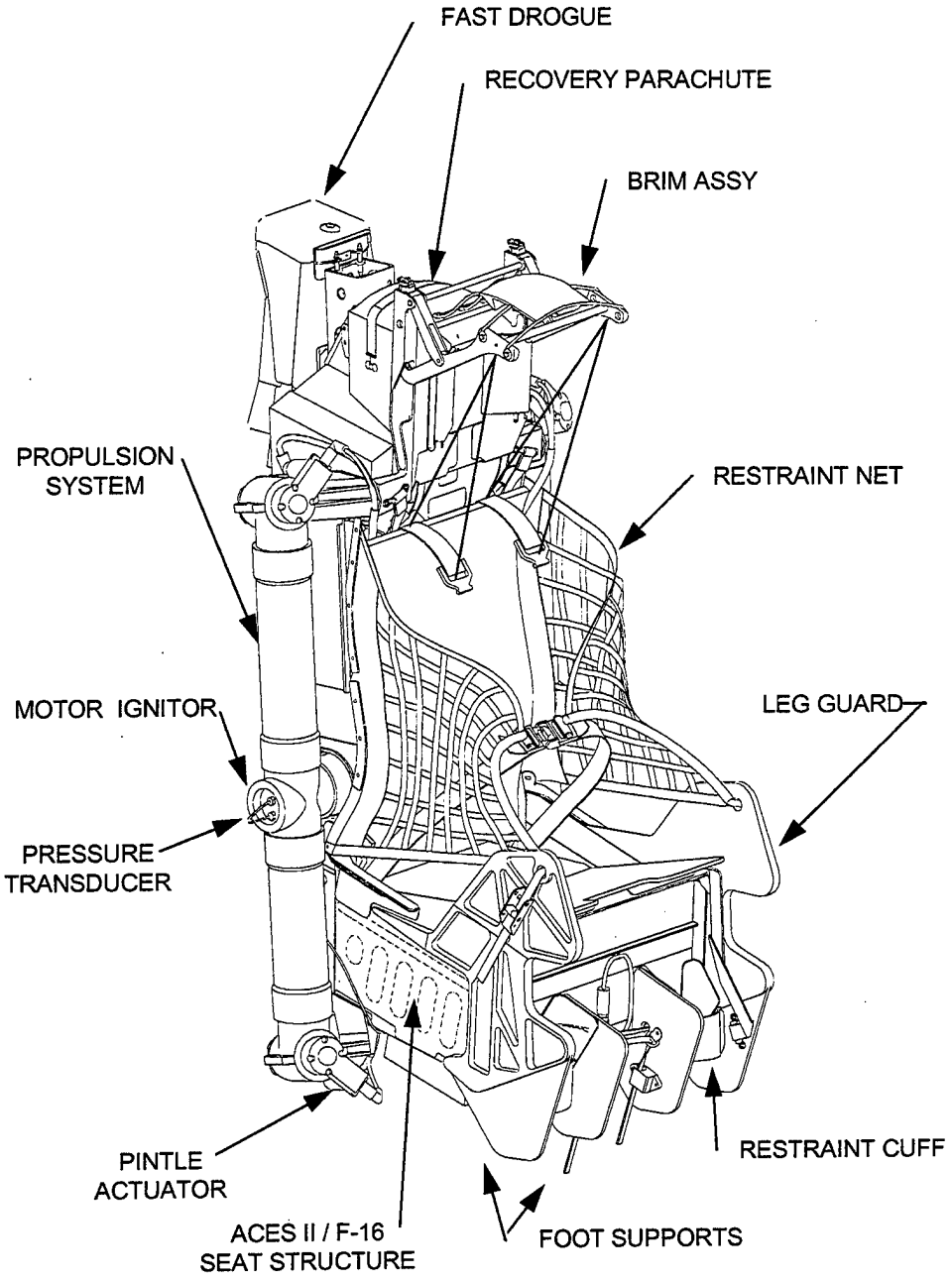

Figure 4-2 Demonstration Seat Assembly

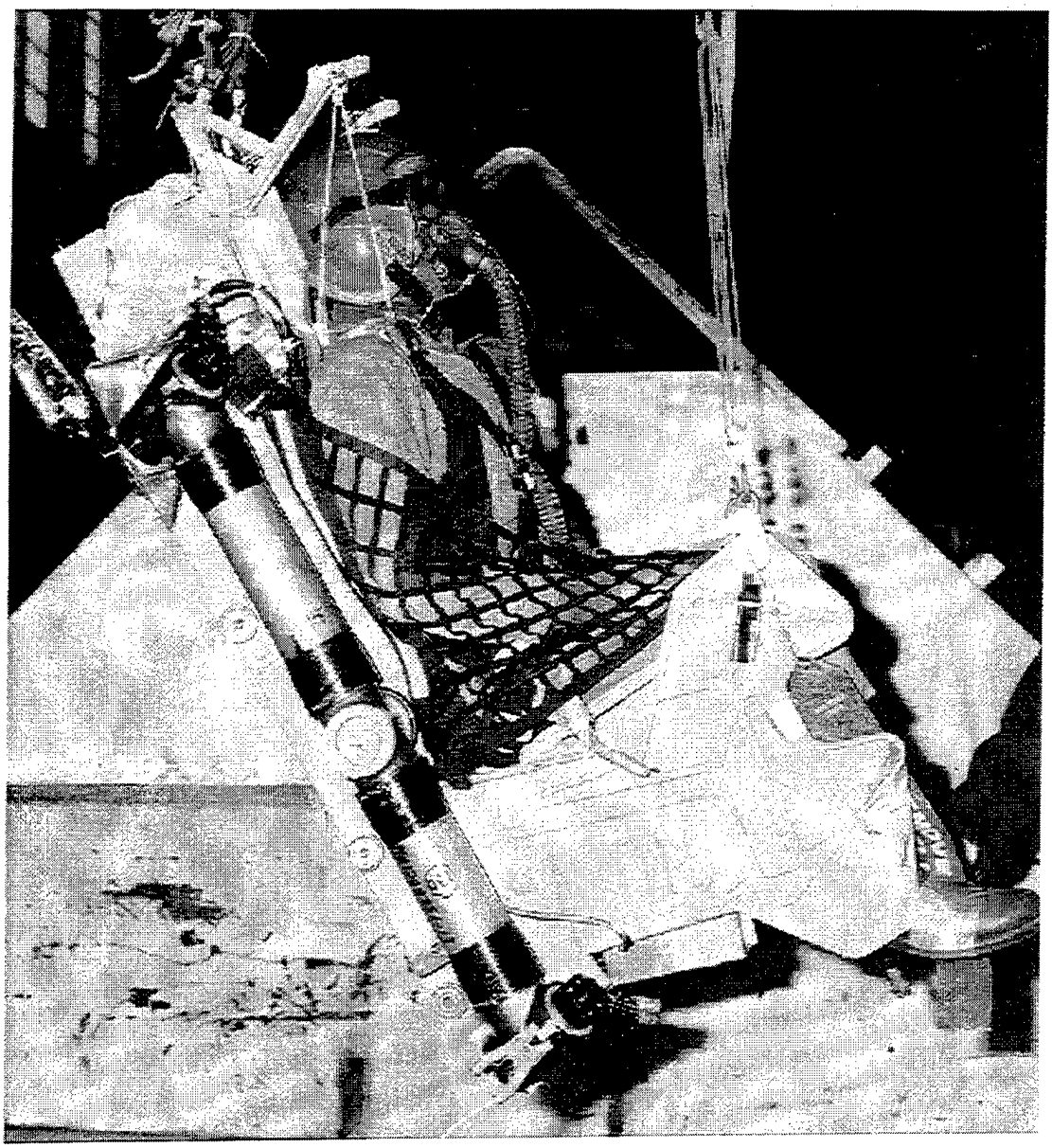

Figure 4-3 Side View of Demonstration Seat Used on Test No. 10

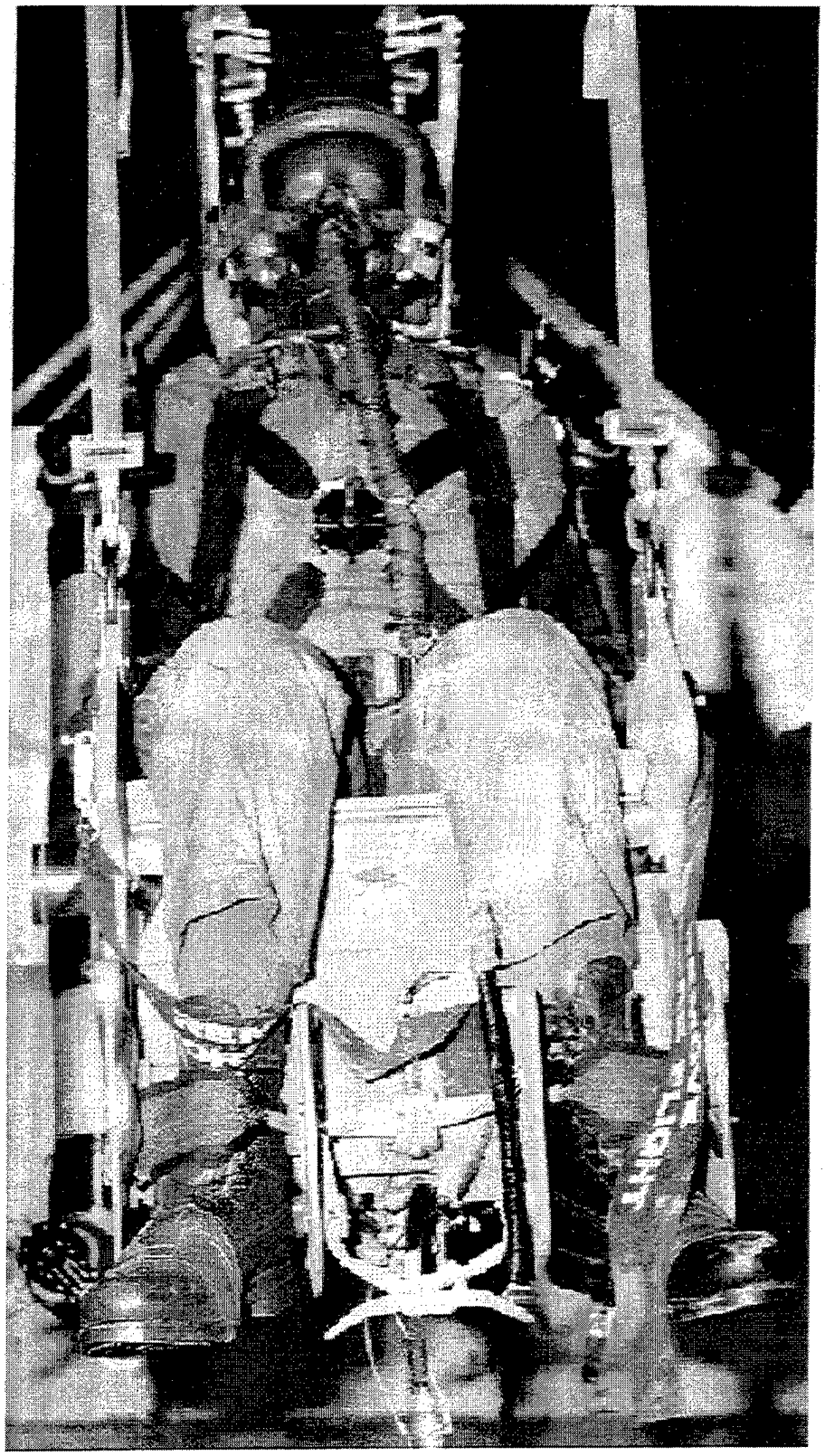

Figure 4-4 Front View of Demonstration Seat Used in Test No. 10

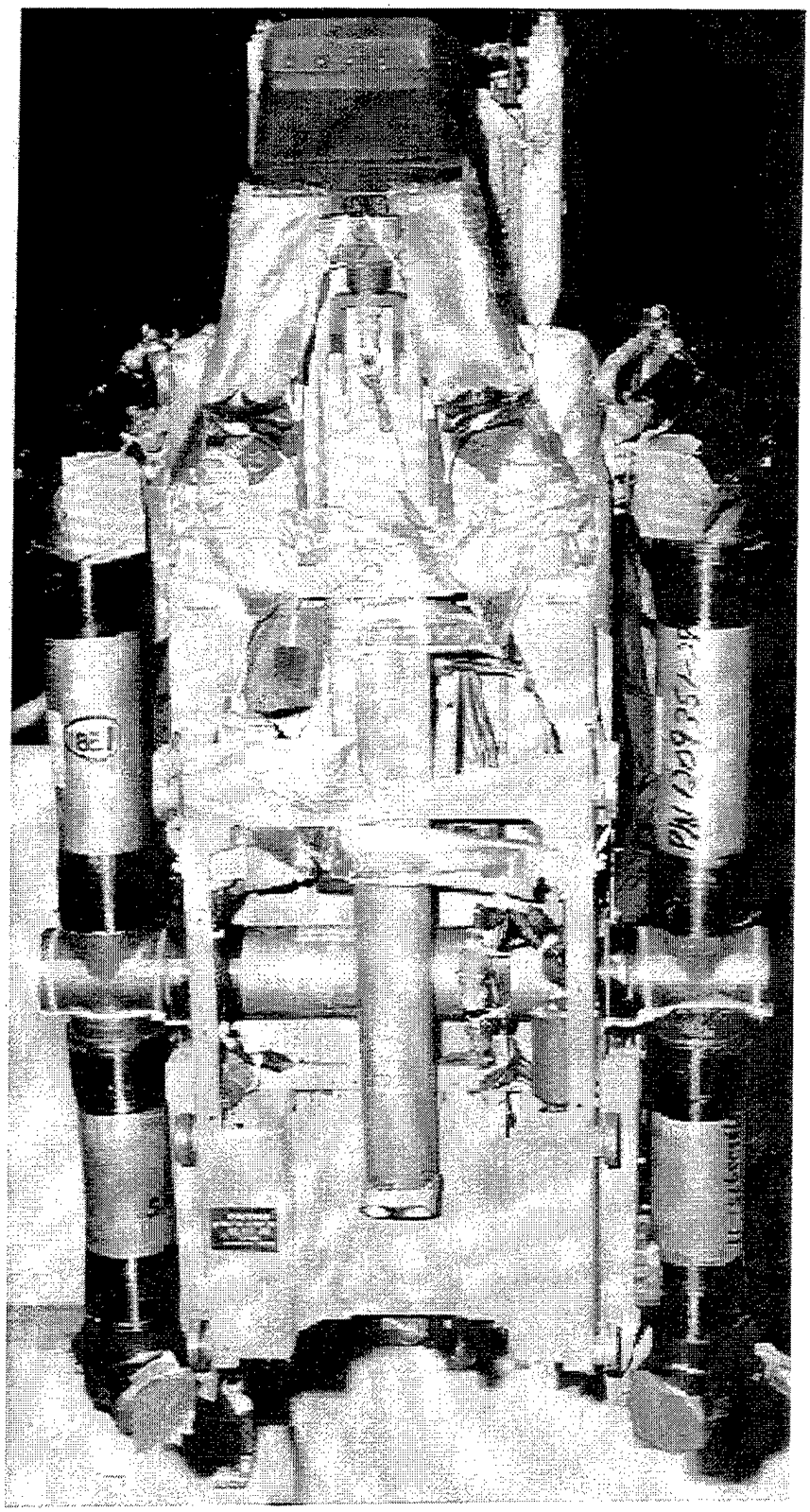

Figure 4-5 Back View of Demonstration Seat Used in Test No. 10

A description of each of the elements of the system is given in the following paragraphs:

4.1 ACES II Test Vehicle

The basic ACES II seats used in the program were seats which had been installed in F-16 aircraft. For the program, these seats were modified to accommodate the new technology systems and to be compatible with other program requirements. The following is a top level description identifying which parts of the ACES II system were retained and which were modified, replaced or deleted.

- Parts Retained
  - Recovery parachute
  - Harness release system
  - Catapult portion of rocket catapult

- Parts Modified
  - Seat structure
  - Inertia reel

- Parts Replaced
  - Seat pan
  - Drogue system (replaced by drogue from F-22 ACES II seat).
  - Lap belt

- Parts Deleted
  - Rocket portion of rocket catapult
  - Recovery sequencer and environmental sensor
  - STAPAC
  - Pop-up pitots
  - Firing control system
  - Survival kit

A brief description of the significant changes to the seat is:

Seat Bucket Structure; The seat bucket structure was modified to accommodate the leg protection system.

Seat Pan: The seat pan was replaced by a sheet aluminum seating surface which was also a part of the leg protection system.

Seat Back Structure: The seat back structure was significantly modified to accommodate the controllable propulsion. Holes were introduced in the seat back sides to allow the installation of the motor cross-tube. Also, the upper

and lower portions of the seat back were modified to provide attachments for the four pintle motor housings.

Rocket catapult: The catapult portion of the CKU-5 rocket catapult was used but the rocket portion was not. This allowed the outer casing of the CKU-5 to be trimmed, Figure 4-6, to allow space for the installation of the controllable propulsion cross-tube.

Drogue Parachute: The standard drogue system was replaced by the FAST (Fast Acting STabilizing) drogue system that is used on the F-22 version of the ACES II seat. The FAST drogue deploys more rapidly than the standard ACES II drogue system and this helps to provide a smooth transition from propulsion to aerodynamic stabilization. Also, the FAST drogue mounts externally on the aft surface of the seat thereby providing internal space for the propulsion cross tube and for other components of the new technology systems.

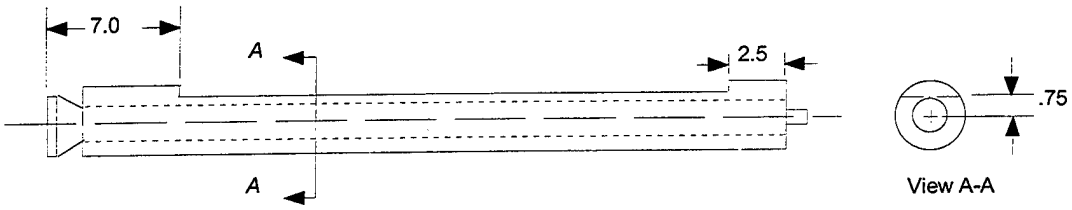

Figure 4-6 Modified CKU-5 Catapult

4.2 Controllable Propulsion System

The controllable propulsion system, designated PEPS (Pintle Escape Propulsion System), was designed and developed by the Aerojet division of the GenCorp Corporation. The operation of the system was demonstrated in Phase I of the program. The system consists of a solid propellant motor which has four pintle-controlled nozzles. The pintles are driven by actuators and the system supplied by Aerojet includes two controllers, with each controller being responsible for the control of two actuators. The motor is in an "H" shaped configuration with propellant in each of the five segments of the motor and with pintle-controlled nozzles at the four ends of the "H". The motor is installed on the seat so that the nozzles are located at the corners of the seat to obtain large moment arms for attitude control. The motor has a regressive thrust profile starting at approximately 5,000 lb. thrust decreasing to approximately 3,000 lb. thrust. The burn time is approximately one second. The nozzles are angled inboard so that modulation of the thrust of each of the

four nozzles can be used to generate moments in the pitch, roll and yaw axes. It is necessary to maintain a constant pressure within the motor and therefore the modulation of the four nozzles must be controlled such that the motor pressure (and total thrust) is maintained. The maximum thrust for one nozzle is 2500 lb. and the minimum thrust for one nozzle is approximately 150 lb.

The operation of the motor is illustrated in Figure 4-7 which presents the motor data for test #8, which was at 450 KEAS and 20 degrees yaw. The upper plot shows how the motor pressure is controlled and the lower four plots show the thrust command changes throughout the propulsion burn.

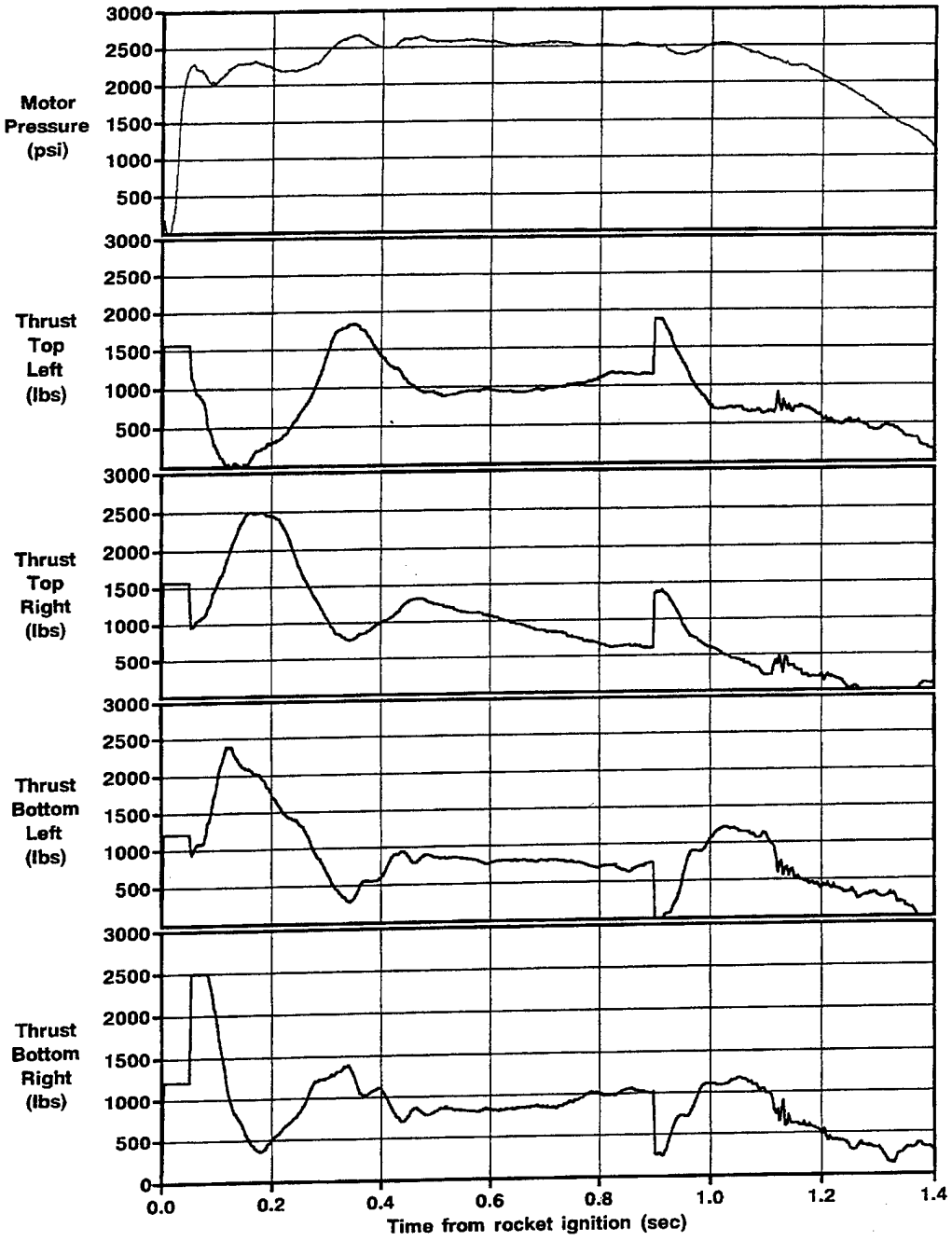

Figure 4-7 Pressure & Thrust Profiles for Test #8

(Yaw=20, KEAS=437)

The plot of motor pressure shows that the pressure was somewhat below the design pressure of 2,500 p.s.i. in the early portion of the ejection, when large thrust command changes were being generated to correct the initial yaw attitude. There are redundant pressure transducers and although the plots of

the data from both are shown, they are so similar that any differences are indiscernible.

In the four plots of thrust command, the initial commands are intended to maintain the pintles in their initial positions until the motor is at pressure. After that period, the commands are generated to correct for the initial yaw and, once this is accomplished, it is necessary to arrest the correction and then to damp out any residual sideslip oscillation. While this is being accomplished, these thrust commands are being overlaid by commands to rotate the seat aft and then, later, to arrest the rotation. Once sideslip has been eliminated and the seat is at 60 to 70 degrees angle of attack, the commands change relatively gradually until 0.9 seconds when the drogue alignment maneuver is executed. When this occurs the two upper thrusters are commanded to increase thrust while the two lower thrusters are commanded to reduce thrust. Partway through the maneuver the commands are reversed to arrest pitch rotation and adjusted to bring the seat into the desired orientation to the wind. The simultaneous implementation of two maneuvers makes it difficult to rationalize each of the commands. However, the flight control achieved in this test was excellent and this is described in the test results in Section 5.0.

The assembly of the motor is illustrated in Figure 4-8, while the installation on the seat and the schematic are shown in Figures 4-9 and 4-10. As indicated in the figures, the thrusters are angled downwards and inwards. The downward angle is 15 degrees below normal in the x-z plane of the seat and the inward angle is 25 degrees in the x-y plane of the seat.

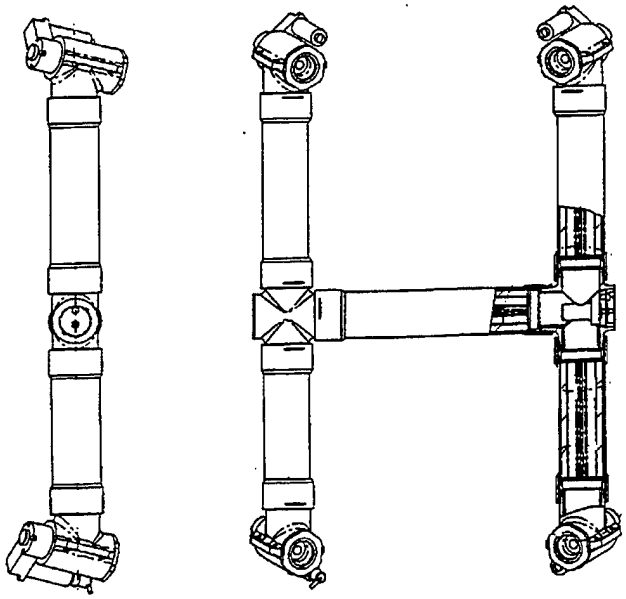

Figure 4-8 Propulsion Motor Assembly

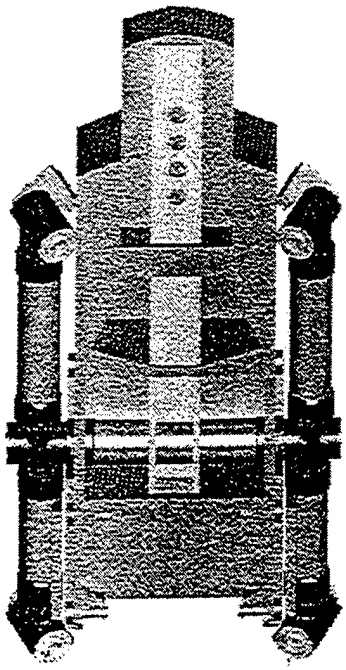

Figure 4-9 Propulsion System Installation

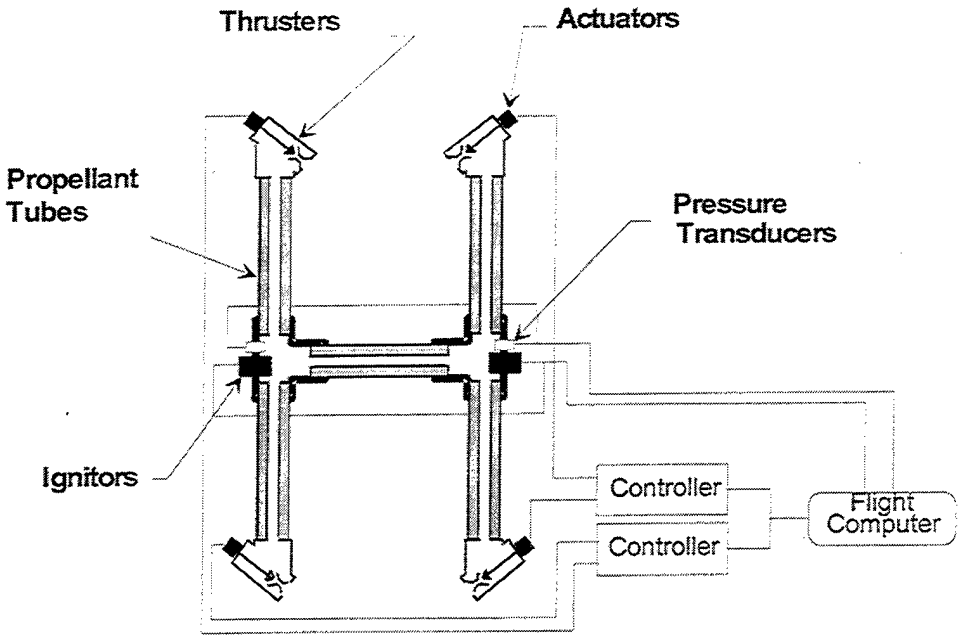

Figure 4-10 Propulsion System Schematic

4.3 Avionics System

The avionics system includes the flight control system and the support hardware required to control the propulsion system and the seat systems. The Guidance and Control Unit (GCU) is a modified version of the GCU developed for the Joint Direct Attack Munition (JDAM) program. The modifications consisted of providing additional interfaces and the addition of new software/algorithms which were required for the control functions.

4.3.1 *Control system*

The GCU provides overall control of the seat functions during flight, see Figure 4-11. These functions include control of motor thrust from each pintle, sequencing of parachute deployment and manikin release from the seat.

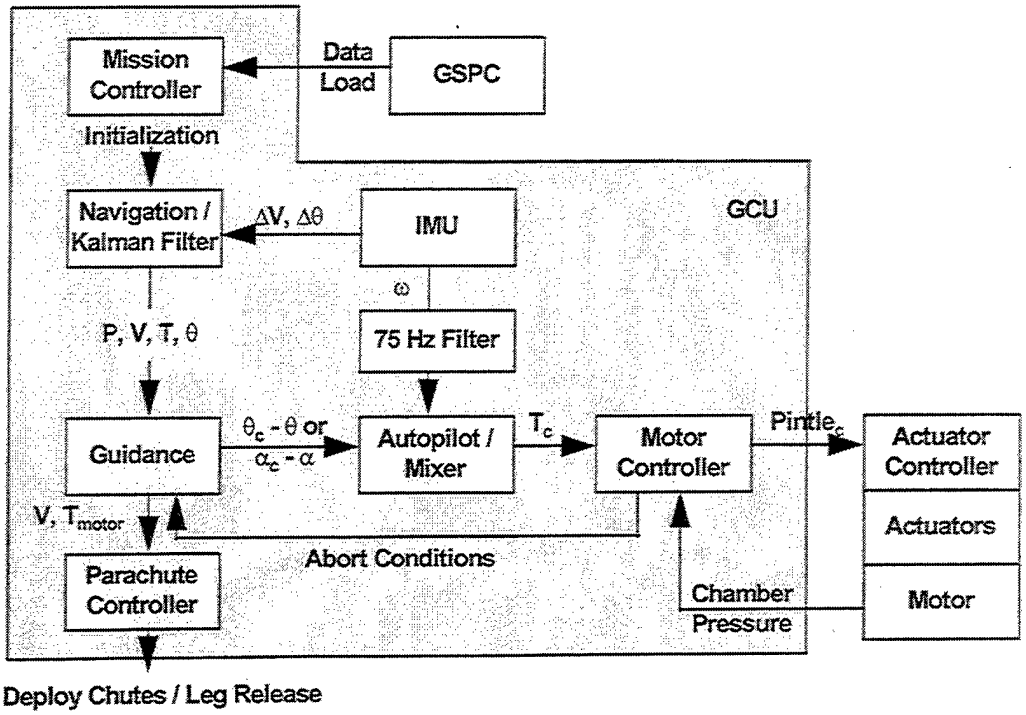

Figure 4-11 Control System Top Level Block Diagram

Initial mission conditions, such as pintle bias and initial seat position and attitude are downloaded from the Ground Support PC (GSPC). The mission controller distributes these inputs to the proper software module and controls the mission state. There are four primary mission states used in the system: Built-In-Test (BIT), transfer alignment, navigation and closed loop motor control.

At power up, BIT is run to ensure system operation. The operator then commands the GCU to begin transfer alignment to refine the controller estimates of roll and pitch (tilts). Since the sled is not moving, the yaw or

azimuth attitude cannot be refined. When sled launch is imminent, the operator commands the GCU to the navigation mode. The navigation algorithms use the IMU outputs to maintain the position, velocity and attitude reference. An arming screenbox is used to provide the signal to allow arming of the seat squib drivers, to provide an update used to align azimuth and to enable arming of the catapult ignition circuit upon successful system health check.

The seat catapult is initiated when a trackside screen box fires a gas initiator and the motor ignition signal is provided by a breakwire located 20 inches up the guide rails. After the rocket motor is ignited, the guidance and autopilot loops are closed. Constant pintle positions are commanded until the motor is at pressure. After the motor is at pressure, the motor control loop is closed. The seat is near the top of the guide rails when this occurs.

After closure of the guidance and control loops, the GCU continues to maintain knowledge of the seat position, velocity, and attitude. The guidance algorithms command seat pitch attitude (θ) or angle of attack (α) based on predefined criteria of speed and time relative to motor burn time. The guidance algorithm and parachute control logic were developed from detailed modeling in the Dynamic Ejection Seat Simulation (DESS) program, to achieve the proper altitude for safe recovery while meeting MDRC goals (Figure 4-12). The seat is initially pitched in the proper attitude to achieve a safe recovery altitude -- initial alignment. At low speeds, the seat is controlled based on pitch attitude. At higher speeds (> 360 KEAS), the seat is controlled based on Angle of Attack (AoA). As motor burnout approaches, the guidance algorithm changes to command seat alignment relative to the wind axis so that the parachute forces will be applied in the desired direction relative to the crewmember (Figure 4-13).

Lateral Directional (Roll and Sideslip)

- Regulated to Zero

Longitudinal (Pitch or AoA)

- Initial Alignment
  - 0 to 70 KEAS --> Inertial Alignment to 45 deg Pitch
  - 70 to 360 KEAS --> Inertial Alignment to 75 deg Pitch
  - >360 KEAS --> Wind Alignment to Schedule
    << Limit to < 75 deg Pitch Attitude
- Chute Alignment to Wind Axis
  - Drogue --> AoA Cmd = 10 deg
  - Recovery --> AoA Cmd = 90 deg

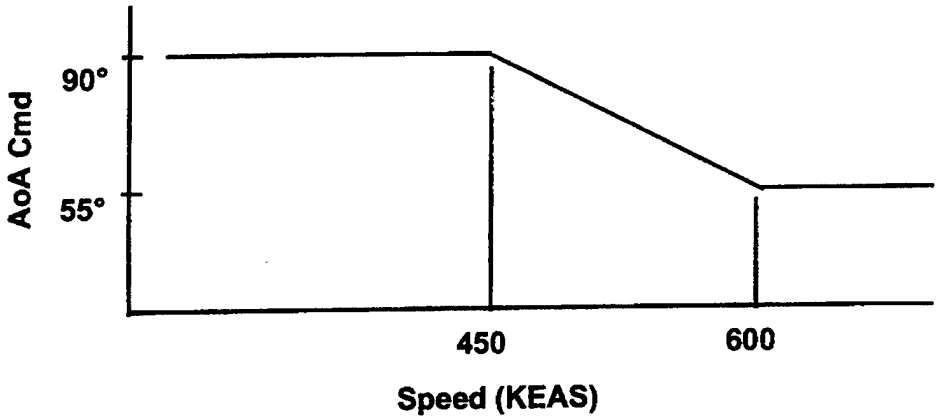

Figure 4-12 Guidance Logic

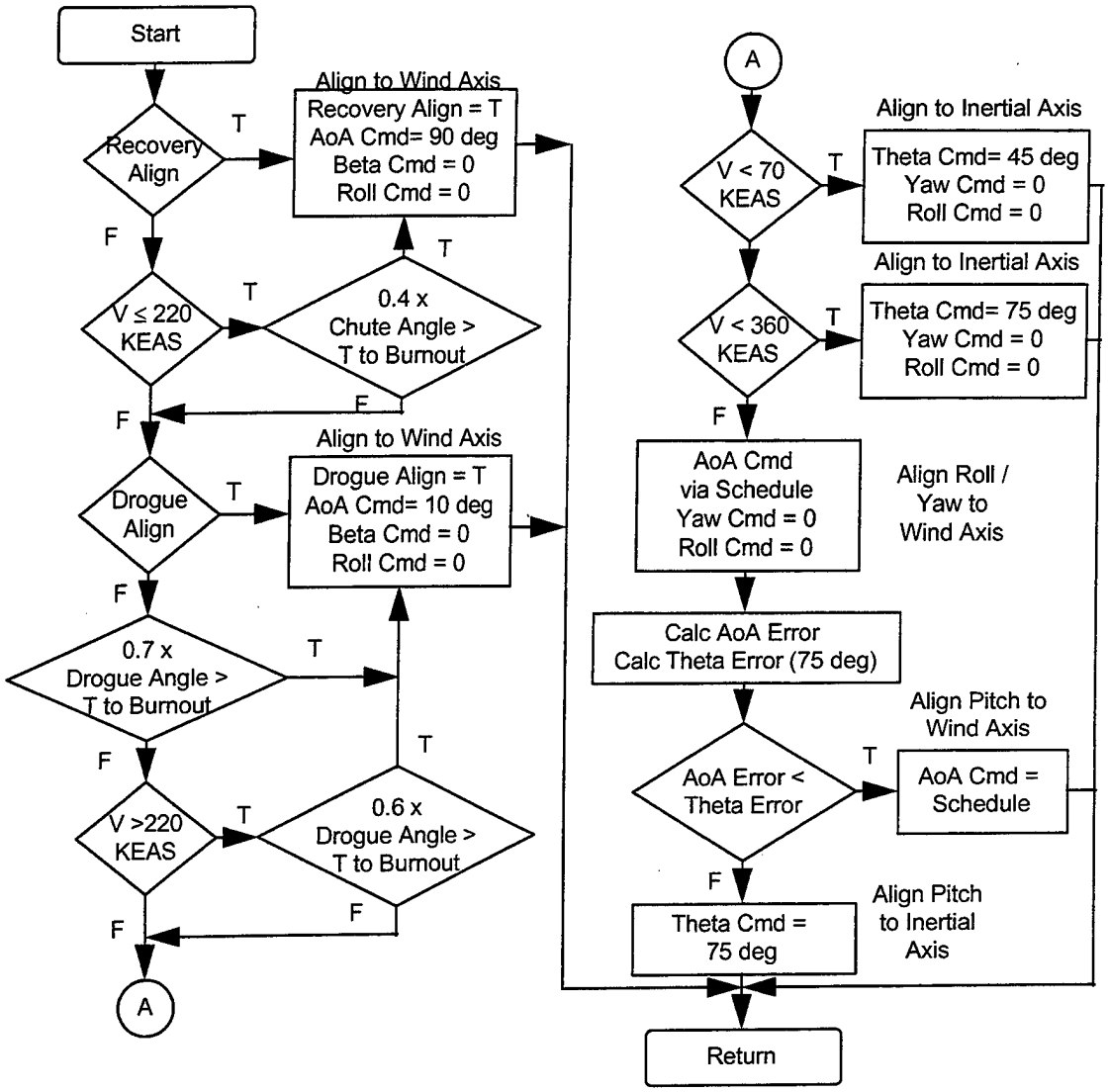

Figure 4-13 Attitude Command Logic

The parachute controller sequences firing of the parachutes, harness release and leg release squibs. The drogue chute is fired at 1.1 seconds after motor ignition if seat speed is greater than 220 KEAS. The main chute is fired at 1.2 seconds after motor ignition or speed less than 220 KEAS, whichever occurs later. The drogue-severance squibs are fired at 0.15 seconds and the harness and leg release squibs are fired at 0.25 seconds after the main chute.

The angle commands are processed by the autopilot to generate thrust commands to each pintle. The autopilot implements a Proportional-Integral (PI) controller in each attitude channel (Figure 4-14). Gains are generated using Linear Quadratic Regulator (LQR) based tools to maximize robustness to aerodynamic and other uncertainties. Thrust limiting logic is implemented

to reflect the physical limits of the rocket motor. If any thruster is commanded above its 2500 lb. limit, the limiting logic proportionately reduces the thrust from each thruster to preserve the direction of the total moment command (Figure 4-15).

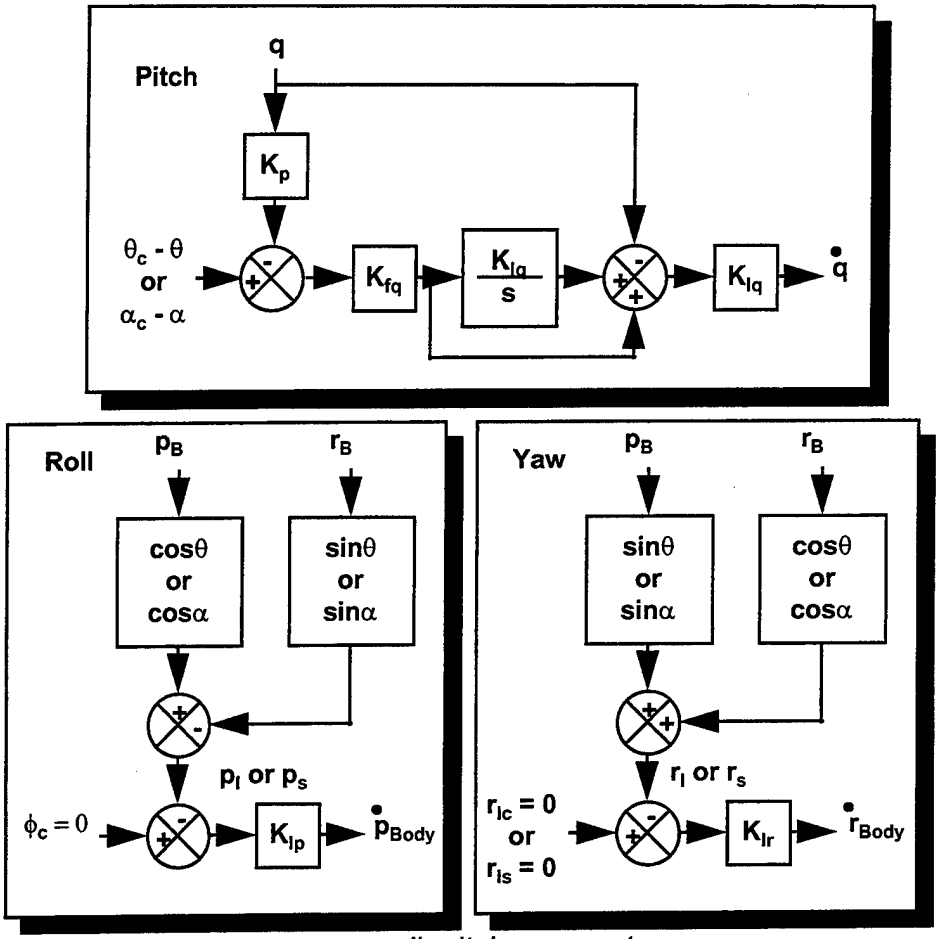

p,q,r = roll, pitch, yaw rate
Subscript b = body axis
Subscript I = inertial axis
Subscript s = stability axis
Kp, Kfq, Klq, Klp, Klr = Autopilot Gains
ϕ,θ,ψ = roll, pitch, yaw attitude
$\phi c,\theta c,\psi c$ = roll, pitch, yaw attitude command
α = angle of attack
αc = angle of attack command
pdot, qdot, rdot = roll, pitch, yaw acceleration command ~ moment command

Figure 4-14 Attitude Control Autopilot

$$\begin{vmatrix} T1 \\ T2 \\ T3 \\ T4 \end{vmatrix}_{Limited} = \begin{vmatrix} T_{sys}/4 \\ T_{sys}/4 \\ T_{sys}/4 \\ T_{sys}/4 \end{vmatrix} + \frac{1}{K_{Lim}} \begin{vmatrix} \Delta T_1 \\ \Delta T_2 \\ \Delta T_3 \\ \Delta T_4 \end{vmatrix}_{Unlimited}$$

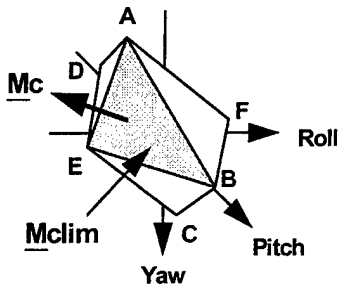

- **Compute Gain, Ki, to Limit Each Thruster to $0 \leq Ti \leq 2500$ lbs**

$$\frac{-T_{sys}}{4} \leq \frac{\Delta T_i}{K_i} \leq 2500 - \frac{T_{sys}}{4}$$

- $K_{Lim} = \max\{1, K_1, K_2, K_3, K_4\}$

Tx = Thrust from each Nozzle, x = 1,2,3,4
Tsys = Total System Thrust (nominally 5500 lbf)
ΔTx = Unlimited Thrust delta from nominal, Thrust command
Ki = Gain calculated from limiting equation given Tsys and ΔTx
Mc = Vector of Unlimited Moment Command
Mclim = Surface Defining Moment Limit
A,B,C,D,E,F = Corners of Moment Limiting Surface

Figure 4-15 Thrust Limiting Logic

The motor controller regulates motor pressure to 2500 psi while responding to the thrust commands. The motor controller was developed by Aerojet for rehosting in the mission computer.

4.3.2 *Avionics Hardware*

The demonstration system avionics hardware consists of the GCU, GSPC, serial data recorder, avionics battery and wire harness (Figure 4-16) and the actuator thermal batteries.

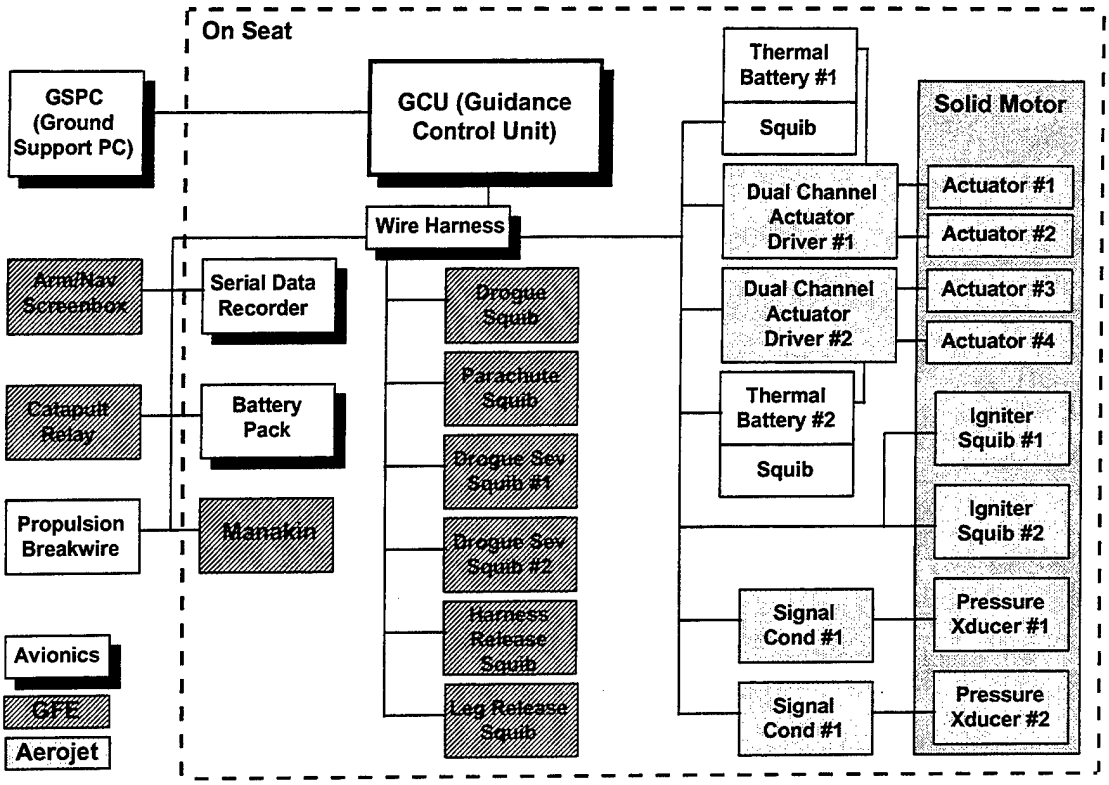

Figure 4-16 Demonstration System Avionics Hardware and Interfaces

The GCU includes six major components (Figure 4-17). The design is the same as the JDAM initial design with the JDAM Global Positioning System (GPS) receiver replaced by the analog converter board and two additional Pyro Initiation Modules (PIMs) (Figure 4-18). The additional PIMs are based on the existing JDAM PIM. An additional internal wire harness was added for the Analog Connector Board (ACB) interface connector and the front cover was modified to accommodate the connector. All other hardware was developed to the JDAM specification.

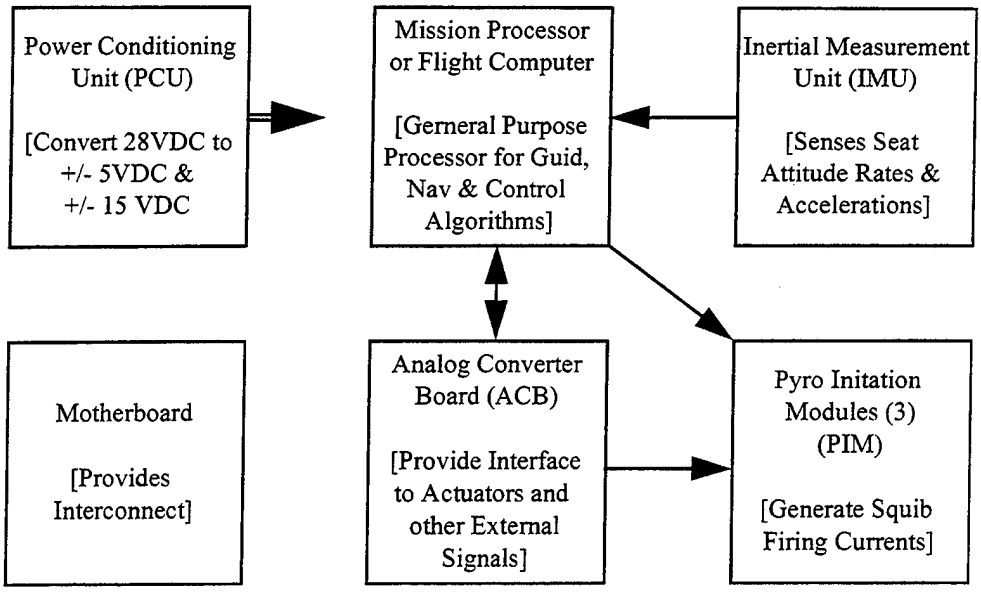

Figure 4-17 GCU Components and Functions

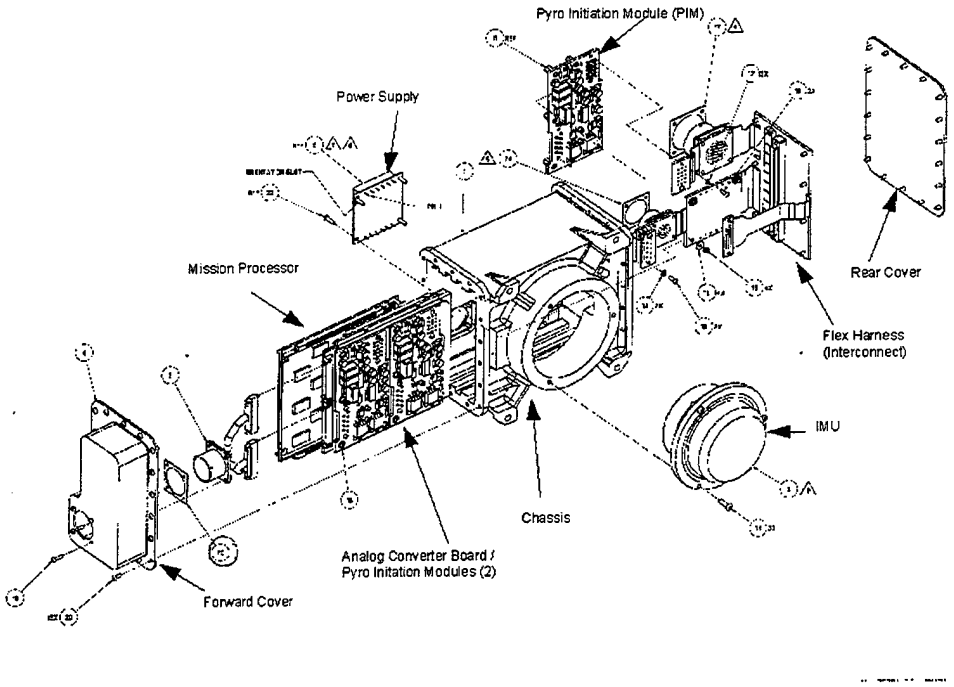

Figure 4-18 GCU Exploded View

As shown in Figure 4-19, the analog converter circuit board includes a separate DC/DC converter to avoid additional load on the existing Power Conditioning Unit (PCU). The filters and D/A converters are the same design used by Aerojet to interface to the actuator controllers and pressure transducers. An Erasable Programmable Logic Device (EPLD) controls the ACB functions, including interface to the mission computer and other external interfaces.

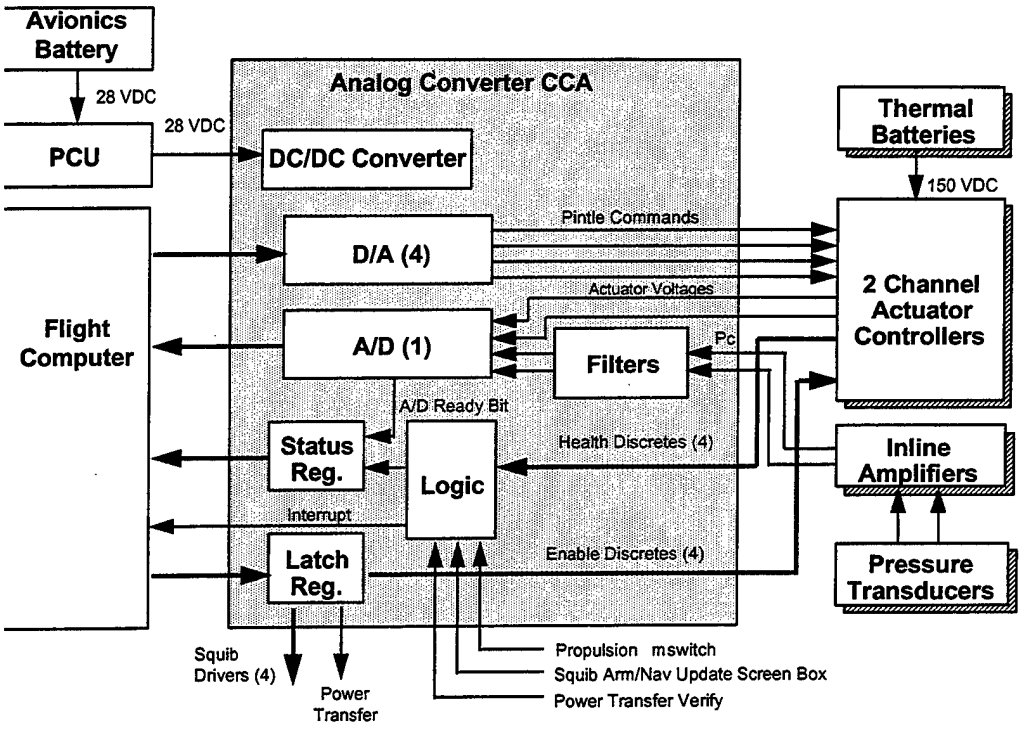

Figure 4-19 Analog Converter Board Block Diagram

The ground support PC is used to communicate to the GCU to provide initialization data and control. It is an off-the-shelf ruggedized 486 based laptop computer. An off-the-shelf MIL-STD-1553B interface card is added to communicate to the GCU. This unit was used on the Tactical High Anti-Jam GPS Guidance (THAGG) program which also used the JDAM GCU. Software modifications were made under the Phase II task for unique BIT and other functions.

The avionics system and the actuator controllers require 28 VDC power. Rechargeable lead-acid batteries were originally selected as the power source but, during the sled test program, the ability of the rechargeable battery pack to operate through the sled test environments became questionable and it was

replaced with a single 28 VDC thermal battery, P/N EAP-12198, from Eagle Pitcher.

Digital telemetry data from the GCU was recorded on a digital data recorder capable of recording 100 Kbytes/sec, Figure 4-20. The recorder was procured from Electronic Professional Services (EPS), Part Number SSR-A1-008-01-CBSP. Data extraction from the recorder is achieved by a separate card hosted in the ground support PC.

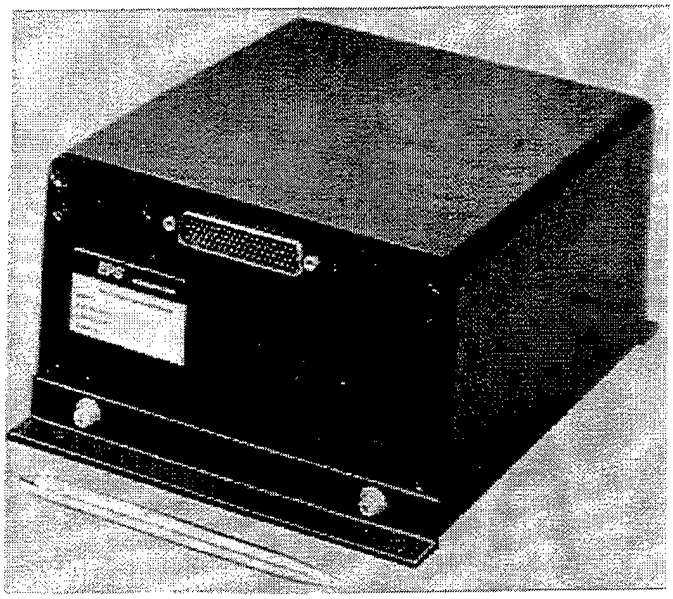

Figure 4-20 Data Recorder

The wire harness provides the interconnect between the various seat subsystems (Figure 4-21).

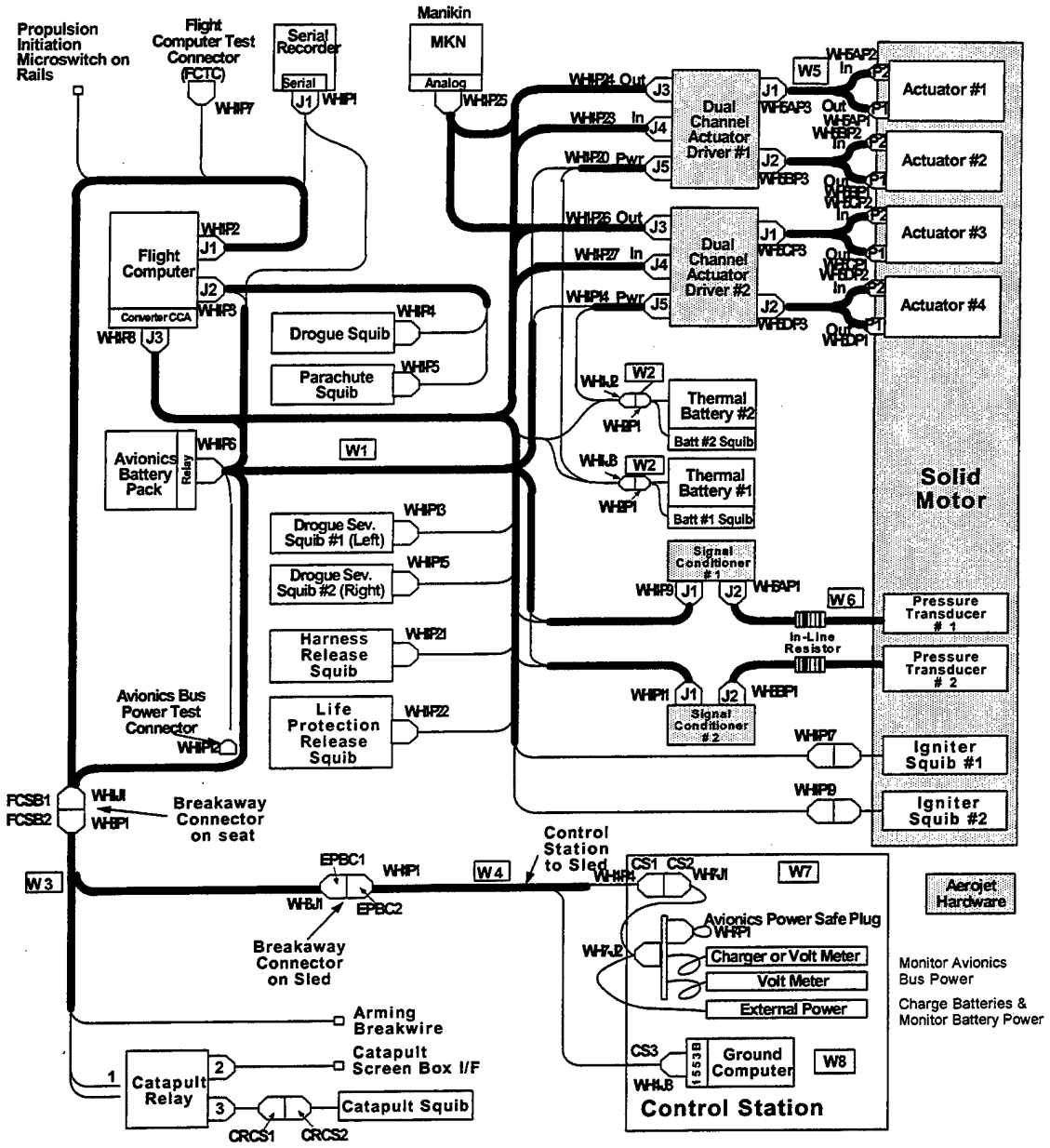

Figure 4-21 Wire Harness

4.4 High Speed Protection Devices

The devices on the seat to provide high speed protection, consist of the following:

- Torso restraint harness
- Arm restraint system
- Leg protection system
- Head protection system

4.4.1 *Torso Restraint*

Torso restraint is provided by a seat-mounted single-point harness that serves as a parachute harness and as a restraint harness in the seat. The arrangement of the harness, as it could be applied to an operational seat, is illustrated in Figure 4-22. The primary advantage of this type of harness is that the crewmember's torso is positively restrained against the backrest by the "X" straps of the harness which are all cinched up for ejection.

For the demonstration seat, the harness was cinched up when the manikin was installed in the seat. The recovery parachute riser attachment arrangement is similar to that used on ACES II and cinch up was achieved by an ACES II inertia reel which had been modified to be retracted by compressed gas from a storage bottle rather than by the normal gas generator. This arrangement helped to minimize the motion of the manikin during the period of sled travel prior to ejection.

Although the single-point harness concept eliminates the conventional lap belt, a lap belt was also used on the demonstration seat. This was done because it was a convenient method of providing centrally located rings needed for the arm restraint lanyards. The lap belt was similar to that used on the ACES II F-22 seat but was integrated into the single-point harness so that the harness and the lap belt could both be anchored by the existing lap belt locking pins. Thus, when the harness release system operated, the withdrawal of the inertia reel strap and lap belt locking pins released both the single point harness and the lap belt from the seat.

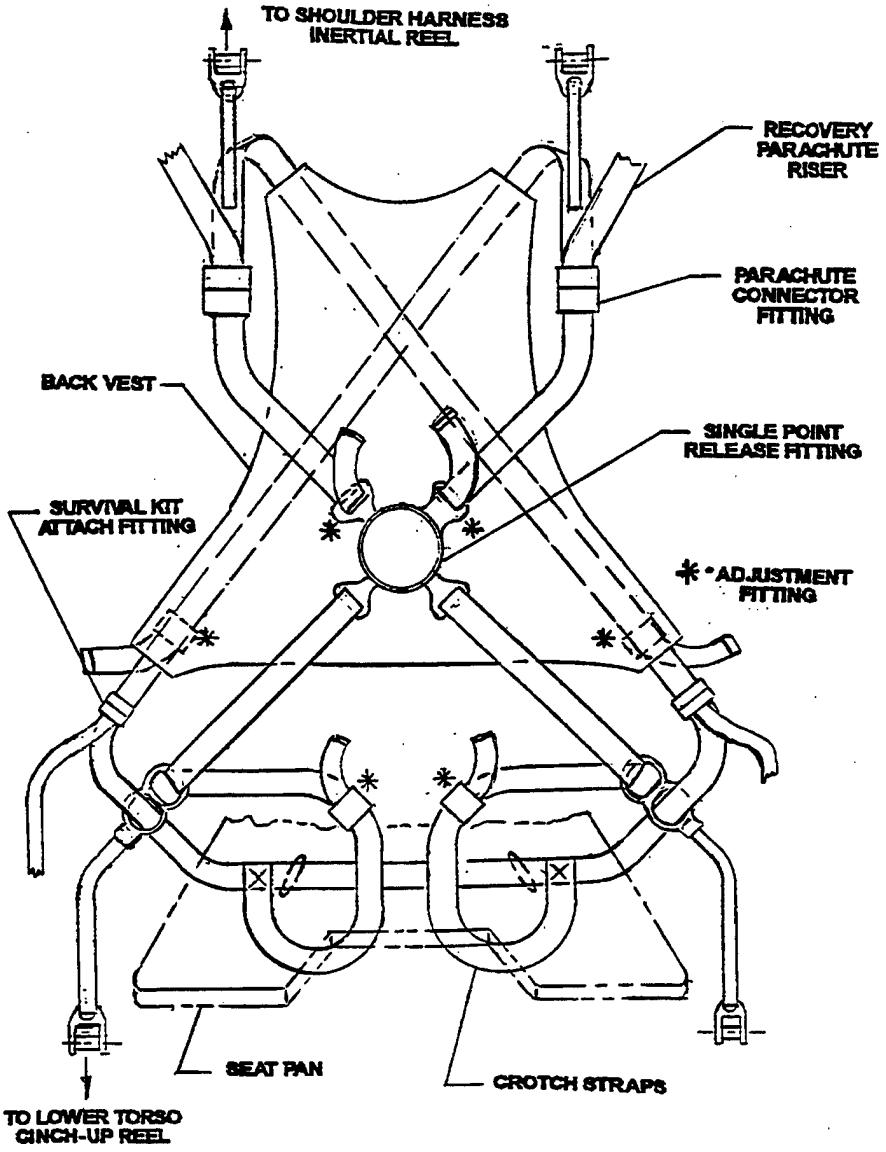

Figure 4-22 Integrated Seat Mounted Harness

4.4.2 *Arm Restraint*

Arm protection is provided by a system of restraint lanyards and nets which deploy around the arms and restrain them against windblast forces. This system is representative of the arm restraint system developed for the ACES II seat in the F-22 aircraft. For the demonstration program, the system was pre-deployed. This avoided the need to conduct tests to verify the compatibility of the arm restraint deployment system with the test vehicle. Also, it helped to avoid the introduction of any adverse arm motion due to the motion of the sled prior to ejection. The arm restraint lanyards are anchored by the lap-belt end

fittings and therefore the restraint system is released when the lap belt becomes detached from the seat during seat-manikin separation.

4.4.3 *Leg Protection*

In the fourth generation seat, provisions are necessary to restrain and support the legs against the forces imposed by the airstream, by maneuvering of the seat and by the deployment of the drogue parachute. It is also important to restrain the legs in a predetermined configuration so that changes in the aerodynamic characteristics, center of gravity and inertial characteristics are minimized.

On the demonstration seat, protection is provided by a combination of three features. One feature is that the legs are raised so that the lower legs are supported by the forward face of the seat bucket. A second, is that surfaces are provided for lateral (outboard) support for the lower legs and to provide lateral (inboard and outboard) support for the feet. The third feature is the provision of lanyards and cuffs that tether the legs to the forward surface of the seat bucket. For the demonstration test program, the geometry of the seat pan was such that the manikins' legs were in the raised position. Also, the leg restraint lanyards were cinched up when the manikin was installed in the seat. The cuffs are released by being severed by a cutter when the harness release system is actuated.

4.4.4 *Head Protection*

Head protection is provided by two devices. One of these is a "brim", which consists of an airfoil that is positioned above the head to reduce the lift force on the helmet by altering the airflow. The other device consists of lateral restraint straps which run between the brim and two anchor points on the parachute risers and are positioned on either side of the helmet when the brim is deployed.. The general arrangement of the brim and the lateral restraint straps is shown in Figure 4-23. The airfoil portion of the brim assembly is of fabric construction, with a solid insert to provide a triangular shaped flow deflector. The lateral restraint straps, as the name indicates, are provided to limit the lateral motion of the head. The approach of anchoring the straps to the parachute risers limits the lateral motion of the head as a function of the position of the head relative to that of both the seat and the torso.

In an operational system, the brim and lateral support straps would most probably be deployed at the time of ejection and, depending on the seat-crewmember separation process, may have to be retracted to clear the path for the crewmember to separate cleanly from the seat. For the demonstration system, the brim and straps were set in the deployed position prior to the test but were retracted for seat-manikin separation.

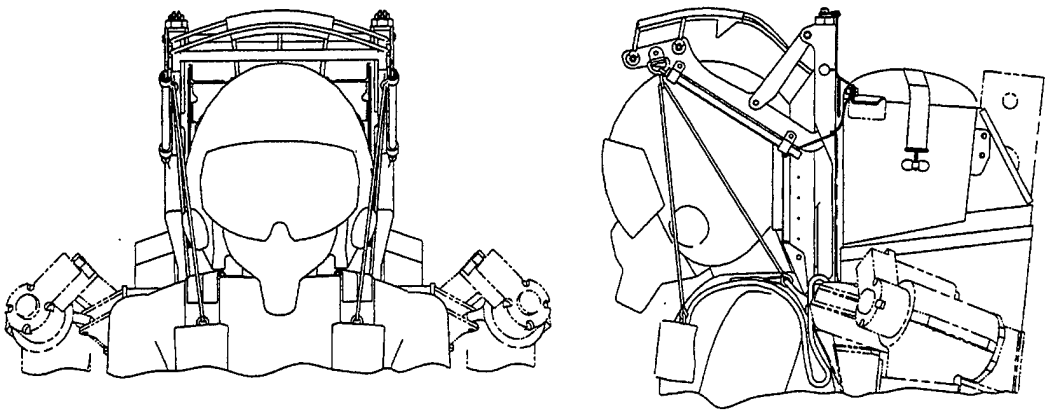

Figure 4-23 Head Protection System

4.5 System Operation

To describe the operation of the fourth generation demonstration system, it is convenient to describe the sequence of events for the three modes relative to the sequence of events for an ejection under high speed, low altitude conditions. The following sequence is for a high speed demonstration sled test. It should be noted that some of the events and practices, while appropriate for a test, may not be appropriate for an operational system. In this respect, care was taken to ensure that the test performance was fully representative of what could be obtained by an operational system. The sequence of events for a high speed demonstration test is as follows:

1. In preparation for the test, the manikin is secured in the seat with the harness tightened and the inertia reel retracted. The legs are in the raised position and the restraint systems for both the arms and legs are deployed and cinched up. In addition, the high speed protection brim and the lateral support straps are in the deployed configuration.

2. The seat and manikin are then installed in the cockpit of the F-16 forebody on the MASE sled and the sled mounted on the track.

3. Prior to the test, the avionics system is powered up and checked out to ensure that the critical elements are functioning satisfactorily. Also, prior to the test, the GCU is set to the initial attitude conditions.

4. Just prior to sled propulsion initiation, the avionics power supply on the seat and the thermal batteries for the propulsion pintle actuators are turned on.

5. When the sled reaches the ejection initiation point, a track-side screen box initiates the ejection catapult causing the seat and manikin to be propelled up the guide rails.

6. After 20 inches of travel, the controllable propulsion motor is fired and the motor begins to pressurize.

7. 50 milliseconds after motor ignition, the GCU issues commands to the four pintle actuators in accordance with the control laws and in response to inputs from the IMU and from the motor pressure transducers.

8. When the seat is in an adverse attitude, such as banked or yawed, the flight control system will act to correct the attitude. Simultaneously, the system may begin to pitch the seat aft to gain altitude in accordance with a schedule that is compatible with controlling the MDRC.

9. The flight control system monitors seat angle of attack and motor burn time and reorients the seat for drogue operation. The drogue is fired 1.1 seconds after motor ignition and, when the opening force occurs, the seat is aligned so that the force vector passes through or close to the center of gravity of the seat, and occupant, thereby minimizing pitch oscillations. With this timing, the drogue becomes effective and begins to stabilize the seat at approximately the same time as the motor begins the process of burning out.

10. When the seat and manikin have slowed down to 220 KEAS, the recovery parachute is fired and then, as in the standard ACES II seat, the drogue is severed and the harness release system is actuated 150 and 250 milliseconds later, respectively. The arm and leg restraint systems are released at the same time as harness release.

11. The initial motion of the recovery parachute container withdraws cotter pins from the brim mechanism and the mechanism then retracts the brim to provide a clear path for the manikin to separate from the seat.

12. The recovery parachute inflates and separates the manikin from the seat.

13. The seats in the demonstration tests were fitted with a recovery parachute which was packed in a fabric container stowed in the seat pan but attached to the manikin so that deployment was achieved by seat-manikin separation.

The above sequence is for a high speed demonstration ejection test. For a low speed demonstration test, the sequence of events would be the same up to step 9. If, during step 9, the speed drops to 220 KEAS and the process of aligning the seat for the drogue has not been initiated then, instead of reorienting the seat for drogue deployment, the flight control system would continue to monitor the seat angle of attack and motor burn time and would reorient the seat for recovery parachute operation. The recovery parachute is fired at 1.2 seconds after motor ignition and, when the parachute opening force occurs, the seat is aligned so that the force is applied in line with the crewmember's spine.

In an ejection at high altitude, above 15,000 feet, the sequence would be the same as described above for the high speed demonstration test except that the recovery parachute would not be deployed above 15,000 feet and the conditions for deployment of the recovery parachute would be a combination of altitude and speed.

5.0 TEST PROGRAM

The Phase II test program consisted of two types of test: "Initial Tests" and "Demonstration Tests". The initial tests were conducted to provide data or verify component or subsystem operation to support the system demonstration tests. The demonstration tests consisted of a series of ten system ejection tests to demonstrate the operation of the fourth generation technologies under a range of conditions.

5.1 Initial Testing

The initial testing included wind tunnel tests and verification testing of components and sub-systems. It also included testing to investigate and resolve problems which occurred in the demonstration ejection tests. A listing of the initial tests is provided in Table 5-1 which also references the test report numbers. Most of the tests are documented in Reference #3, report MDC 97K7017, however, some of the tests were documented in individual reports and others are described in ejection test reports. A brief description of the initial tests is given in the following paragraphs:

5.1.1 *Wind Tunnel Tests*

Two series of wind tunnel tests were conducted. One was a series of full scale, low speed tests which was conducted primarily to develop the brim concept proposed for reducing the forces on the head at high speed. The other was a series of transonic tests using a 40% scale model to obtain aerodynamic data for the fourth generation demonstration configuration.

5.1.1.1 *Low-Speed Wind-Tunnel Tests*

The objectives of these tests were 1) to investigate various brim configurations and develop the most effective design and 2) to obtain aerodynamic data for the demonstration seat configuration.

The tests were conducted in the Micro Craft Low Speed Wind Tunnel in San Diego, California. The tunnel has a cross-section of eight feet by twelve feet. Blockage limited the speed to Mach 0.26 and all of the tests were run at this speed. The test article was an ACES II F-15 seat which was modified to be representative of the demonstration seat configuration. A total of 88 runs were made and data was obtained at pitch angles from -10 to +60 degrees and yaw angles up to 30 degrees. The brim concept is to locate an airfoil above the head to reduce the lifting force on the helmet and tests were conducted on a fabric airfoil and a rigid airfoil. The data showed that there was not a significant performance difference between the two and, the fabric brim was selected because it should be considerably easier to stow than a rigid brim.

Table 5-1 Initial Tests and Investigative Tests

Test	Report Reference
Drogue Bridle Burn Test	Ref. #2 (MDC 95K0192)
Arm Restraint Snubber Test	Ref. #3 (MDC 97K7017)
Thermal Battery Isolation Test	Ref. #3 (MDC 97K7017)
Rocket Motor Load / Deflection Test	Ref. #3 (MDC 97K7017)
Rocket Motor Free Vibration Test	Ref. #3 (MDC 97K7017)
Footman Loop Pull Test	Ref. #3 (MDC 97K7017)
Leg Restraint Strap Cutter Test	Ref. #3 (MDC 97K7017)
Seat Vibration Test	Ref. #3 (MDC 97K7017)
Seat / Manikin Separation Test	Ref. #3 (MDC 97K7017)
Pyro Initiation Test	Ref. #3 (MDC 97K7017)
Seat Recovery Parachute Extraction Test	Ref. #3 (MDC 97K7017)
Low Speed Wind Tunnel Test	Ref. #4 (MDC 96K0201)
Transonic Wind Tunnel Test	Ref. #5 (MDC 96K0228)
Avionics Battery Vibration Test	Ref. #3 (MDC 97K7017)
Brim Retraction Test	Ref. #3 (MDC 97K7017)
Structural Windblast Test	Ref. #6 (MDC 97K0104)
Avionics Initial Test	Ref. #7 (MDC 96P0048)
Brim Strap Pull Test	Ref. #3 (MDC 97K7017)
Pressure Transducer Drift Test	Ref. #8 (MDC 97K7036)
Seat and Rail Characterization Test	Ref. #9 (MDC 97K0123)

The configuration of the brim was refined as the tests progressed and a total of twelve configurations were tested. In the course of the tests, the horizontal and vertical locations and the angle of the brim relative to the head were changed. Also, the location of the deflector on the brim was altered as was the brim width. The configuration comparison tests were conducted using a 95th percentile male manikin then, once the configuration refinement process had been completed, the final configuration was also tested with a 5th percentile male manikin.

The runs to obtain aerodynamic data showed that the fourth generation seat has greater drag and higher aft pitching moments than the ACES II seat, but that it has less lift near 0 degrees angle of attack.

5.1.1.2 *Transonic Wind Tunnel Tests*

These tests were conducted to obtain the aerodynamic data required to support the design and development of the flight control system. The tests were conducted in the Micro Craft Trisonic Wind Tunnel in El Segundo, California. The test article, shown in Figure 5-1, was a 40% scale model of the demonstration seat and crewmember. The model crewmember was a 5th percentile male, located such that the head was in the correct position for a seat with a movable bucket. The legs were in the raised ejection configuration.

Tests were run at Mach 0.26, 0.6, 1.0 and 1.2 and data were obtained for pitch angles from -20 to +70 degrees and from 0 to 30 degrees in yaw. The data obtained were axial, side and normal forces, lift and drag forces and pitch, yaw and roll moments. The data were compared with the data from the low speed wind tunnel test program and with data for ACES II. On the basis that the comparison showed that the data exhibited similar trends and were generally of the same magnitude, it was concluded that the data were valid. Both the low speed and transonic tests showed the demonstration seat to be statically stable at small angles of yaw, whereas the ACES II seat is statically unstable at similar angles.

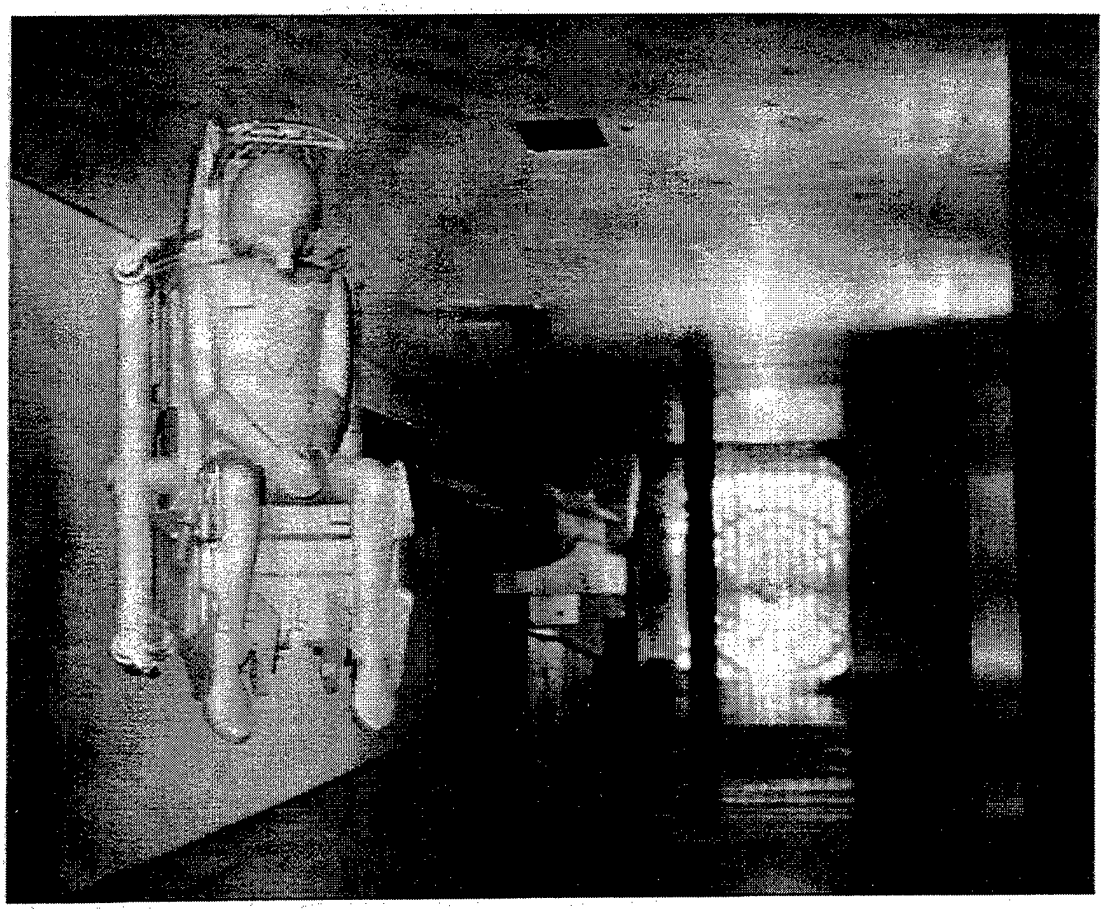

Figure 5-1 Transonic Wind Tunnel Test

5.1.2 *Avionics Tests*

The primary testing of the avionics system was the Avionics Initial Test Program which was conducted to demonstrate that the avionics system provided satisfactory initialization and control of all functions. The program was structured to provide operational verification at increasing levels of fidelity and integration. This approach is illustrated in Figure 5-2. The tests were conducted by MDA at their St. Louis, Missouri, facility during the period from November 1995 to October 1996.

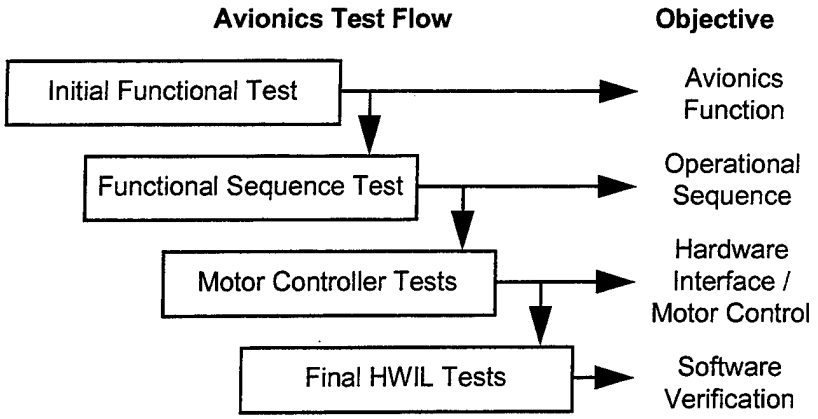

Figure 5-2 Avionics Initial Test Flow

Initial Functional Tests: These tests verified the operational function of the GCU processor, analog converter board and seat pyro initiator module. It also verified the functioning of the GSPC hardware. The interface control software and the ability to download and execute GCU software from the GSPC were tested. Also tested were the GCU processor to analog converter board interface and the converter board external I/O interfaces.

Functional Sequence Tests: During these tests, the function of the GCU software that controls the sequence of events during an ejection was verified. The testing included verifying the normal operational sequence together with all abort sequences using simulated GCU inputs. This testing also encompassed verification of the Aerojet motor control algorithm software. In order to incorporate the Aerojet motor control algorithm software in the GCU, it was converted to Ada code using an XD Ada compiler. The tests verified the operation of the rehosted motor control algorithm.

Motor Controller Tests: These tests verified the closed loop motor control system operation using the GCU combined with the Aerojet actuator drivers and actuators. This test allowed verification that the GCU control system response compared satisfactorily with simulation results and verified the GCU/actuator interface and wiring harness. The interface with the serial data recorder was also verified in these tests.

Final Hardware-In-The-Loop (HITL) Tests: The final HITL tests verified the operation of the software by closed loop testing with simulated environments. These tests verified closed loop operation of the motor controller, seat attitude control and guidance algorithms with the sled-test operational flight program for all of the demonstration test cases.

5.1.3 *Drogue Bridle Burn Tests*

In an ejection at high altitude or at low altitude and high speed, the drogue parachute is deployed to continue to stabilize the seat and crewmember once the propulsion system burns out. As burn-out occurs over a relatively long period of time and the timing of the event is influenced by several variables, the drogue parachute has to be deployed such that there can be a significant period of time between drogue fire and motor burn-out. During this period, the motor plumes can impinge on the drogue bridle. The purpose of these tests was to develop a satisfactory thermal protection scheme for the bridles.

The tests were conducted in conjunction with the controllable propulsion demonstration tests which were conducted by Aerojet at their facility in Sacramento California. For the tests, four samples of the drogue bridle were covered with candidate protection systems and the bridles were inserted into the rocket plumes during the burn-out phase of the motor operation. In the first test, in July 1995, four different protection systems were tested and the one selected consisted of inner and outer sleeves of Fiberglass which had an aluminized outer surface and a Silicon rubber inner surface. The other protection schemes that were tested were: 1) an inner sleeve of Nextel with an outer sleeve of Fiberglass, 2) an inner sleeve of Nextel with an outer sleeve of Nomex and 3) a single sleeve of Fiberglass. Satisfactory operation of the selected system was verified in a second test, in February 1996, in which the selected protection system was installed on all four bridle samples.

5.1.4 *Structural Windblast Tests*

These tests were conducted to verify the structural integrity of the demonstration seat assembly which included the brim installation. Four tests were conducted in which the seat was exposed to a 660 KEAS windblast. This was the maximum capability of the test facility. The same seat and manikin were used in every test but a new brim assembly was installed for each test. The seat and brim installation withstood the windblast without damage. The tests were also used to verify the retraction of the brim under appropriate air load conditions. The brim retraction system is triggered by the motion of the recovery parachute container and the container was fired when the airspeed had decayed to the recovery parachute deployment speed of 220 KEAS. The brim retracted satisfactorily in all four tests.

5.1.5 *Miscellaneous Functional, Structural And Environmental Tests*

In the course of the Phase II program, a variety of tests were conducted to verify the satisfactory operation of different components or to investigate anomalies which occurred in the demonstration ejection tests. The following is a summary of each test:

Arm Restraint Snubber Tests: For the demonstration program, it was believed that the snubbing requirements could be met by a low-cost commercial cargo

strap snubber, Part Number ANCAM/100-1500. A total of twenty-five tests were conducted on the cargo strap snubber and on two different snubbers designed for ejection seat restraint systems. It was concluded that the cargo strap snubber would be adequate for the demonstration program.

Thermal Battery Isolation Tests: The purpose of these tests was to establish the capability of candidate insulation materials to withstand the battery temperature. The tests were conducted at the MDA, Long Beach, California, facility in April 1996. Two materials were tested; Nextel 312, a woven ceramic cloth, and EPDM (Ethelene-Propylene Diene Modified) synthetic rubber sheet. The tests showed that both materials performed satisfactorily and the EPDM synthetic rubber sheet was selected based on cost.

Rocket Motor Load/Deflection Tests: The purpose of these tests was to investigate the stresses that would be developed in the motor when subjected to the simultaneous application of internal operating pressure and thrust loads. The tests generated data on the deflection versus load characteristics of the motor and the data were used in conjunction with motor/seat deflection data to verify that the motor deflection during operation on the seat would not result in deflections which would cause unacceptable stresses in the motor.

Rocket Motor Free Vibration Tests: The purpose of these tests was to obtain deflection data for the motor, both by itself and when installed on the seat. The tests were carried out by MDA at F & L Enterprises, Cypress, California, in June 1996. The results of these tests, in conjunction with the Rocket Motor Load/Deflection Tests, verified that the deflections of the installed motor were such that the motor would not be subjected to unacceptable stresses during a demonstration test.

Leg Restraint Strap Cutter Tests: In order to avoid the development of a mechanical release system for the leg restraint straps, it was proposed to sever the two straps using the ACES II drogue bridle severance cutter, Teledyne McCormick-Selph Part Number 81138-6. A series of six tests was conducted and the straps were successfully severed in each test. The tests were conducted by MDA at their Long Beach, California, facility in July 1996.

Seat Vibration Tests: This test was conducted to verify the structural integrity of the seat and the functional performance of the GCU during random vibration. The power spectral density in these tests was shown to be similar to that measured on the seat in a sled run at 700 KEAS. Also, these tests did not indicate any problems with the seat structure or with the performance of the electronic equipment. The tests were conducted by NTS at their facility in Fullerton, California in June and July 1996.

Seat Manikin Separation Tests: The purpose of these tests was to verify the satisfactory separation of the manikin from the seat. Four tests were conducted with a 95th. percentile male manikin and two with a 5th. percentile male manikin. The arm restraint straps did not release properly in two tests due to incorrect rigging of the straps relative to the torso restraint harness. With the proper rigging, separation was successfully demonstrated. The tests were conducted by MDA at their Long Beach, California, facility in July 1996.

Pyro Initiation Tests: In the first demonstration ejection test, the connectors which connected to the seat mounted pyros were incorrectly wired. The purpose of these tests was to obtain data on two methods of providing the firing pulse to the pyros. In one method, power was supplied to both of the squib bridgewires in series and in the other method, power was supplied to only one of the two bridgewires. As a result of the tests, the approach of supplying power to one bridgewire was selected because the tests showed that this provided a greater margin of power from the avionics battery. The tests were conducted by MDA at Holloman AFB, New Mexico.

Seat Recovery Parachute Extraction Test: In the first demonstration ejection test, the parachute system used to recover the seat was a system developed by MDA for their Minipac seat. This used a 26-foot conical parachute packed in a laced-up fabric container. After the first test, it was decided that the ACES II reefed C-9 28-foot flat circular parachute should be used as this would reduce the rate of descent and thereby reduce the risk of damaging the seat. There was only sufficient volume in the seat bucket for the Minipac container and the ACES II chute had to be modified to fit into the container. The purpose of this test was to verify that the chute could be extracted from the container with an extraction force which was compatible with the demonstration system. In the test the packed parachute was suspended and the dynamic deployment conditions were simulated by allowing a 100-lb. mass to drop approximately 1 foot. When the mass was released it dropped smoothly and deployed the entire parachute from the container. The test was conducted by MDA at Holloman AFB, New Mexico, in August 1996.

Avionics Battery Vibration Tests: A premature failure of the avionics batteries occurred prior to the first demonstration ejection test. It was believed that this was due to excessive vibration testing and the purpose of these tests was to verify the batteries were suitable to be used in the program. As a result of these tests, the duration of the environmental stress screening was reduced. The tests were conducted by MDA at their St. Louis, Missouri facility in September 1996.

Brim Retraction Test: In the demonstration tests, the brim was retracted so that it would not interfere with the manikin during separation from the seat.

The primary purpose of this test was to verify the operation of the retraction system and to verify that the actuation of the retraction system did not adversely affect the main recovery parachute assembly. A secondary purpose was to verify a method of snubbing the recovery parachute container which was needed to allow the recovery parachute to be fired in the windblast tests. In the test, the brim retracted smoothly and the head lateral restraint straps released freely from the brim structure. Also, the test provided the data needed to finalize the design of the parachute snubbing system. The tests were conducted by MDA at Holloman AFB, New Mexico, in December 1996.

Brim Strap Pull Tests: These tests were conducted to identify a satisfactory configuration of brim cross strap. A total of 14 tests were conducted and a configuration was selected. The tests were conducted by MDA at their Long Beach facility in May 1996.

Pressure Transducer Drift Test: In the first two demonstration tests, one of the two motor pressure transducers, Sensotec Part Number 060-975-03, exhibited an unacceptable degree of drift relative to the other. The purpose of these tests was to investigate possible causes. Analysis of the data indicated the possibility that the transducer was being affected by the high temperature gas, as only the tip of the transducer was protected. The tests confirmed this and showed that protecting the transducer with grease would resolve the problem.

Seat Mode Characteristics Tests: In demonstration test #3, the GCU failed as the seat was leaving the guide rails. It was concluded that this was caused by the shock resulting from rebound of the guide rails when the middle rollers exited the rails. It was decided to add supports to stiffen the rails and this was done by introducing struts which were bolted between the guiderails and the cockpit aft bulkhead. The upper portions of the guiderails, approximately 12 inches, are cantilevered and the struts were located approximately six inches from the top of the rails. The tests were conducted to establish the frequency characteristics of the unstiffened and stiffened rails and of the GCU and they showed that the GCU exhibited significant resonances in the frequency that coincided with the unstiffened rail but which were below the frequencies for the stiffened rails.

5.2 Demonstration Testing

5.2.1 *Test Program*

The demonstration test program consisted of a series of ten ejection tests which were conducted on the high speed test track at Holloman AFB using the MASE sled vehicle which had an F-16 forebody. The crewmember was represented by a biofidelic manikin. In six of the tests the Advanced Dynamic Anthropomorphic Manikin (ADAM) was used and in the other four tests the Hybrid III manikin was used.

The objectives of the program were:

- To demonstrate controlled flight of an ejection seat at speeds up to 450 KEAS with adverse launch conditions.

- To demonstrate safe escape at speeds up to 700 KEAS.

In accordance with the test objectives, the tests covered a speed range from 0 to 700 KEAS. Also, tests at speeds up to 450 KEAS were run with adverse attitudes so that the flight control system was required to correct for the initial attitude as part of the attitude and trajectory control process. During the course of the program, problems were encountered and, as a result, the test conditions were selected on a test-by-test basis. Some test conditions were repeated in order to provide data and to verify that the system could successfully operate under those specific adverse conditions.

5.2.2 *Evaluation Criteria*

The evaluation criteria for the program consisted of criteria for restraint and criteria for recovery parachute opening forces. In addition, in order to provide requirements for system design, values for the MDRC were established.

Restraint Criteria (Neck Loads):- A review of the restraint criteria indicates that, because of the comprehensive limb restraint provisions on the demonstration system, the only important criteria for the demonstration program was the evaluation criteria for neck loads. These criteria stated that the tension load on the neck shall be limited to 300 lb and the lateral load on the neck shall be limited to 50 lb. It was later agreed that the 50 lb. evaluation criterion was too low and 250 lb. was a more appropriate criterion.

Recovery Parachute Force Criteria:- The recovery parachute evaluation criteria provided limits for the parachute opening force (25G), rate of onset (250 G/sec) and a requirement that the opening forces not cause hyperextension of the neck. As the fourth generation program evolved, it became apparent that these criteria were somewhat academic. While recovery parachute operation could be critical in a fourth generation system under dive

or sink conditions, when ground avoidance is not practical, this was not the case for the demonstration test conditions. For all of the demonstration test conditions the flight control system guides the seat and manikin into an upward trajectory such that there is no need to impose stressful recovery parachute loads.

MDRC Criteria:- In order to provide meaningful requirements for the design of the flight control system, values were assigned for the MDRC. These were that the maximum value for the MDRC should be 1.0 using the high risk criteria and that as a goal, the MDRC should be less than or equal to a value of 1.0 using the low risk criteria. The method used to calculate the MDRC is described in Appendix A.

5.2.3 *Summary of Results*

Table 5-2 lists the conditions for the ten tests while Table 5-3 lists weight data and Table 5-4 the event times for each test. Table 5-5 summarizes the overall test results and Table 5-6 lists the detailed objectives for each test and indicates which objectives were met. The results of the tests relative to the operation of the flight control system are presented in Appendix B, which contains plots of trajectory, angle of attack, angle of sideslip and MDRC. Included in these data are plots generated by DESS simulations. In addition, Appendix C contains plots of significant parameters which were recorded by the seat mounted data recorder and by the manikin data acquisition system. In the case of the ADAM manikin, the data was recorded by the ADAM data recorder and, in the case of the Hybrid III manikin, the data was telemetered to a data recording facility.

Table 5-2 Test Conditions

Test	Date	Run	Speed (KEAS)	Roll (Deg)	Yaw (Deg)	Manikin Type	Report Ref
1	7/25/96	85E-B2	0	0	0	Large ADAM	Ref #10 (MDC 97K7013)
2	9/5/96	85E-B3A	0	60	0	Small ADAM	Ref #8 (MDC 97K7036)
3	10/29/96	85E-C1	325	60	0	Small ADAM	Ref #9 (MDC 97K0123)
4	2/1/97	85E-C3A	325	60	0	Small Hybrid III	Ref #11 (MDC 97K0124)
5	4/3/97	85E-D1A	325	0	20	Small Hybrid III	Ref #12 (MDC 97K0127)
6	6/13/97	85E-D2A	325	0	20	Small Hybrid III	Ref #13 (MDC 97K0128)
7	8/13/97	85E-D3A	325	0	20	Small Hybrid III	Ref #14 (MDC 97K0158)
8	9/4/97	85E-E1	450	0	20	Small ADAM	Ref #15 (MDC 97K0157)
9	10/15/97	85E-F1	600	0	0	Small ADAM	Ref #16 (MDC 97K0156)
10	11/10/97	85E-G2	700	0	0	Small ADAM	Ref #17 (MDC 97K0155)

Table 5-3 Weight Data

Test	Speed (KEAS)	Manikin	Nude W4t.(lbs)*	Gear Wt.(lbs)	Dressed Wt.(lbs)	Seat Wt.(lbs)	Ejected Wt.(lbs)
1	0	LG ADAM	~195	~10	~205	~291	502
2	0	SM ADAM	~146	~10	~157	~291	440
3	320	SM ADAM	~146	~10	~157	~291	449
4	320	SM Hybrid III	~166	~10	~176	~295	469
5	325	SM Hybrid III	166	9	175	~295	469
6	317	SM Hybrid III	~166	~10	~176	~295	472
7	325	SM Hybrid III	167	10	176	296	472
8	437	SM ADAM	145	11	156	295	451
9	589	SM ADAM	147	10	157	297	454
10	708	SM ADAM	145	12	157	293	450

*Nude weight of manikin includes instrumentation

Table 5-4 Event Times

EVENT	Test 1	Test 2	Test 3	Test 4	Test 6	Test 7	Test 8	Test 9	Test 10
Sled Launch	-0.895	-0.900	-10.097	-10.182	-10.792	-10.690	-7.493	-10.127	-10.934
Squib Arm	-0.895	-0.900	-0.902	-0.915	-0.879	-0.868	-0.912	-0.892	-0.884
Catapult Initiation	-0.150	-0.136	-0.145	-0.150	-0.137	-0.131	-0.135	-0.137	-0.106
Propulsion Breakwire	0.000	0.000	0.000	0.000	0.000	0.000	0.000	0.000	0.000
Drogue Alignments Start	na	na	na	na	na	0.904	0.908	0.868	0.780
Drogue Mortar Initiation	na	na	na	na	0.377	1.104	1.104	1.101	1.103
Parachute Alignment Start	0.766	0.863	na	0.964	na	na	na	na	na
Parachute Mortar Initiation	na	1.203	na	1.204	1.674	1.934	2.084	2.275	2.456
Drogue Severance Initiation	na	1.356	na	1.354	1.824	2.084	2.238	2.428	2.606
Restraint Release Initiation	na	1.456	na	1.454	1.924	2.184	2.334	2.525	2.706
Seat / Manikin Separation	na	1.467	na	1.658	2.306	2.420	2.603	2.824	3.078
Main Chute 1st Inflation	na	5.603	na	2.971		3.592	4.010	4.056	
Manikin Ground Impact	11.560	20.075	10.905	9.764	9.321	20.849	20.395	35.000	14.517
Seat Ground Impact	11.560	na	10.905	9.764	9.441	21.840	21.808	21.035	11.720

Table 5-5 Test Results

Test	Speed (KEAS)	Mach No.	Altitude (Feet)	MDRC Medium Risk	Results	Cause
1	0	.00	495	0.70	Controlled Flight, No Recovery Chute	Wiring Error
2	0	.00	390	0.73	Success	
3	320	.53	n/a	n/a	GCU Failed	Mech. Shock
4	320	.53	n/a	n/a	IMU Failed	Mech. Shock
5	325	.53	n/a	n/a	No Test, Ejection Not Initiated	Elect. Short
6	317	.53	n/a	0.76	Propulsion Shut Down In Mid-Burn	Mech. Vibration
7	325	.52	410	0.76	Success	
8	437	.71	370	0.97	Success	
9	589	.97	300	0.83	Success, But Neck Loads Exceeded Criteria	Para. 5.2.5.4.1
10	708	1.14	220	1.03	Success, But Neck Loads Exceeded Criteria	Para. 5.2.5.4.1

Table 5-6 Test Objectives

OBJECTIVE	Test 1	Test 2	Test 3	Test 4	Test 6	Test 7	Test 8	Test 9	Test 10
Propulsion Initiation	Yes	Yes	Yes	Yes	Yes	Yes	Yes	Yes	Yes
Propulsion Burn	Yes	Yes	No	Yes	No	Yes	Yes	Yes	Yes
Control Propulsion	Yes	Yes	No	No	No	Yes	Yes	Yes	Yes
Stabilize Seat	Yes	Yes	No	Yes	Yes	Yes	Yes	Yes	Yes
Reorient Seat	Yes	Yes	No	Yes	Yes	Yes	Yes	Yes	Yes
Control Pitch/Angle of Attack	Yes	Yes	No	No	No	Yes	Yes	Yes	Yes
Restrain Torso	Yes	Yes	-	Yes	Yes	Yes	Yes	Yes	Yes
Restrain Arms	Yes	Yes	-	Yes	Yes	Yes	Yes	Yes	Yes
Restrain Legs	Yes	Yes	-	Yes	Yes	Yes	Yes	Yes	Yes
Restrain Head	N/A	N/A	N/A	No	No	No	No	No	Yes
Meet Head Load Criteria	Yes	Yes	-	No	Yes	No	No	No	No
Meet MDRC	Yes	Yes	-	Yes	Yes	Yes	Yes	Yes	Yes
Reorient for Chute Deployment	Yes	Yes	-	No	No	Yes	Yes	Yes	Yes
Recover Seat and Manikin	No	Yes	No	Yes	Yes	Yes	Yes	Yes	Yes

The results of the demonstration test program can be summarized as follows:

- The flight control system was successfully demonstrated in six of the ten tests.
- Although the flight control system failed in tests 4 and 6, it was functioning satisfactorily when the dynamic environment caused mechanical failures of the system.
- Test #5 was a "no test" because an electrical harness short caused the test to be aborted prior to initiation of the catapult.

Review of the test results shows that the test failures were caused by the effect of the mechanical environment on the avionics hardware and were not the result of systematic problems related to the new technologies. It is also significant that, once the characteristics of the mechanical environment were established and the avionics components were revised to withstand the environment, the system provided a spectacular demonstration of fourth generation seat system capabilities in four successive successful tests. When the tests are evaluated relative to the demonstration of new technologies, it is clear that the program objectives were successfully achieved. This conclusion is supported by the following list of program accomplishments:

- Flight control was successfully demonstrated over the speed range from 0 to 700 KEAS.

- Ground avoidance or "upward seeking" maneuvers were successfully demonstrated from initial adverse attitude conditions of 60 degrees roll at 0 and 325 KEAS and 20 degrees yaw at 325 and 450 KEAS.
- "Safe" escape was demonstrated at speeds up to 700 KEAS.
- The MDRC was successfully controlled in every test with values of 0.83 and 1.03 being attained for the 600 and 700 KEAS tests using medium risk criteria.
- The manikin's torso and limbs were successfully restrained and protected.
- The head protection system achieved reduced lift, however, tests 9 and 10 showed higher neck loads (404 and 408 lbs respectively) than the evaluation criteria (300 lbs) requirement.
- The helmet was retained throughout the 0-700 KEAS speed range.
- Alignment for parachute loads was successfully demonstrated.

The operation of the demonstration system is illustrated in Figure 5-3 which shows a sequence of the shots of the seat and manikin in test #2, which was at zero speed and 60° roll. Figure 5-4 shows several photographs of test #8 which was at 437 KEAS and 20 degrees yaw. In this case, the first two photographs show the attitude of the seat being corrected. In the third photograph, the seat has been pitched aft and is being propelled upward. In the final photograph the seat has been pitched forward so that the force vector of the drogue, which is in the process of deploying, will be in the desired orientation to minimize MDRC.

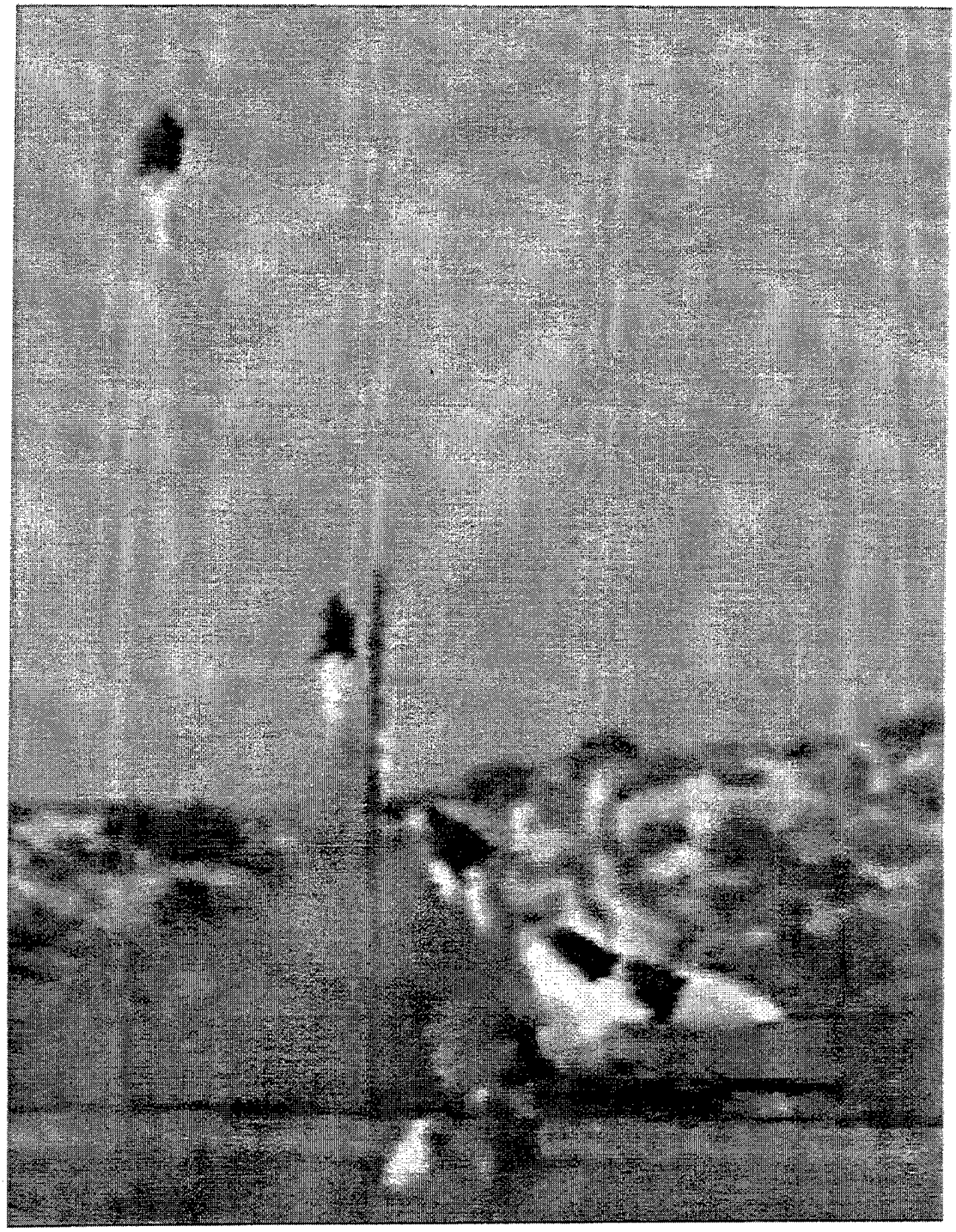

Figure 5-3 Demonstration Test #2 Superimposed Photographs

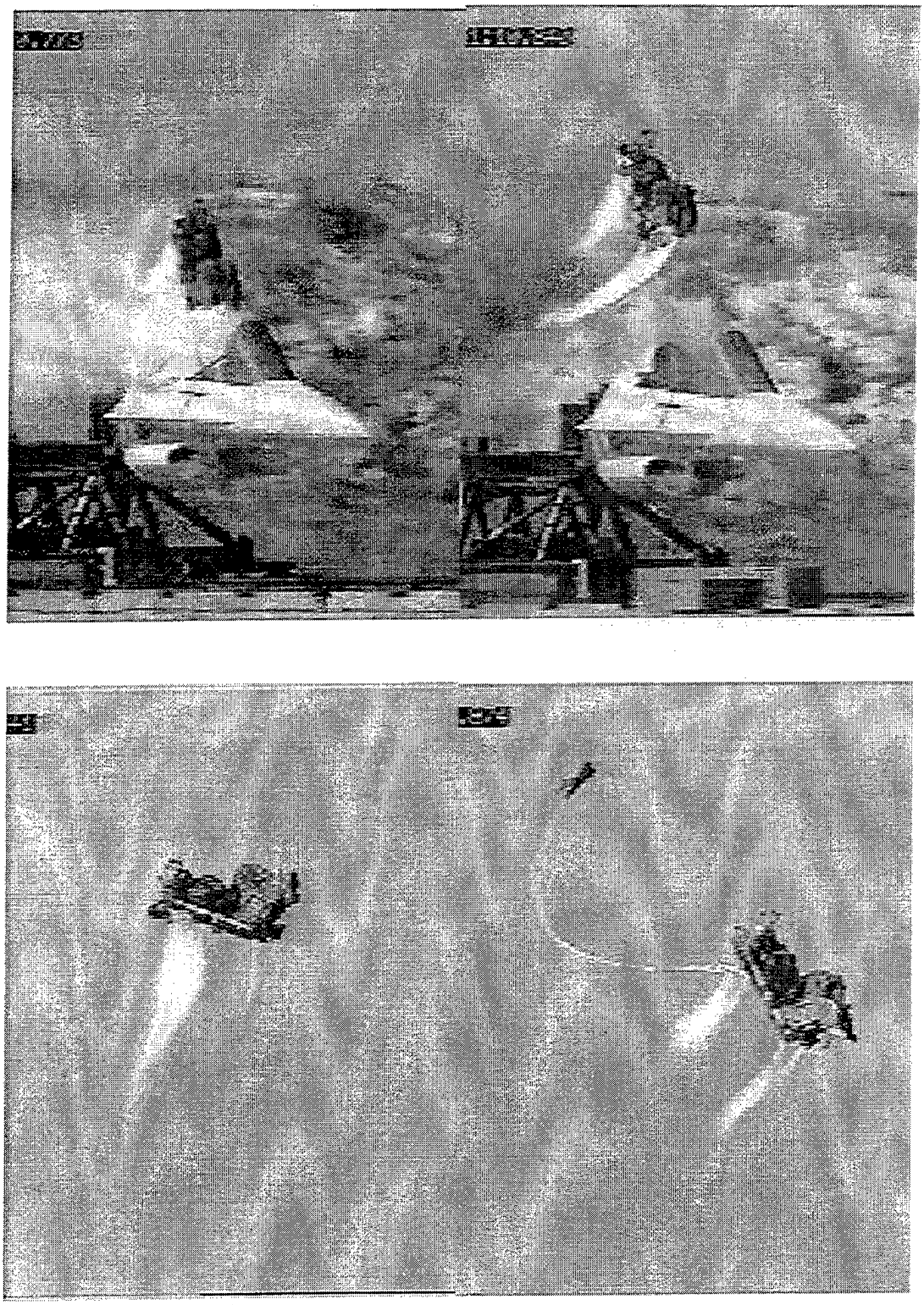

Figure 5-4 Demonstration Test #8 Four Photographs

The performance data for the tests are contained in Appendix B. These data consist of trajectory plots together with plots of angle of attack, sideslip and MDRC.

The most significant data are those that show the degree of seat attitude control during the propulsion phase of the test. Figures 5-5 and 5-6 show data for what are judged to be the two most demanding tests, test #8, 450 KEAS and 20 degrees yaw, and test #10, 700 KEAS. In these plots, motor ignition is at 0.0 seconds and the seat separates from the guiderails approximately 50 milliseconds later.

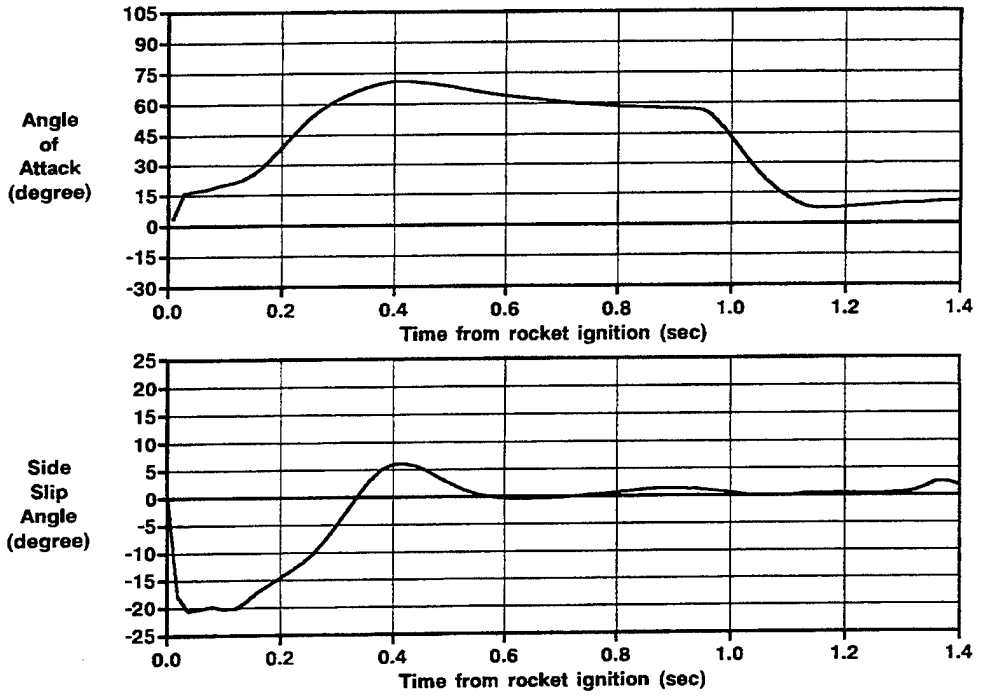

Figure 5-5 Attitude Control Performance in test #8 (KEAS=437, Yaw=20 degrees)

The plot of sideslip for test #8, shows that the system did not allow the seat to yaw beyond the initial angle of 20 degrees. Subsequently, the initial yaw angle was corrected in approximately 0.3 seconds after the seat separated from the guiderails. The plot of angle of attack shows that the seat starts off at an angle of about 15 degrees then, to increase the upward component of the propulsion vector, it progressively rotates aft until the angle of attack is 60 to 70 degrees. At about 0.9 seconds, the process of alignment for the drogue begins so that, by the time the drogue is fired at 1.1 seconds, the seat is aligned to an angle of attack of 5-10 degrees, so that the drogue force will be in the desired orientation.

In the 700 KEAS test, sideslip is totally controlled and the plot of sideslip shows that excursions were limited to about 2 degrees. The plot of angle of attack is similar to that for test #8 except, because of the higher speed, the seat is rotated aft at a much lower rate in order to control the spinal component of the MDRC.

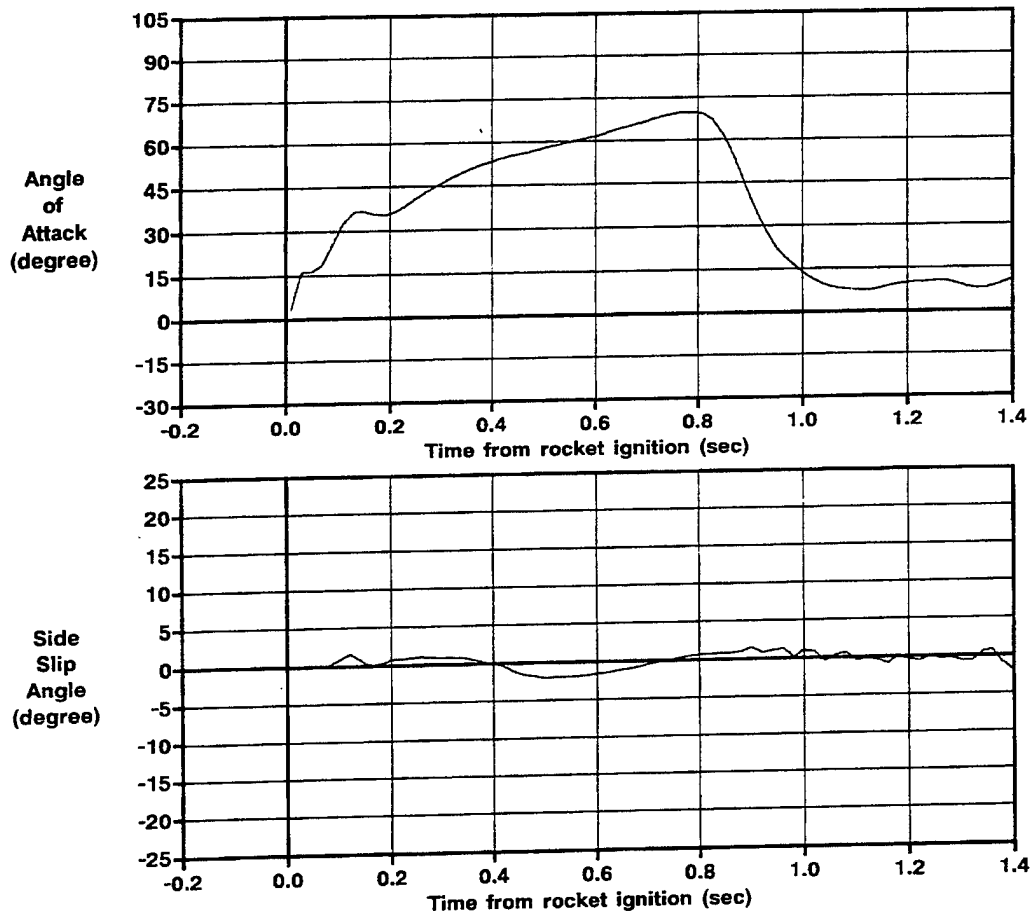

Figure 5-6 Attitude Control Performance Test #10, (KEAS=708)

The ultimate objective of the fourth generation escape system technologies program was to establish the technical base for the design and development of a fourth generation operational system and, on the basis of the demonstrated successful operation coupled with the lack of systematic failures, this objective was achieved.

5.2.4 *Demonstration Tests Results - Avionics System*

The new technologies, "flight control system" and "high speed protection devices" have such different attributes that it is convenient to address them separately. This section describes the results of the individual tests relative to

the operation of the flight control or avionics system and the results relative to the operation of the high speed protection devices are described in section 5.2.5.

5.2.4.1 *Demonstration Test #1*

This test, at zero speed and altitude, was intended to demonstrate system performance in a benign (static) test condition. The catapult and seat / aircraft separation performed as expected with no interference or anomalies. The initiation and control of the propulsion system also performed as expected and the proper seat attitudes were attained. However, due to incorrect definition of the pyro squib interfaces, the recovery systems were not initiated. Simulation of the test showed good correlation between the DESS and test data. Several anomalies occurred and these, together with the cause and resulting modifications, are summarized in Table 5-7.

Lessons Learned:

(1) Use flight hardware vs. surrogates for development tests. Using live squibs versus squib simulators would have revealed the squib interface issue prior to sled testing and may have also revealed the pressure spikes due to low bus voltage. Using flight pressure transducers in the flight configuration versus a tee for a third instrumentation pressure transducer may have revealed the pressure drift problem.

(2) Development tests should duplicate predicted flight duty cycles in addition to "engineering" duty cycles. 4th Generation Phase 1 development tests focused on engineering pintle command duty cycles as representative of flight duty cycles and to gather the maximum amount of engineering data on motor performance. Use of predicted flight duty cycles might have revealed pressure rise at 0.3 seconds and the command spikes at 0.836 seconds.

(3) Propulsion Demonstration Test #8, the full up demonstration, should have been repeated with lessons (1) and (2) applied. Demonstration test #8 should have been further modified to include a proper test fixture to prevent the seat from experiencing environments introduced by the test fixture, such as banging against the wall.

(4) Perform static tests with control loops closed. This static test is typically conducted with systems using aerodynamic control surfaces to ensure that no parasitic effects exist in the control system. This type of test is much more difficult to perform with a propulsive control system, requiring a special test fixture, but may have identified the 100 Hz limit cycle.

Table 5-7 Demonstration Test #1 Anomalies and Modifications

	Test Anomaly	Cause	Resulting Modification
1A	ACES II Pyros not fired	Squib Interface had been miscommunicated / misinterpreted	Wiring Harness Modified. Verified via Squib Tests
1B	Limit cycle on thrust command	100 Hz limit cycle possibly due to skip sampling or aliasing.	Filter bandwidth on attitude rate feedback signal to autopilot reduced from 75 Hz to 25 Hz Reduced filter BW does not substantially impact performance at low speed.
1C	Motor pressure rise with peak at tmotor + ~ 0.3 seconds	Aerojet suspects combustion instability but data is insufficient to evaluate	None
1D	PC2 drift low relative to PC1, PC2 marked bad at tmotor + 0.226 seconds	Electrical interference was primary suspect, but testing could not duplicate the problem. (Thermal drift was identified as the cause after sled test 4.)	None for Sled Test 2. (Transducers were sealed with grease as a thermal barrier after sled test 4)
1E	PC1 spike at motor initiation (tmotor + 0.003 seconds)	Post sled test 2 tests revealed that pressure readings become erratic when the voltage to the signal conditioners falls toward the low end of the specified range (18 to 30 V). Since the avionics bus voltage can fall to 19 to 20 volts during squib firing, this may contribute to this effect. Low bus voltage is caused by high internal resistance of rechargeable batteries	Prevent motor control loop closure on pressure spikes observed in sled test 1. Minimum of 3 pressure samples above threshold to close motor loop
		Pressure transducers were improperly terminated.	Pressure transducer shield terminated at signal conditioner
1F	Pintle command 2 spike at tmotor + 0.836 seconds	Pintle command spikes when pintle commands approach zero	Motor controller modification to efficiency calculation (Aerojet)
1G	Premature failure of the avionics batteries during pretest checkout	Evaluation of the batteries revealed that internal plates had shifted causing a loss of capacity. Suspected cause was vibration and/or shock. The batteries had been vibrated twice to the ACES II flight worthiness levels for one minute in each axis. This is an overtest of the 4th Gen. flight duration.	None
	Other Modifications	N/A	Minor BIT check modifications for easier pretest checkout
		N/A	Drogue sever 0.15 seconds after chute deploy to correct conflicting requirement. Previously drogue sever was at 0.20 seconds.

5.2.4.2 *Demonstration Test #2*

This test was a second static ejection with a 60 degree initial roll angle. The seat performed as expected with minor anomalies (See Table 5-8). Simulation of the test showed good correlation between the DESS and test data.

Table 5-8 Demonstration Test #2 Anomalies and Modifications

Re	Test Anomaly	Cause	Resulting Modification
2A	Recorded data stopped at tmotor + 8.699 sec	Unknown. May be related to bit errors on some data. A control bit error might stop the recorder	None. Further diagnostics to software deemed unwarranted
2B	Motor pressure rise with peak of 2750 psi at tmotor + 0.273 sec	Combustion Instability? Similar to Sled Test 1	None
2C	PC2 drift low relative to PC1, PC2 marked bad at tmotor + 0.203 sec	Unknown. (Thermal Drift identified after sled test 4)	(Add grease to thermally isolate transducers from motor after sled test 4)
			Increased delta pressure from 200 to 450 psi before marking a transducer as bad
2D	PC1 spike at tmotor + 0.0195 sec TCMD3 spike at tmotor + 0.01596 Harness release data bit error at tmotor + 0.0195	Data Bit Error. The 3rd bit of the byte is in error. Since the software would have squibbed the release if it tried to write that bit and since the software limits the thrust command it appears there is a noise problem on the output bit to the data recorder. The data spikes are within 100 bytes of each other in the recorded file. This suggests the noise is related to some event, potentially motor initiation. The RS-422 output driver checked out OK.	None
2E	Pintles not retracted at end of flight	When the motor pressure drops below 50 psi (burnout), the pintles should be retracted. Because the motor pressure is oscillating around 50 psi, all 4 pintle commands cycle between full retract and full in..	A latch has been added to the sled test 3 software to keep the pintles retracted once the chamber pressure falls below 500 psi for 3 samples and the time since motor initiation is greater than 1.5 seconds.
	Other Modifications	Abort down the track	New abort logic between catapult enable and motor initiation to sequence chutes based on time
		Simulation of higher speed ejection	Modified control angle schedule based on simulation results

5.2.4.3 *Demonstration Test #3*

In this test the GCU failed when the seat was at the top of guiderails. As a result, the motion of the seat was not controlled and it impacted the ground 0.7 seconds after propulsion ignition. Investigation indicated that the GCU hardware was marginal for the vibration and shock environment experienced when the seat middle rollers exit the rails. Modifications were made to harden the GCU electronics and to attempt to reduce the shock environment (See Table 5-9).

Table 5-9 Demonstration Test #3 Anomalies and Modifications

Ref	Test Anomaly	Cause	Resulting Modification
3A	GCU failed at top of rails	Shock	GCU Electronics hardened (removed EPLD socket and epoxied large components to boards)
			Mount GCU on isolators. No autopilot modifications were required to maintain stability margins
			Stiffen Rail Structure by adding supports to reduce cantilever and move shock to higher frequency
		SW error found after sled test 3	Run time system modifications to eliminate exception on move with floating underflow
		Processor halts on internally generated exceptions and unhandled interrupts.	Run time system modifications to handle all exceptions and interrupts. Attempt to keep running - may have little benefit
	Other Modifications	Ensure positive control during drogue alignment for 325 KEAS cases with initial pitch & yaw conditions	Modify drogue alignment logic: 0.7 * Drogue Angle > Time to Burnout OR Time to Burnout < 0.6 seconds
		Shock and Vibration Environment	Replaced lead acid avionics battery with thermal battery due to uncertainty about operation through vibration and shock environments

Lessons Learned:

(1) Better understand the test environment. Detailed analysis of the seat / rail systems may have revealed this issue. Dynamic testing is preferred but may not be possible for this system.

(2) Include better, more reliable environmental instrumentation to fully characterize the environment. The telemetry / data recording system must be designed to accommodate a larger amount of data. Steps should be taken to reduce the noise on the data.

(3) Test all development units to the full flight worthiness level. Limited margin testing should be conducted if a unit can be sacrificed and the additional cost absorbed.

(4) Provide additional oversight (detailed reviews) for design and build to improve product quality and reliability. This is difficult to implement on low budget development programs but worth the additional expense up front.

5.2.4.4 *Demonstration Test #4*

In this test the accelerometers in the IMU failed 0.116 seconds after motor ignition. Prior to failure of the accelerometers, the seat had zeroed out the initial roll attitude and was following the desired trajectory. After the failure of the accelerometers, the seat no longer followed the prescribed trajectory due to improper calculation of seat velocity and angle of attack (α) based on erroneous acceleration data from the IMU. Failure analysis by Honeywell concluded that the accelerometers failed due to shock. The most likely cause of the shock is the IMU being struck by the seat / sled umbilical (Table 5-10). The accelerometers are extremely sensitive to low shock levels at high frequency.

Table 5-10 Demonstration Test #4 Anomalies and Modifications

Ref	Test Anomaly	Cause	Resulting Modification
4A	The accelerometers failed (output went full scale) 0.116 seconds after motor ignition	Shock broke the pendulous mass suspension system in one accelerometer and distorted the mass suspension system in the other accelerometers, resulting in the pegged outputs. Most likely cause is the seat/sled umbilical impacting the IMU.	Add cover to seat bottom to protect IMU.
			Add IMU accelerometer check and abort code to ignore velocity
		Although the GCU isolators may have bottomed, it is now considered unlikely that this caused the IMU failure due to the IMU isolator. It is doubtful that the IMU contacted seat structure.	Mounting configuration modified to prevent contact between the GCU or IMU and seat structure
		Aerodynamic loading caused larger IMU / GCU displacements	Add cover to seat bottom to protect IMU
4B	Drogue did not deploy	Calculated seat speed was less than 220 KEAS. Logic properly followed.	None
4C	Data recorder S/N 5087 failed check at T-30 seconds (replaced)	Could not duplicate failure at STL or manufacturer (A software mod writes power up records to the data recorder before it is ready resulting in a failed BIT test)	(The cause was identified after sled test 7.) Added display of prelaunch abort conditions to GSPC. Added check for squib arm & propulsion breakwire to BIT to identify BIT fail modes
4D	Data recorder S/N 5084 power down at ~ 3 seconds after motor ignition	Shock associated with parachute opening probably caused the power on reset. The shock loads were not measured directly since the accelerometers failed, but there are large rates near the data dropouts .	None. Since the seat was not at the proper attitude for chute deployment and the main chute was deployed at high speed (~300 KEAS), we believe that the chute opening load was larger than normal and do not anticipate this problem to repeat

Lessons Learned:

(1) A more thorough analysis of the system design may have identified seat umbilical impact on the IMU as a potential failure mode.

(2) Last minute results of isolator displacement analysis were not properly considered relative to the final installation and available sway space.

5.2.4.5 *Demonstration Test #5*

Test #5 was a " no test" because the seat was not ejected from the sled. This was due to a fault in the catapult enable relay circuit (Table 5-11). Post test analysis revealed a burned trace in the GCU motherboard on the power return for the catapult enable signal that prevented the relay from pulling in. A short in the wire harness caused the trace to fail, most likely during T-2 hr checks. The catapult enable return signal isolation from ground (structure) was violated by the sled track monitoring circuit, contributing to the failure.

Table 5-11 Demonstration Test #5 Anomalies and Modifications

Ref	Test Anomaly	Cause	Resulting Modification
5A	Squib Arm signal at sled first motion	Noise. Switch did not close at first motion	Require a squib arm signal in excess of 4 msec before arming
			The time out between the squib arm screen box and the motor initiation break wire is increased from 30 to 90 seconds. This change will prevent a system shut down in the event of an early squib arm signal.
5B	Catapult did not fire.	A short between the 28 VDC and the shield in the main wire harness	Hi-Pot test all cables
			Provide L-1 end to end checks of catapult fire circuit and squib arm signal Provide L-0 check of catapult fire circuit and squib arm signal. Modify catapult enable BIT test to toggle on / off.
	Other Modifications	Provide an additional safety by retracting the pintles in the event that the seat will need to be disarmed.	Retract pintles on no start conditions
		The ESS test software exhibited a problem with the interrupt enable function. The flight OFP did not exhibit this problem.	The interrupt enable will now be done first thing in a task in order to guarantee it is done after the connect to the interrupt handler.

Lessons Learned:

(1) More thoroughly document and coordinate external (track) interfaces. The harness failure would not have caused the trace damage had the catapult enable return signal not been tied to ground. The actuator batteries had a requirement that the 28 VDC be isolated from ground (structure) which was violated by the track instrumentation.

(2) End to end test everything, even things you didn't think were testable (think again) or think don't require test. If end to end tests are not achievable, the test should be aborted on any anomaly. Overvoltage /

overcurrent conditions were experienced prior to the test but the in place system tests did not detect the damage to the catapult enable circuit.

5.2.4.6 *Demonstration Test #6*

The sixth system sled test repeated the 325 KEAS, 20 degree yaw ejection condition. This test resulted in a motor over pressure abort, 0.374 seconds after motor initiation. At the time of the abort, the system had completed the yaw correction maneuver and was in the pitch-up maneuver. Analysis of the test data indicated two problem areas: (1) autopilot instability and (2) motor controller performance (Table 5-12).

Table 5-12 Demonstration Test #6 Anomalies and Modifications

Ref	Test Anomaly	Cause	Resulting Modification
6A	Motor overpressure 0.374 seconds after ignition	Autopilot Instability caused by seat modes and GCU isolators.	Remove GCU Isolators. Tested GCU to 450 g shock.
		Pintle Controller does not stabilize pressure loop for any command time history.	None. Although any command should not cause the motor to overpressure, GCU modifications should prevent the command instability and pintle control algorithm modifications could not be accomplished without significant schedule / cost impact
6B	Data recorder intermittently not ready (fails BIT test)	Power bus glitch at ~ 12 V due to actuator controllers and/or writing to recorder before it is ready.	Delay writing to data recorder at power up on hold pending need for other SW mod

The test data showed that the flight controller was commanding an ~30 Hz roll axis oscillation. Evaluation of the acceleration data from the GCU mount locations revealed that the seat bottom structure has an ~30 Hz vibration mode that was exciting the natural frequency of the GCU shock mounts in the lateral direction and inducing a ~30 Hz mode into the autopilot. The acceleration data obtained in test 6 at the shock mount interface to the seat indicated that the shock environment is significantly less than what was predicted from the extrapolated data. Additional lab testing of a GCU under 230g 2ms shocks and 450g 1ms shocks verified that the GCU can withstand the environment measured at the GCU mounts in test 6.

Lessons Learned:

(1) Understand the seat modal characteristics. Perform modal tests. Prior analysis assumed that seat modes were high frequency relative to autopilot bandwidth.

5.2.4.7 *Demonstration Test #7*

Sled test #7 successfully demonstrated system performance at 325 KEAS with an initial 20 degree yaw attitude. Minor anomalies are noted in Table 5-13. Poor correlation with the predicted trajectory was seen, primarily due to unmodeled tip-off effects.

Table 5-13 Demonstration Test #7 Anomalies and Modifications

Ref	Test Anomaly	Cause	Resulting Modification
7A	Higher than predicted overshoot / tip-off	Unmodeled aerodynamics possibly due to rocket plume effects and proximity aero possibly related to windscreen.	None. Tip-off models were modified to match this test case but general prediction of aero is still in error
			Remove windscreen
7B	Pintle chatter post test	Actuator controllers powered after GCU drops off line. Thermal batteries keep bus energized (vs. lead acid batteries) and controller DC converter drops out lower than GCU DC converter	None. Significant schedule impact to modify actuator controllers or avionics bus power to eliminate post test pintle chatter. Limited probability of damage to actuators / controllers due to chatter.
7C	Catapult enable drive transistor burnout	After sled test 8, discovered that limiting diode on sled catapult relay was not installed	Added limiting diode after sled test 8.

5.2.4.8 *Demonstration Test #8*

This test demonstrated successfully demonstrated safe escape at 450 KEAS, 20 degrees initial yaw. Minor anomalies are noted (Table 5-14)

Table 5-14 Demonstration Test #8 Anomalies and Modifications

Ref	Test Anomaly	Cause	Resulting Modification
8A	Higher than predicted overshoot / tip-off	Unmodeled aerodynamics possibly due to rocket plume effects and proximity aero possibly related to windscreen.	None. Tip-off models were modified to match this test case but general prediction of aero is still in error
			Replace windscreen for high speed tests
8B	Pintle chatter post test	Actuator controllers powered after GCU drops off line. Thermal batteries keep bus energized (vs. lead acid batteries) and controller DC converter drops out lower than GCU DC converter	None. Significant schedule impact to modify actuator controllers or avionics bus power to eliminate post test pintle chatter. Limited probability of damage to actuators / controllers due to chatter.
8C	Catapult enable drive transistor burnout	After sled test 8, discovered that limiting diode on sled catapult relay was not installed	Added limiting diode after sled test 8.

5.2.4.9 *Demonstration Test #9*

Sled test #9 was conducted at 600 KEAS, straight and level. While the performance of this seat was acceptable in terms of MDRC and recovery of the crewman and seat, it was not acceptable in terms of neck loads on the crewman. In addition, post test analysis indicated unmodeled forces acting on the seat caused both alpha and beta overshoots (Table 5-15).

Table 5-15 Demonstration Test #9 Anomalies and Modifications

Ref	Test Anomaly	Cause	Resulting Modification
9A	Higher than predicted overshoot / tip-off	Unmodeled aerodynamics probably due to rocket plume effects. Unmodeled tip-off	None. A plume impingement model was developed and aerodynamic parameters modified to match the sled test 9 data. The tip-off model was modified
9B	Drogue risers deployed early, 0.15 seconds after motor initiation	Nylon locking loops that retain drogue cover were melted by the rocket plume	Replace nylon loop with Kevlar loop and pot with RTV on the exposed side of the drogue container
9C	Brim provided less than expected attenuation of neck axial loads - 350 lb. vs. 120 lb. predicted	Brim > 1.9 inches above helmet due to catapult acceleration loads compressing manikin and/or airloads inflating brim	Rig brim to reduce nominal clearance and restrict billowing

5.2.4.10 *Demonstration Test #10*

Sled test #10 was conducted at 700 KEAS, straight and level. The seat trajectory was as predicted with the following anomalies (Table 5-16).

Table 5-16 Demonstration Test #10 Anomalies and Modifications

Ref	Test Anomaly	Cause	Resulting Modification
10A	17 Hz limit cycle in lateral channels	Unknown. Possible causes include: • Aerodynamics, cross-coupling • Inertial cross-coupling • Plume impingement, Plume interaction with aerodynamics • A/P or Motor Control Loop • Hardware failure • Actuator rate limit	TBD
10B	Trajectory / attitude prediction mismatch	Plume effects / aerodynamics not properly modeled	
10C	Failed actuator health BIT test on first test attempt	Intermittent open in wire harness	N/A. Take more care during installation

A 17 Hz oscillation in the roll and yaw channels was observed during test #10. Fig 5-7 through 5-9 show the three angular seat rates, attitudes, angles-of-attack and speed. Time zero corresponds to rocket motor ignition. The 17 Hz response appears to change in magnitude at three times. At approximately 0.05 seconds, the seat exits the guide rails and tip-off occurs. Tip-off introduces pitch rates of 500 deg/sec and roll/yaw rates of 100 to 150 deg/sec. Response to tip-off appears to be well damped in all three rate and attitude channels. This time corresponds to the highest speed portion of the flight at small angles-of-attack and small pitch attitudes.

The 17 Hz response increases at approximately 0.3 seconds. The roll/yaw attitude and rate responses appear to be unstable or very lightly damped from 0.3 to 0.7 seconds. The seat is approaching the maximum angle-of-attack and pitch attitude and speed is decreasing to approximately 500 knots. The response could be due to an excitation event or because the seat is simply less

stable as the angle-of-attack increases. Note that the linear stability analysis indicated a gain margin of 5.7 dB and phase margin greater than 25 degrees throughout the speed, alpha, pitch attitude regime of sled #10. Nonlinearities, errors in the aerodynamic data base, aerodynamic or inertial cross coupling or other unmodeled effects all contribute to reduce these margins.

The 17 Hz oscillation increases in magnitude again at approximately 0.7 seconds. This excitation appears slightly prior to the drogue-alignment, pitch-attitude command change at ~ 0.78 seconds. The response is lightly damped to unstable in roll rate and lightly damped in yaw rate. The roll and yaw attitudes are both underdamped, but stable – converging to zero from the 8 deg disturbance. Seat speed is approximately 500 knots and the angle-of-attack and pitch attitude are small.

Examination of the data indicates that the seat is significantly less stable than predicted at high angles of attack at speeds greater than 500 knots. Since the linear stability analysis indicated sufficient margins, the test results imply that unmodeled aerodynamics, aerodynamic cross-coupling, inertial cross-coupling and/or plume effects or other system nonlinearities may be significantly reducing the stability margins at these conditions. The cause appears to be related to the aerodynamics, since sled test #10 was at a higher speed. The persistence of the oscillation at lower speeds and lower angles of attack at approximately one second contradict this argument, since the oscillation was not observed at similar conditions on sled test #9. Potential causes are summarized in Table 5-17.

Lessons Learned:

(1) Develop better aerodynamic models. Conduct separation wind tunnel testing.
(2) Develop better tip-off models. Conduct tip-off tests.
(3) Consider plume effects on aerodynamics and plume impingement effects.

Table 5-17 Test #10 Potential Causes of 17 Hz Oscillation

Potential Cause	Merits	Issues
Aerodynamics	• Seat is not a "clean" aerodynamic configuration. • Manikin can effect aero • Cross coupling aerodynamics unknown • Transonic aerodynamics uncertain • First test at 700 KEAS	• Speed / alpha regime similar to Test #9 after 0.4 seconds
Inertial cross-coupling	• Manikin movement can introduce disturbances and modify aerodynamics • Cross products of inertia can introduce similar effect as aerodynamic cross coupling • Most plausible cause of a disturbance at 0.3 seconds (?)	• Movement not apparent, but possible • Not seen on test # 9 in similar speed / alpha regime • Seat / manikin configuration unchanged from test #9 • Prelaunch mass properties measurements consistent with previous tests.
Plume impingement, plume interaction with aerodynamics	• Effected previous sled tests • Effects not well understood	• Did not introduce 17 Hz mode on previous tests
Autopilot or motor control loop	• Motor control loop stability not completely characterized	• Not seen on previous tests • Autopilot linear stability analysis indicates 6 dB gain margin, 25 degree phase margin for baseline aero / mass properties
Hardware failure	• Soft failure in actuators, pintles, motor can introduce instability in control loop • Some seat structure failed changing mechanical modes	• Other than limit cycle, seat system performed as expected • No structure failures apparent
Actuators rate limited	• Actuator rate limiting can produce limit cycles	• Apparent rate limiting on pintle 4 position data is most likely noise on the data

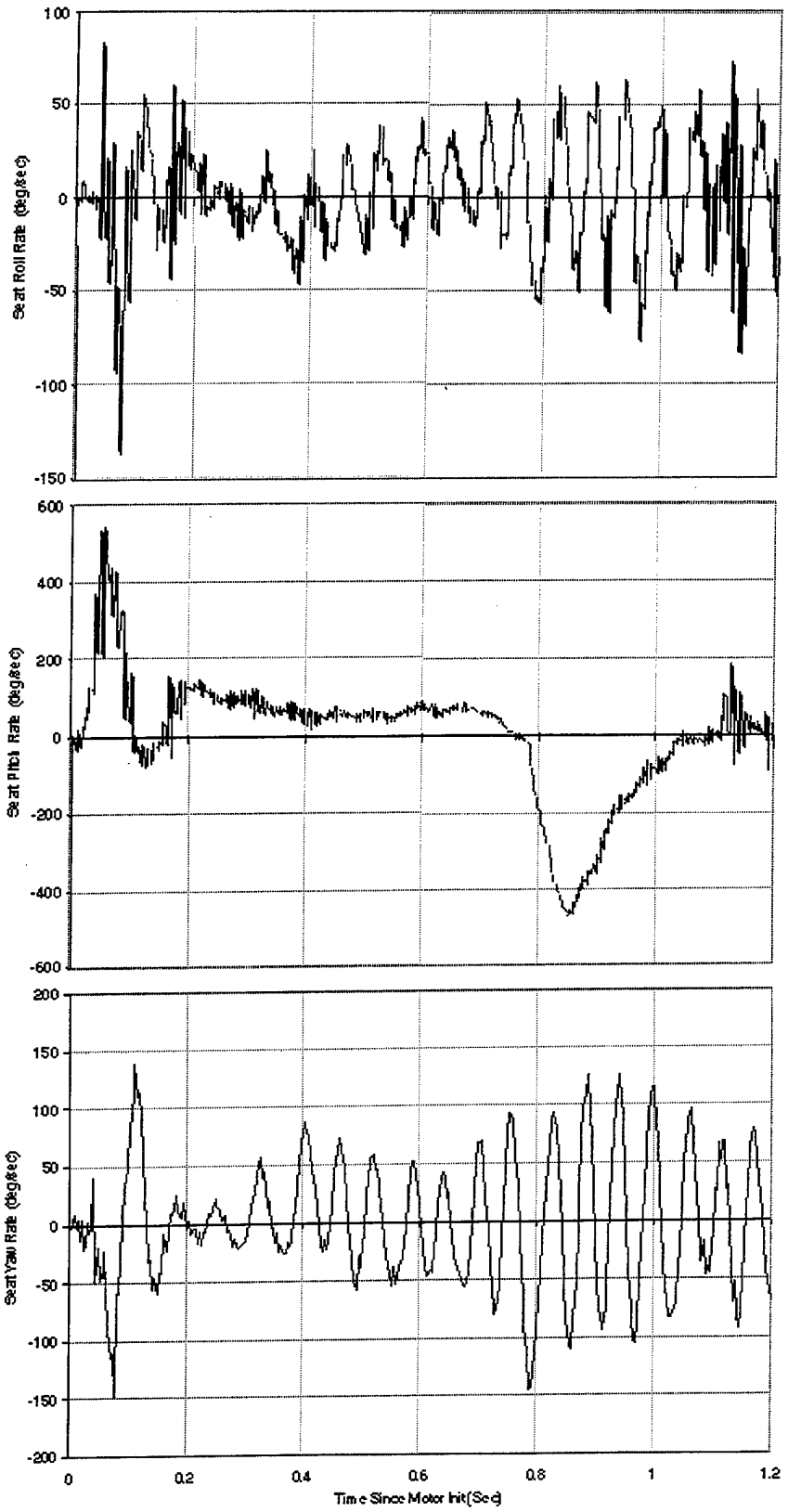

Figure 5-7 Sled Test #10 Seat Angular Rates

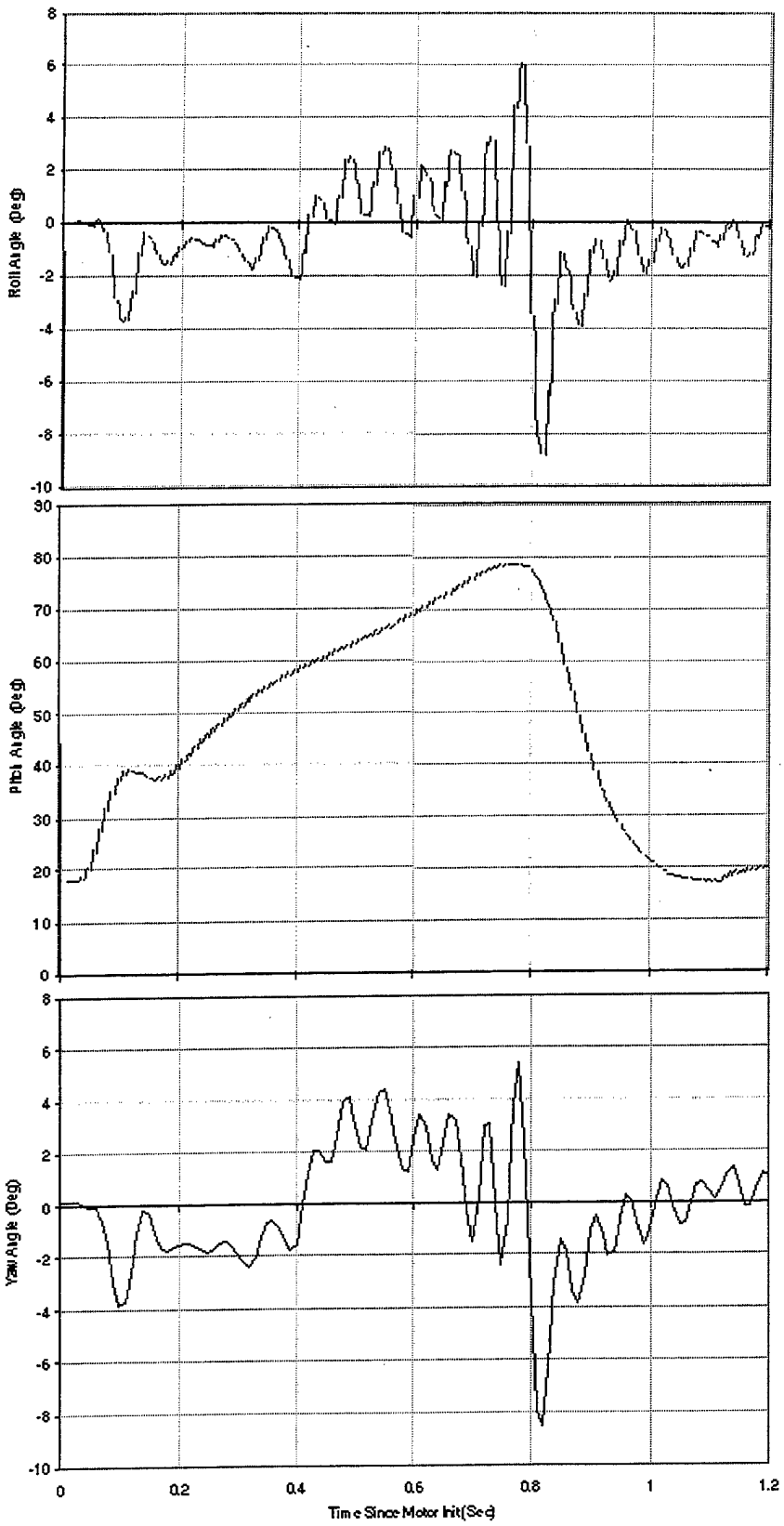

Figure 5-8 Sled Test #10 Seat Attitudes

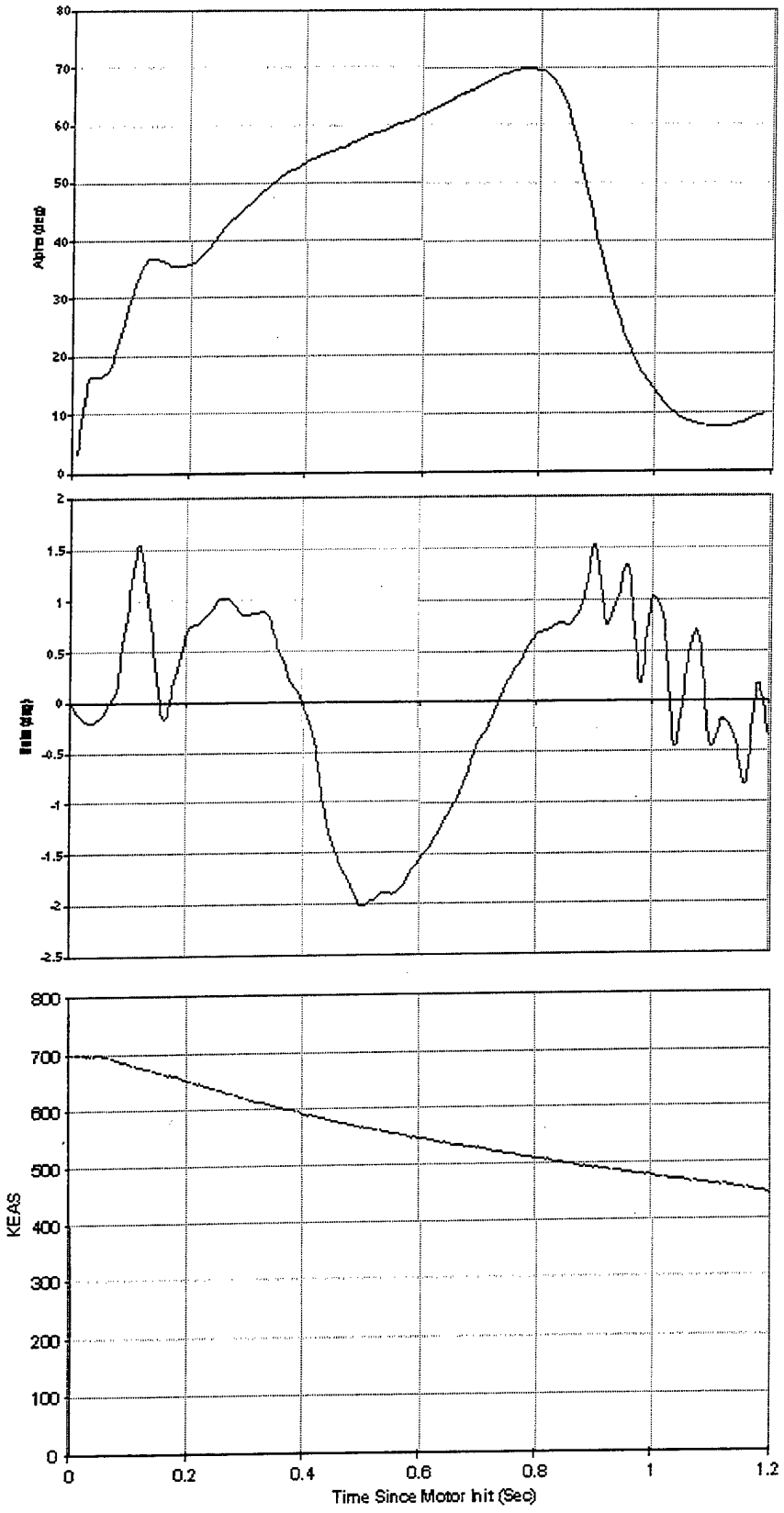

Figure 5-9 Sled Test #10 Seat Angles of Attack and Speed

5.2.5 *Demonstration Test Results - High Speed Protection Devices*

Of the high speed protection devices, the torso restraint, arm restraint and leg protection system were installed on every test, whereas the head protection system was installed on tests #4 and subsequent. The operation of each of the high speed protection devices is discussed in the following paragraphs:

5.2.5.1 *Torso Restraint*

The single-point torso harness did not appear to be as effective as anticipated in limiting lateral movement of the manikin in the adverse attitude tests where the harness has to provide restraint against adverse gravitational and windblast forces. Review of the situation indicates that the effectiveness of the harness was compromised by the approach of cinching up the harness several days prior to the test and by the use of a retraction process that was not adequately representative of what would be used in an operational system.

The torso single-point restraint harness used in the program was representative of the arrangement proposed for an operational seat, but relied on the tensioning of the inertia reel straps to cinch up the "X" configuration of straps. Normally, the inertia reel is actuated at the time that ejection is initiated but, in order to limit manikin movement during the sled acceleration period, the reel was cinched up when the manikin was installed in the seat. As mentioned previously, the inertia reels used in the program were modified such that they could be cinched up using nitrogen gas pressure. Initially, a pressure of 4,000 psi. was requested however, in tests 2, 3 and 4 the available pressure was 3,250, 2,500 and 2,100 psi. respectively. It was apparent from these tests that the torso restraint was not as effective as anticipated and the track was asked to provide a source of 5,000 to 6,000 psi. The situation did improve and tests 6 through 10 had pressures of 4,700, 4,800, 4,000, 4,500 and 5,000 psi. Despite this it is probable that, at the time of ejection, the harness tension was significantly less than at the time of cinch up. This assessment is based on the fact that the harness is cinched up several days prior to the test and the tendency for the tension to drop off with time would be aggravated by the handling movement and by the dynamic environment during sled acceleration. There is little doubt that the tension in the harness straps would be very significantly less than the tension that would be applied by the actuation of the inertia reel with the gas generator which typically retracts the reel with a peak pressure of 7,000 - 10,000 psi.

5.2.5.2 *Arm Restraint System Effectiveness*

The arm restraint system was deployed and cinched-up prior to each test and successfully restrained the arms in every test.

5.2.5.3 *Leg Protection System Effectiveness*

The manikin was installed in the seat with the seat pan fixed in the "legs raised" configuration and the leg restraint cuffs were cinched up at that time. The protection provided by these devices combined with the lateral supports for the legs and feet effectively restrained the legs in every test.

5.2.5.4 *Head Protection System Effectiveness*

The head protection system, consisting of the brim and lateral restraint straps, were installed in test 4 and subsequent tests. The head protection system was not effective in tests 4, 6, 7 and 8. In test 4 the brim inadvertently retracted as the seat exited the cockpit, while in tests 6 and 7 (325 KEAS and 20 degrees yaw), the lateral component of the windblast caused the head to move outside the restraint straps and beyond the influence of the brim. In test 8 (450 KEAS and 20 degrees yaw), the right side head restraint strap failed and the head again moved beyond the influence of the brim. In tests 9 and 10 (600 and 700 KEAS),the full effectiveness of the brim was not achieved because the gap between the brim and the helmet increased during the ejection. Nevertheless, in the SE tests, the neck loads recorded were significantly lower than would be expected without the head protection system. Also, it is important to note that, despite the degraded effectiveness of the head protection system, the helmet remained on the head in every test. The neck load data recorded in the tests correlates reasonably well with the wind tunnel data and, although the neck tensile load criterion was not met, this provides a basis for the position that the demonstration test data, in combination with the wind tunnel data, justify the position that the validity of the head protection concepts was successfully demonstrated in the program.

5.2.5.4.1 *Individual Test Results - Head Protection System*

A description of the operation of the head protection system in each of the last four tests is as follows:

Test #4 - In this test, at 325 KEAS with 20 degrees yaw, the head protection system was not effective because the brim retracted to the stowed position as the seat was exiting the cockpit. It was found that this could occur as a result of tension in the head restraint straps unloading the brim mechanism springs and allowing the release cotter pins to be vibrated out of the locking position. The cotter pins were wire-locked in the locking position for the subsequent tests.

Test #6 and 7 - In these tests, at 325 KEAS with 20 degrees of yaw, the head protection system was not effective due to the movement of the manikin's head. During the catapult stroke the manikin's head rotated forward and then, when the seat and manikin entered the airstream, the lateral component of the windblast caused the head to rotate sideways and move aft around the lateral

restraint straps and into a position where it was beyond the influence of the brim.

Test #8 - In this test, at 450 KEAS with 20 degrees yaw, the lateral restraint strap system failed, allowing the head to move laterally out of the influence of the brim. The failure occurred on the starboard side which would be loaded by the lateral component of the airblast due to the yawed attitude. It was concluded that the failure was caused by the tensioned nylon strap being cut by contact with the relatively sharp edge of the visor snap on the helmet. The profile of the neck tensile load indicates that the lateral restraint strap failed approximately 2.7 seconds prior to ejection initiation. Once this occurred, it appears that the lateral component of the airflow caused the head to be moved sideways out of the influence of the brim. The peak neck loads recorded on this test, 300 lb tension and 60 lb lateral, were of the magnitude that would be expected with no head protection system. It should be noted that the windscreen was not installed on the forebody for this test and therefore the helmet would be applying an increasing load on the lateral restraint strap as the sled was accelerated along the track. For test #9, measures were introduced to protect the straps.

Test #9 - In this test, at 600 KEAS, the peak neck tension and lateral loads were approximately 400 and 90 lb respectively. There were two anomalies. 1) the lateral restraint strap system on the port side failed at the anchor loop on the riser and 2) the distance between the brim and the helmet increased during the ejection. The forebody attitude for this test was straight and level and there is no indication that the failure of the lateral restraint strap system adversely affected the effectiveness of the head protection system. However, the photographic data indicates that the gap between the helmet and brim was significantly more than the intended gap of ~2.0 inches. It is difficult to assess what the actual gap was but data on the effect of gap on the neck tensile load, from the wind tunnel test program, indicates that the recorded loads are equivalent to a gap of the order of 5.3 inches.

It was postulated that the most probable cause of the failure of the lateral restraint strap system was that the strap may have been rigged too tightly during installation and a change in the rigging was made for test #10. Investigation of the spatial relationship between the helmet and the brim during the test, led to the conclusion that a major cause of the increase in the gap between the helmet and the brim was "billowing" of the fabric brim. For test #10, in an effort to reduce billowing, the configuration was revised to obtain a pre-test gap of ~ 0.75 inches. This is illustrated in Figure 5-10.

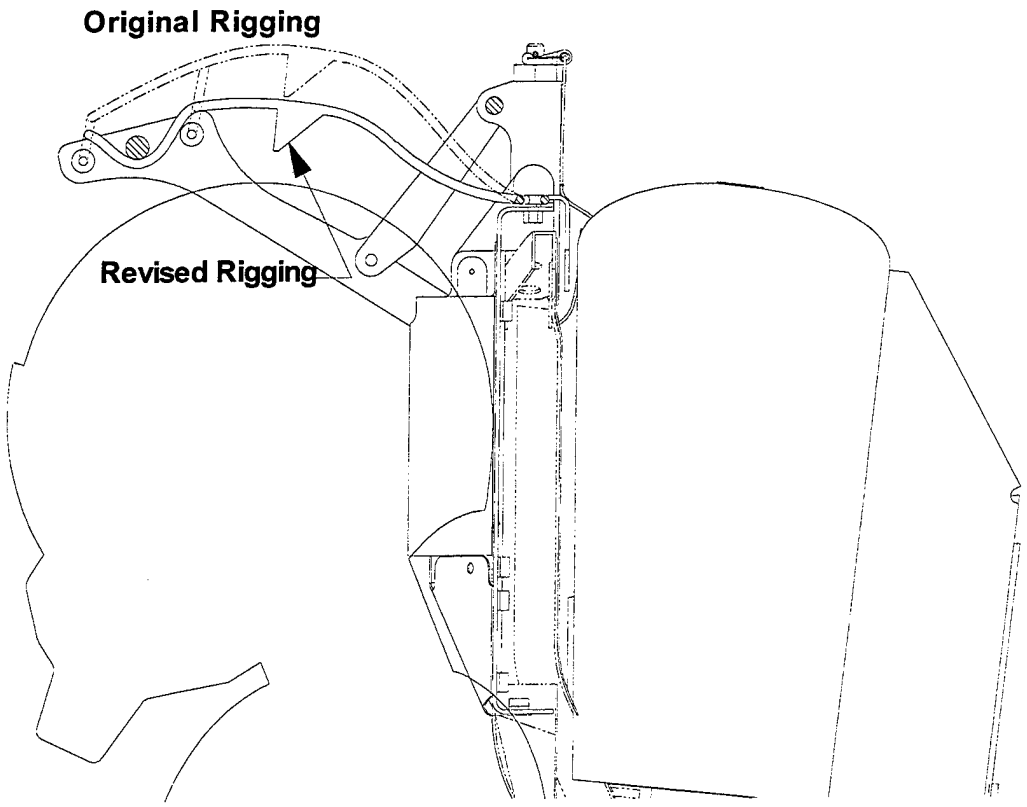

Figure 5-10 Brim - Revised Rigging

Test #10 - in this test, at 700 KEAS, the peak neck tension and lateral loads, were approximately 400 and 90 lb respectively, and the vertical load profile was very similar to that recorded in test #9. The lateral restraint straps withstood the loads but, despite the brim configuration change, the gap between the helmet and the brim again increased significantly during the ejection. Although an accurate measurement is not possible, it appears from the photographic records, Figure 5-11, that the gap was of the order of 4.0 inches. This would significantly affect the reduction in neck tensile force due to the brim. The photographic data also indicates that, while the increase in gap between the helmet and the brim during ejection may be partially due to billowing of the brim, it appears that a significant portion of the gap increase was due to the relative downward movement, or slump, of the ADAM manikin.

Figure 5-11 Seat Emerging from Cockpit in Test #10

5.2.5.4.2 *Head Protection System - Operation Under Yaw*

In test #7, the lateral restraint straps did not restrain the manikin's head because the head rotated forward in reaction to the catapult force and, when it was subsequently rotated aft by the airblast, the yaw angle caused the head to translate laterally beyond the restraint straps. Although there may have been mitigating circumstances, such as the torso restraint not being fully effective, it has to be recognized that the lateral restraint straps have a limited lateral capture area which will not be adequate under extreme circumstances.

5.2.5.4.3 *Head Protection System - Neck Load Evaluation*

The neck load evaluation criteria were that the lateral and tensile loads should not exceed 250 and 300 lb., respectively. In the 600 and 700 KEAS tests the lateral loads were within the criteria but the tensile loads, at approximately 400 lb., exceeded the criteria. The photographic evidence indicates that the brim would not be as effective as intended because the gap between the helmet and the brim increased significantly during the ejection, apparently due to a combination of brim distortion and manikin slump. The wind tunnel testing of the brim system provided data on the relationship between the helmet-brim gap and tensile load and these data, together with the magnitude of the loads which could be expected at these speeds without the brim, are

presented in Table 5-18. As indicated in the table, the neck tensile loads measured in the 600 and 700 KEAS tests are significantly lower than the loads that could be expected without a brim. Based on the wind tunnel data, the loads recorded in tests #9 and 10 correspond to gaps of 5.3 and 4.5 inches respectively. On this basis, it appears to be relatively certain that a brim configuration that achieved a gap closer to the desired 2.0 inches, would control the neck tensile loads to below the 300 lb criterion.

Table 5-18 Neck Tensile Load

Test	Speed	Peak Measured Tensile Load	Gap Corresponding to Measured Load	Expected Load with 2.0 inch Gap
9	600 KEAS	~400 lbs	5.3 inches	120 lbs
10	700 KEAS	~400 lbs	4.5 inches	150 lbs

6.0 OPERATIONAL FOURTH GENERATION SYSTEM

The fourth generation program demonstrated the successful operation of flight control and advanced high speed protection devices, which are the new technologies required to support the development of an operational fourth generation system. However, the system was designed as a demonstration system and was not configured to be a prototype of an operational system. As described earlier, a primary reason for this was to concentrate the program efforts on the design, development and demonstration of the new technologies and to avoid the effort, expense and risk associated with the design and development of hardware to perform functions which could be performed by existing hardware. To some extent, the approach of minimizing design and development effort and risk was also applied to the new technologies, particularly in the case of the flight control system. This is reflected in the fact that while the flight control system used in the demonstration program had performance which was representative of an operational system, other characteristics, such as redundancy, were not. This approach was justified on the basis that the design of the operational system would not be based on 1992 avionics but would be based on the significantly more advanced hardware which would be available at that time. Also, it was predicted that a fourth generation seat may well be volume and/or weight limited, as the capability tends to be a function of the amount of propulsion fuel that the weapon system designer is prepared to allocate. In this environment, the physical characteristics and degree of integration of the flight control components may be critical to the assembly of an efficient system and therefore they may well be tailored to optimize volume and weight. The purpose of this section is to discuss the implementation of the technologies which were demonstrated in this program with regard to an operational fourth generation system.

During the fourth generation program, an initial design of a fourth generation system was created. This was done to support the propulsion trade study effort and considerable effort was made to ensure that the design was feasible. As stated above, the capability of a fourth generation seat is largely a function of the weight and volume of the fuel that can be accommodated and therefore it is important to establish weight and volume constraints so that the capability is similarly realistic. The weight of the operational seat was limited to 250 lb. and the volume issue was addressed by specifying that the seat be compatible with the existing F-22 cockpit accommodations. This initial design of an operational seat is still considered to be a valid point of departure. The following is a description of the operational system including comparisons with the demonstration system and the identification of issues associated with various features of the operational system.

6.1 General Arrangement

The general arrangement of the operational seat is illustrated in figure 6-1 and a weight breakdown is shown in table 6-1. The weight for the propulsion system is 74 lb. which comprises 51.5 lb. for hardware and 22.5 lb. for propellant. More recent estimates result in a hardware weight of 30.0 lb. and this poses a choice between having a lighter system or having more fuel. The advantage of having more fuel is that it increases the range of low altitude, adverse attitude conditions for which a ground avoidance trajectory can be implemented.

An important feature of the operational configuration is the fact that the seat uses controllable propulsion for stabilization and, when the propulsion is about to burn out, either a drogue or recovery parachute is deployed, depending on the speed and altitude conditions. A task in the program was to investigate the use of fins or booms to augment the stability function and thereby reduce the capability required of the propulsion system. The conclusion then and now, is that the combination of controllable propulsion and drogue parachute provides the most effective combination of characteristics for enabling a "smart" controller to optimize the operation of the system over the entire escape envelope. It appears that fins or booms would only become candidates if it was not possible to provide a propulsion system that would meet the high speed stabilization requirements.

Another important feature of the configuration is that seat adjustment is provided by means of a moveable bucket. For a fourth generation seat, this approach, as opposed to that of raising and lowering the entire seat, is selected because it provides more space for the propulsion system and fuel and because it facilitates the accommodation of crewmembers of very small stature. In a seat with a moveable bucket, the fixed aft portion of the seat can be longer, and therefore have more volume, than a comparable single-piece seat. In the proposed operational design, the propulsion system occupies the major portion of the seat back and any reduction in seat length would require a decrease in the amount of fuel. This, in turn, would cause a reduction in escape envelope capability. Future seats will be required to accommodate an increased range of crewmember sizes and this will probably introduce a requirement for increased vertical travel. With a moveable bucket seat, the upper portion of the seat is fixed whereas, with a single-piece seat, upward adjustment raises the top of the seat relative to the aircraft canopy. The potential problem with a single-piece seat, is that the additional upward travel required to accommodate crewmembers of very small stature may be unacceptable because of the additional space required beneath the canopy.

Table 6-1 Operational Weight Estimates

Major Component	Weight
Seat Back Structure and Mechanisms	33.0
Seat Bucket Structure and Mechanisms	38.9
Ejection Catapult (seat mounted portion)	3.5
Drogue Parachute	10.0
Main Recovery Parachute	24.9
Survival Kit and Oxygen	31.6
Flight Computer Suite	11.9
Life Protection Devices	19.0
Propulsion	74.0
Miscellaneous Fittings	3.2
Total System Weight	**250.0 lbs**

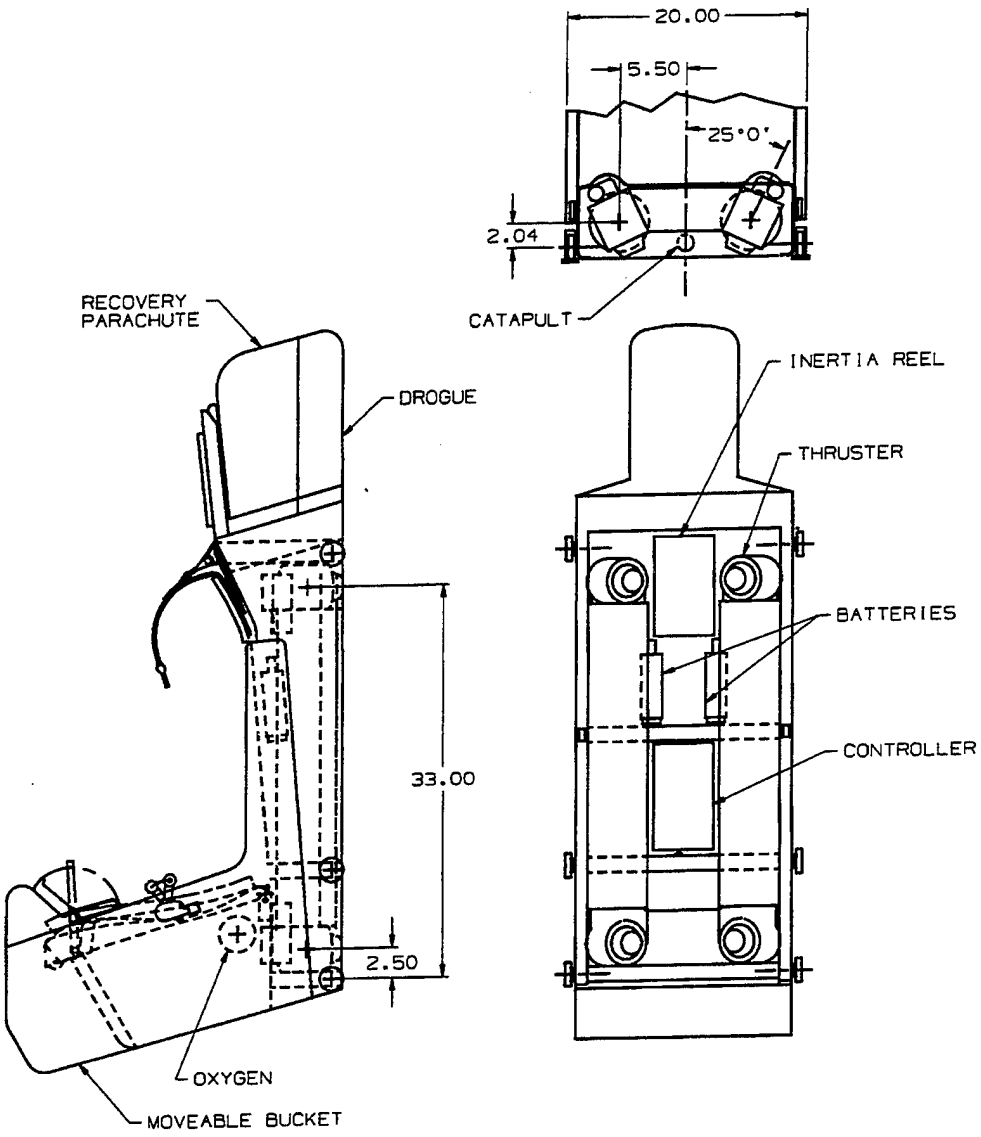

Figure 6-1 Operational Configuration

A second important feature is the fact that the seat uses controllable propulsion for stabilization and, when the propulsion is about to burn out, either a drogue or recovery parachute is deployed, depending on the speed and altitude conditions. A task in the program was to investigate the use of fins or booms to augment the stability function and thereby reduce the capability required of the propulsion system. The conclusion then and now, is that the combination of controllable propulsion and drogue parachute provides the most effective combination of characteristics for enabling a "smart" controller to optimize the operation of the system over the entire escape envelope. It appears that fins or booms would only become candidates if it was not

possible to provide a propulsion system that would meet the high speed stabilization requirements.

6.2 Conventional Subsystems

With the exception of the "new technologies", the fourth generation operational seat is assumed to utilize current technology subsystems and therefore these, such as the drogue and the recovery parachute, can be assumed to be similar to those used in the demonstration seat.

6.3 Controllable Propulsion System

The controllable propulsion envisioned for an operational seat would be a development of the demonstration system which would incorporate some important physical and operational improvements. As indicated in the seat general arrangement, a "U" shaped motor, with the rocket grains in the upright legs and the cross tube used for gas transfer, is envisaged for the operational configuration. Relative to the demonstration system, the most significant characteristics of the operational system are:

- The motor would have two operating pressures and thrust levels so that the thrust level most appropriate to the emergency conditions could be selected. The high thrust value would be derived from the requirements for stabilization at maximum speed, while the low thrust value would be appropriate for other circumstances, such as adverse attitude cases, where a significant amount of maneuvering is required.

- The propellant would be extinguishable. This feature will allow a controlled transition from propulsion to parachutes. Extinguishable propellant, pintle nozzle rocket motors have been evaluated for other non-escape applications, but were not a requirement for this demonstration program.

- The motor would be "fail-safe" such that if electrical power to the pintle actuators or the controllers is lost, the pintles would move to their initial position and provide a predetermined thrust and thrust vector.

6.4 Operational Avionics

Table 6-2 Demonstration vs. Operational Configuration

System	Demonstration	Operational	Issues
Flight Control (Avionics)	Single Channel	Redundant	Redundancy Architecture Commercial Parts Reliability / Environments
Interface	1553 to Ground Controller	TBD to A/C	Autonomy
Flight Computer	NDI JDAM 24 Mhz M68040	TBD	Throughput
IMU	NDI Honeywell HG1700 (JDAM) Navigation Quality RLG	Low Cost Flight Control Quality Accelerometers and Gyros	Cost, Accuracy
Pyro Initiation Modules	NDI JDAM Single Bridgewire	Redundant Bridgewire Capability	
Power Conditioning	NDI Modular Devices Hybrid Module (JDAM)	TBD	
Power	NDI Eagle Pitch 12198 28VDC thermal batteries	Thermal batteries Transfer keepup source TBD	Rise Time / Instant On
Wire Harness	Single Channel	Redundant	
Data Recorder	NDI EPS Solid State Data Recorder	TBD	Data buffering
GPS	None	TBD	A/C autonomy

The demonstration avionics subsystem provides most of the functions required for an operational system. Table 6-2 summarizes the demonstration configuration and identifies a potential operational configuration and associated issues. The key issues in the evolution of these avionics to an operational system are: redundancy architecture, initialization and aircraft interface, and final component / subsystem selection. Details of the component / subsystem requirements must be identified through a complete design trade study of an operational system. Candidate approaches and technologies, along with issues that must be addressed, are identified below:

Concept: A potential avionics concept for an operational escape system is illustrated in Figure 6-2. Functionally, it is similar to the demonstration avionics with the potential addition of a Global Positioning System GPS receiver. The aircraft will download initialization data to the escape system computer through the 1553 interface, initialize the GCU, and provide a position and velocity reference until GPS acquisition is complete. Following acquisition, the GPS receiver will provide the primary position and velocity reference for the flight controller. During flight, the aircraft will provide air speed for estimating wind velocity, radar altitude, and backup navigation data over the avionics bus.

The flight controller may operate in a continuous transfer alignment mode receiving position and velocity aiding from either the GPS receiver (primary)

or the aircraft system (back up). The escape system computer will use radar altitude from the avionics bus when that is available. If required, the system can estimate altitude Above Ground Level (AGL) by differencing the inertial with preloaded Digital Terrain Elevation Database (DTED) altitudes. It will maintain an estimate of wind velocity by differencing its own inertial velocity and the aircraft air speed. If air speed becomes unavailable, the computer will employ a fading memory using the last valid estimate of wind velocity. Data from the Ground Proximity Warning System (GPWS), available on the avionics bus, will be used to monitor aircraft sensor validity and to support guidance mode decisions.

During an escape sequence, the navigation mode transitions from transfer alignment to pure inertial navigation. The proper guidance mode is selected on the basis of inertial velocity (speed and sink rate), inertial attitude, and altitude AGL. Guidance commands are generated using inertial attitude (low speed) or estimated AoA (high speed). Autopilot rate and acceleration feedback is obtained directly from the IMU.

Interface issues associated with each of the candidate aircraft must be considered on a case by case basis. As a minimum, power and avionics bus interfaces will be required. On those aircraft for which a seat-mounted GPS antenna is not feasible, access to the IF signal output from the aircraft antenna electronics box (AE1) will be required.

Reliability can be addressed through the proper selection of technology and use of redundancy where feasible. The system should be designed so that it maintains a third generation capability in the event circumstances preclude a fourth generation escape.

Architecture: Current aircraft (F-15, F-18) flight control systems employ quad-redundant architectures to ensure integrity of the flight control system and achieve the desired level of reliability. Separate, redundant control and instrumentation channels are used. The processors are tied together using cross channel data link or other interface approaches and voting is used to develop an integrated control solution. If a channel/component fails, that channel/component is ignored. Future aircraft systems are evaluating tri-channel systems to achieve the same level of reliability. Figure 6-2 illustrates redundant channel seat avionics architecture with a backup sequencer. The number of redundant channels needs to be evaluated versus the reliability requirements. The backup sequencer provides a final fail-safe control for the system. The backup sequencer may eliminate the need for redundant flight computers, IMUs, etc. Configuration and redundant interface of the motor controllers needs to be addressed in more detail.

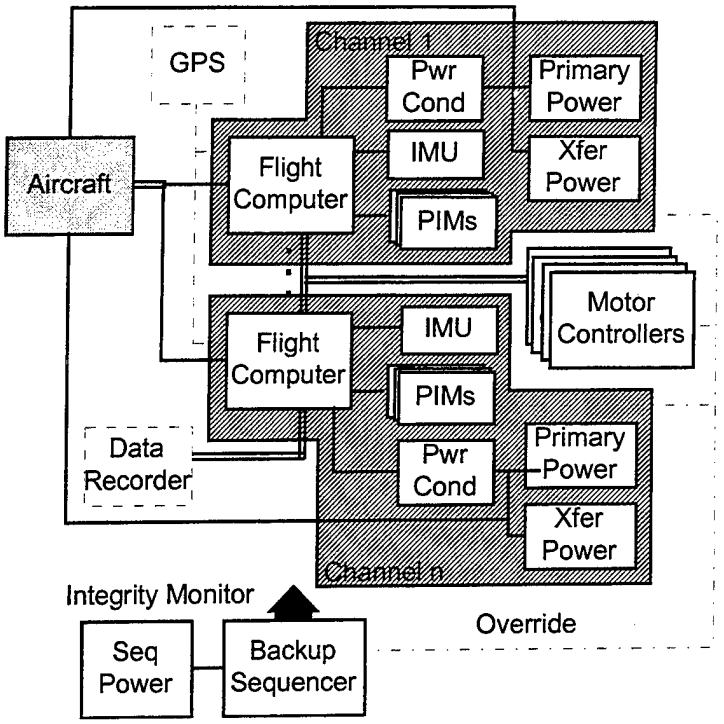

Figure 6-2 Avionics Concept for Operational System

An alternate architecture, illustrated in Figure 6-3 provides an integrated approach to redundancy versus separate channels. In this architecture, each flight computer is tied to each instrument and actuation device. The number of each component / subsystem can be optimized based on the reliability of the device. This approach may provide lower cost by requiring fewer hardware components but complicates the interfaces and voting logic.

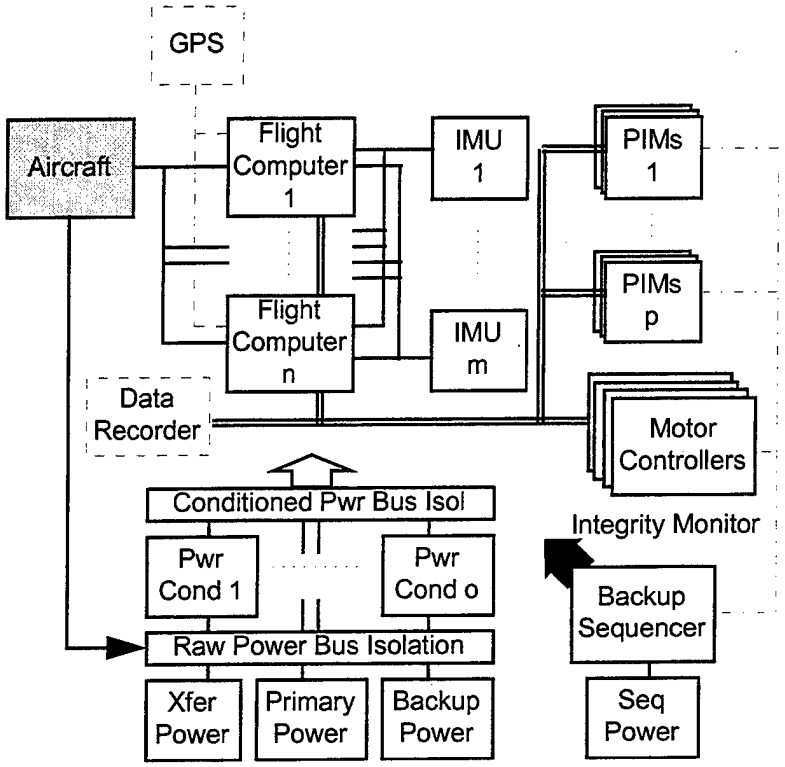

Figure 6-3 Integrated Redundancy Approach

Initialization: The guidance and control algorithms drive the seat trajectory based on knowledge of attitude, angles of attack, altitude and velocity. The IMU provides measurements of acceleration and attitude rates to maintain knowledge of these parameters from a set of initial conditions. Those initial conditions are the aircraft attitude, angles of attack, velocity, altitude and acceleration at ejection. Key initialization issues are validity of the aircraft data at time of ejection and operating life of the seat avionics system.

The ejection system avionics needs to operate for a few seconds. Lower acquisition and logistics costs can be achieved by operating the seat avionics only during the ejection event, but system start-up time is an issue. This is the current ACES II approach.

The aircraft data can not be assumed valid at the time of ejection since the aircraft data may be degraded by the cause of the emergency. Independent knowledge of the aircraft altitude, inertial velocity and possibly attitude could be maintained by a seat mounted GPS system without powering the flight computer or IMU. Requirements for angle of attack need to be addressed. Attitude from GPS requires multiple antennas and accuracy is dependent on separation of these antennas. The GPS could be tied into the aircraft navigation data as secondary data source. Alternatively, one channel of the IMU / Flight Computer could be powered along with the GPS. This would

provide a full navigation solution to the seat. This hardware channel could be configured as a line replaceable unit to minimize logistics costs. Since attitude alignment accuracy requirements are modest, continuous alignment of the seat may not be required for accuracy purposes. Accuracy of the initial sideslip (β) angle may be an issue for high-speed ejections.

BIT Test: Complete test of the seat control system integrity is needed as part of aircraft preflight checks and for maintenance. The requirement and utility for subsequent in-flight BIT tests should be evaluated.

A/C Data Interface: Aircraft data needed for seat initialization is available from the aircraft navigation and flight control computers. Data would be transmitted across the 1553 data bus. Required seat data is similar to transfer alignment messages that are typically provided to weapons. Reliability of the data must be addressed given that the aircraft is in a casualty mode.

Flight Computer: The primary requirements of the flight computer are sufficient throughput and memory to accommodate the seat control functions. The 24 MHz 68040 used for the demonstration system is adequate, but obsolete. Commercially available processors will make the flight computer performance a non-issue. Use of an existing aircraft or weapon flight computer, as was done for the demonstration system, will help minimize software development for the operational system

Guidance & Control Algorithms: The guidance logic has been optimized for the demonstration sled test conditions. Additional simulation and analysis is required to extend the guidance logic to the entire escape envelope. Likewise, the autopilot used fixed gains for the flight test program. Each attitude channel received equal priority. Previous versions of the autopilot included optimized gain schedules based on altitude, speed and angle-of-attack derived from Boeing's AUTOGAIN tool. Alternative autopilot structures may be considered to increase response and robustness at certain flight conditions. The demonstration autopilot bandwidth was approximately 15 Hz with a 300 Hz command rate. The operational bandwidth should probably be slightly higher (20 Hz). The command rate may be reduced to preserve throughput.

The primary autopilot issue is the mixing logic when the thrust commands are saturated. The current logic proportionally ratios each thrust command to preserve the moment direction if any thruster is commanded beyond the maximum 2500 lb. thrust limit. Linear programming and other approaches that prioritize the moment direction based on flight condition should be considered.

The motor control algorithm developed by Aerojet, needs to be further refined and a complete stability analysis conducted. Demonstration test #6

demonstrated that the motor control algorithm did not properly control motor pressure independently of the autopilot commands.

IMU: IMUs fall into two classes of performance and cost: navigation quality and flight control quality. Since the seat time of flight is short and attitude accuracy is not critical, flight control quality instruments are preferred. Micromachined IMUs, available in the 2001-2003 time frame, promise to provide the low cost, rugged construction needed for an operational seat. The IMU must be operating prior to seat first motion to properly track the seat trajectory. Typical startup times of 1 second need to be addressed to meet the rapid startup requirement for an operational seat. Bandwidth of 50-100 Hz with good roll-off of higher frequencies is desired. An analog filter is desired to roll-off the high frequencies to alleviate any aliasing issues. Noise characteristics must be considered but should not be a significant issue. Discrete sensors versus an IMU may be a lower cost option. Three rate gyros are required to maintain knowledge of attitude and three accelerometers are required to maintain knowledge of velocity and angles of attack.

GPS: Need for a GPS receiver must be addressed in terms of the overall architecture trade study. GPS will provide an independent means of position, velocity and, potentially, attitude. Location of the GPS antenna and effect of the canopy on GPS reception will be issues. Attitude determination will require multiple antennas and attitude accuracy will be dependent on antenna separation length. Increased maintenance will be required since the GPS will be operating continuously. Integration with the Combat Survivor Evader Locator (CSEL) GPS receiver, currently in development, should be addressed.

Pyro Initiation Modules: The pyro initiation circuits need to be capable of meeting the squib all fire requirement. The power source must be capable of generating the required currents without significant voltage drop. This was an issue with the rechargeable batteries in the demonstration system.

Motor Controllers: The motor controllers drive the motor pintles based on the commands from the flight computer. The controllers used in the demonstration system had an analog interface, requiring an analog output module in the flight computer. A digital (RS-422) interface may be desired. The controllers should be designed to retract the pintles if no command is present or the interface is lost (no connection).

Backup Sequencer: A backup sequencer may be desired as a final fail-safe measure. It may also reduce or eliminate the need for redundant flight control channels. The sequencer may require the addition of monitoring circuits / messages to assess the health of the primary seat flight control system. This will include power bus monitors, BIT status monitoring, actuator monitoring, etc. The backup sequencer requires an autonomous power source with backup

from the primary power source. The sequencer could be implemented with separate PIMs or use the primary PIMs to sequence parachutes and other events. Override of the pintle control actuators is not easily implemented and requires significant design trade studies. Parachute and other discrete events could be accomplished by sequencing those events at a maximum fail-safe time. This may eliminate some integrity monitoring requirements. The backup sequence time could be fixed or based on initial ejection conditions if validity of those conditions can be ensured.

Power: Thermal batteries are traditional power sources that provide high reliability, long storage life and good environmental robustness. Rise time needs to be minimized to alleviate transfer power requirements. A rechargeable power source may be a viable alternative as it would eliminate the transfer power requirement and allow constant integrity monitoring.

Transfer Power: The transfer power subsystem is required to provide seat power prior until the primary power source is energized. Sizing and maintenance of the transfer power source are the primary issues. Size limits will preclude the system from operating for an indefinite period without aircraft power. A rechargeable source is probably the only instant on system. Battery size to accommodate the short duration transition between start of the ejection event and full power from the primary power source should not be an issue.

Interconnect: Wire harness failures subsequent to seat installation occurred in the demonstration program. The harness should be fully redundant, possibly including redundant connectors to each component.

Data Recorder: An on-seat recorder may be desired to assist in post ejection investigations. The demonstration system data recorder provided quality recording of critical flight parameters for all ejection sled tests. Non-volatile (FLASH, EEPROM), non-buffered recording at the maximum rate possible is desired for complete analysis of system performance.

6.5 High Speed Protection Devices

For an operational seat, it appears that the high speed protection devices selected and demonstrated in this program would be satisfactory candidates.

6.5.1 *Torso Restraint*

Good torso restraint is required for an operational fourth generation seat and the system used must have the capability of being cinched up automatically for ejection such that both the crewmembers shoulders and hips are pinned to the seat. The approach selected for the demonstration program appears to be an excellent concept but, although a considerable amount of development work was done, there are still many details to be finalized. Integration into the

seat and the cinch up of the lower straps are design challenges which cannot be fully resolved until the configuration of the seat system is being established.

6.5.2 *Arm Restraint*

The system used in the demonstration program was based on that developed for the ACES II seat in the F-22 aircraft. It has the advantages of having minimal encumbrance and being almost entirely mounted on the seat. This system, or an equivalent, should be satisfactory for an operational system.

6.5.3 *Leg Protection*

The approach of raising the legs and providing comprehensive support and restraint appears to be an excellent one. The method of raising the legs will have to be decided. This is a feature which will have a significant impact on the design of the system and alternative concepts should be defined in detail before a selection is made.

6.5.4 *Head Protection*

Head protection is perhaps the most difficult challenge for the fourth generation system. The brim concept effectively reduced the tensile neck loads in the demonstration program and it appears that this is a viable solution. The issue of slump has to be addressed. A moveable bucket seat will help to minimize the range of positions the head is likely to be in but, nevertheless, it appears that some approach that will position the brim relative to the head may be needed.

Clearly, the brim will not be effective if the crewmember's head in out of the brim's influence, which can happen in certain circumstances. However, the neck loads and helmet retention successes in the 600 and 700 KEAS demonstration tests are significant achievements. It can be argued that head excursions may be significantly reduced if the torso is more effectively restrained. Also, it may be that head movement can be related to adverse attitudes which are normally associated with speeds at which neck loads and helmet loss are not issues.

The use of the lateral restraint straps concept on an operational seat needs to be examined. The approach of anchoring the straps to the parachute riser is a good concept that successfully avoids the dangers associated with restraining the head independently of the torso. However, in test #7 it was illustrated that if the head rotates forward under the influence of the catapult then, when it subsequently rotates aft, it can either move within the straps or around them. The straps, therefore, may cause the head to move further sideways than would otherwise be the case. This does not appear to be an acceptable characteristic.

7.0 LESSONS LEARNED

Lessons learned have also been included in the text in section 5.0 where the related circumstances are described. The following is a discussion of the important lessons:

1. Use actual parts for test

In demonstration test #1, the squibs for the seat pyros were not fired and the seat and manikin were not recovered, because a mistake was made regarding the function of the squib connector pins. Several tests had been conducted which involved firing squibs but, for a variety of reasons, the actual squib was not used in any of these tests and the error was not detected until the correct squibs were used.

2. Establish dynamic environment for avionic hardware

The most serious problem in the program was the failure of the GCU because it could not withstand the dynamic environment. The primary problem was caused by shock resulting from seat-guide rail tip-off dynamics. Another problem was caused by shock due to a loose connector striking the IMU. In future programs, the dynamic environment for avionic components should be determined by test and the mechanical robustness of the avionics should be emphasized.

3. Keep seat and sled systems apart

In every ejection test program there are electrical systems for the seat and for the sled. These should not be commingled.

4. Investigate potential issues

Late in the program several issues arose that should have been the subject of earlier study. One was the proximity effects of the very large windscreen when the forebody was yawed. A second was the effect of the impingement of the upper rocket plumes with regard to the flow field around the seat and on the thrust vector and a third was the effect of the rocket plumes on the aerodynamic characteristics of the seats. Fortunately, the impingement and plume effects had previously been examined in a Computational Fluid Dynamics (CFD) study, reference 18, and data from this source helped to permit a more accurate analysis.

5. Don't degrade operation for test purposes

The practice of cinching up the restraint harness several days prior to the test using relatively low pressure gas is not a satisfactory process and some means must be found to satisfy the pre-ejection and ejection requirements.

8.0 CONCLUSIONS AND RECOMMENDATIONS

Based on a review of the demonstration tests, the broad conclusion that can be made is that the demonstration system performed well and, indeed, demonstrated the characteristics which will enable a fourth generation system to achieve the desired improvements in escape envelope capability.

Although the test series included failures which caused no-tests and partial no-tests, the failures were incidental to the main technical thrust of the program and did not reflect adversely on the potential of the concepts being demonstrated.

In the six successful tests and in the two partial no-tests, the demonstration flight control system operated correctly in response to the available inputs and provided data that allows every aspect of the system operation to be analyzed and verified.

The demonstration system successfully executed the "upward seeking" maneuvers in the adverse attitude cases and did so with such authority that in the most demanding case, 450 KEAS at 20 degrees yaw, the seat yaw was not allowed to exceed the initial angle of 20 degrees.

The demonstration system successfully controlled the motion of the seat in the high speed tests to provide stability such that in the most demanding 700 KEAS test, seat yaw was held to $\pm$ 2 degrees.

The restraint harness and limb restraint systems performed successfully in the demonstration program and provided a valid basis for future operational applications.

The head protection brim successfully produced reduced neck loads and can no doubt be credited with the successful retention of the helmet at 700 KEAS. Although the neck tensile criterion of 300 lb. was exceeded, the available data indicates that if the brim can be located to compensate for slump, then this device should be capable of meeting the criterion without difficulty.

The significant aspect of the lateral head restraint straps is that they did not capture the head in the ejection at 325 KEAS and 20 degrees yaw. Further evaluation of this approach is required.

The program successfully demonstrated that the selected technologies had the capability to recover a crewmember from extreme adverse attitude conditions and from extremely high speed conditions with such control and precision that the loads on the crewmember, as indicated by the demonstrated MDRC, promise to be in the range where only minimal injury can be anticipated.

The program also demonstrated that the capabilities of the technologies are not only reflected in flight control and stability but in the ability to precisely align the seat and crewman to accept the drogue and recovery parachute loads in the optimum manner.

On the basis of this demonstration program it is recommended that a follow on program be initiated to design and develop an operational fourth generation ejection seat which will incorporate the demonstrated technologies and make these advanced capabilities available to accomplish the following objectives:

1) to improve the probability of successful escape under the high risk low altitude, adverse attitude conditions and the equally high risk high speed conditions and,

2) to reduce the risk of injury in every ejection.

9.0 REFERENCES

1. James Schoen, Fourth Generation Escape System Technologies Demonstration Phase I Final Report; 28 February 1997, Report No. MDC 97K7016, AF Contract No. F33615-92-C-2290, CDRL Item A009

2. Fred Duskin, Fourth Generation Escape System Technologies Demonstration Drogue Bridle Burn Test Report, Revision A DTD 22 November 1996; 29 August 1995, Report No. MDC 95K0192, AF Contract No. F33615-92-C-2290, CDRL Item A008

3. Fred Duskin, Fourth Generation Escape System Technologies Demonstration Program Phase II Initial Test Report; 14 February 1997, Report No. MDC 97K7017, AF Contract No. F33615-92-C-2290, CDRL Item A001

4. Joe D'Allura, Fourth Generation Escape System Technologies Demonstration Low Speed Wind Tunnel Test Report; 28 March 1996, Report No. MDC 96K0201, AF Contract No. F33615-92-C-2290, CDRL Item A009

5. Joe D'Allura, Fourth Generation Escape System Technologies Demonstration Transonic Speed Wind Tunnel Test Report; 22 December 1996, Report No. MDC 96K0228, AF Contract No. F33615-92-C-2290, CDRL Item A001

6. Joe D'Allura, Fourth Generation Escape System Technologies Demonstration Structural Windblast Test; 5 March 1997, Report No. MDC 97K0104, AF Contract No. F33615-92-C-2290, CDRL Item A003

7. James W. Brooks, Fourth Generation Escape System Technologies Demonstration Avionics Initial Test Report; 31 October 1996, Report No. MDC 96P0048, AF Contract No. F33615-92-C-2290, CDRL Item A008

8. James Schoen, Fourth Generation Escape System Technologies Demonstration Ejection Sled Test 2 Report; 11 April 1997, Report No. MDC 97K7036, AF Contract No. F33615-92-C-2290, CDRL Item A008

9. James Schoen, Fourth Generation Escape System Technologies Demonstration Ejection Sled Test 3 Report; 20 June 1997, Report No. MDC 97K0123, AF Contract No. F33615-92-C-2290, CDRL Item A008

10. P. Jackson, Fourth Generation Escape System Technologies Demonstration Ejection Sled Test 1 Report; 15 January 1997, Report No. MDC 97K7013, AF Contract No. F33615-92-C-2290, CDRL Item A008

11. James Schoen, Fourth Generation Escape System Technologies Demonstration Ejection Sled Test 4 Report; 17 September 1997, Report No. MDC 97K0124, AF Contract No. F33615-92-C-2290, CDRL Item A008

12. James Schoen, Fourth Generation Escape System Technologies Demonstration Ejection Sled Test 5 Report, Revision A DTD 18 June 1997; 4 June 1997, Report No. MDC 97K0127, AF Contract No. F33615-92-C-2290, CDRL Item A008

13. James Schoen, Fourth Generation Escape System Technologies Demonstration Ejection Sled Test 6 Report; 29 September 1997, Report No. MDC 97K0128, AF Contract No. F33615-92-C-2290, CDRL Item A008

14. James Schoen, Fourth Generation Escape System Technologies Demonstration Ejection Sled Test 7 Report; 3 October 1997, Report No. MDC 97K0158, AF Contract No. F33615-92-C-2290, CDRL Item A008

15. James Schoen, Fourth Generation Escape System Technologies Demonstration Ejection Sled Test 8 Report; 10 October 1997, Report No. MDC 97K0157, AF Contract No. F33615-92-C-2290, CDRL Item A008

16. James Schoen, Fourth Generation Escape System Technologies Demonstration Ejection Sled Test 9 Report; 14 November 1997, Report No. MDC 97K0156, AF Contract No. F33615-92-C-2290, CDRL Item A008

17. P. Jackson, Fourth Generation Escape System Technologies Demonstration Ejection Sled Test 10 Report; 12 December 1997, Report No. MDC 97K0155, AF Contract No. F33615-92-C-2290, CDRL Item A008

18. G. Rock, S. D. Habchi, T. J. Marquette, Numerical Simulation of Controllable Propulsion for Advanced Escape Systems; 23-25 June 1997, Report No. AIAA-97-2254, AIAA Applied Aerodynamics Conference, Atlanta, GA

APPENDIX A - MDRC Definition.

APPENDIX A

MDRC (Multi-Axial Dynamic Response Criteria)

As stated in the report, Paragraphs 1.0 and 5.2.2, the MDRC is the criteria used to judge the severity of the accelerations imposed on the seat occupant. The purpose of this appendix is to provide a brief description of MDRC and to describe the process that was used for calculating the MDRC during this program. The development of the MDRC approach is described in AGARD Conference Proceedings No. 472, Implications of Advanced Technologies for Air and Spacecraft Escape, in a technical paper titled " Development of Acceleration Exposure Limits for Advanced Escape Systems", by James W. Brinkley and Lawerence J. Specker, Armstrong Laboratory, Wright-Patterson AFB, Dayton, Ohio. The AGARD paper refers to the "injury-risk criterion". The injury-risk criterion and the MDRC are equivalent.

The MDRC approach to quantifying the severity of the accelerations imposed on the seat occupant uses simple lumped-parameter models to evaluate the effects of linear acceleration components acting in the orthogonal axes of the body. The models are based on the dynamic characteristics of the human body and the accelerations are considered to be most injurious when acting at the "critical point", which is defined as the center of mass of the upper torso.

In this program, the sensors which provided the data used to calculate the MDRC consisted of accelerometers and rate gyros which recorded these parameters in three axes. The sensors were located in the IMU which was installed in the forward portion of the seat bucket. Figure A-1 shows the relationship of the critical point to the seat reference point and the relationship of the sensors to the critical point in the x and z axes. In the y axis, the IMU was located 3.7 inches to the right of the seat centerline.

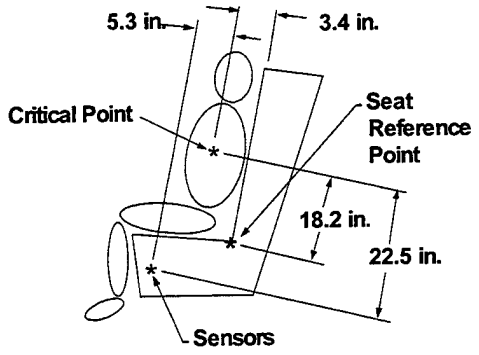

Figure A-1 Critical Point and Sensor Location

To calculate the MDRC, the accelerometer-time histories are first rotated to provide the acceleration component-time histories in the three orthogonal axes. In this system, the z-axis is parallel to the spine and the x-axis is forward and aft. The next step in the process is to transform these acceleration-time histories to the critical point using the angular acceleration-time histories which are obtained by differentiating the angular rates recorded by the rate gyros.

The transformation formulae used are:

$$\ddot{S}_x = A_x + D_y(\omega_x \omega_y - \alpha_z) - D_x(\omega_y^2 + \omega_z^2) + D_z(\omega_z \omega_x + \alpha_y)$$
$$\ddot{S}_y = A_y + D_z(\omega_y \omega_z - \alpha_x) - D_y(\omega_z^2 + \omega_x^2) + D_x(\omega_x \omega_y + \alpha_z)$$
$$\ddot{S}_z = A_z + D_x(\omega_z \omega_x - \alpha_y) - D_z(\omega_x^2 + \omega_y^2) + D_y(\omega_y \omega_z + \alpha_x)$$

Where:

- $\ddot{S}$ is the acceleration component along the pertinent axis acting at the critical point (ft/sec^2).
- A is the linear acceleration in the pertinent axis (ft/sec^2).
- D is the distance between the sensor and the critical point in the pertinent axis (ft).
- ω is the angular rotation rate in the pertinent axis (rad/sec).
- α is the angular acceleration in the pertinent axis (rad/sec^2)

Each of the transformed acceleration-time histories is then used in a second order equation:

$$\ddot{\delta} + 2\zeta\omega_n\dot{\delta} + \omega_n^2\delta = \ddot{S}$$

Where:

- $\ddot{\delta}$ is the acceleration of the dynamic response model mass relative to the critical point acceleration (ft/sec^2).
- $\dot{\delta}$ is the relative velocity between the critical point and the model mass (ft/sec).
- δ is the compression of the model spring (ft).
- ζ is the damping coefficient ratio (0.2 for the x axis, 0.09 for the y axis and 0.224 for the z axis).
- ω_n is the undamped natural frequency of the model (62.8 rad/sec for the x axis, 58.0 rad/sec for the y axis and 52.9 rad/sec for the z axis).

The dynamic response in each axis is obtained from:

$$DR = \frac{\omega_n{}^2 \delta}{g}$$

Where:

g is the acceleration due to gravity (ft/sec^2)

The injury-risk criterion or MDRC is then calculated based on the DR values for the three axes and on the DR limit values:

$$\text{Injury-Risk Criterion or MDRC} = \sqrt{\left(\frac{DRx}{DRxL}\right)^2 + \left(\frac{DRy}{DRyL}\right)^2 + \left(\frac{DRz}{DRzL}\right)^2}$$

Where:

DRx, DRy and DRz are the dynamic responses for the X, Y and Z axes.

DRxL, DRyL and DRzL are the X, Y and Z DR limit values.

The limit values for the acceleration components in the three axes are 40 and 35 for forward and aft accelerations in the x axis, 17 for the y axis and 18.0 and 16.5 for upward and downward accelerations in the z axis.

The injury-risk criterion or MDRC is considered to have been exceeded when the injury-risk criterion has a value greater than one.

The maximum MDRC value for the demonstration ejection tests are included in Table 5-5 of the report. Additional items relative to the MDRC calculations in the test program are:

- The data sample rate was 300 Hz.
- In Test #1, the angular rate data was extremely noisy and as the seat rotation rates were low, the accelerations were not transformed to the critical point.
- In Test #9, the roll rate history had excessive noise and a 30 Hz filter was used. In all other cases the angular rates were filtered at 80 Hz.

APPENDIX B

Test Data Vs. Simulation Data

This appendix contains the primary seat performance data for tests 1, 2, 4, 6, 7, 8, 9, and 10. For tests 4 and 6, the control system ceased to function correctly part-way through the test and only valid data is shown. The performance parameters are listed below, and the data includes validated DESS simulation plots of these parameters.

o Trajectory

o MDRC versus time

o Angle of attack, alpha, versus time.

o Angle of sideslip, beta, versus time.

It should be noted that time 0.0 seconds on these plots is motor ignition and motor control starts 50 milliseconds later, as does seat separation from the guiderails.

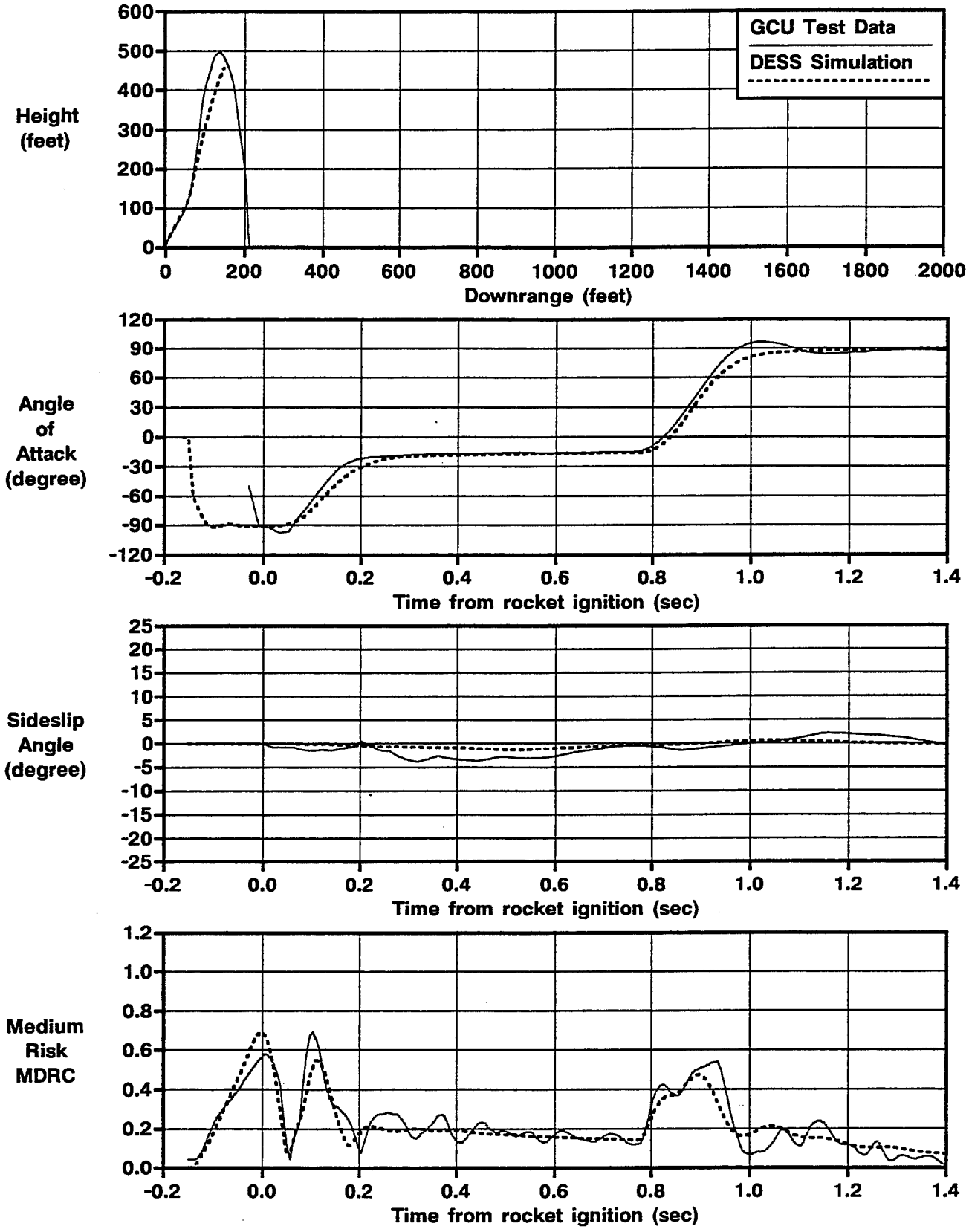

Figure B-1 Simulated and Actual Performance
Sled Test=1, KEAS=0, 95th%

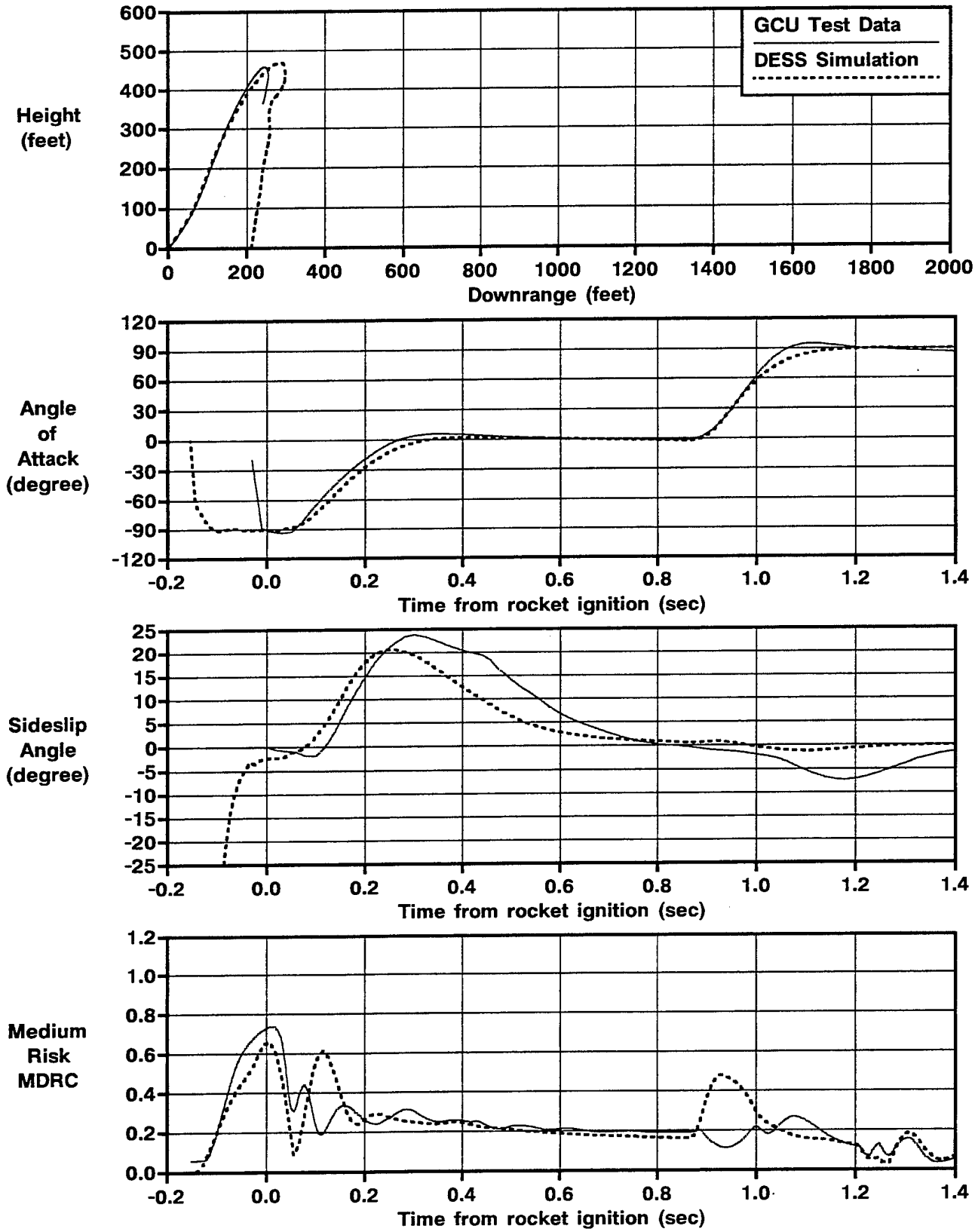

Figure B-2 Simulated and Actual Performance
Sled Test=2, KEAS=0, 5th%, Roll=60

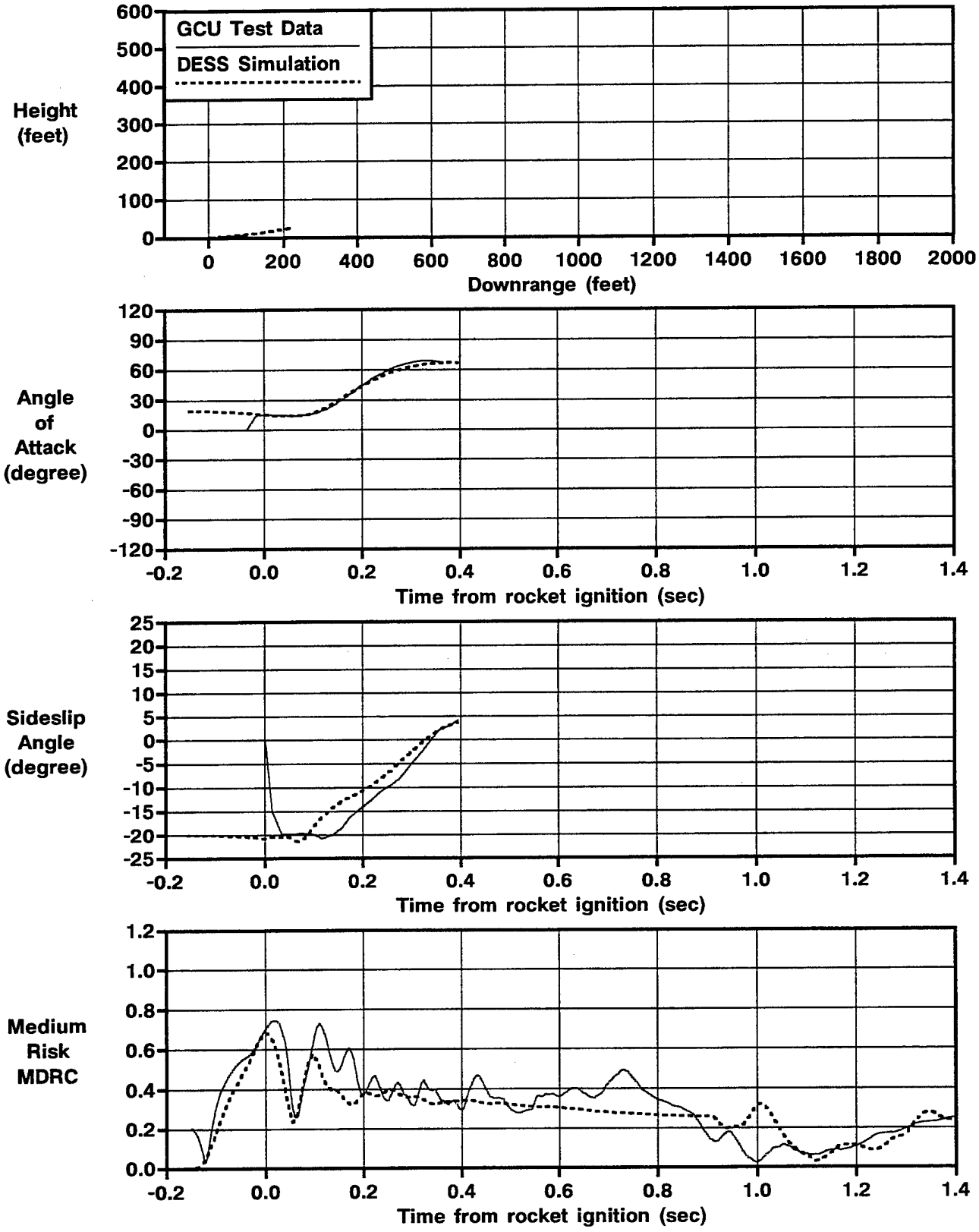

Figure B-3 Simulated and Actual Performance
Sled Test=6, KEAS=325, 5th%, Yaw=20

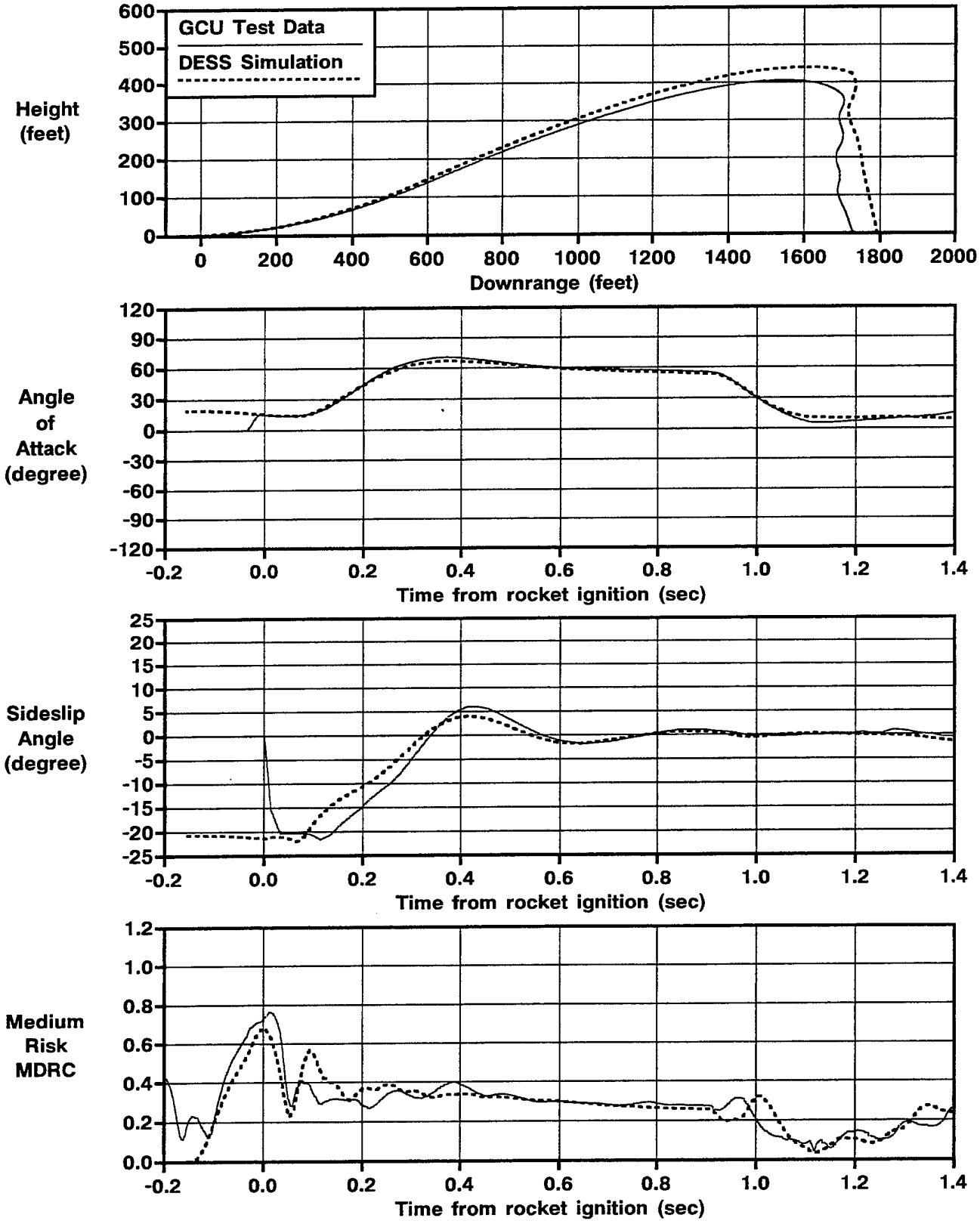

Figure B-4 Simulated and Actual Performance
Sled Test=7, KEAS=320, 5th%, Yaw=20

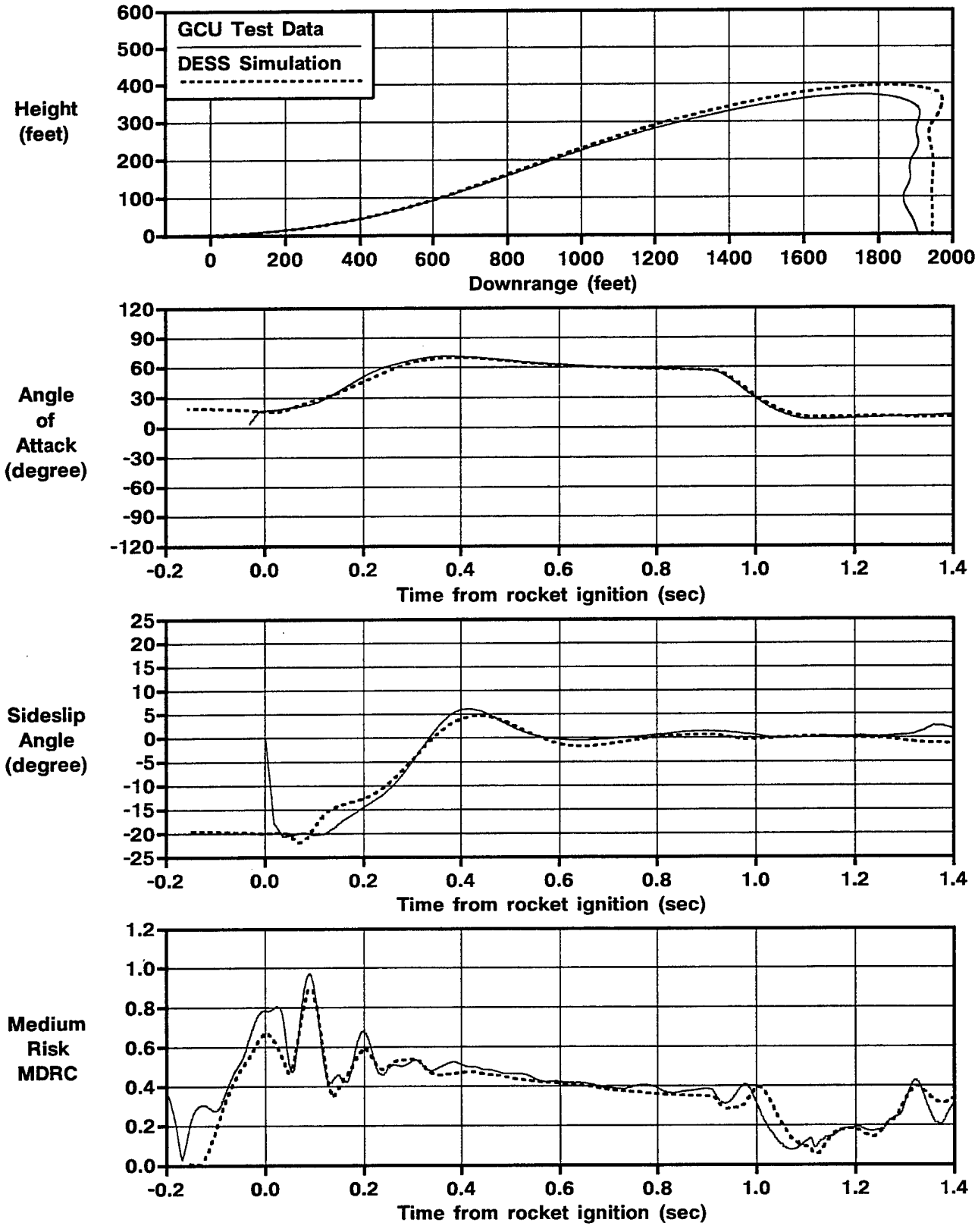

Figure B-5 Simulated and Actual Performance
Sled Test=8, KEAS=438, 5th%, Yaw=20

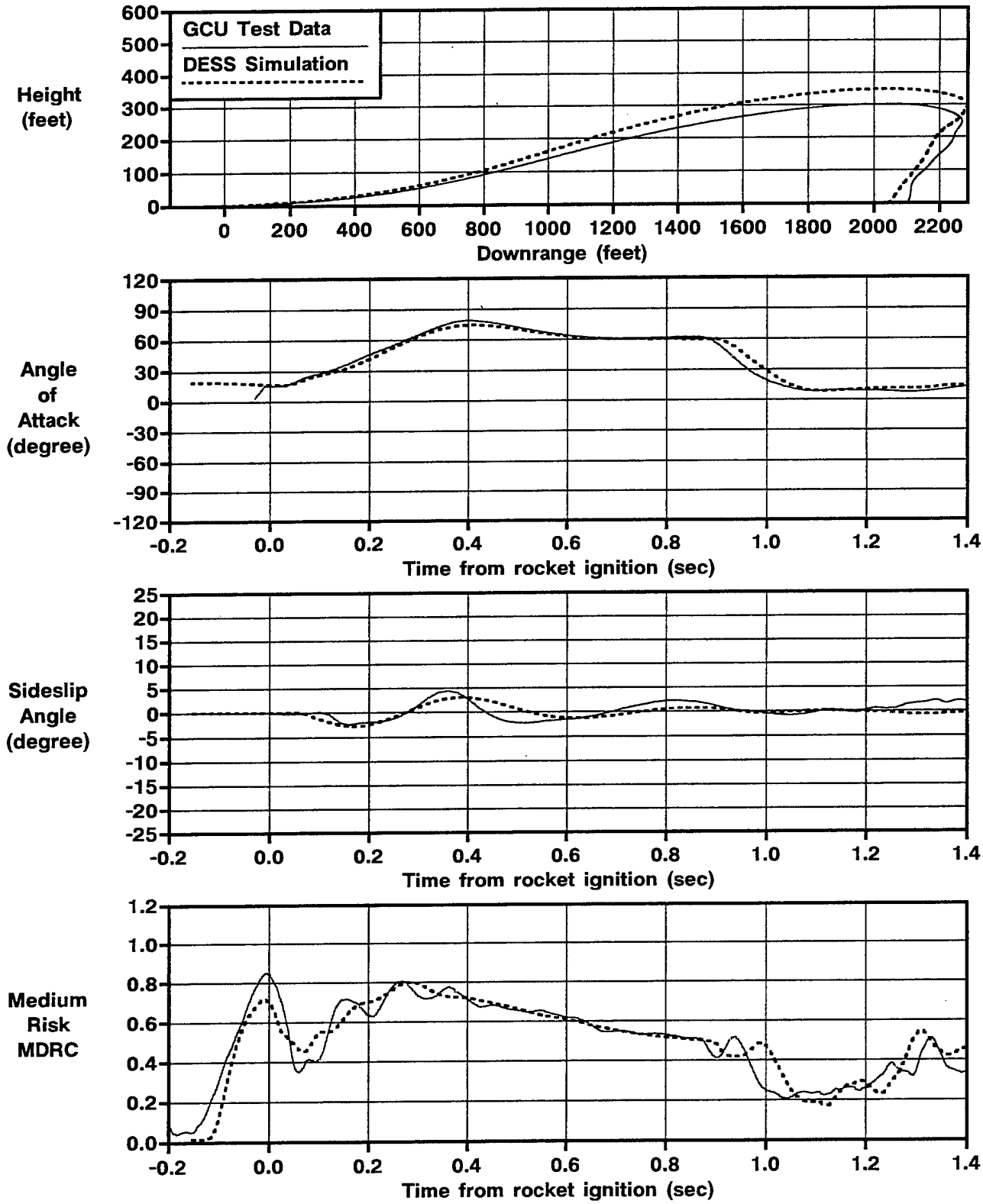

Figure B-6 Simulated and Actual Performance
Sled Test=9, KEAS=589, 5th%

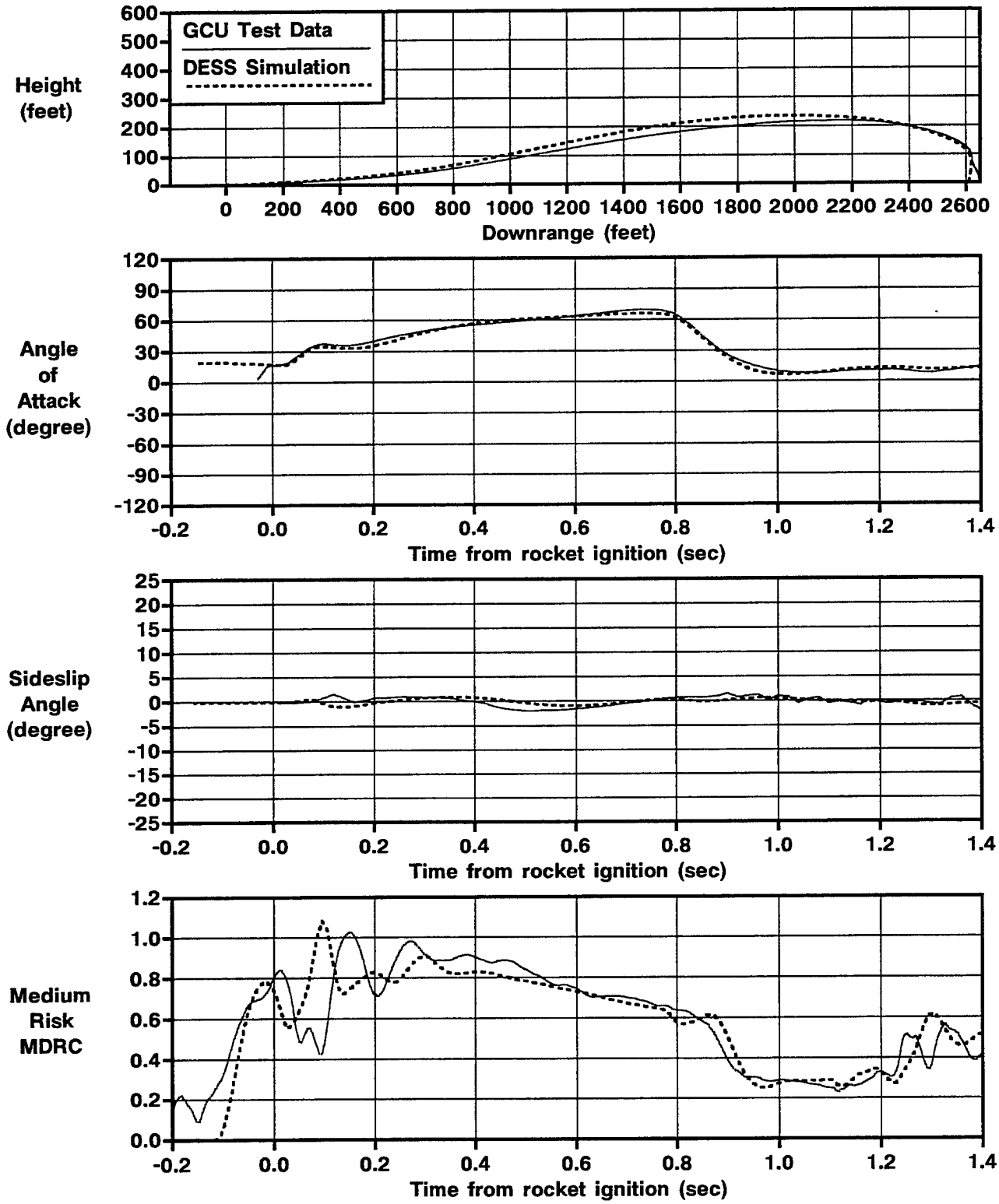

Figure B-7 Simulated and Actual Performance
Sled Test=10, KEAS=700, 5th%

APPENDIX C - Test Summaries and Recorded Data

APPENDIX C

Test Summaries and Recorded Data

Individual test reports were prepared for each of the demonstration ejection tests and these were referenced previously in Table 5-2. This Appendix includes an Appendix for each test, Appendices C-1 through C-10, which contain extracts from the individual reports. These extracts summarize the results of the tests and present the primary parameters which were recorded. Table C-1 lists the IMU data while Table C-2 and C-3 list the data which were recorded by the ADAM and Hybrid III manikins was used and data was obtained. In all of the data plots, time "0.0 seconds" is propulsion initiation. Also, Table C-4 shows the event times for all tests, with propulsion initiation being the "Propulsion Breakwire" event.

Table C-1 Figure Numbers for IMU Data

IMU Data	Test 1	Test 2	Test 3	Test 4	Test 6	Test 7	Test 8	Test 9	Test 10
Displacements	C-1-1	C-2-1	C-3-1	C-4-1	C-6-1	C-7-1	C-8-1	C-9-1	C-10-1
Velocities	C-1-2	C-2-2	C-3-2	C-4-2	C-6-2	C-7-2	C-8-2	C-9-2	C-10-2
Accelerations	C-1-2	C-2-2	C-3-2	C-4-2	C-6-2	C-7-2	C-8-2	C-9-2	C-10-2
Rotation Angles	C-1-3	C-2-3	C-3-3	C-4-3	C-6-3	C-7-3	C-8-3	C-9-3	C-10-3
Rotation Rates	C-1-3	C-2-3	C-3-3	C-4-3	C-6-3	C-7-3	C-8-3	C-9-3	C-10-3
Thrust Comands	C-1-4	C-2-4	C-3-4	C-4-4	C-6-4	C-7-4	C-8-4	C-9-4	C-10-4
Pintle Commands	C-1-5	C-2-5	C-3-5	C-4-5	C-6-5	C-7-5	C-8-5	C-9-5	C-10-5
Chamber Pressure	C-1-5	C-2-5	C-3-5	C-4-5	C-6-5	C-7-5	C-8-5	C-9-5	C-10-5
Aero Angles	C-1-6	C-2-6	C-3-6	C-4-6	C-6-6	C-7-6	C-8-6	C-9-6	C-10-6
Control Angles	C-1-6	C-2-6	C-3-6	C-4-6	C-6-6	C-7-6	C-8-6	C-9-6	C-10-6
Total Speed	C-1-6	C-2-6	C-3-6	C-4-6	C-6-6	C-7-6	C-8-6	C-9-6	C-10-6

No added filtering applied to above data

Table C-2 Figure Numbers for ADAM Data

ADAM Data	Test 2	Test 8	Test 9	Test 10
Head Accelerations	C-2-7	C-8-7	C-9-7	C-10-7
Lumbar Accelerations	C-2-7	C-8-7	C-9-7	C-10-7
Chest Linear Accelerations	C-2-8	C-8-8	C-9-8	C-10-8
Chest Angular Accelerations	C-2-8	C-8-8	C-9-8	C-10-8
Neck Forces	C-2-9	C-8-9	C-9-9	C-10-9
Lumbar Forces	C-2-9	C-8-9	C-9-9	C-10-9
Neck Moments	C-2-10	C-8-10	C-9-10	C-10-10
Lumbar Forces	C-2-10	C-8-10	C-9-10	C-10-10
Seat Rotation Rates	C-2-11	C-8-11	C-9-11	C-10-11
Seat Ref. Point Accelerations	C-2-11	C-8-11	C-9-11	C-10-11
Pintle Positions	C-2-12	C-8-12	C-9-12	C-10-12

Data filtered at 250 Hz, and averaged to eliminate time shifting.

Table C-3 Figure Numbers for Hybrid III Data

Manikin Recorded Data	Test 4	Test 6
Manikin Head Accelerations	C-4-7	C-6-7
Manikin Chest Accelerations	C-4-7	C-6-7
Manikin Head force	C-4-8	C-6-8
Manikin Head Moment	C-4-8	-
Seat Angular Rates	C-4-9	C-6-9
Seat Pan Accelerations	C-4-9	C-6-9
Manikin Chest rates	C-4-10	-
Manikin Lumbar Force	C-4-10	-
Pintle Positions	C-4-11	C-6-11

Table C-4 Event Timing

EVENT	Test 1	Test 2	Test 3	Test 4	Test 6	Test 7	Test 8	Test 9	Test 10
Speed (KEAS)	0	0	320	320	317	320	437	589	709
Roll Angle (degrees)	0	60	60	60	0	0	0	0	0
Yaw Angle (degrees)	0	0	0	0	20	20	20	0	0
Sled Launch	-0.895	-0.900	-10.097	-10.182	-10.792	-10.690	-7.493	-10.127	-10.934
Squib Arm	-0.895	-0.900	-0.902	-0.915	-0.879	-0.868	-0.912	-0.892	-0.884
Catapult Initiation	-0.150	-0.136	-0.145	-0.150	-0.137	-0.131	-0.135	-0.137	-0.106
Propulsion Breakwire	0.000	0.000	0.000	0.000	0.000	0.000	0.000	0.000	0.000
Drogue Alignments Start	na	na	na	na	na	0.904	0.908	0.868	0.780
Drogue Mortar Initiation	na	na	na	na	0.377	1.104	1.104	1.101	1.103
Parachute Alignment Start	0.766	0.863	na	0.964	na	na	na	na	na
Parachute Mortar Initiation	na	1.203	na	1.204	1.674	1.934	2.084	2.275	2.456
Drogue Severance Initiation	na	1.356	na	1.354	1.824	2.084	2.238	2.428	2.606
Restraint Release Initiation	na	1.456	na	1.454	1.924	2.184	2.334	2.525	2.706
Seat / Manikin Separation	na	1.467	na	1.658	2.306	2.420	2.603	2.824	3.078
Main Chute 1st Inflation	na	5.603	na	2.971		3.592	4.010	4.056	
Manikin Ground Impact	11.560	20.075	10.905	9.764	9.321	20.849	20.395	35.000	14.517

APPENDIX C-1: TEST #1

TEST SUMMARY

Objective

The objective of this test was to demonstrate the flight controls and controllable propulsion system of the 4th Generation Escape System in a 0/0 flight condition.

Test Conditions

	Run Number	85E-B2
	Test Date	25 July 1996
	System Launch Time	10:57 AM MDT
	Temperature	73 deg F
(1)	Wind	calm
	Barometric Pressure	12.745 lb/in^2
	Velocity	0 KEAS
	Roll	0 deg
	Pitch	0 deg
	Yaw	0 deg
	ADAM Size	Large

(1) 0 degree angle is a head wind. Positive to the right (clockwise).

Summary And Conclusions

This test successfully demonstrated the operation of the controllable propulsion system and the flight controls, however recovery of the seat and manikin was not achieved. After system initiation by the test facility, the catapult phase and seat / aircraft separation performed as expected with no interference or anomalies. The initiation and operation of the controllable propulsion system also performed as expected. Once in free flight, the control system oriented the seat to a 45° pitch attitude for the climb-out portion of the rocket burn, and then reoriented the seat to 90 degrees angle of attack for parachute deployment.

After completion of the propulsion phase of the ejection sequence, the recovery phase is initiated by the deployment of the recovery parachute and separation of the manikin from the seat. In this test, the signals to initiate the recovery parachute and harness release were initiated, as verified by the flight data recorder, however the pyrotechnic devices were not fired. Due to the lack of parachute deployment, the seat and manikin impacted the ground after a free fall from approximately 500'.

Post test investigation revealed that the failure to fire the ACES II pyro devices was caused by an incompatibility with the demonstration escape system squib cabling and the ACES II pyro devices. The squib cabling was revised and a series of live squib fire tests were successfully completed to verify the corrective action.

This test is considered successful in terms of the primary objective of demonstrating the controllable propulsion and flight controls. Corrective actions have been implemented and tested to verify proper squib operation.

Data.

The primary data obtained from the IMU are presented in Figures C-1-1 through C-1-6.

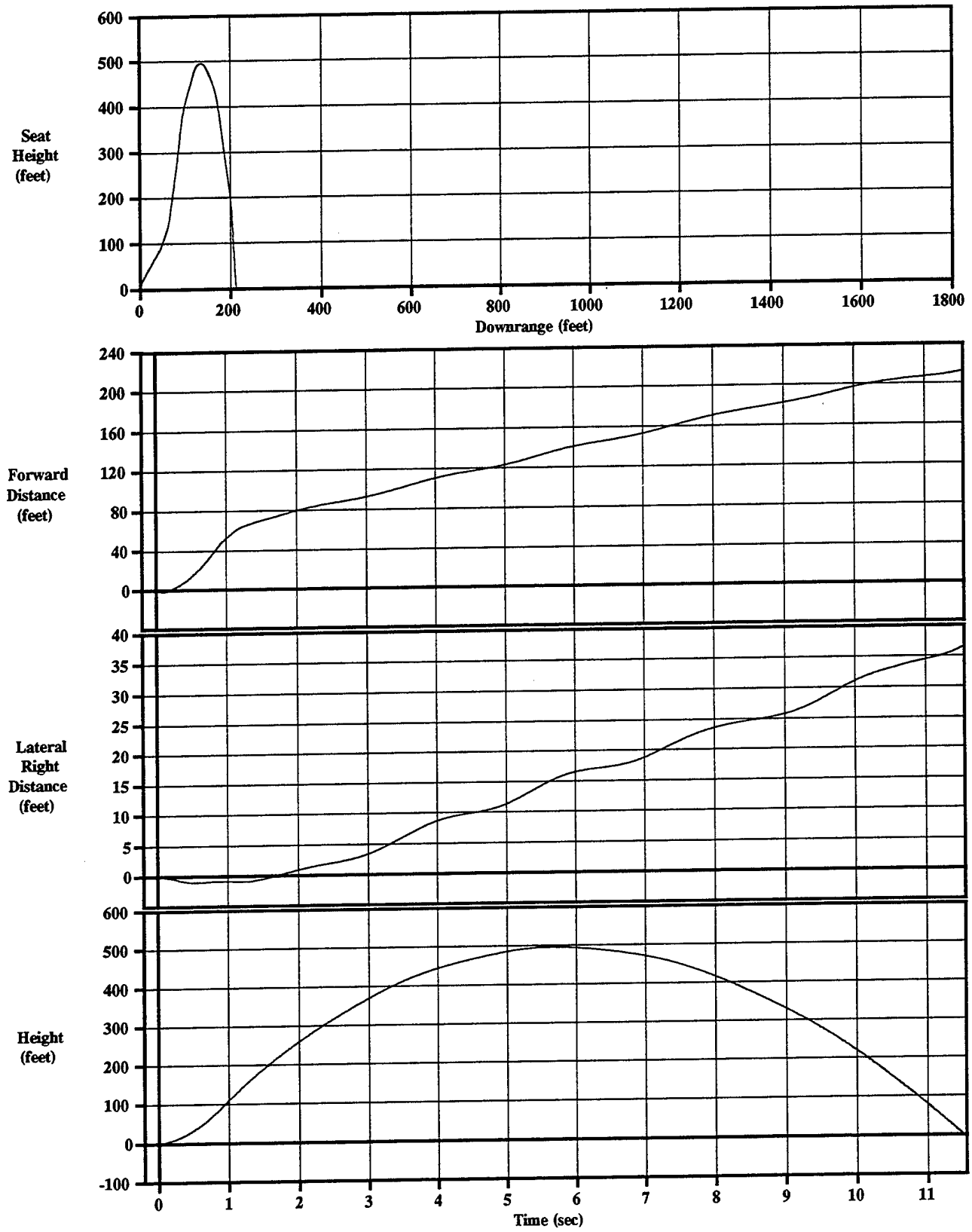

Figure C-1-1 IMU Displacements
Sled Test=1, KEAS=0, 95th%

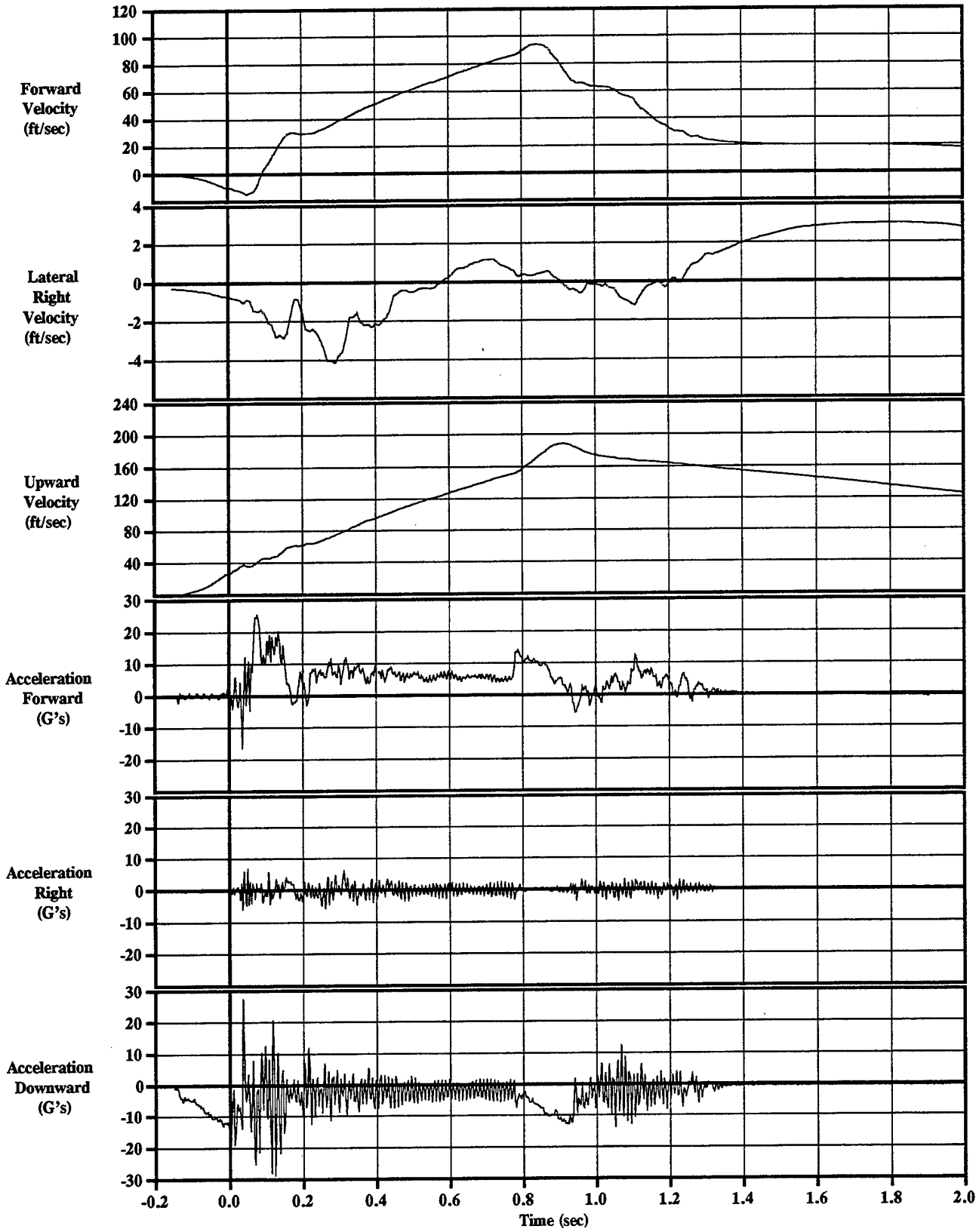

Figure C-1-2 IMU Velocities & Accelerations
Sled Test=1, KEAS=0, 95th%

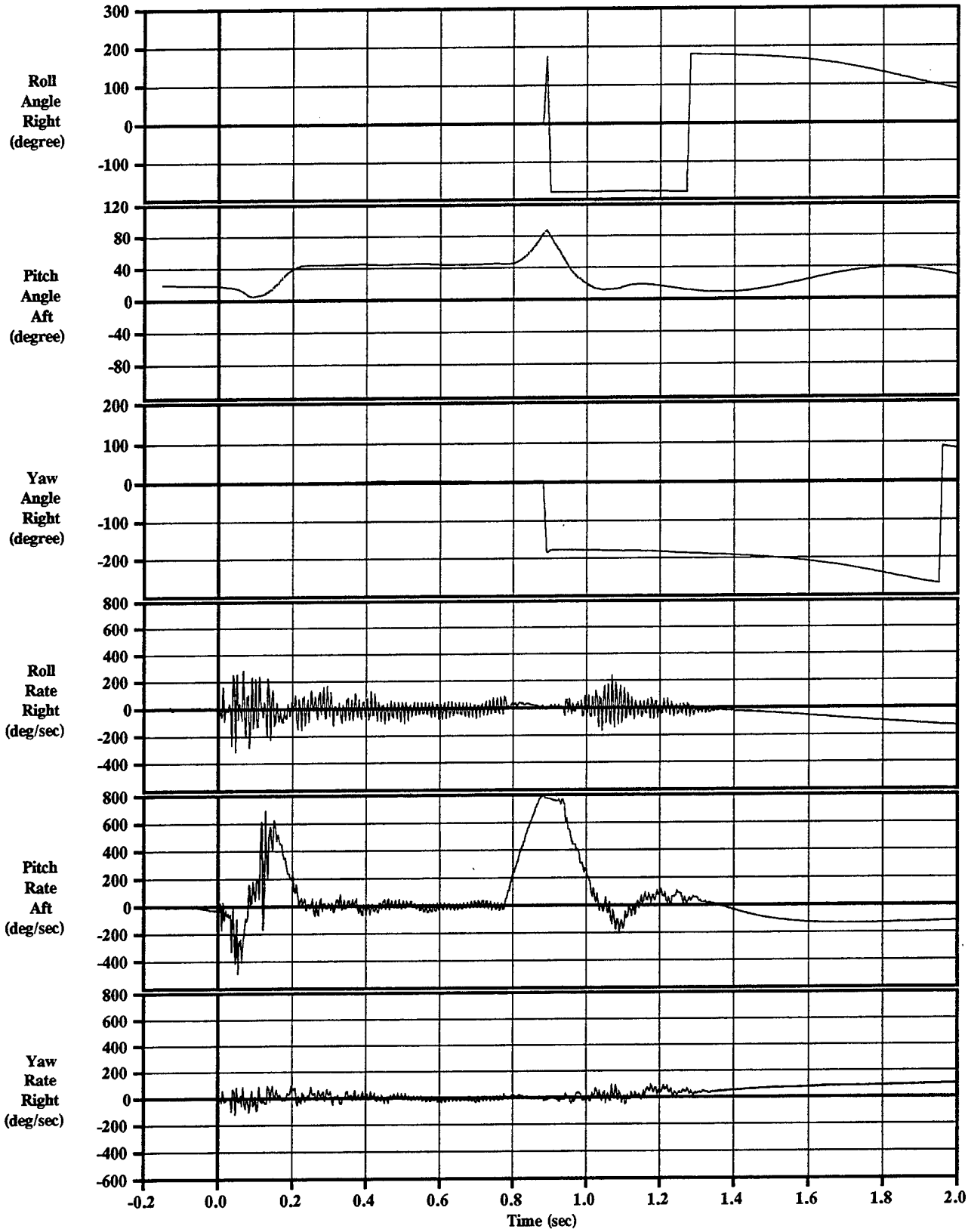

Figure C-1-3 IMU Rotation Angles & Rates
Sled Test=1, KEAS=0, 95th%

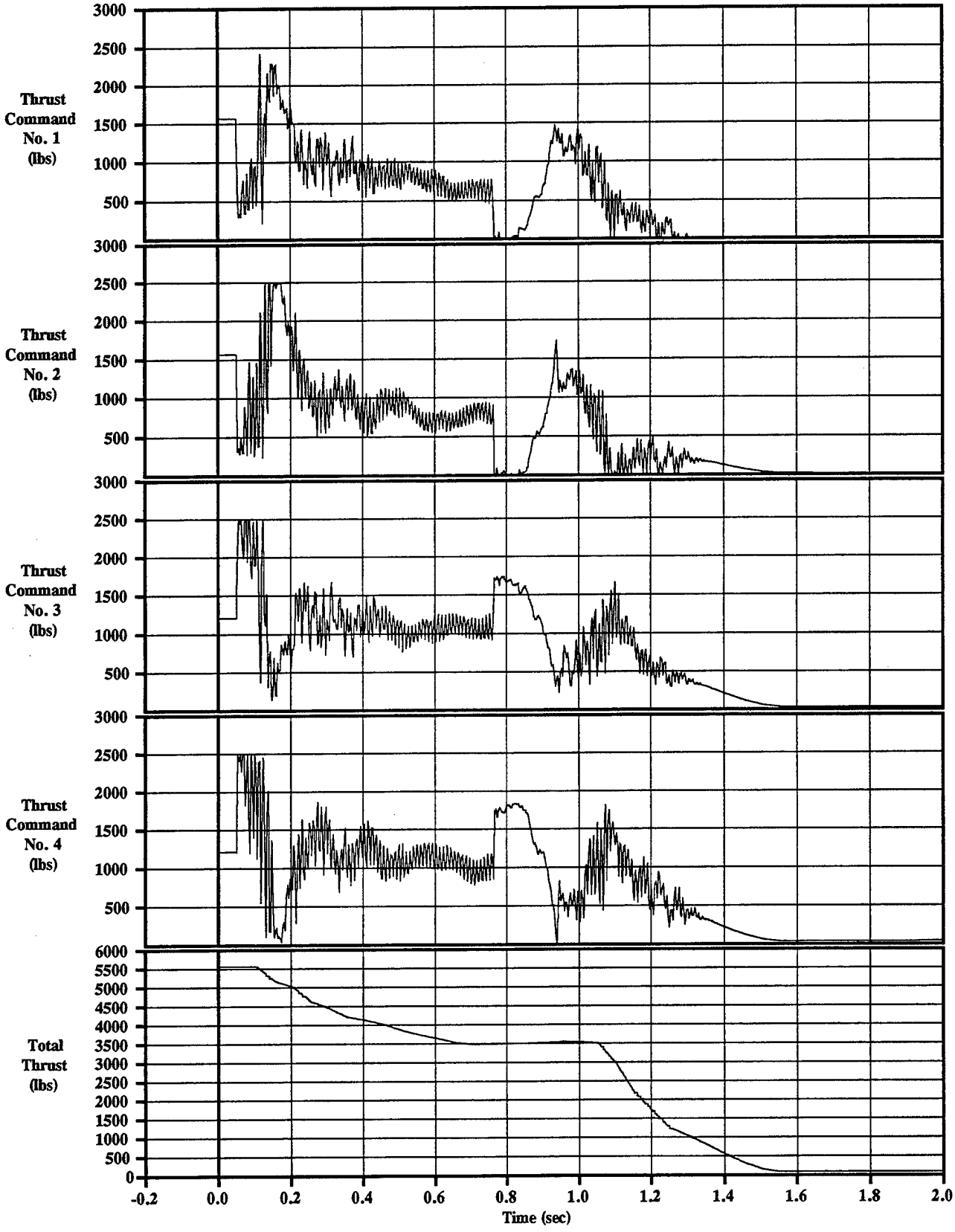

Figure C-1-4 Thrust Commands
Sled Test=1, KEAS=0, 95th%

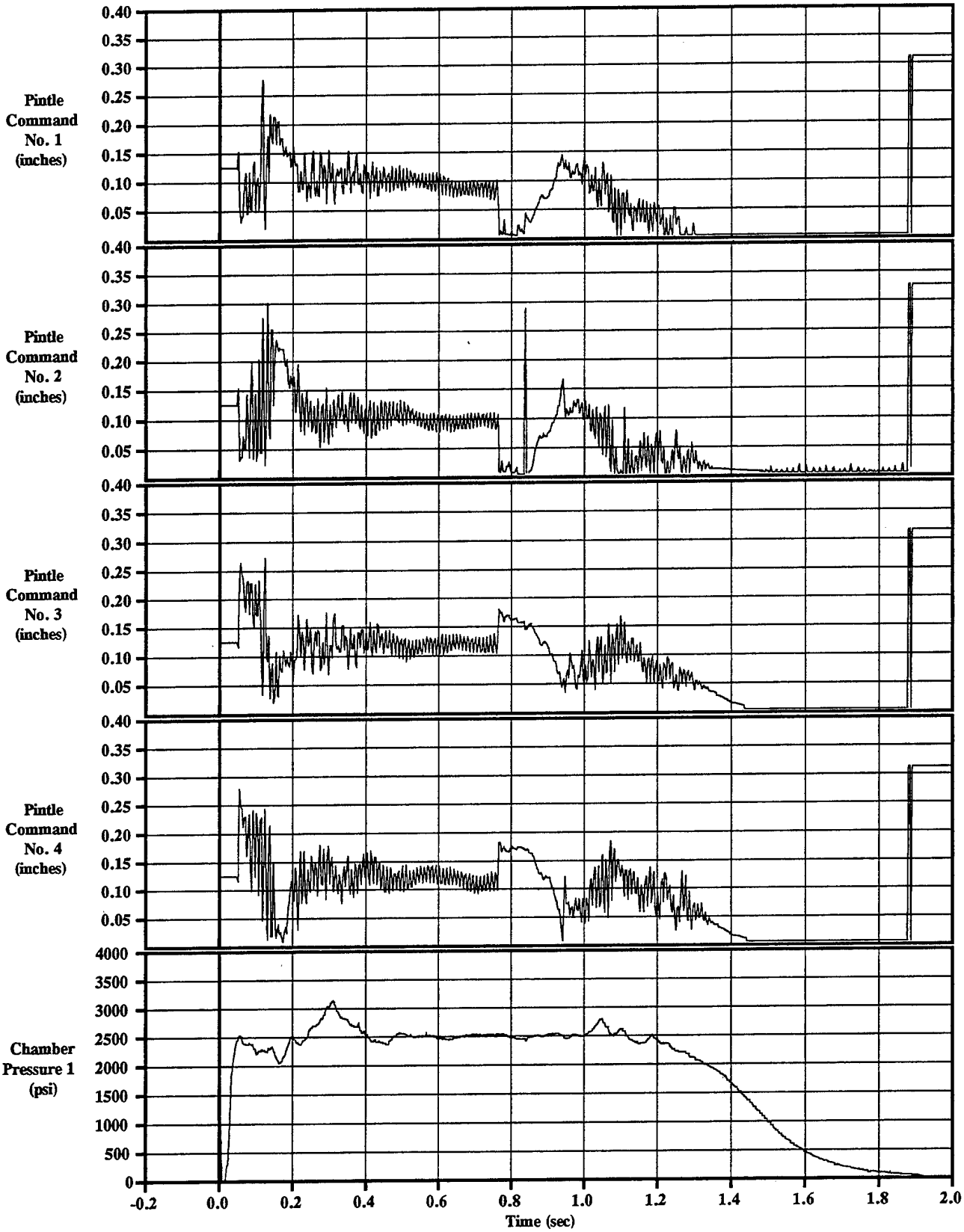

Figure C-1-5 Pintle Commands & Chamber Pressure
Sled Test=1, KEAS=0, 95th%

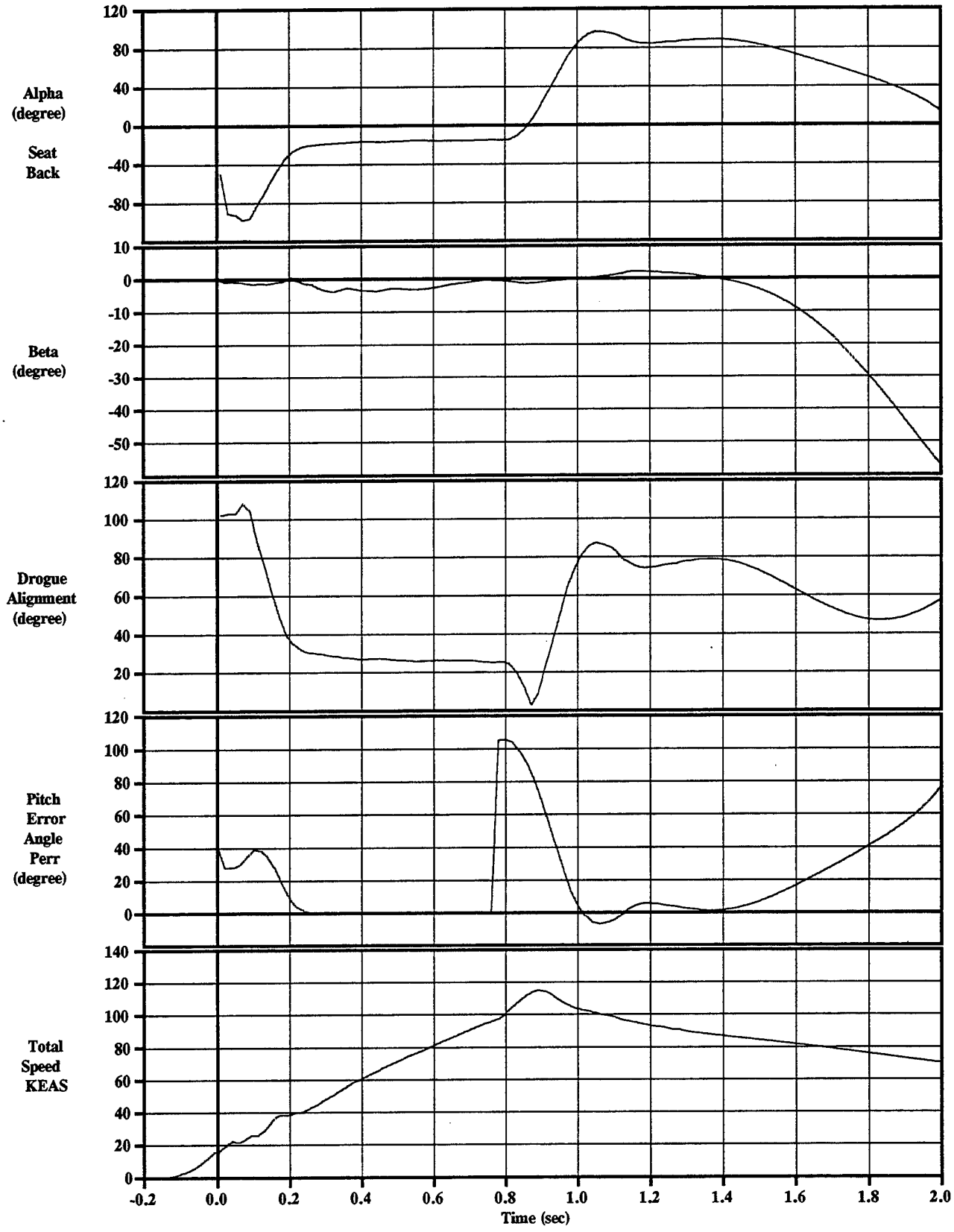

Figure C-1-6 IMU Control Angles and Total Velocity
Sled Test=1, KEAS=0, 95th%

APPENDIX C-2: TEST #2

TEST SUMMARY

Objective

The objective of this test was to demonstrate the flight controls and controllable propulsion system of the 4th Generation Escape System in a 0 KEAS, 60° roll flight condition.

Test Conditions

	Run Number	85E-B3A
	Test Date	5 September 1996
	System Launch Time	10:52 AM MDT
		249:16:52:00 IRIG
	Launch Point	TS 8036.15, on W Track Rd
	Temperature	76 deg F
	Relative Humidity	58.2%
(1)	Wind	5.9 KTS from 287° (NW)
	Barometric Pressure	12.60 lb/in^2
	Velocity	0 KEAS
	Roll	60 deg
	Pitch	0 deg
	Yaw	0 deg
	ADAM Size	Small

(1) 0 degree angle is a head wind. Positive to the right (clockwise).

Summary And Conclusions

This test successfully demonstrated the operation of the controllable propulsion system and the flight controls. After system initiation by the test facility, the catapult phase and seat/aircraft separation performed as expected with no interference or anomalies. The initiation and operation of the controllable propulsion system also performed as expected. Once in free flight, the control system rolled the seat to an upright position at a 45° pitch attitude for the climb-out portion of the rocket burn. Just prior to rocket burnout, the seat was reoriented to 90° angle of attack for parachute deployment. Recovery parachute deployment and separation of the manikin from the seat were achieved and both the ADAM manikin and 4th Gen seat were successfully recovered.

The Dynamic Response Index was 13.1 and is within the requirement of 18.0. Head and neck loads were measured as 288 lb. in the z-axis and 103 lb. in the x-axis, again within the requirements of 300 lb. and 250 lb. respectively. The medium risk

Multiaxial Dynamic Response Index (MDRC) was 0.73 and occurred at the end of the catapult stroke. Parachute loads were measured as approximately 305 lb. for each riser for 610 lb. total. Acceleration values measured during parachute opening were approximately 6 G's as measured in the lumbar region of ADAM. Arm loads and pressures were not measured for this test.

This test is considered successful in terms of the primary objective of demonstrating the controllable propulsion and flight controls.

Data.
The primary data obtained from the IMU and ADAM are presented in Figures C-2-1 through C-2-12.

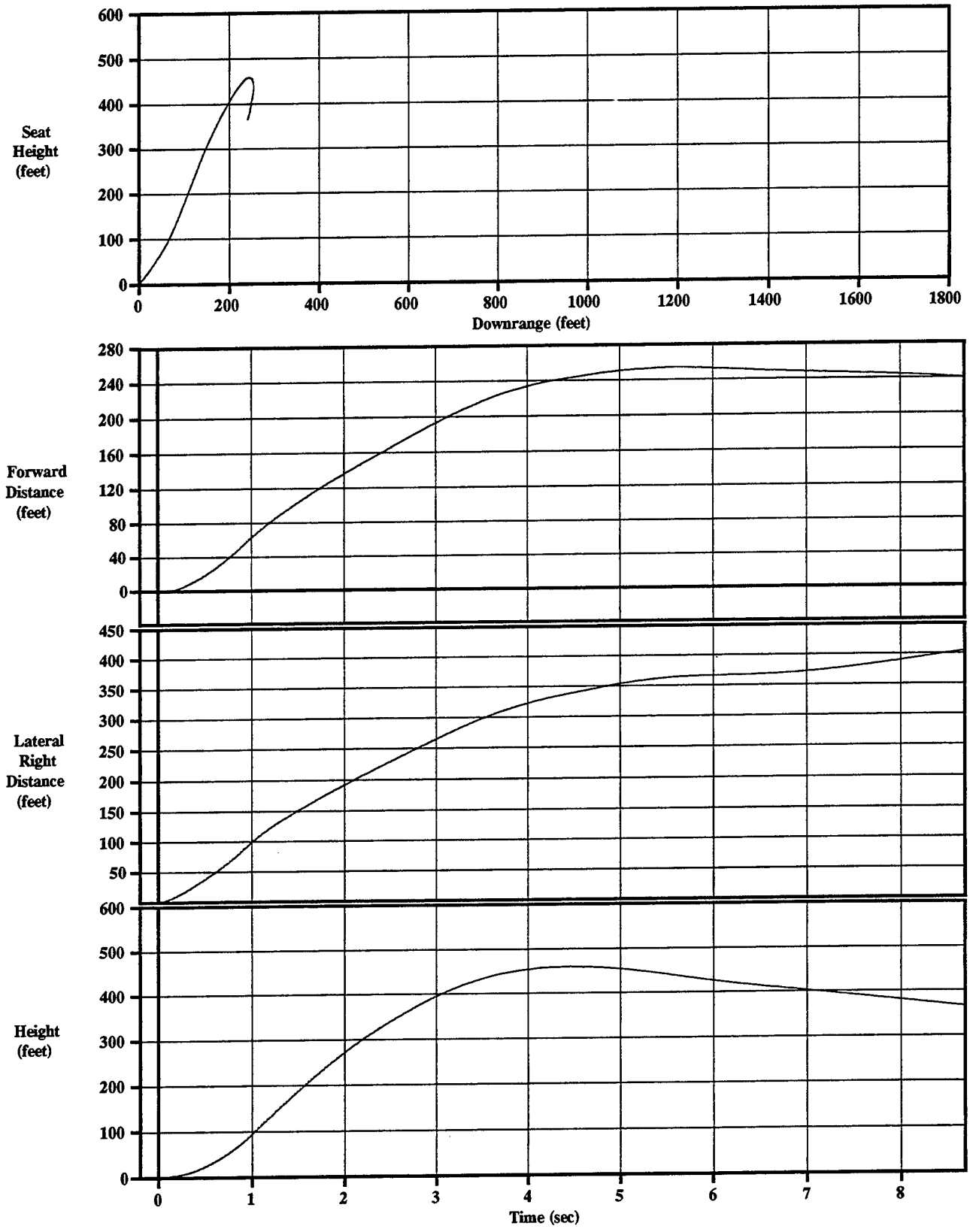

Figure C-2-1 IMU Displacements
Sled Test=2, KEAS=0, 5th%, Roll=60

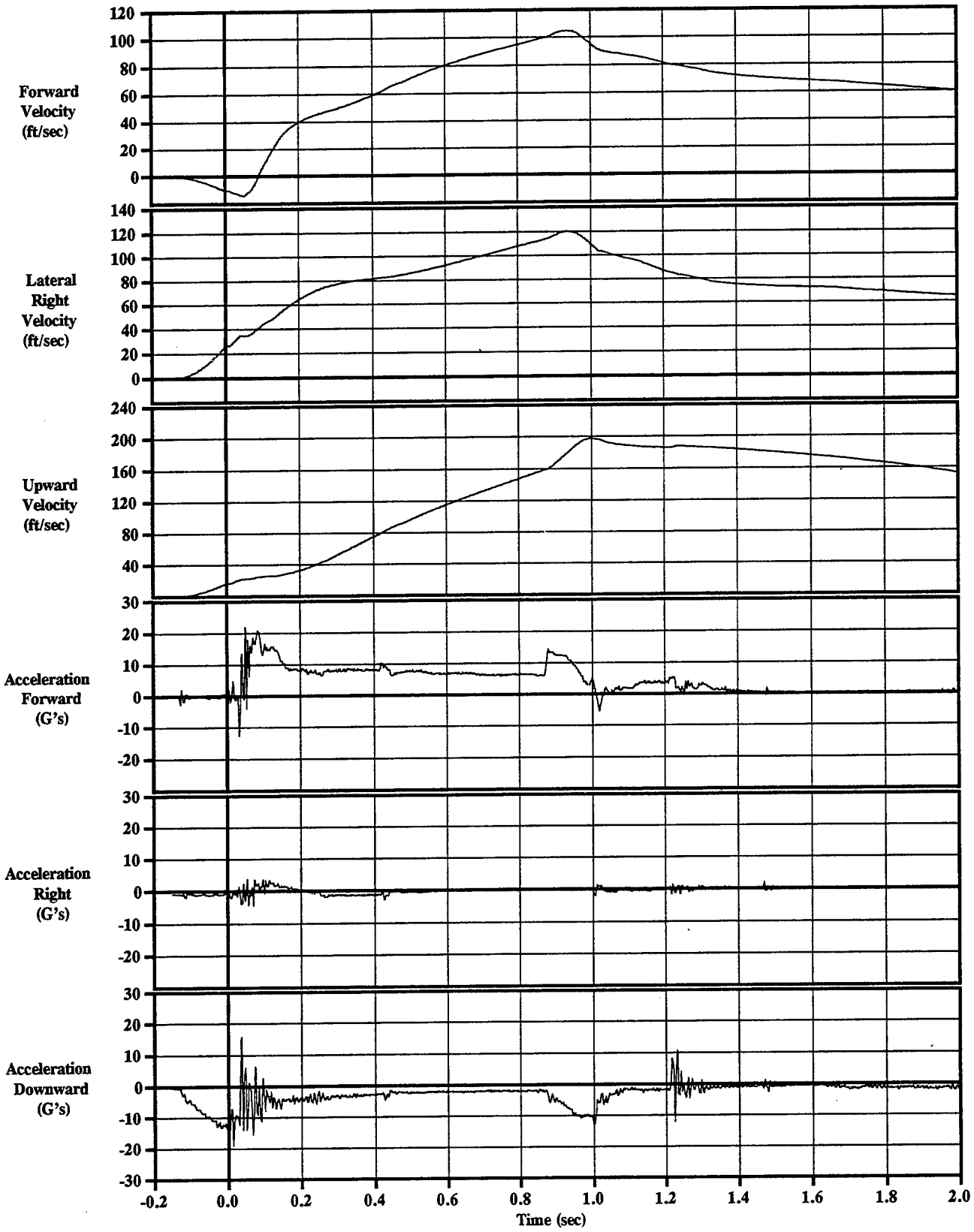

Figure C-2-2 IMU Velocities & Accelerations
Sled Test=2, KEAS=0, 5th%, Roll=60

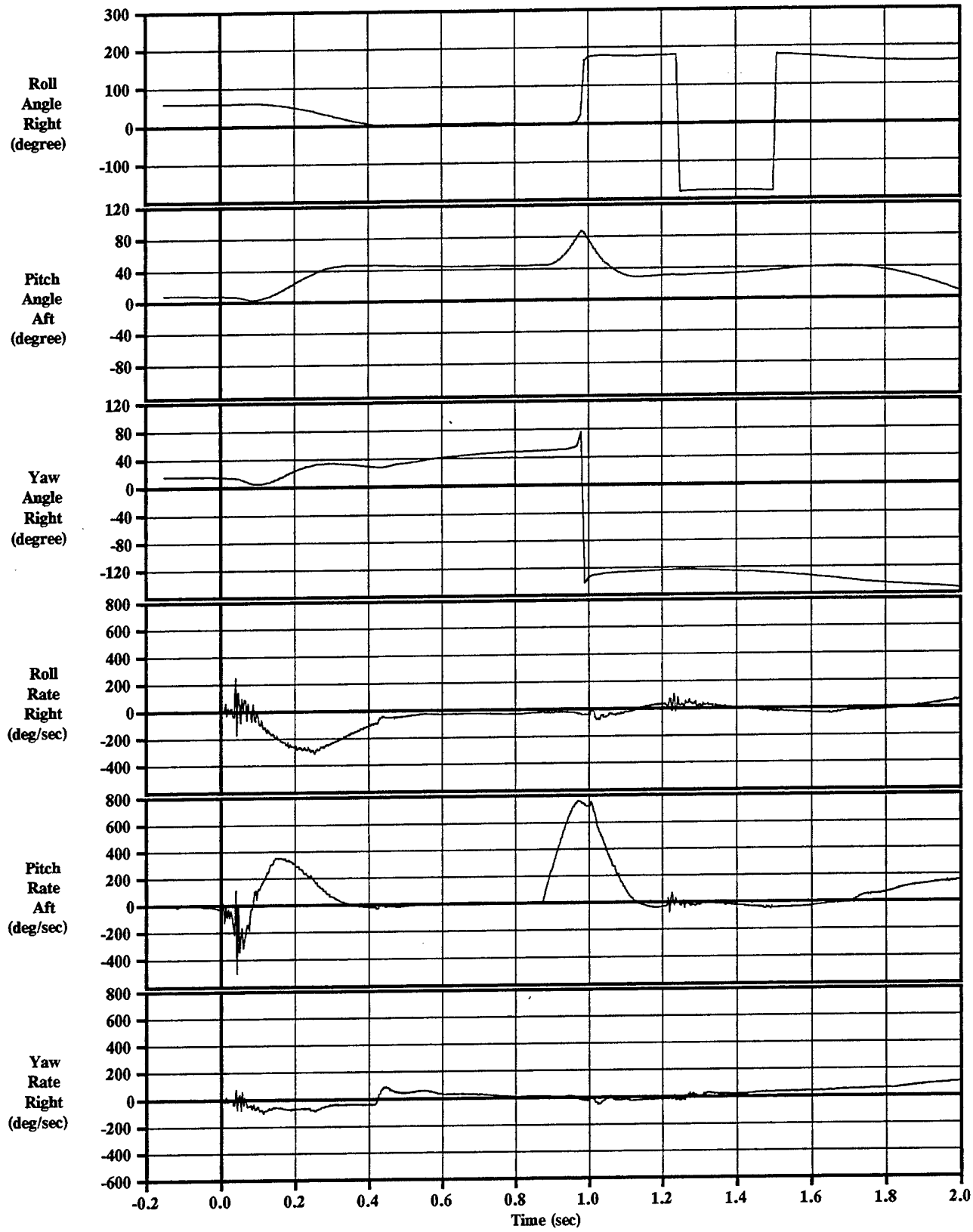

Figure C-2-3 IMU Rotation Angles & Rates
Sled Test=2, KEAS=0, 5th%, Roll=60

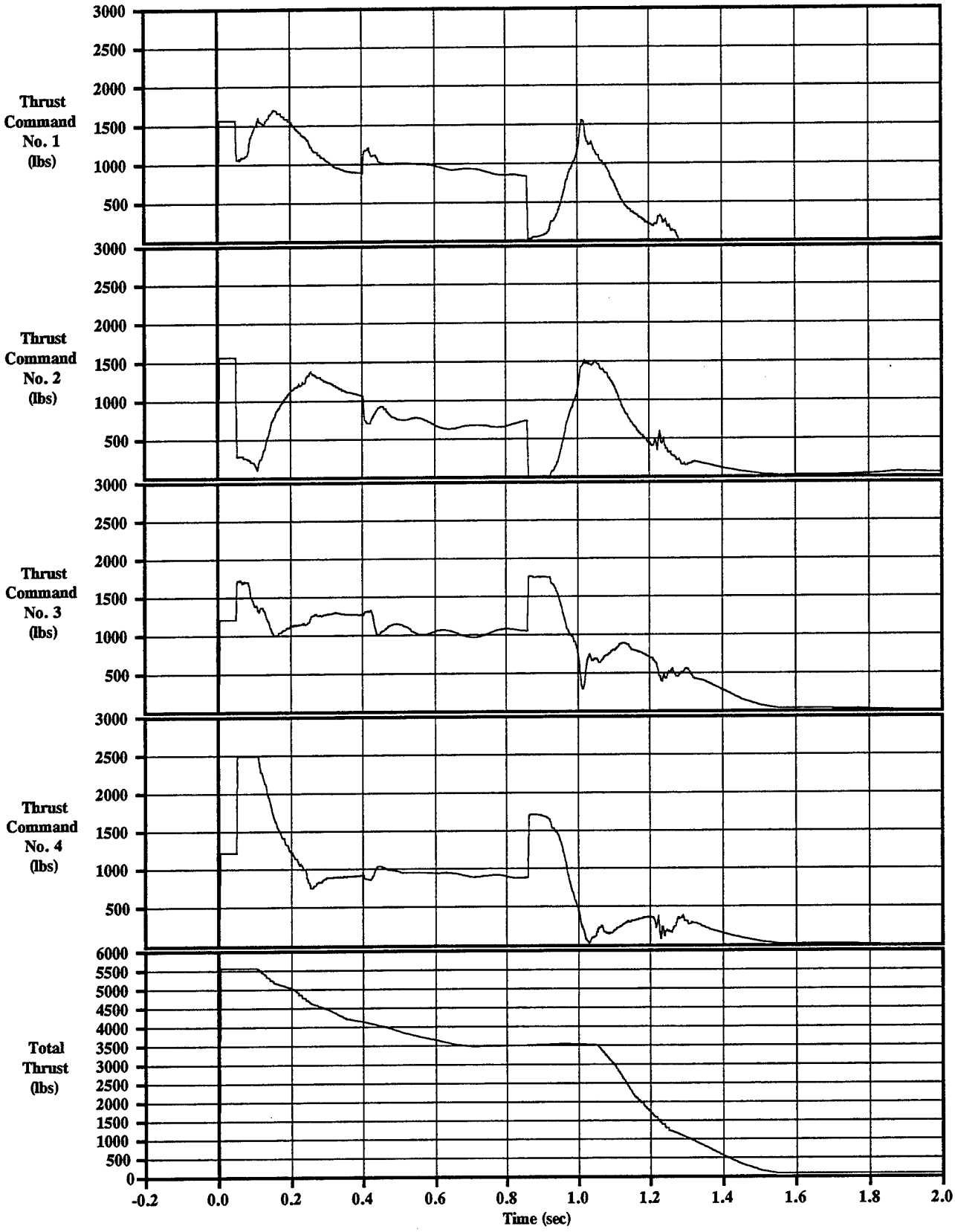

Figure C-2-4 Thrust Commands
Sled Test=2, KEAS=0, 5th%, Roll=60

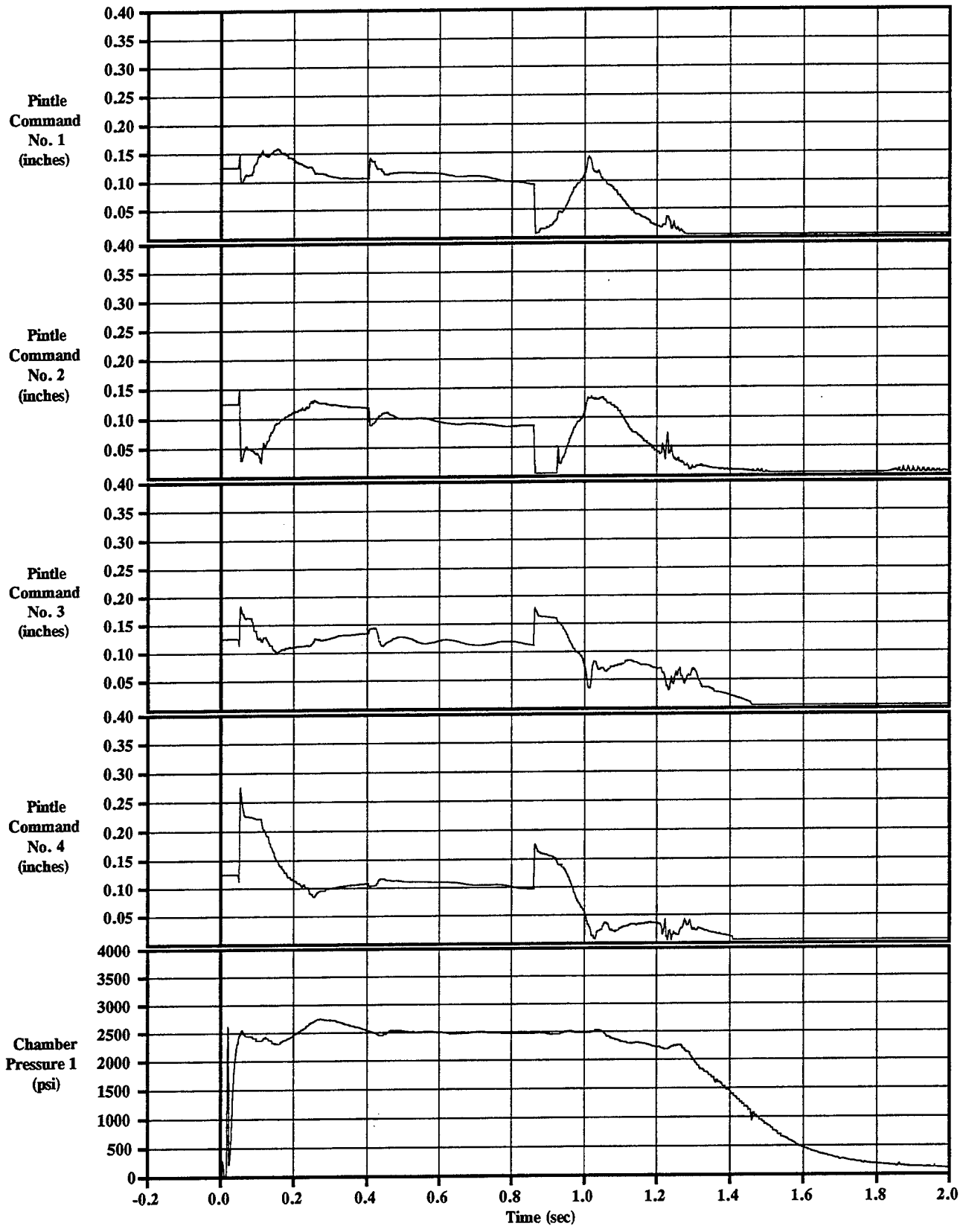

Figure C-2-5 Pintle Commands & Chamber Pressure
Sled Test=2, KEAS=0, 5th%, Roll=60

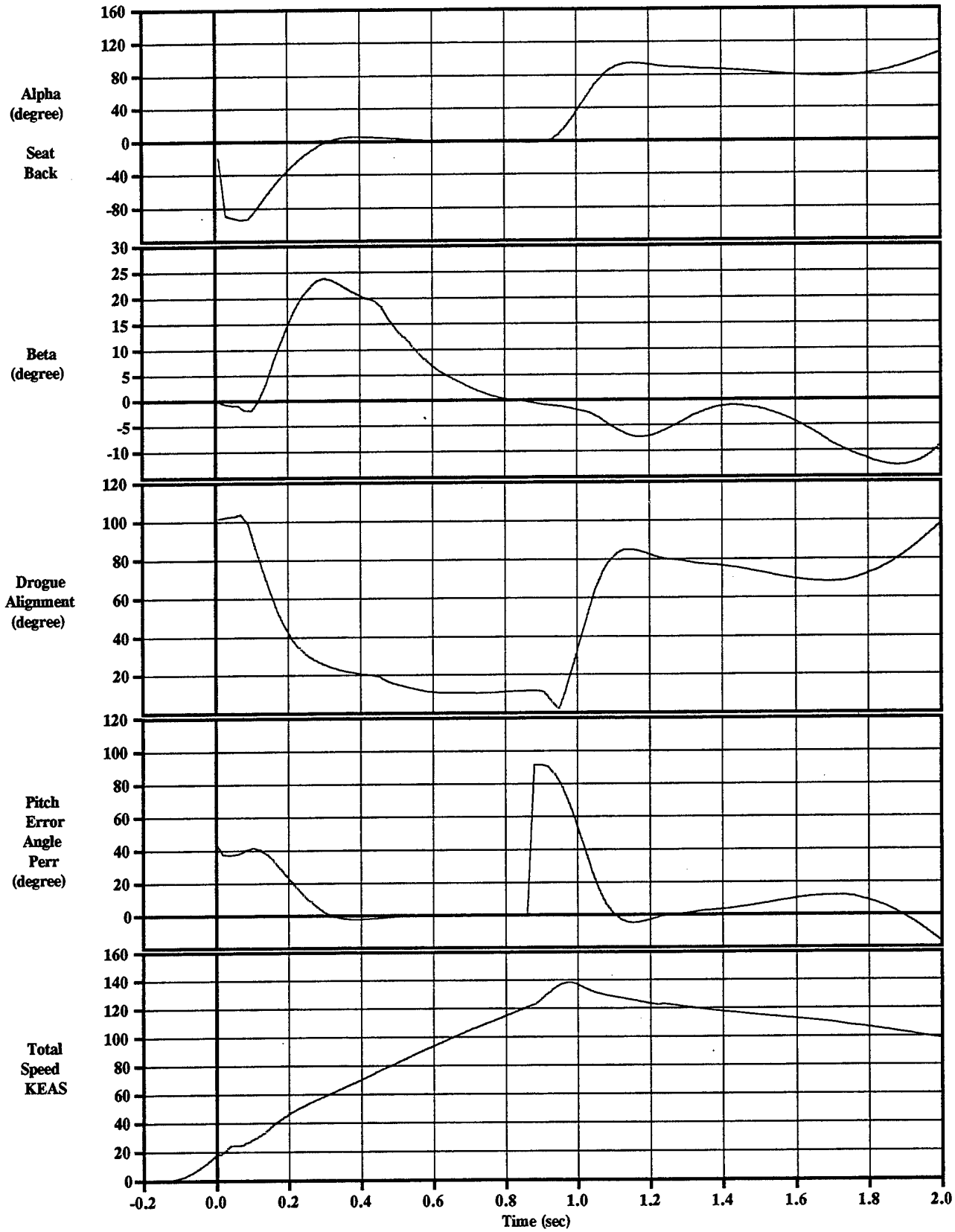

Figure C-2-6 IMU Control Angles and Total Velocity
Sled Test=2, KEAS=0, 5th%, Roll=60

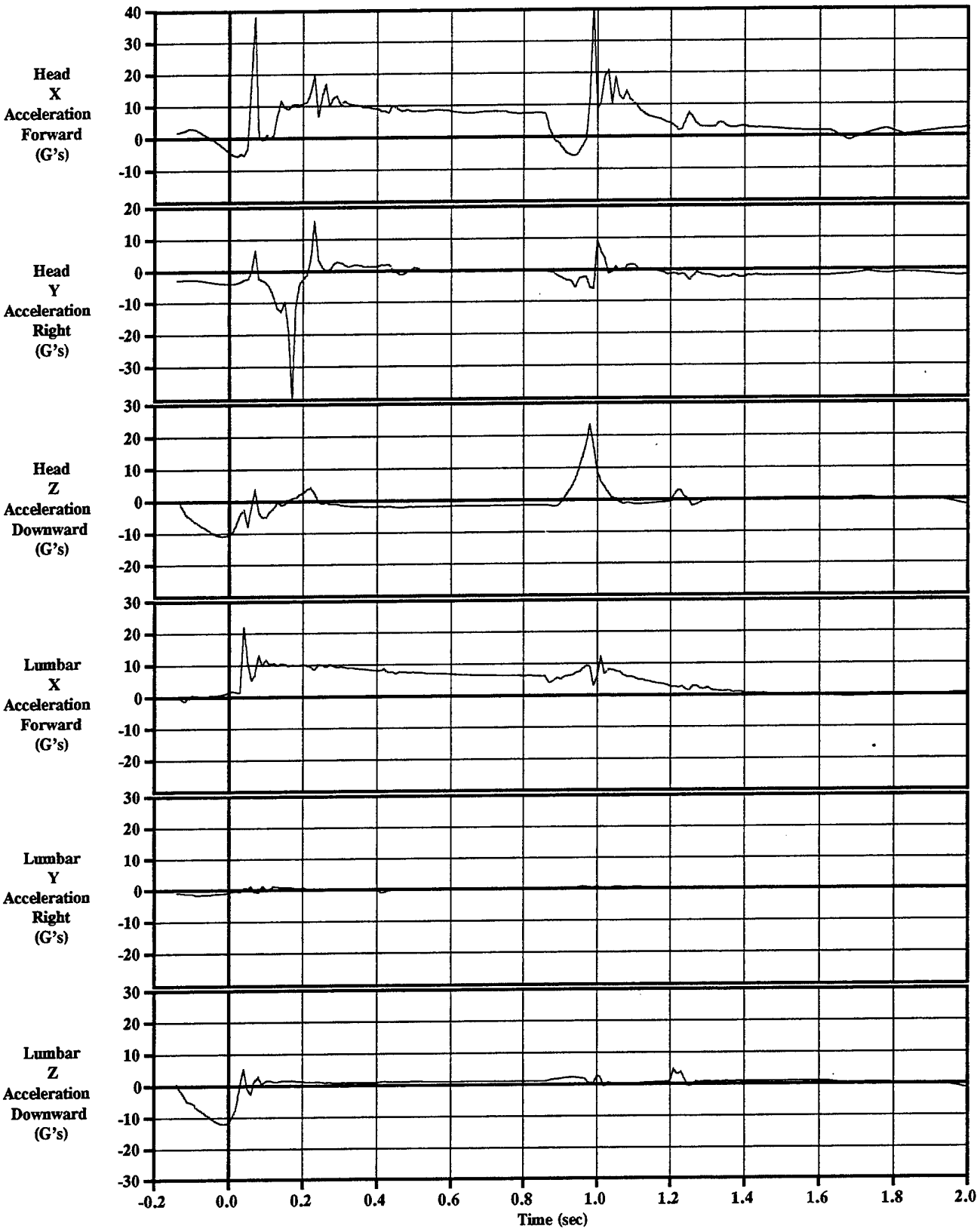

Figure C-2-7 ADAM Head & Lumbar Accelerations
Sled Test=2, KEAS=0, 5th%, Roll=60

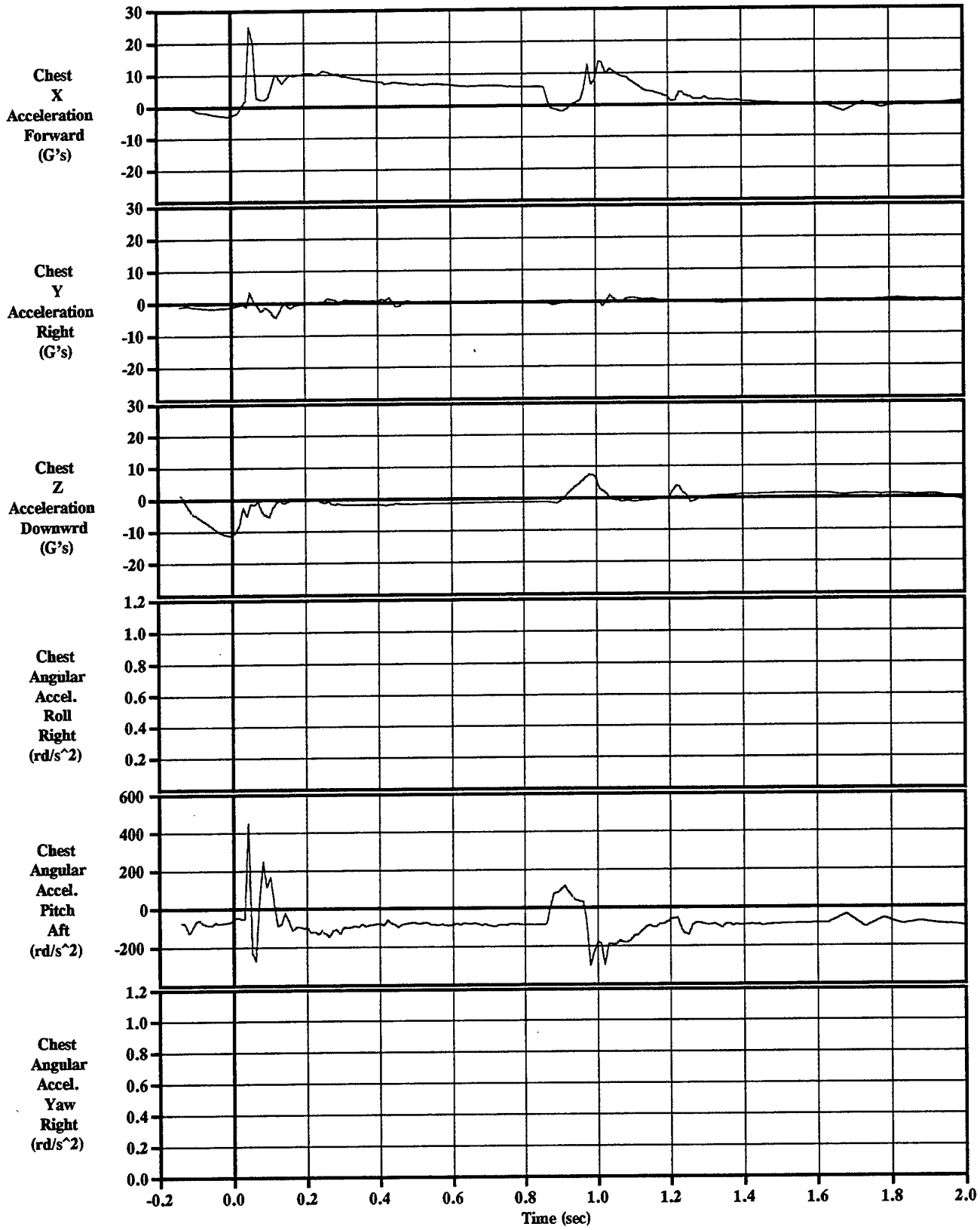

Figure C-2-8 ADAM Chest Linear & Angular Accelerations
Sled Test=2, KEAS=0, 5th%, Roll=60

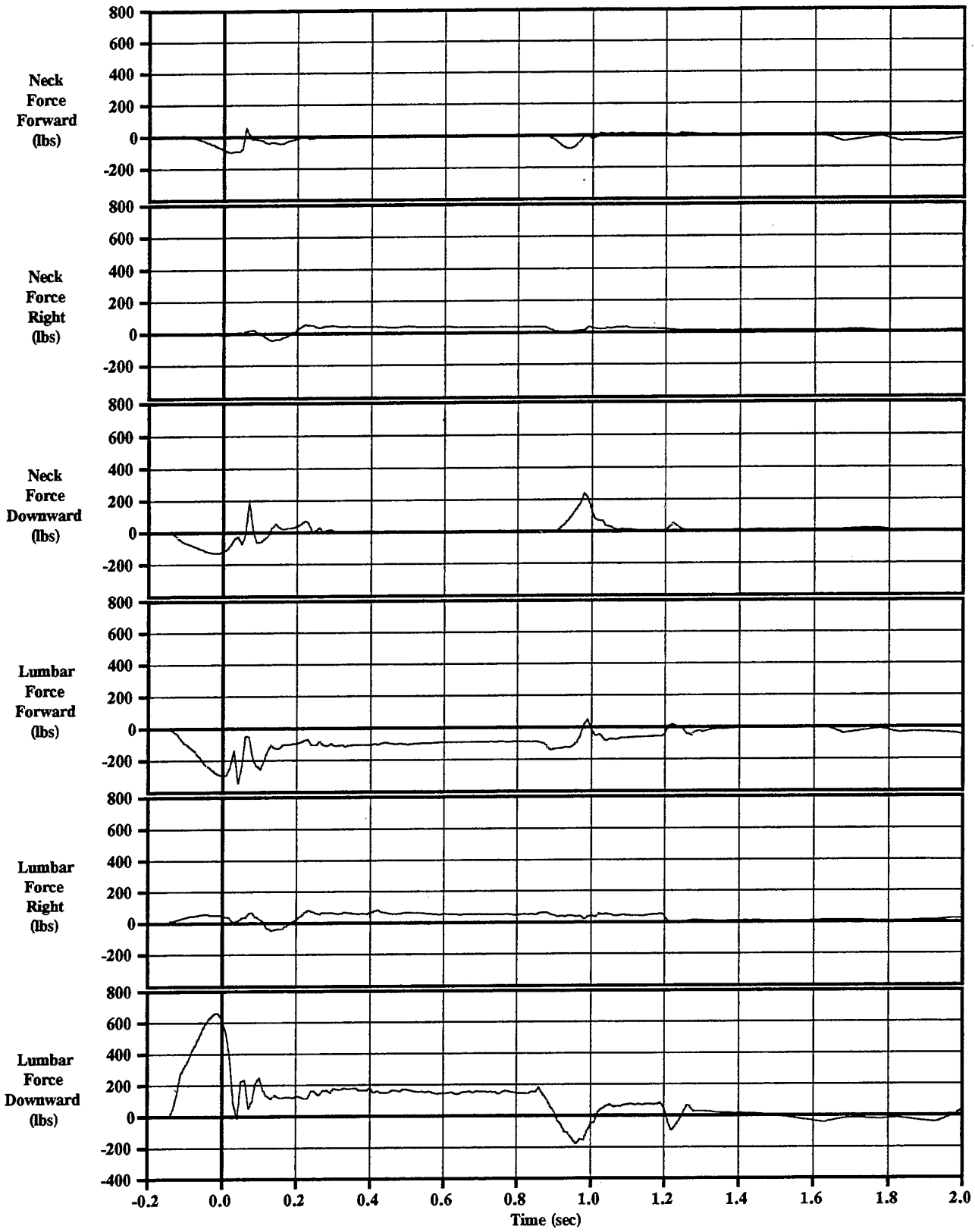

Figure C-2-9 ADAM Neck & Lumbar Forces
Sled Test=2, KEAS=0, 5th%, Roll=60

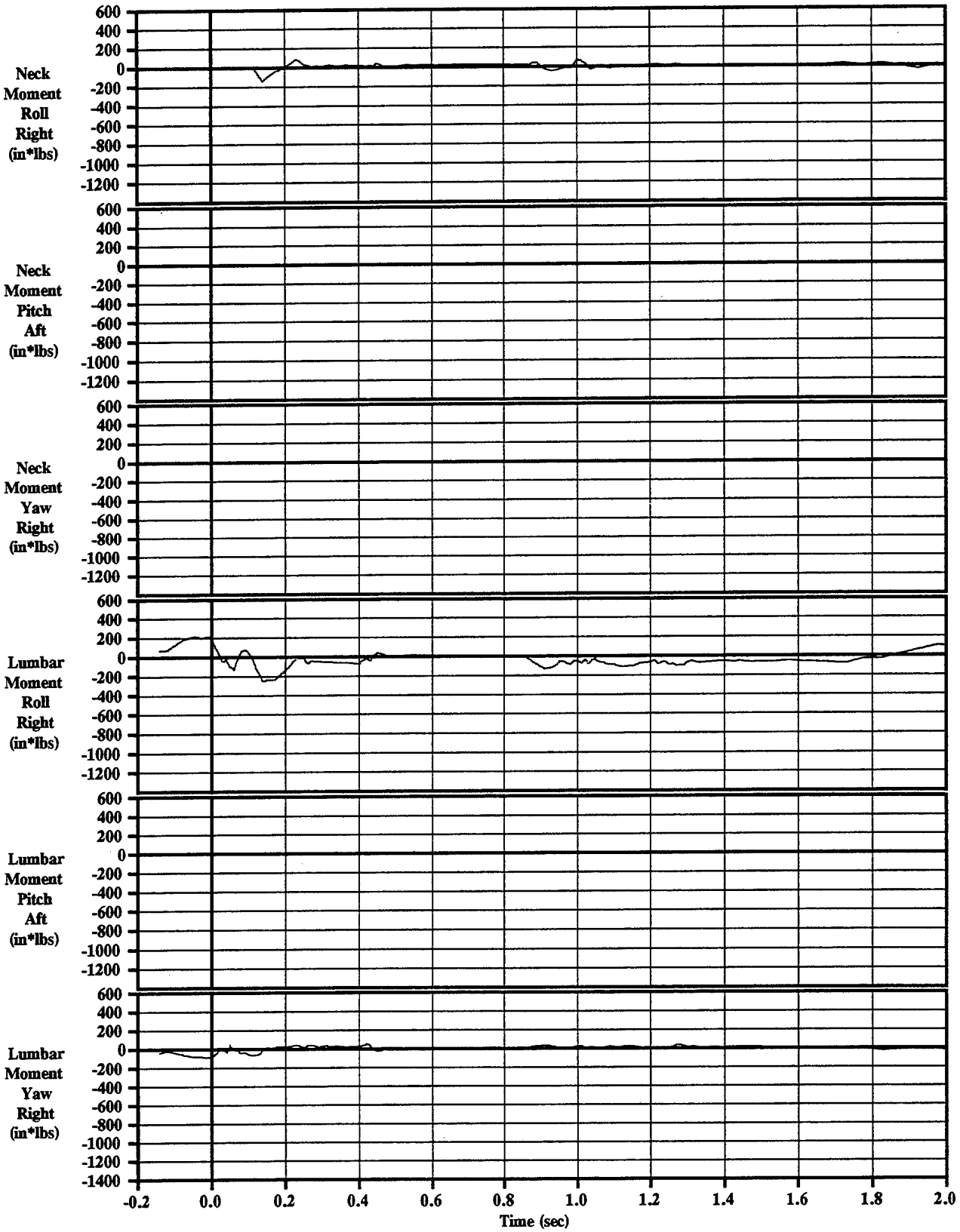

Figure C-2-10 ADAM Neck & Lumbar Moments
Sled Test=2, KEAS=0, 5th%, Roll=60

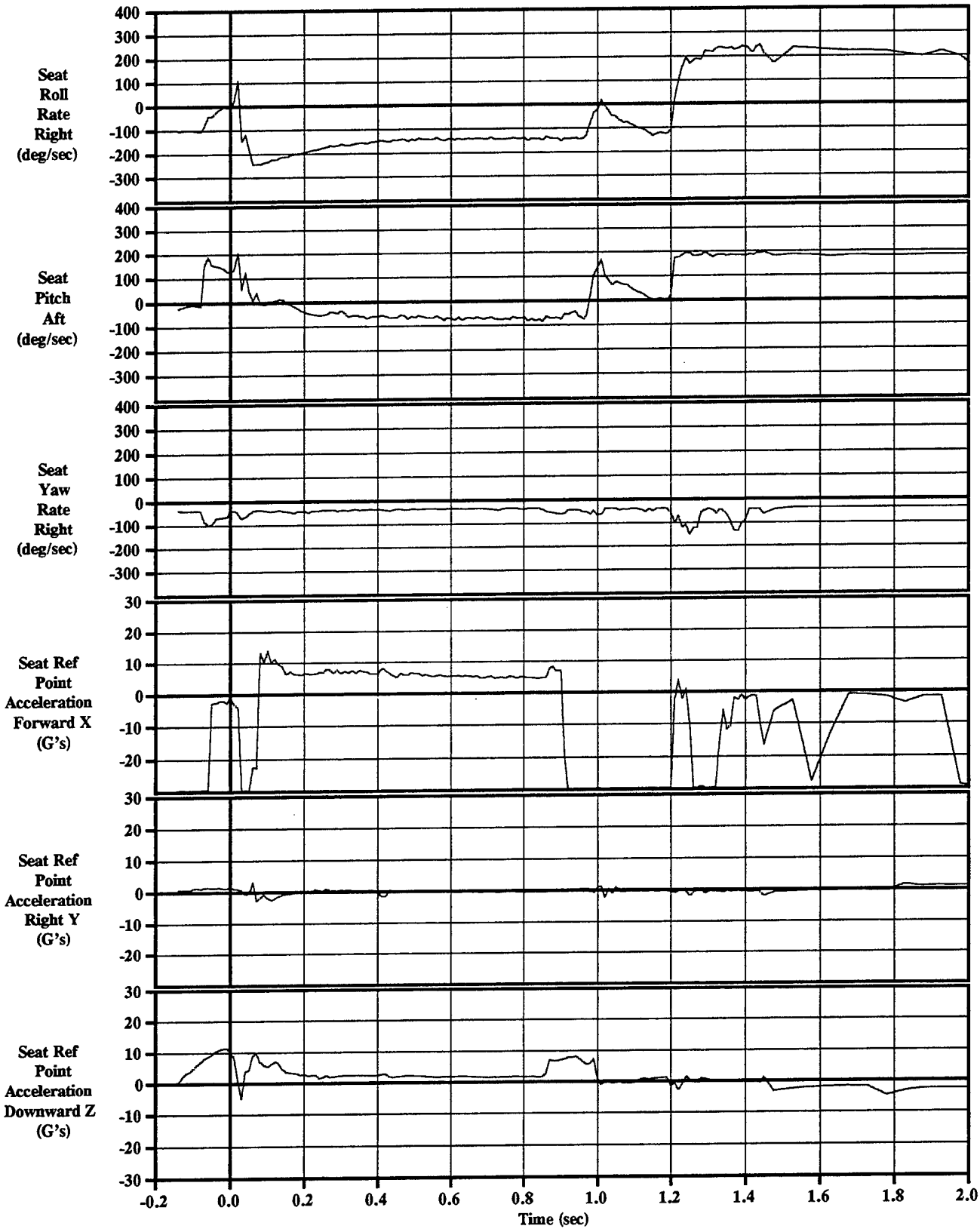

Figure C-2-11 ADAM Recorded Seat Rotation Rates and Accelerations
Sled Test=2, KEAS=0, 5th%, Roll=60

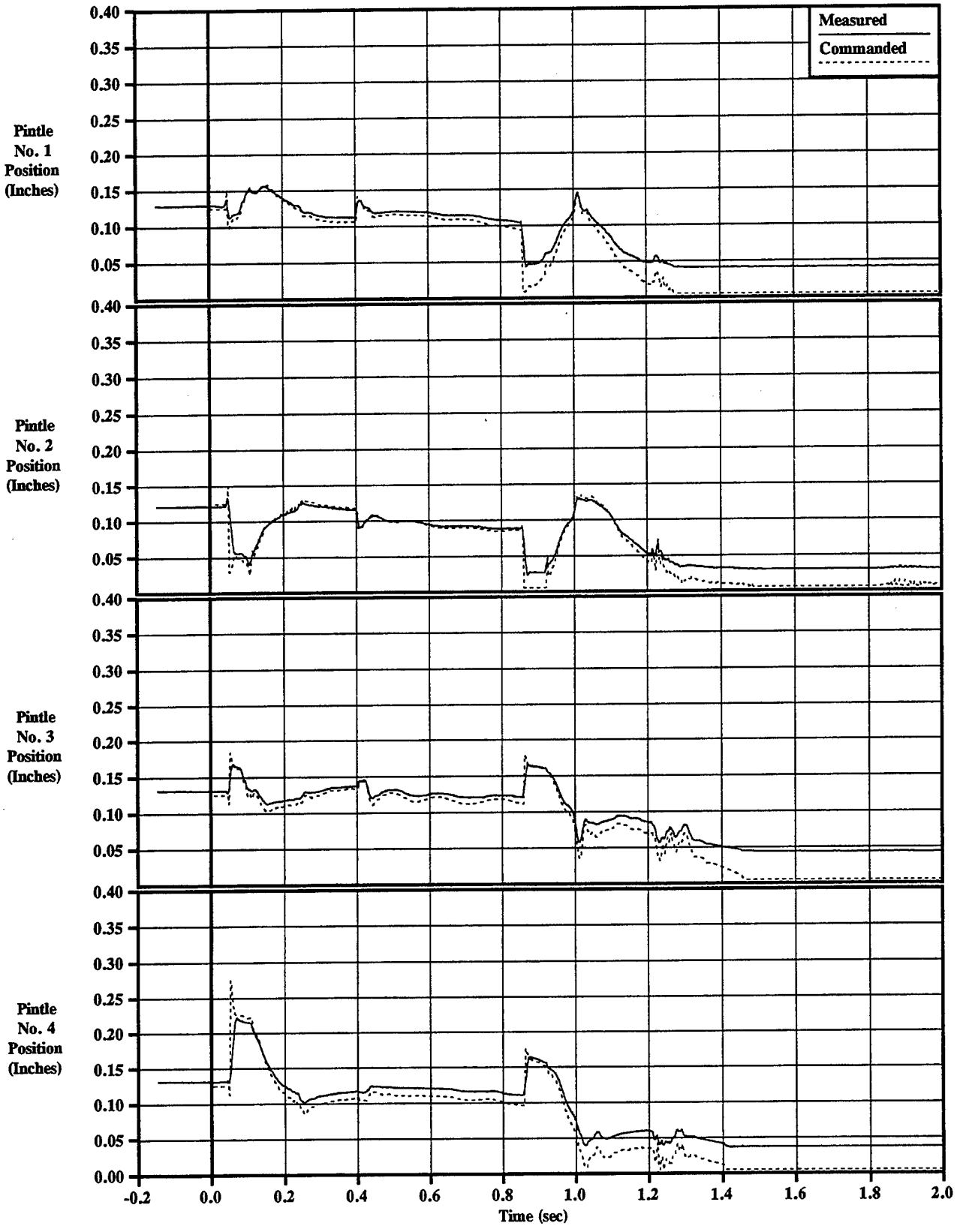

Figure C-2-12 Pintle Positions & Commands
Sled Test=2, KEAS=0, 5th%, Roll=60

APPENDIX C-3: TEST #3

TEST SUMMARY

Objective

The objective of this test was to demonstrate the flight controls and controllable propulsion system of the 4th Generation Escape System in a 325 KEAS, 60° roll flight condition.

Test Conditions

	Run Number	85E-C1
	Test Date	29 October 1996
	System Launch Time	12:30 PM MST
		303:19:30:00 IRIG
	Sled Launch Point	TS 3178
	Seat Eject Point	TS 6998 @ 9.952 sec
	Temperature	57 deg F
	Relative Humidity	29.0%
(1)	Wind	1.9 KTS from 296° (WNW)
	Barometric Pressure	12.73 lb/in^2
	Velocity	320 KEAS
	Sled Gx at Catapult Init	-1.25 G
	Roll	59.8 deg
	Pitch	0 deg
	Yaw	0 deg
	ADAM Size	Small

(1) 0° angle is a head wind. Positive to the right (clockwise).

Summary And Conclusions

The third system sled test of the 4th Gen demonstration ejection seat was conducted on 29-Oct-96 at Holloman AFB, NM. In this test, catapult firing and rocket motor ignition occurred as expected. However, flight control was not achieved and the seat impacted the ground approximately 0.7 seconds after rocket motor ignition. Post test analysis indicated that the Guidance Control Unit (GCU) stopped functioning approximately 0.03 seconds after rocket ignition due to a hardware failure induced by a shock load from the guide rail / seat interface. After the GCU stopped functioning, there were no commands issued to the pintle actuators of the rocket motor and the pintles remained in their initial positions. The 60° initial roll angle of the seat and the constant thrust vector of the rocket motor resulted in an uncontrolled trajectory and eventual ground impact.

The time of the shock load corresponds to the time that the middle set of rollers leaves the guide rails. The shock is caused by tip-off loads deflecting the rail forward,

and then releasing the rail when the middle roller comes out. This causes the guide rail to vibrate, and input a shock load into the seat via the lower roller which is still engaged in the guide rail.

Post test analysis indicated that the shock environment (caused by the seat rail interface) in the sled tests is worse than was anticipated and exceeds the limits of the GCU. To eliminate these problems, modifications to the GCU will be made to make it less susceptible to the shock environment. These modifications include staking of large components and isolation of the GCU from the seat structure. We further recommend switching from the rechargeable avionics battery to a single use thermal battery to withstand the higher than predicted vibration and shock environments as earlier evaluation of the rechargeable batteries indicated that they were sensitive to vibration and shock. The rail structure will also be stiffened to lessen the shock environment. These fixes when implemented are expected to resolve system level and component level deficiencies associated with the shock environment.

Data.
The primary data obtained from the IMU are presented in Figures C-3-1 through C-3-6.

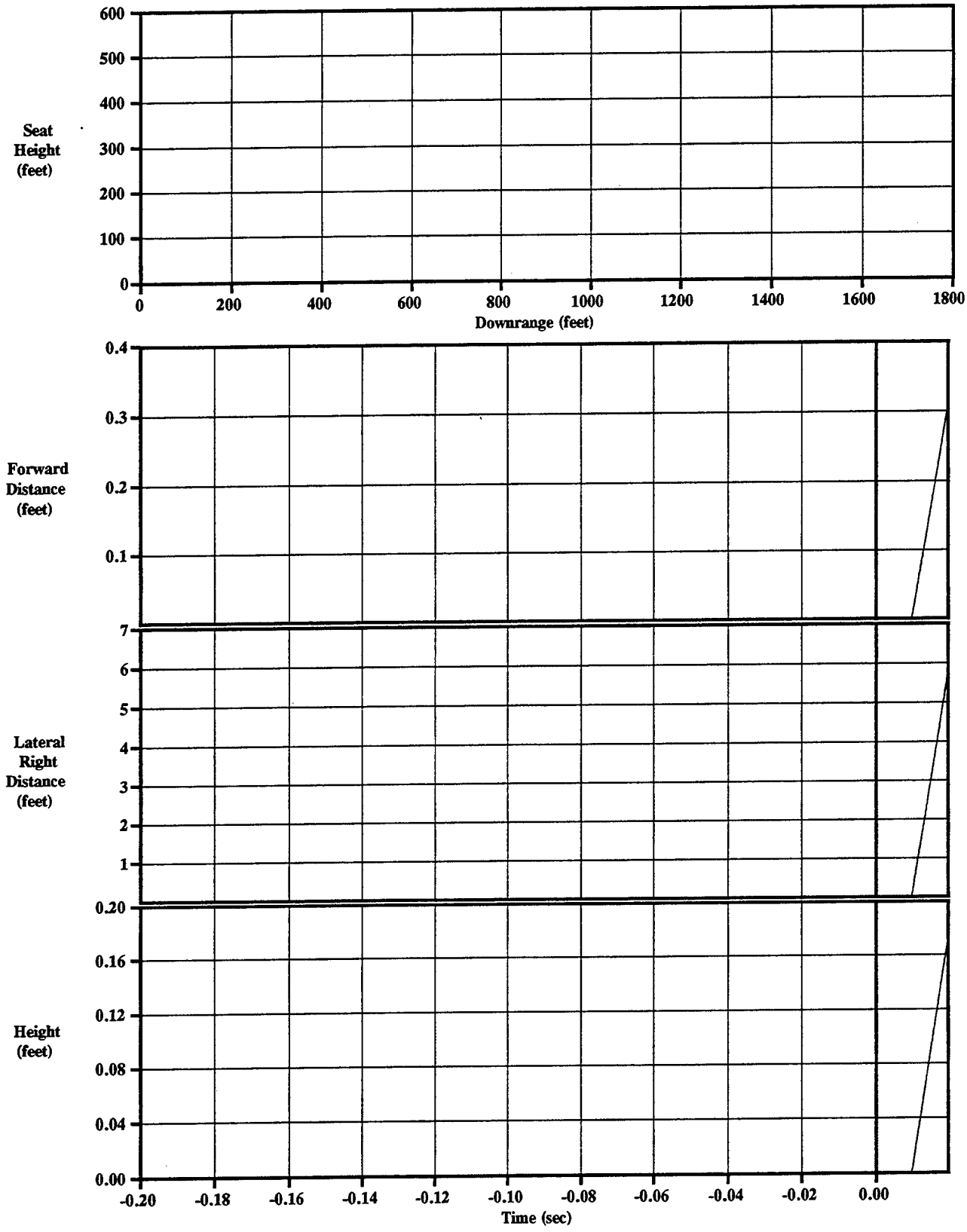

Figure C-3-1 IMU Displacements

Sled Test=3, Controller Quit at .03 sec, KEAS=320, 5th%, Roll=60

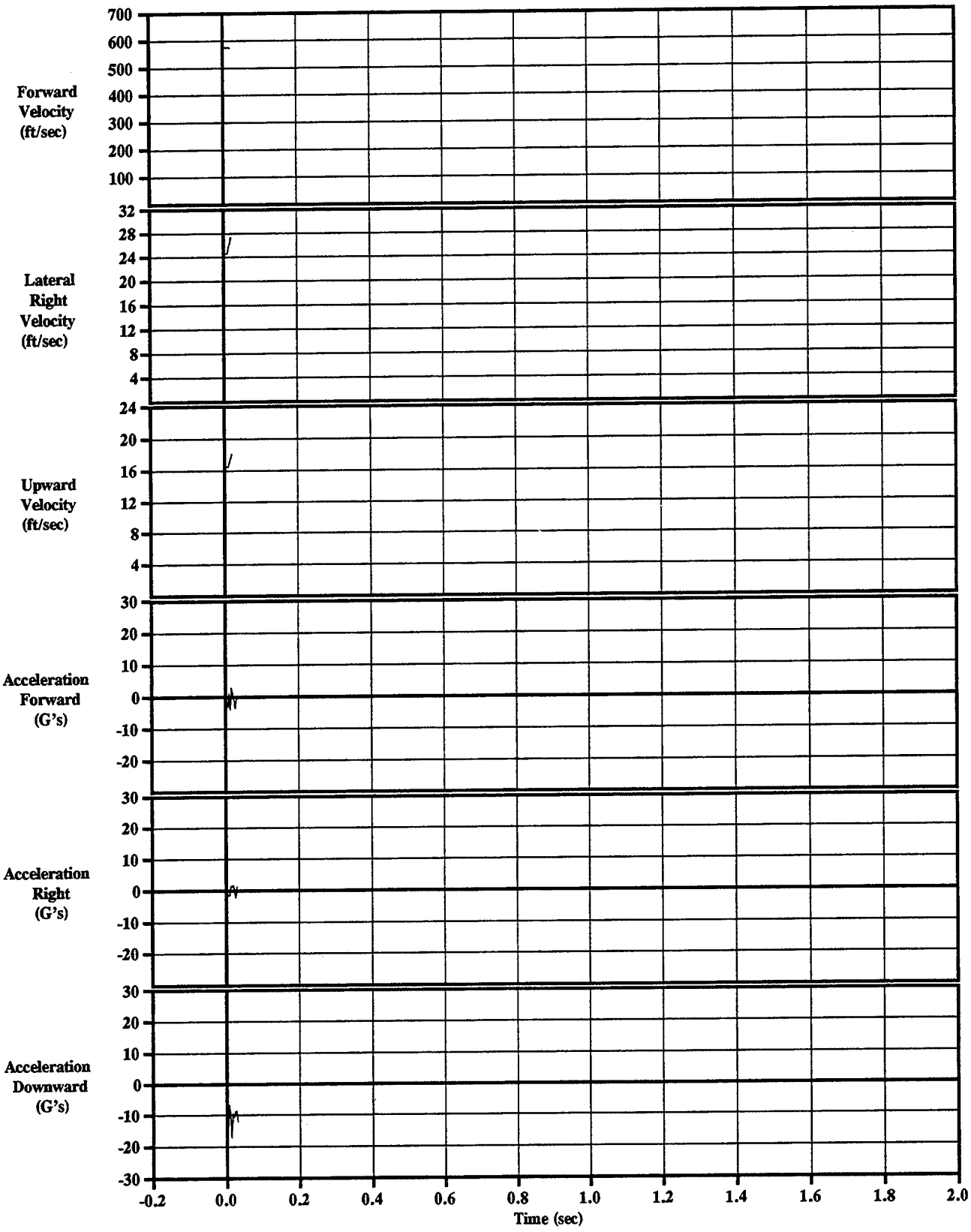

Figure C-3-2 IMU Velocities & Accelerations
Sled Test=3, Controller Quit at .03 sec, KEAS=320, 5th%, Roll=60

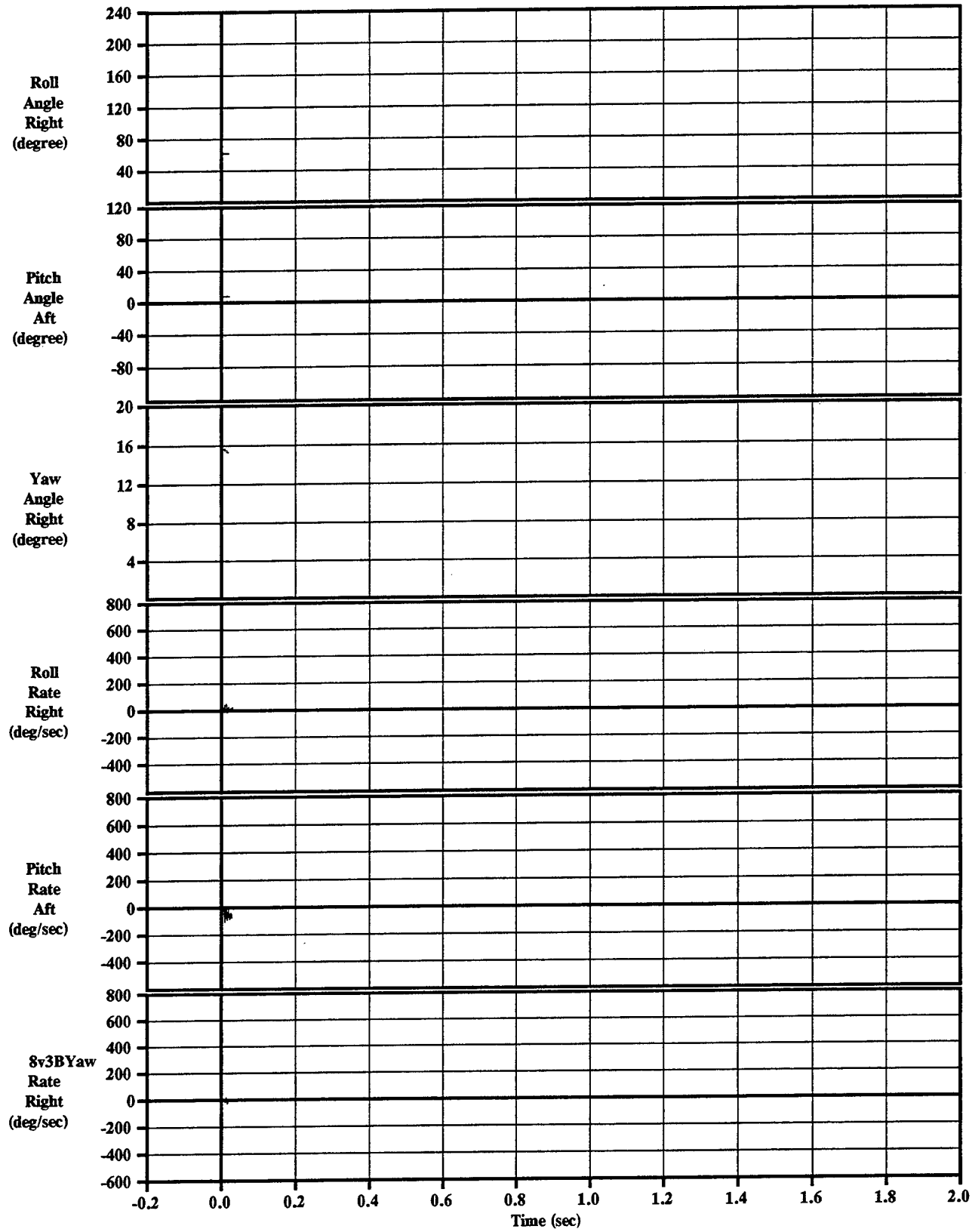

Figure C-3-3 IMU Rotation Angles & Rates
Sled Test=3, Controller Quit at .03 sec, KEAS=320, 5th%, Roll=60

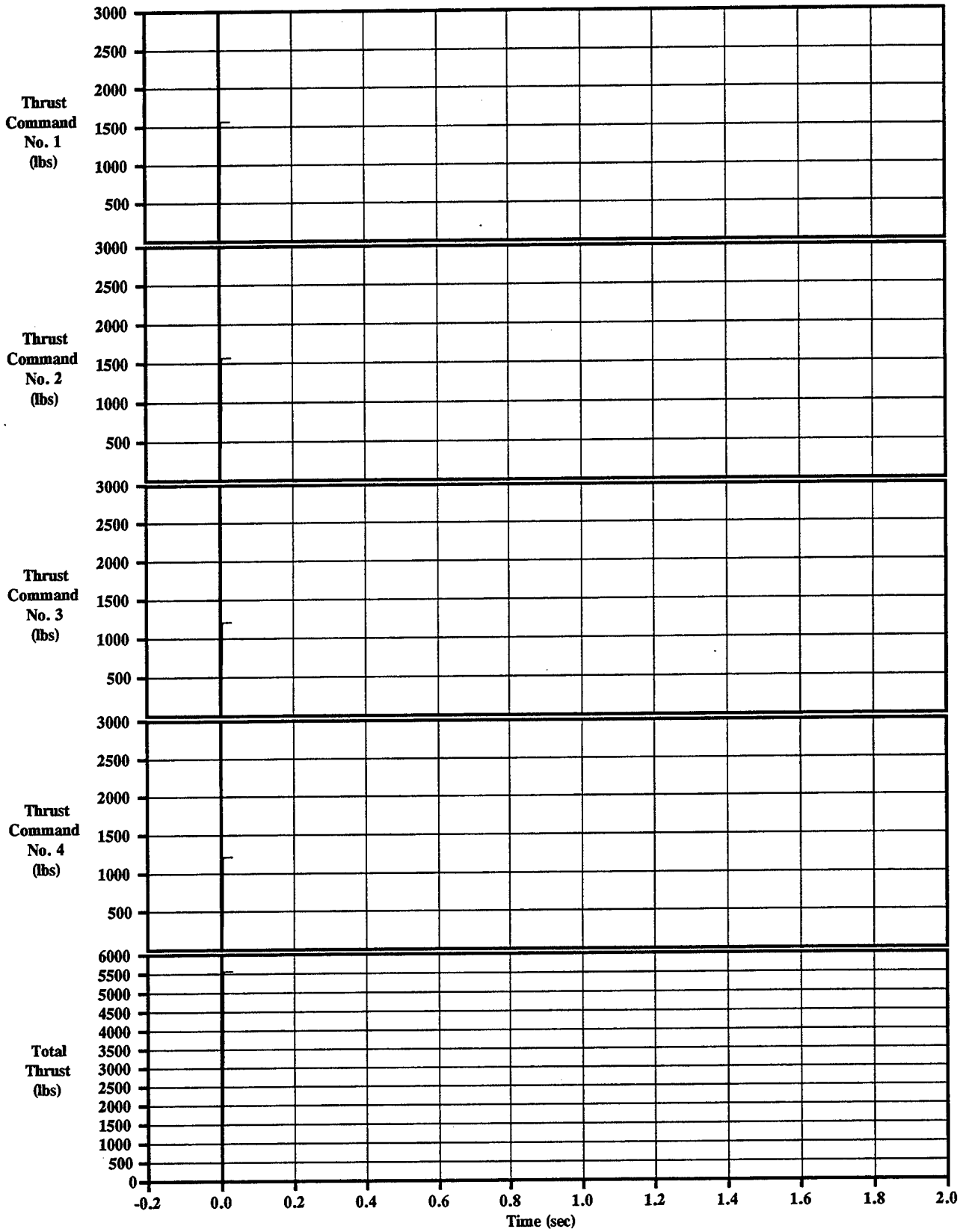

Figure C-3-4 Thrust Commands

Sled Test=3, Controller Quit at .03 sec, KEAS=320, 5th%, Roll=60

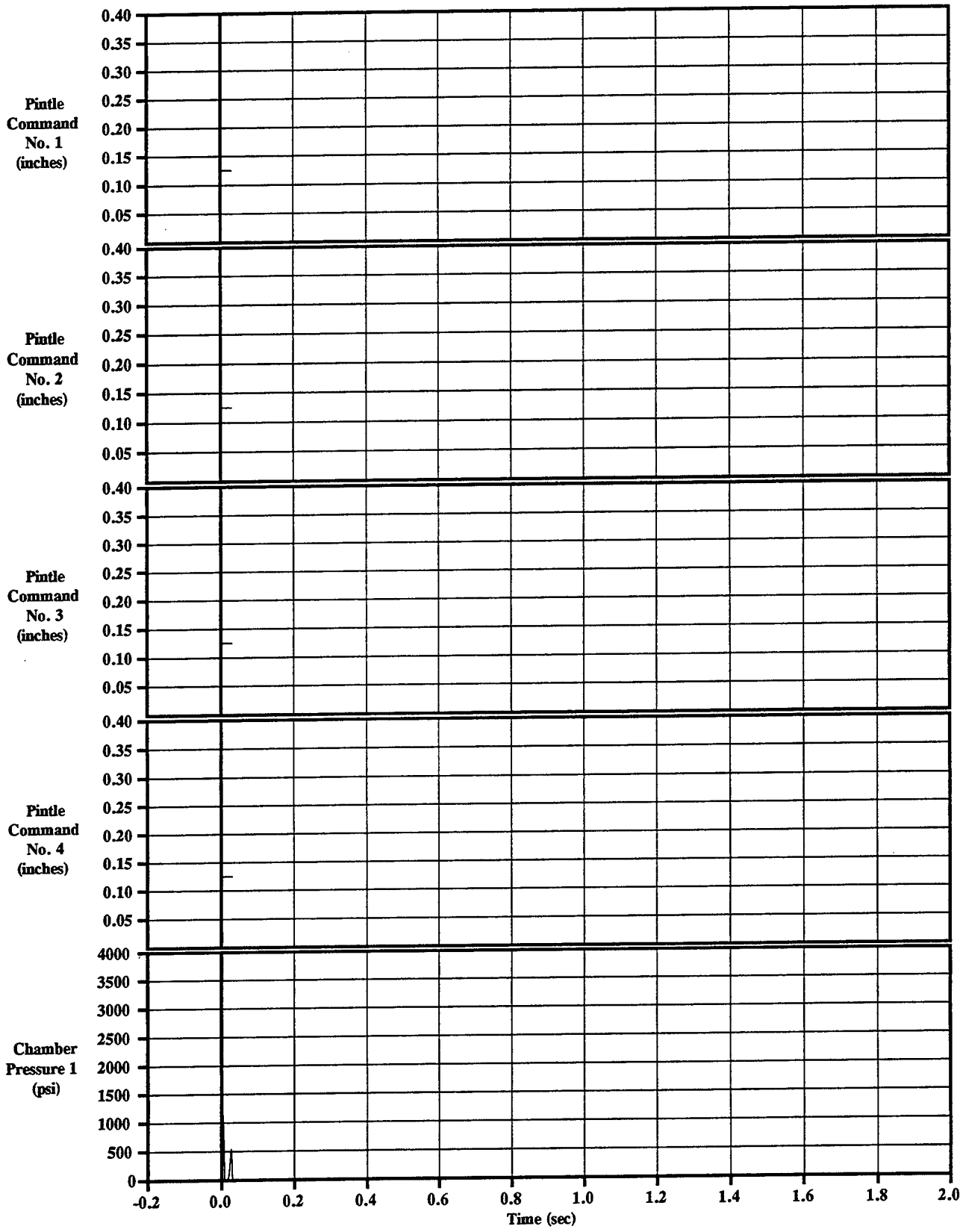

Figure C-3-5 Pintle Commands & Chamber Pressure
Sled Test=3, Controller Quit at .03 sec, KEAS=320, 5th%, Roll=60

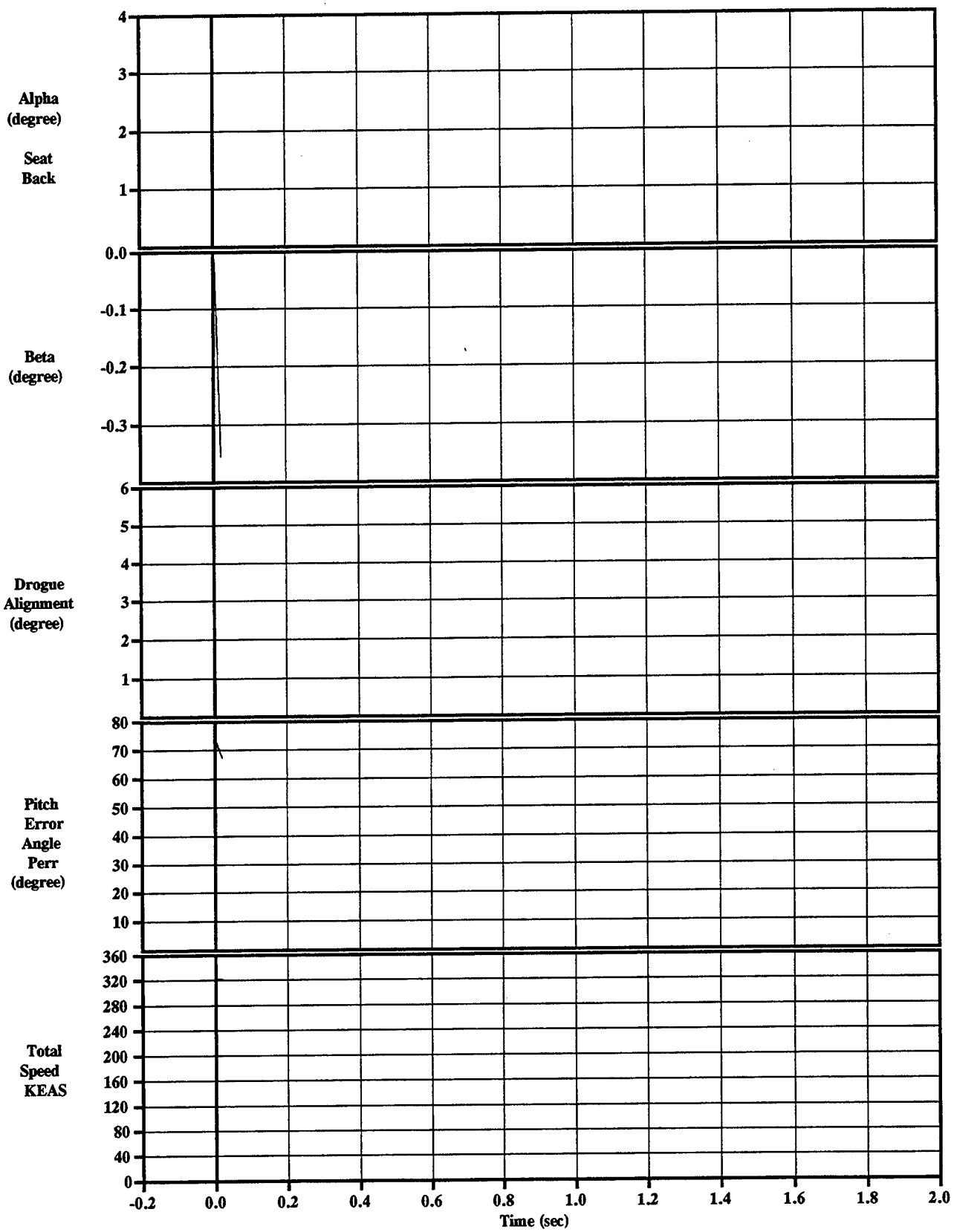

Figure C-3-6 IMU Control Angles and Total Velocity
Sled Test=3, Controller Quit at .03 sec, KEAS=320, 5th%, Roll=60

APPENDIX C-4: TEST #4

TEST SUMMARY

Objective

The objective of this test was to demonstrate the flight controls and controllable propulsion system of the 4th Generation Escape System in a 325 KEAS, 60° roll flight condition.

Test Conditions

	Run Number	85E-C3A
	Test Date	1 February 1997
	System Launch Time	1:14 PM MST 032:20:14:00 IRIG
	Sled Launch Point	TS 3178
	Seat Eject Point	TS 6998 @ 10.034206 sec
	Temperature	61 deg F
	Relative Humidity	41.3%
(1)	Wind	7.9 KTS from 285° (W)
	Barometric Pressure	25.898 lb/in^2
	Velocity	320 KEAS
	Sled Gx at Catapult Init	-0.81 G
	Roll	60 deg
	Pitch	0 deg
	Yaw	0 deg
	Hybrid III Manikin Size	Small

(1) 0° angle is a head wind. Positive to the right (clockwise).

Summary And Conclusions

The fourth system sled test of the 4th Gen demonstration ejection seat was conducted on 1 February 97 at Holloman AFB, NM. The seat was ejected from the MASE sled at ~325 KEAS at 60° right roll. Catapult firing and rocket ignition were achieved successfully. Upon leaving the rails, the seat achieved controlled, stable flight and performed a 60° left roll and pitch-back maneuver resulting in proper reorientation and upward trajectory. At 0.116 seconds after rocket ignition, the IMU accelerometers failed resulting in erroneous propulsion commands. The seat did not maintain the attitude and trajectory which were expected for this ejection condition, however the seat did gain more than enough altitude for operation of the recovery parachutes and both the manikin and the seat were recovered with no apparent damage. All data were successfully recorded throughout the ejection sequence.

Post test analysis showed that the system functioned normally in the initial stage of the ejection. After the IMU failure, the IMU began reporting false acceleration and

position data, resulting in incorrect guidance and control for the actual flight condition. However the thrust commands to the rocket were correct based on the false IMU data. The rocket motor maintained pressure control throughout the duration of burn despite the erratic thrust commands.

The two most likely causes of the shock load input that caused the failure of the IMU were determined to be:

1. Insufficient sway space in the GCU shock mount assembly which would allow the GCU to "bottom out"

2. The IMU being struck by the seat mounted portion of seat / sled umbilical during free flight.

Based on the failure analysis, the following modifications are recommended prior to the next test:

- Modify the GCU installation to provide additional sway space
- Add an aerodynamic cover over the IMU to mitigate potential aerodynamic loading
- Add logic to the flight software to maximize probability of seat recovery in event of accelerometer failure
- Modify the prelaunch check procedures to perform all avionics checks prior to squibbing the avionics battery

Data.
The primary data obtained from the IMU are presented in Figures C-4-1 through C-4-6.

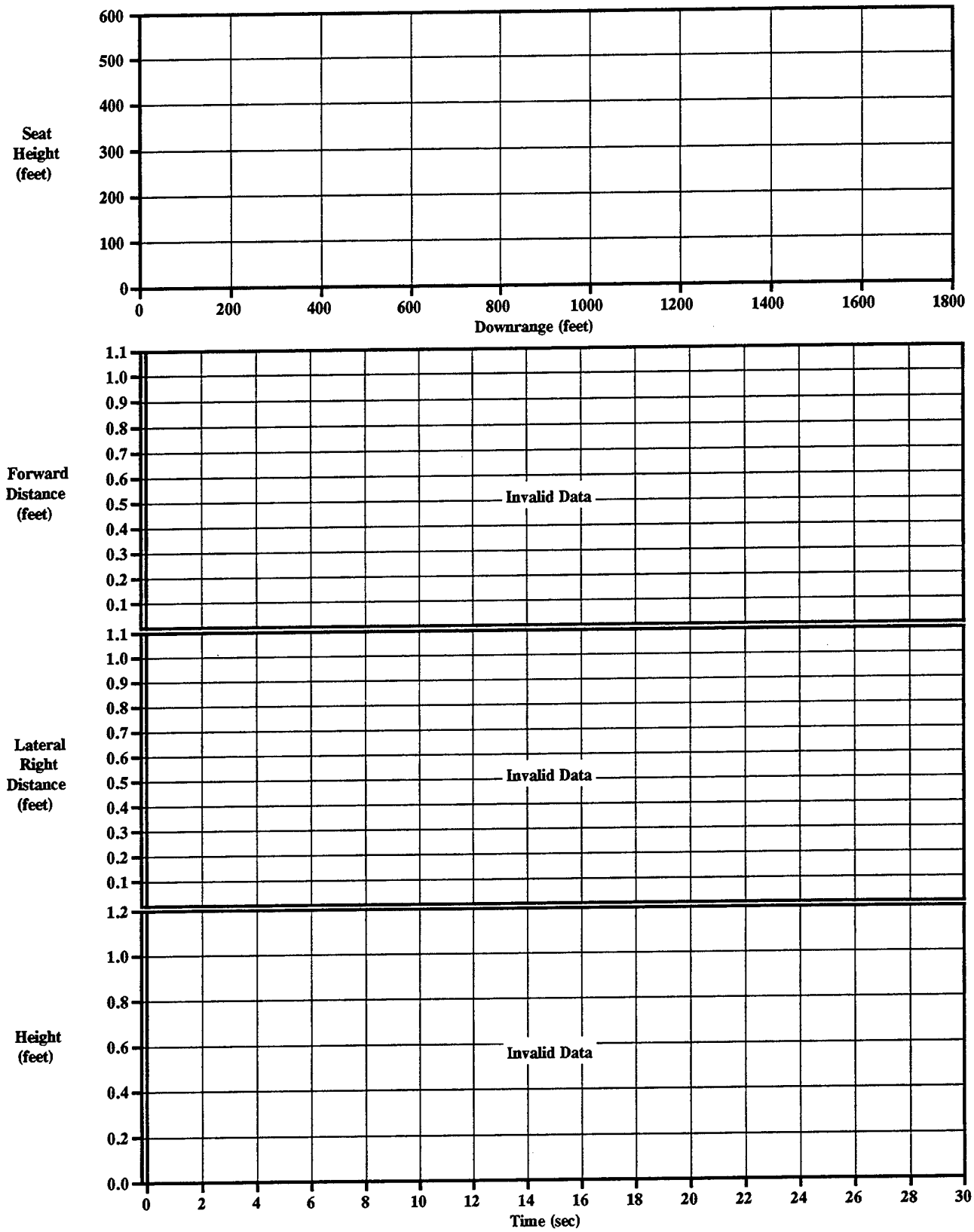

Figure C-4-1 IMU Displacements
Sled Test=4, Accels Broke at .116 sec, KEAS=330, 5th%, Roll=60

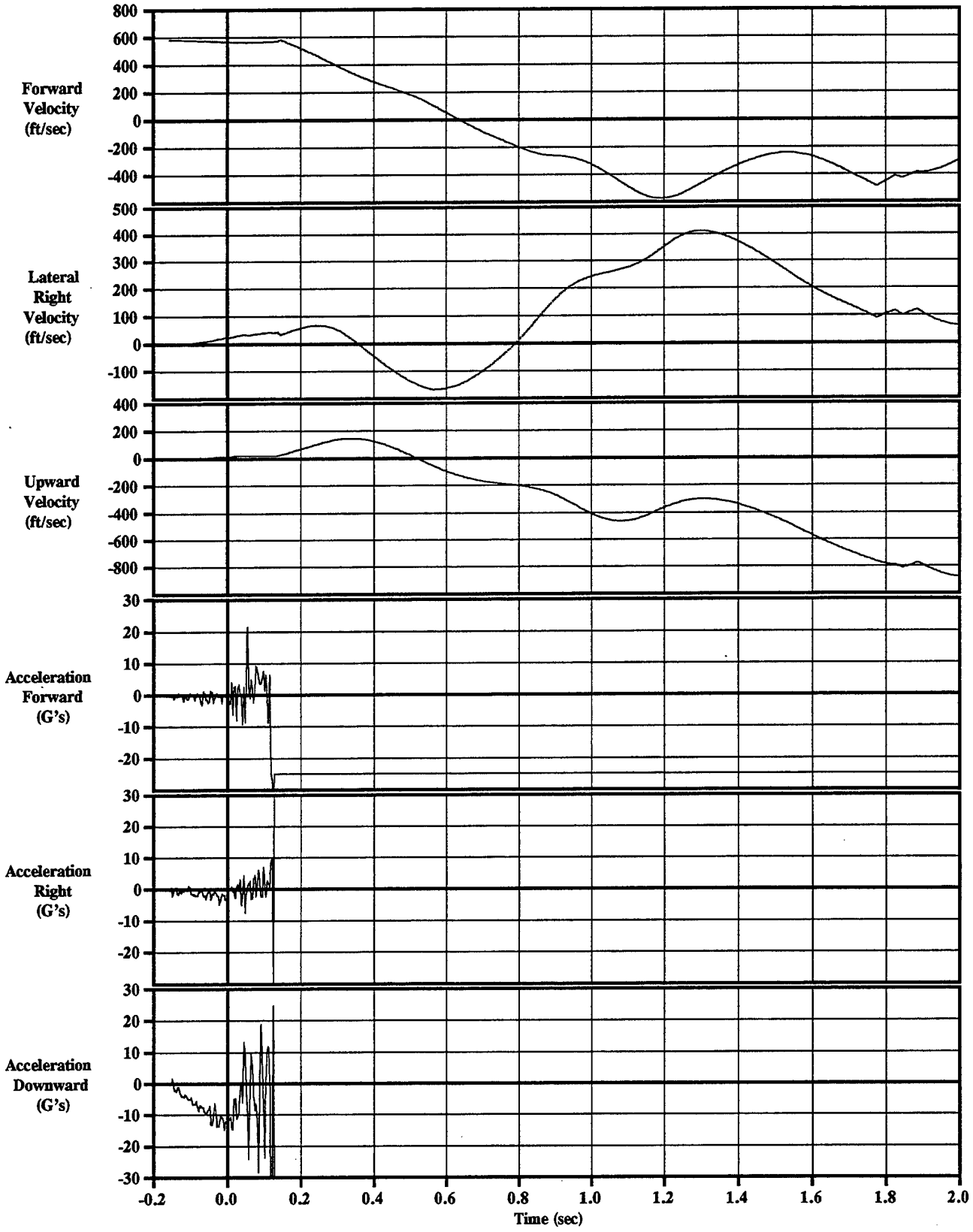

Figure C-4-2 IMU Velocities & Accelerations
Sled Test=4, Accels Broke at .116 sec, KEAS=330, 5th%, Roll=60

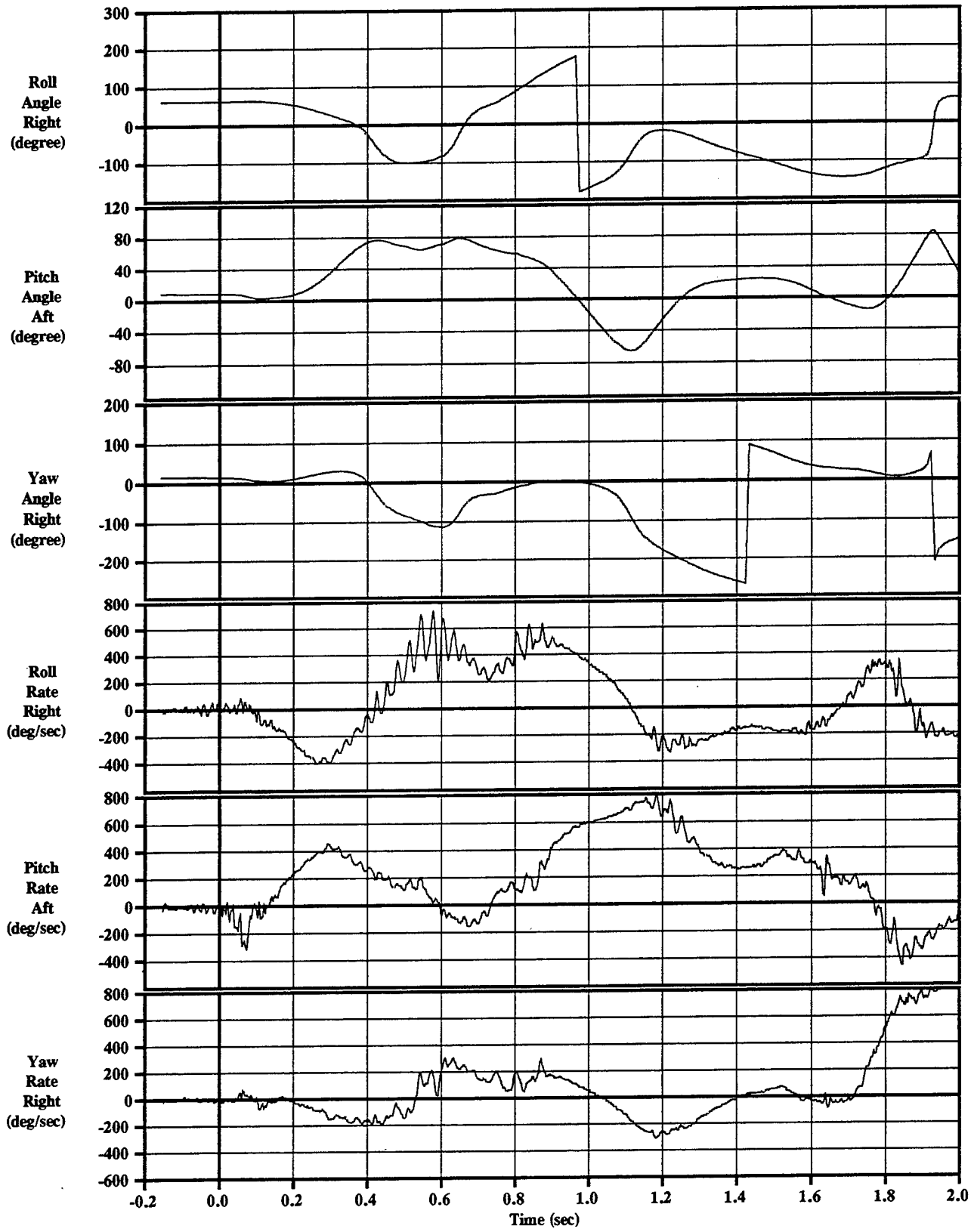

Figure C-4-3 IMU Rotation Angles & Rates
Sled Test=4, Accels Broke at .116 sec, KEAS=330, 5th%, Roll=60

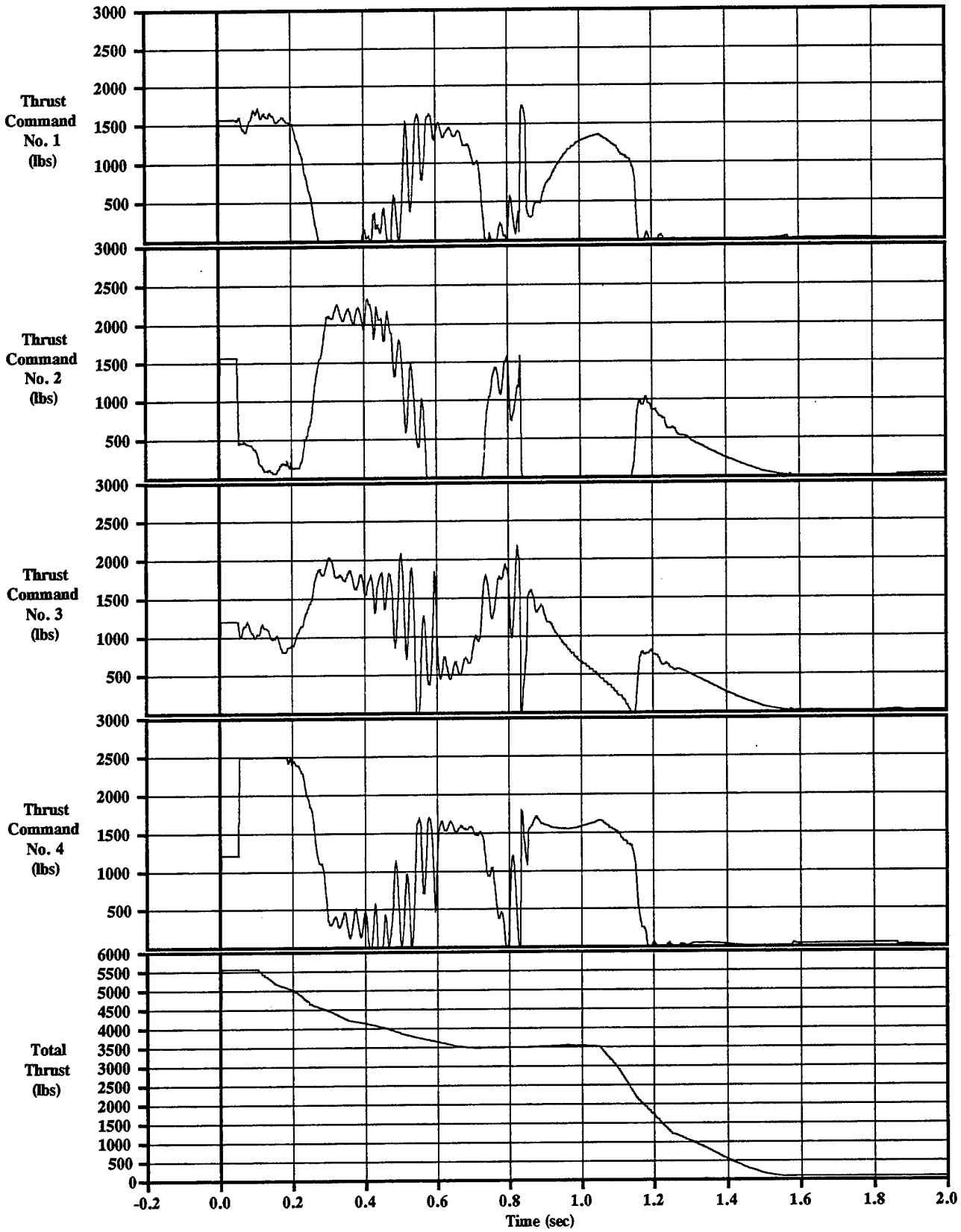

Figure C-4-4 Thrust Commands

Sled Test=4, Accels Broke at .116 sec, KEAS=330, 5th%, Roll=60

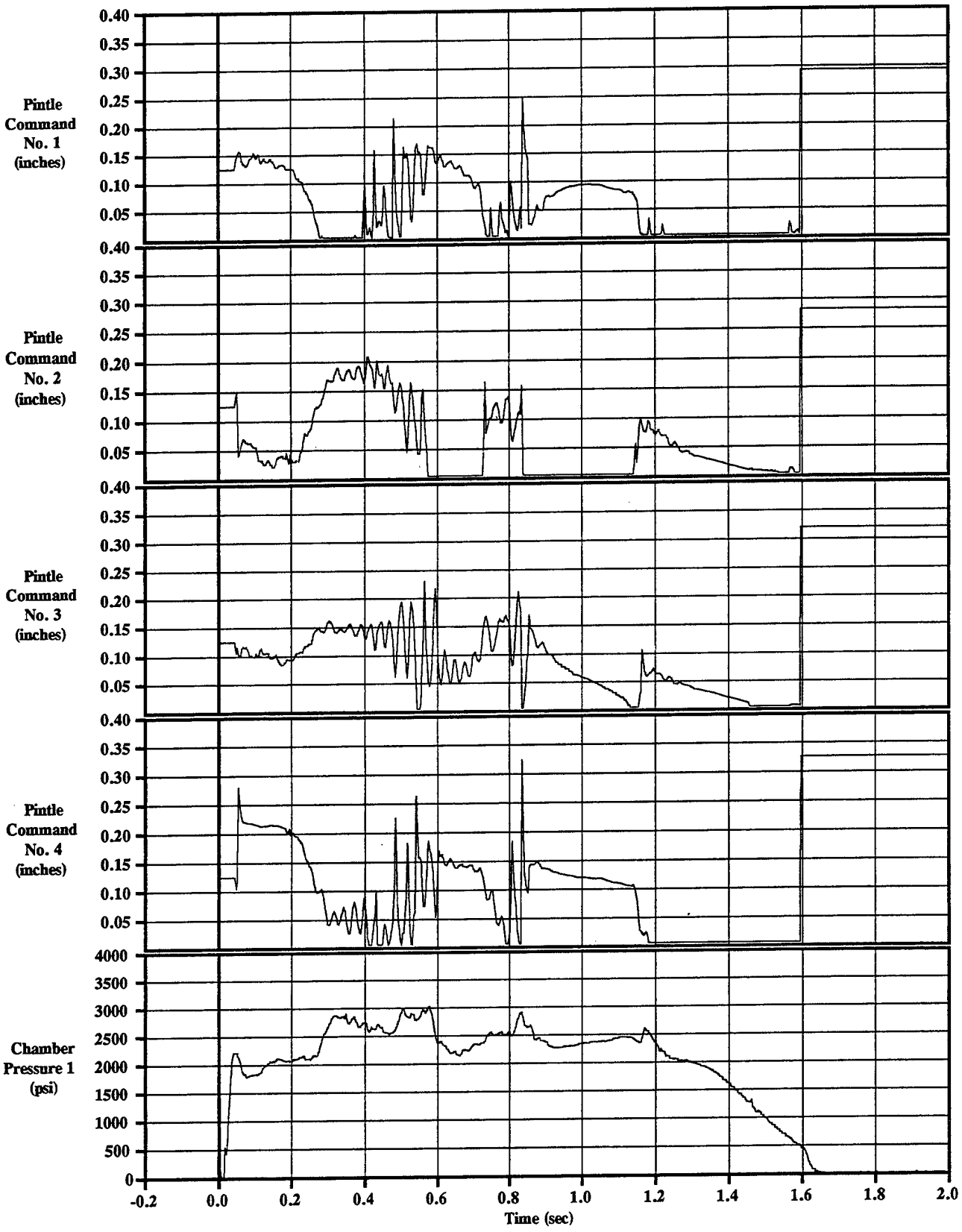

Figure C-4-5 Pintle Commands & Chamber Pressure
Sled Test=4, Accels Broke at .116 sec, KEAS=330, 5th%, Roll=60

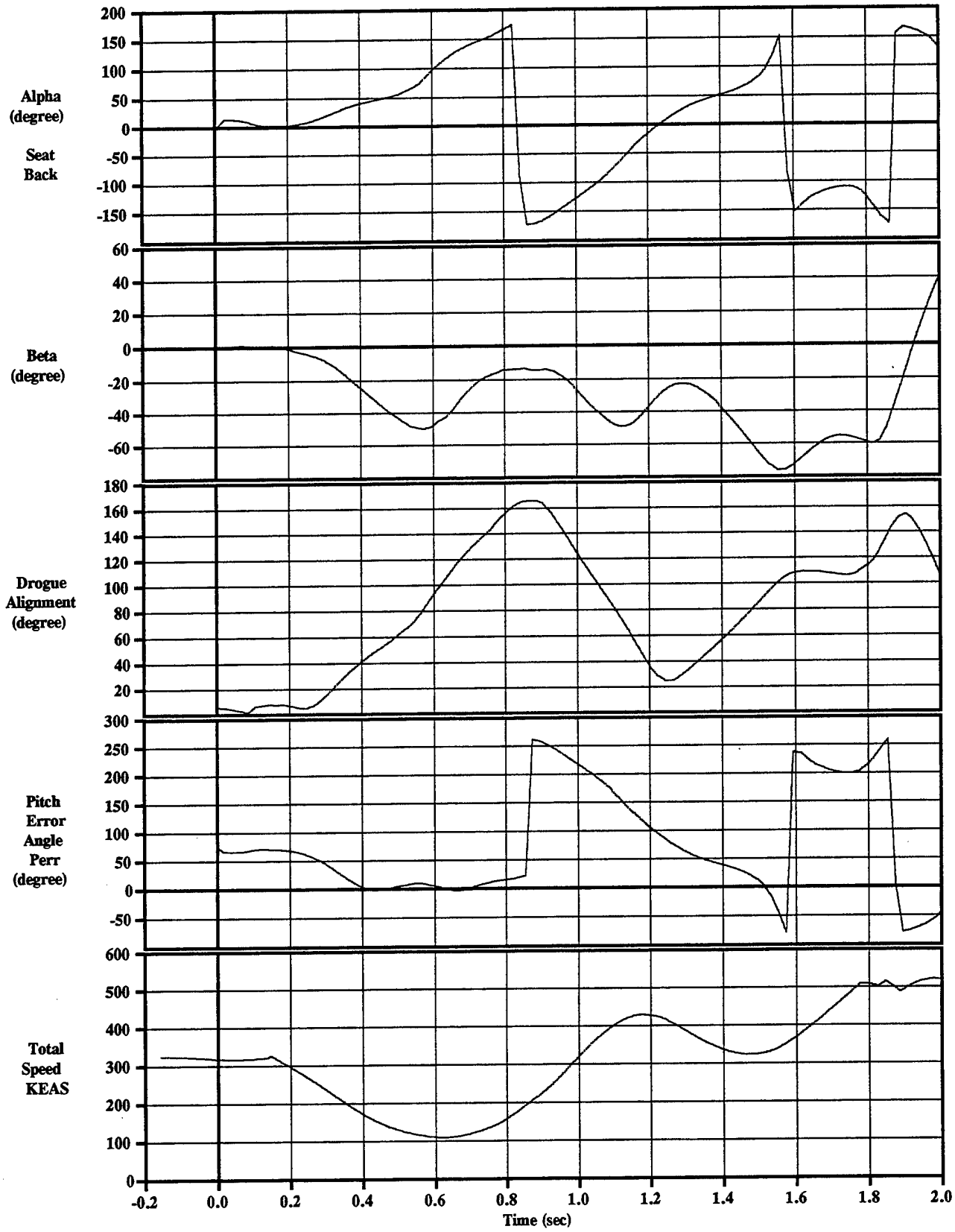

Figure C-4-6 IMU Control Angles and Total Velocity
Sled Test=4, Accels Broke at .116 sec, KEAS=330, 5th%, Roll=60

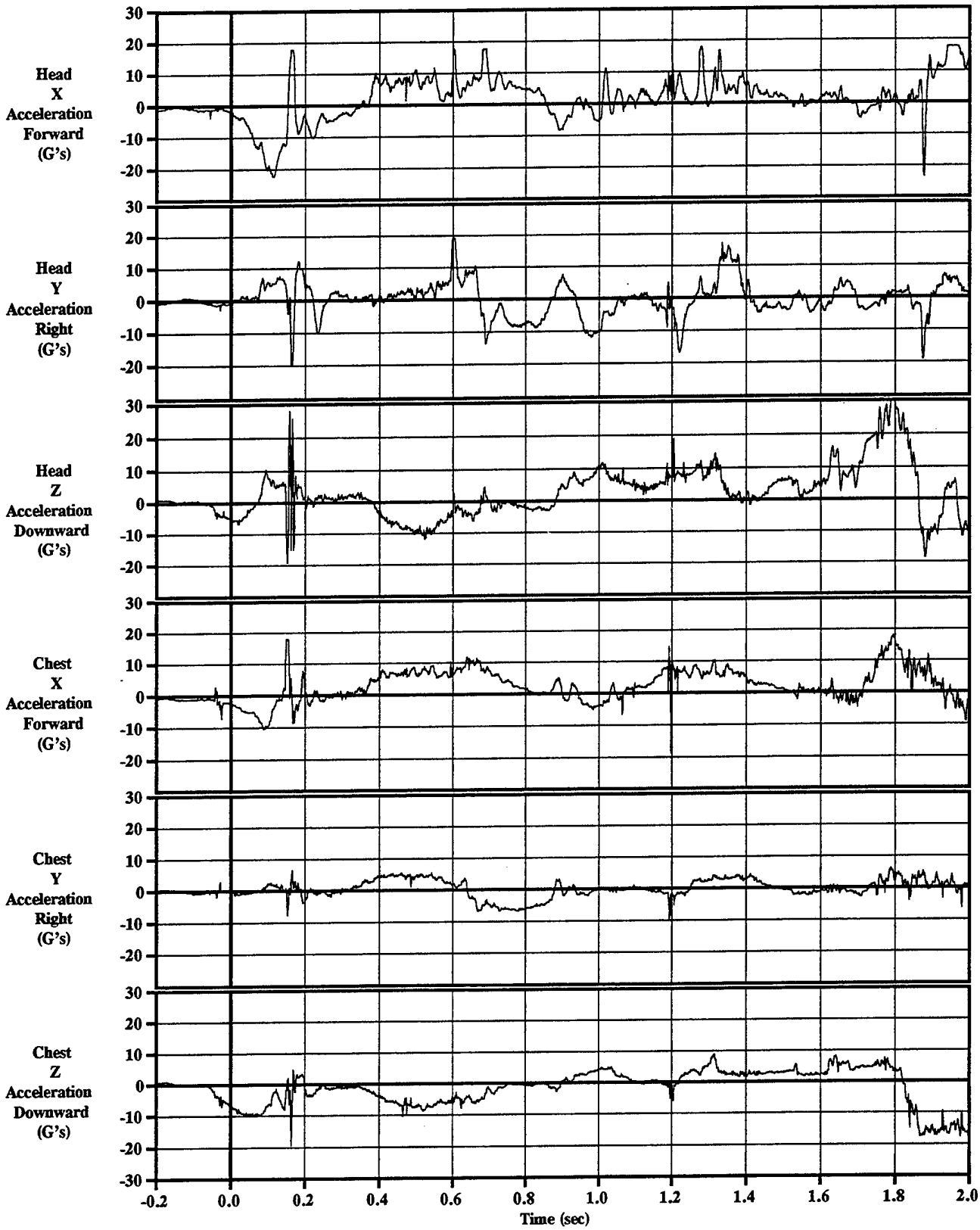

Figure C-4-7 Manikin Head & Chest Accelerations
Sled Test=4, KEAS=325, 5th%, Roll=60

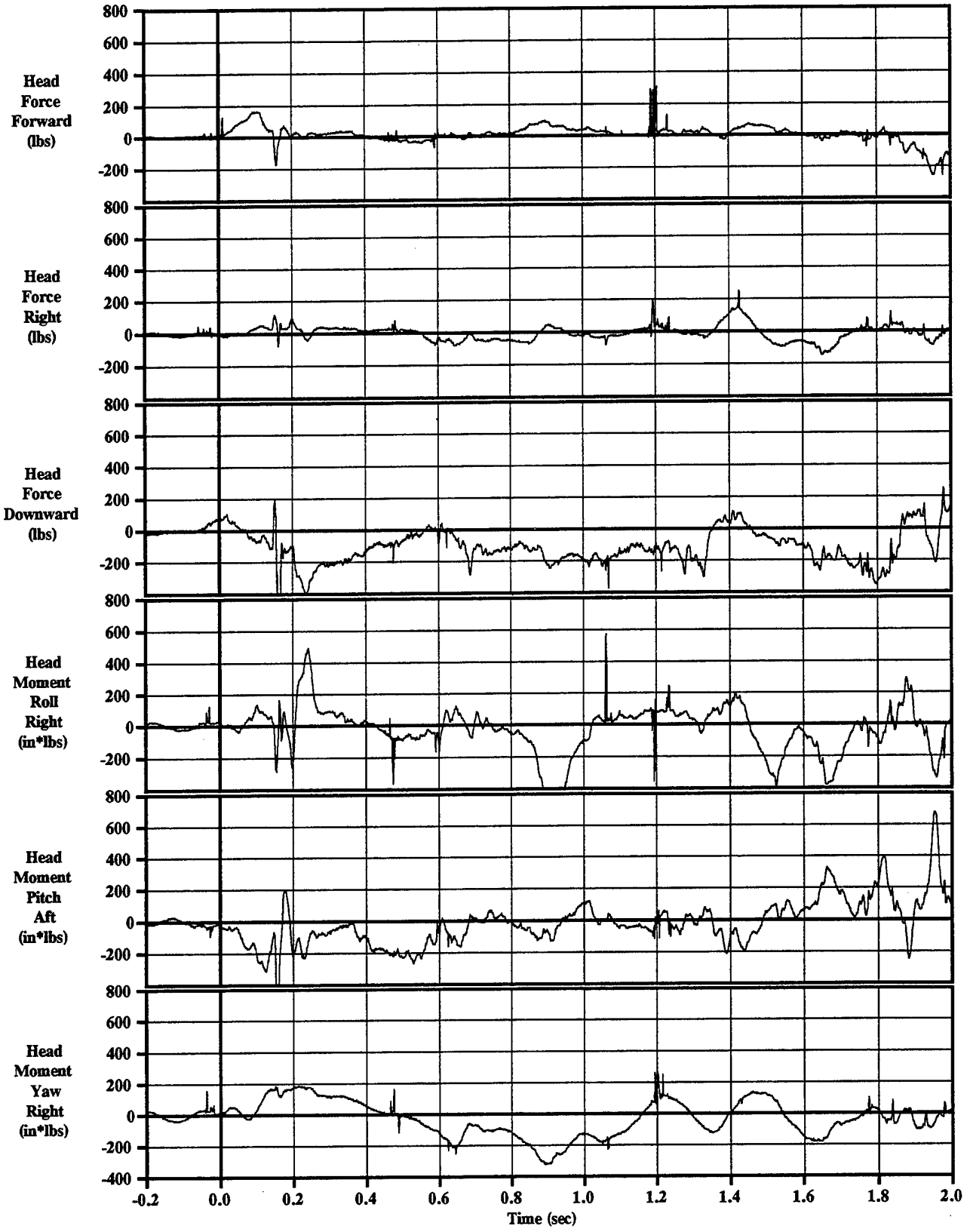

Figure C-4-8 Manikin Head Force & Moment
Sled Test=4, KEAS=325, 5th%, Roll=60

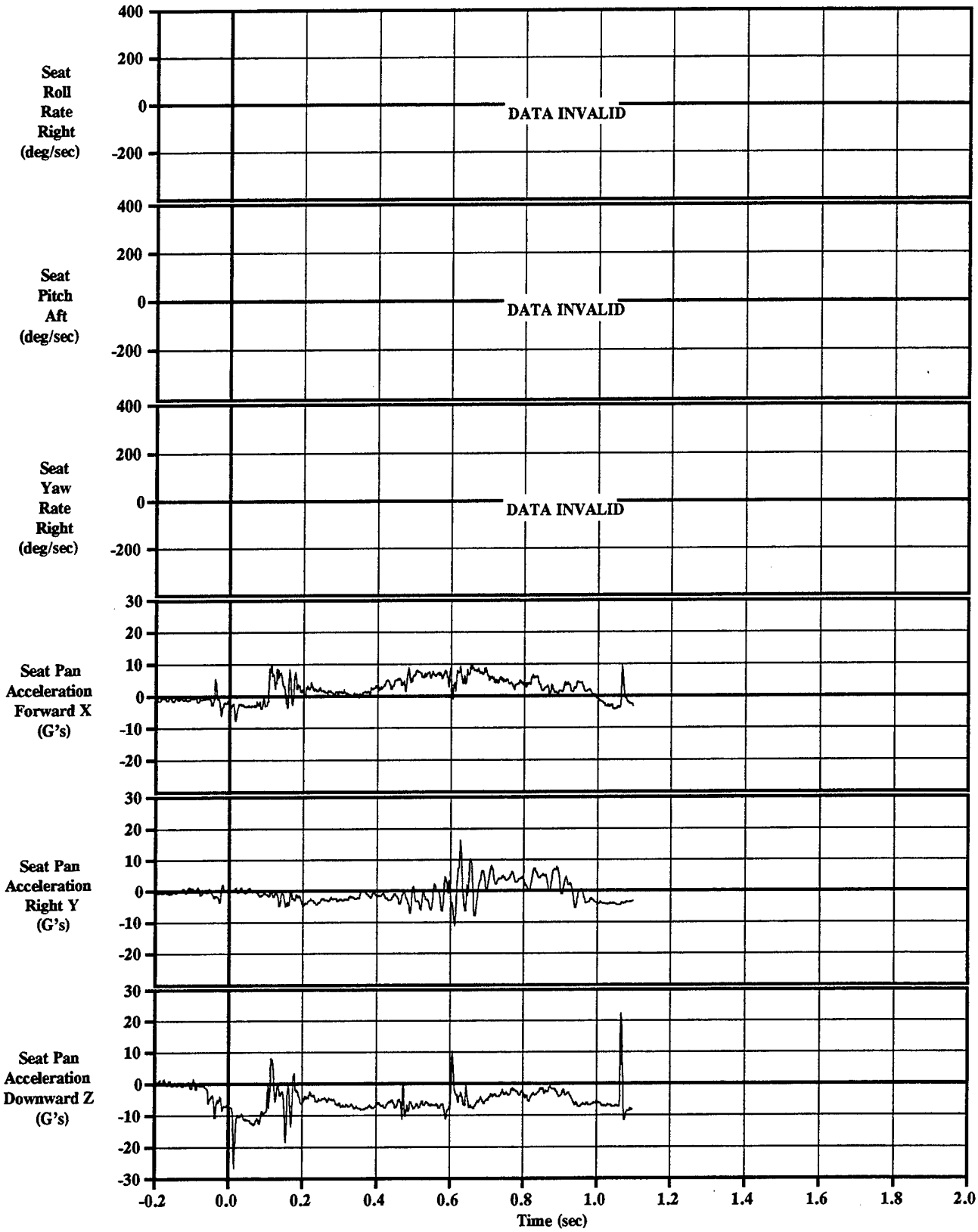

Figure C-4-9 Seat Angular Rates & Seat Pan Acceleration (80 Hz filter)
Sled Test=4, KEAS=325, 5th%, Roll=60

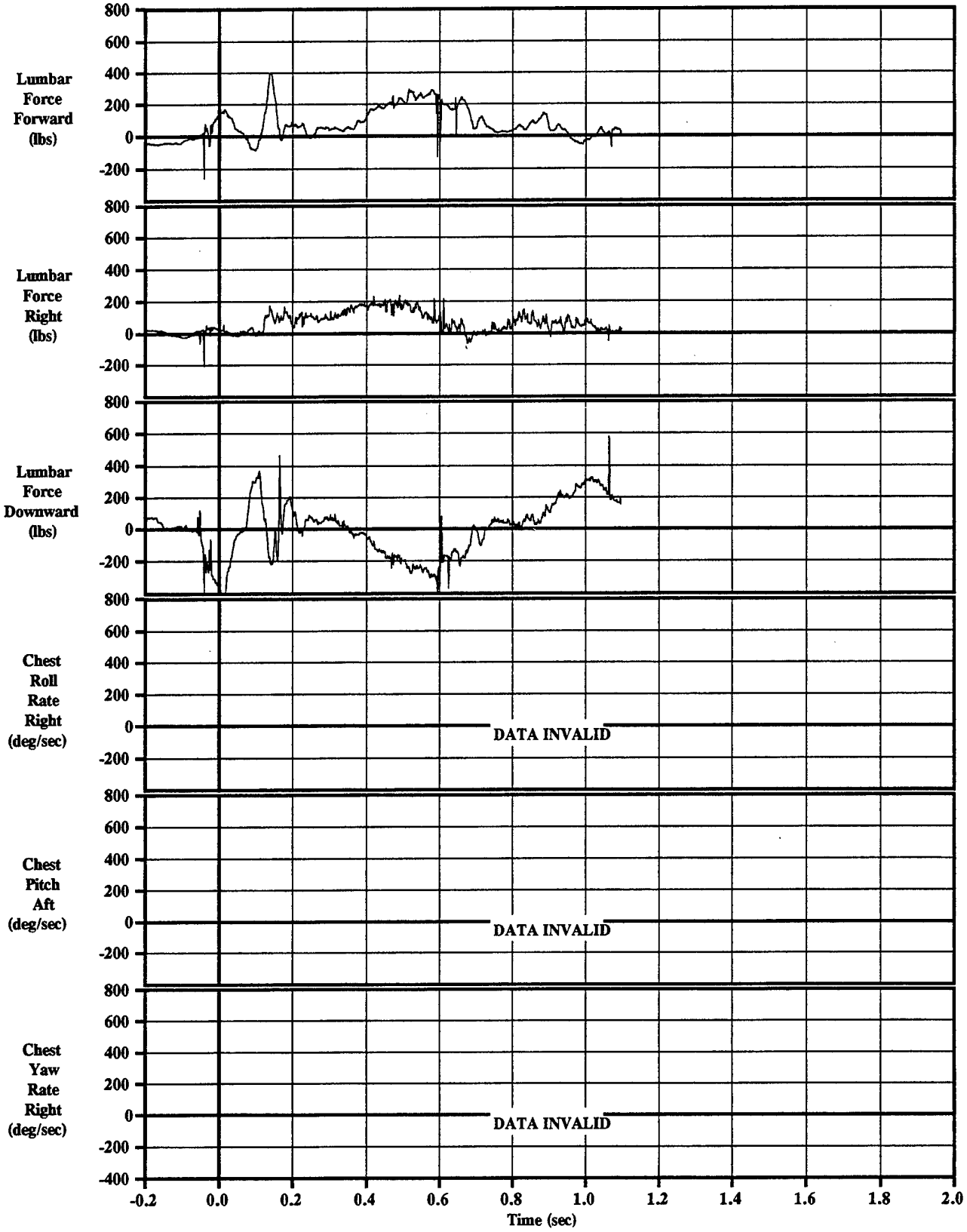

Figure C-4-10 Manikin Chest Rates & Lumbar Force
Sled Test=4, KEAS=325, 5th%, Roll=60

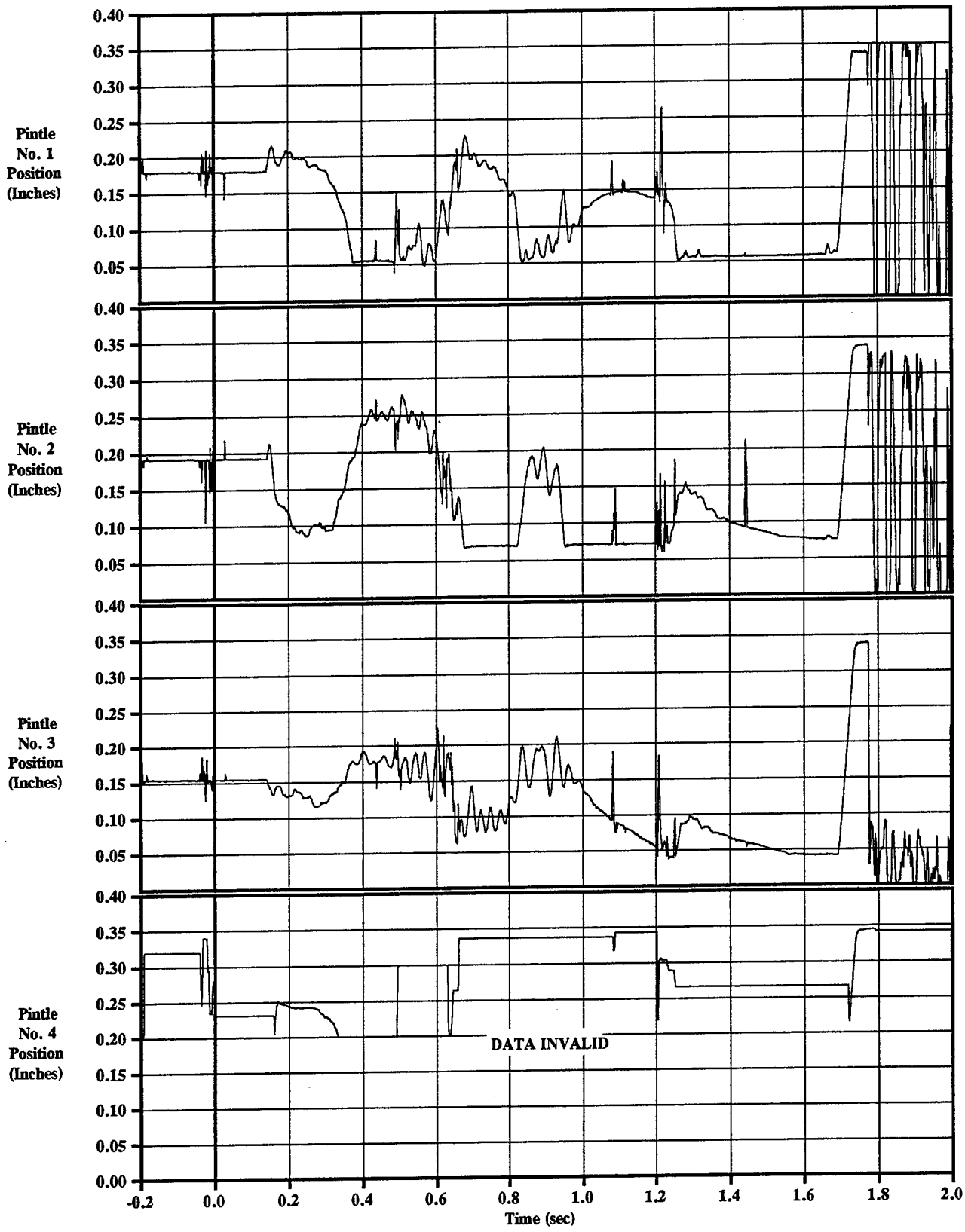

Figure C-4-11 Pintle Positions
Sled Test=4, KEAS=325, 5th%, Roll=60

Appendix C-5: Test #5

TEST SUMMARY

Objective

The objective of this test was to demonstrate the flight controls and controllable propulsion system of the 4th Generation Escape System in a 325 KEAS, 20° yaw flight condition.

Test Conditions

	Run Number	85E-D1A
	Test Date	3 April 1997
	System Launch Time	12:53 PM MDT
	Sled Launch Point	TS 2904
	Seat Eject Point	na
	Temperature	72 deg F
	Relative Humidity	na
(1)	Wind	13.6 KTS from 158° (SSE)
	Barometric Pressure	25.691 lb/in^2
	Velocity	325 KEAS
	Sled Gx at Catapult Init	na
	Roll	0 deg
	Pitch	0 deg
	Yaw	20 deg
	Hybrid III Manikin Size	Small

(1) 0° angle is a head wind. Positive to the right (clockwise).

Summary And Conclusions

The fifth system sled test of the 4th Generation demonstration ejection seat was conducted on 3 April 97 at Holloman AFB, NM, and the seat did not eject from the sled due to a fault in the catapult enable relay circuit. This cause of the fault was found to be a damaged (failed open) trace on the GCU motherboard resulting in an open circuit condition on the circuit. The damaged trace was caused by a short circuit condition between the 28 VDC and catapult enable relay return signal. The short circuit path was from a 28 VDC wire and the cable shield in the main seat wire harness (W1), and a common ground point at the TM interface used to detect the catapult relay closure. The complete seat system is checked out just prior to installation in the MASE sled on L-2 day. For this test all systems, including the catapult enable circuit, passed the pre sled installation checks. The procedures inplace for this test did not include the conduct of a complete end-to-end test of the catapult enable circuit with the seat installed in the sled.

However, subsystem checks, that exercise the catapult enable relay, were conducted. It is apparent therefore, that the system failed some time between the L-2 day checks and the time of sled launch.

There was also an unrelated problem with the squib arm circuit. The data indicate that the squib arm signal was detected by the GCU at the time of sled propulsion initiation instead of when the sled reaches the squib arm screen box. The cause of the premature arming has not been positively identified. However it is suspected that the extremely short (200 μsec) closure time required for the squib arm switch detect allowed a brief intermittent in a cable connection, due to the mechanical environment of propulsion initiation, to be detected as the squib arm event.

The assets expended on this test include the sled pusher motors, and the three seat mounted thermal batteries. The catapult and controllable propulsion system were not initiated during the test and can be reused along with the rest of the seat assembly.

The corrective actions resulting from this test are:

- Increase squib arm filter time to 4 msec
- Conduct a vibration test of the catapult enable relay to ensure it can withstand repeated use under the test conditions.
- Use a new relay for each test.
- Conduct a TRR 1 week prior to test to ensure all test hardware and procedures are in order
- Electrically isolate the track TM system from the MDA avionics system
- Move the sled onto the track on L-2 day to ensure a full L-1 day for TM and system checks
- Conduct an end-to-end test of the squib arm and catapult enable circuits trackside using the MDA flight computer and the track TM system
- Conduct a final TRR on L-1 day to verify all checks are complete

Appendix C-6: Test #6

TEST SUMMARY

Objective

The objective of this test was to demonstrate the flight controls and controllable propulsion system of the 4th Generation Escape System in a 325 KEAS, 20° yaw flight condition.

Test Conditions

	Run Number	85E-D2A
	Test Date	13 June 1997
	System Launch Time	9:17 AM MDT 164:15:17:00 IRIG
	Sled Launch Point	TS 2903
	Seat Eject Point	TS 6998 @ 10.53064 sec
	Temperature	72 deg F
	Relative Humidity	50%
(1)	Wind	6.8 KTS from 264° (W)
	Barometric Pressure	12.575 lb/in^2
	Velocity	317 KEAS (586 fps)
	Sled Gx at Catapult Init	-1.8 G
	Roll	0 deg
	Pitch	0 deg
	Yaw	20 deg
	Hybrid III Manikin Size	Small

(1) 0° angle is a head wind. Positive to the right (clockwise).

Summary And Conclusions

The sixth system sled test of the 4th Generation Escape System demonstration ejection seat was conducted on Friday, 13 June at Holloman AFB, NM. This test resulted in a motor over-pressure abort 0.374 seconds after motor initiation. At the time of the abort, the system had completed the yaw correction maneuver and was in the pitchup maneuver. The maximum pressure that the propulsion system achieved was 3917 psi. After the abort command, the pintles were retracted and the drogue deployed. When the system velocity decelerated to less than 220 KEAS the main recovery parachute was deployed. Both the seat and manikin were successfully recovered by parachute. Analysis of the test data indicated two problem areas:

- Autopilot instability
- Motor controller performance

Autopilot Instability

The test data showed that the flight controller was commanding a ~30 Hz roll axis oscillation. Evaluation of the acceleration data from the GCU mount locations revealed that the seat bottom structure has a ~30 Hz vibration mode that was exciting the natural frequency of the GCU shock mounts in the lateral direction and inducing an ~30 Hz mode into the autopilot. At this point the analysis that indicated the need for the shock mounts was reevaluated, using the new data obtained in this test. All previous acceleration data had been extrapolated from seat locations remote to the GCU mounts and had indicated a shock environment that would require isolation to protect the GCU. The data obtained in test 6 at the shock mount interface to the seat indicated that the shock environment is significantly less than what was predicted from the extrapolated data. Additional lab testing of a GCU under 230g 2ms shocks and 450g 1ms shocks verified that the GCU can withstand the environment measured at the GCU mounts in test 6. Future sled tests will be conducted without the GCU shock mounts.

Motor Controller Performance

The motor controller algorithm is intended to limit the thrust commands (i.e. pintle position) to maintain the proper chamber pressure, however in this test pressure control was not maintained. Analysis has shown that the actuation system hardware performed properly, but that motor controller software has a limit of pintle command frequency and amplitude that it can control motor pressure to. In this test the ~35 Hz command generated by the autopilot resulted in a command duty cycle that the motor controller could not follow. Various approaches to revise the pressure control algorithm were evaluated to eliminate the duty cycle limit condition. However it was determined that the risk associated with changing the controller was higher than the risk associated with ensuring that the autopilot would not command a limit duty cycle.

Data.

The primary data obtained from the IMU are presented in Figures C-6-1 through C-6-6.

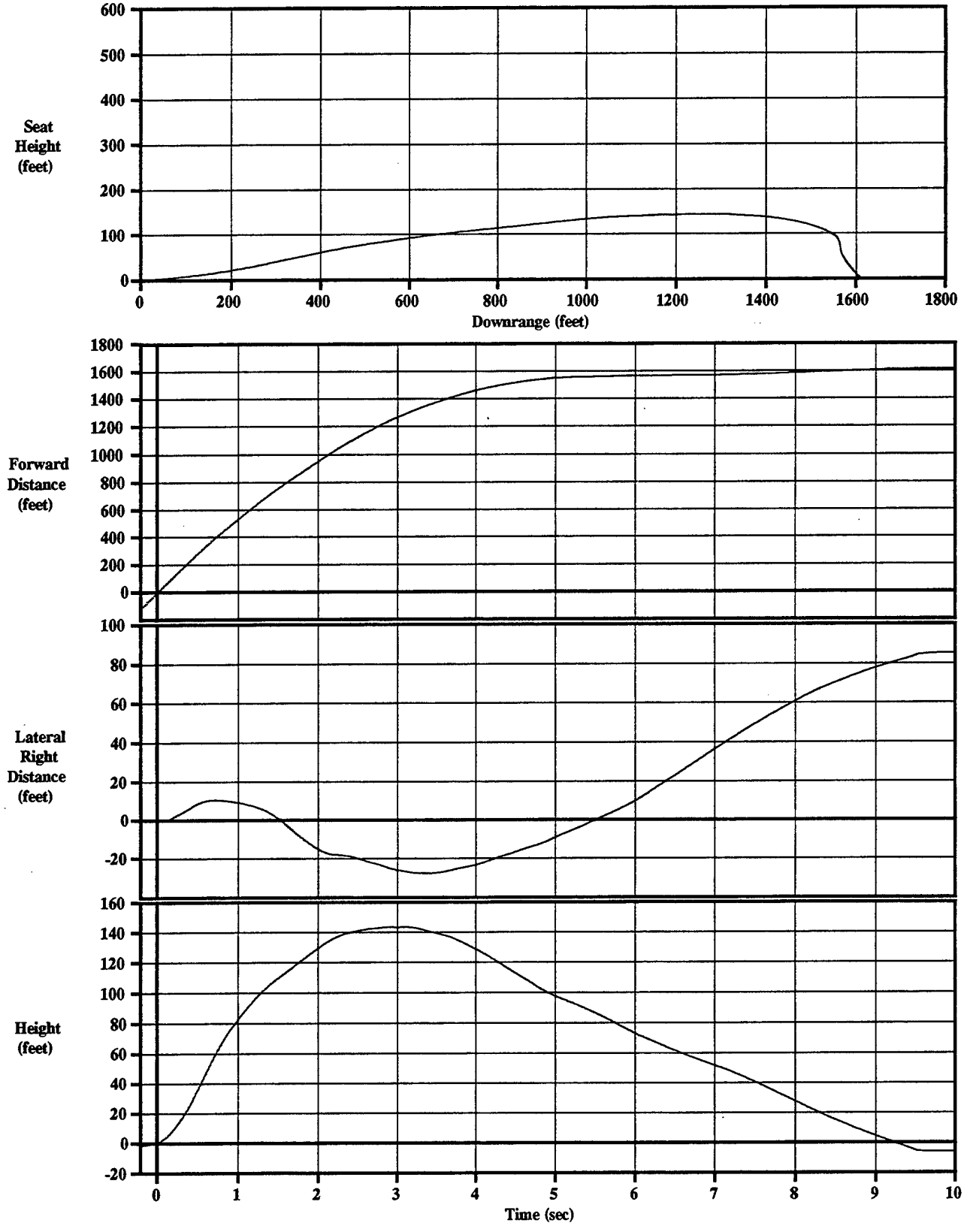

Figure C-6-1 IMU Displacements
Sled Test=6, Over-pressure KEAS=325, 5th%, Yaw=20

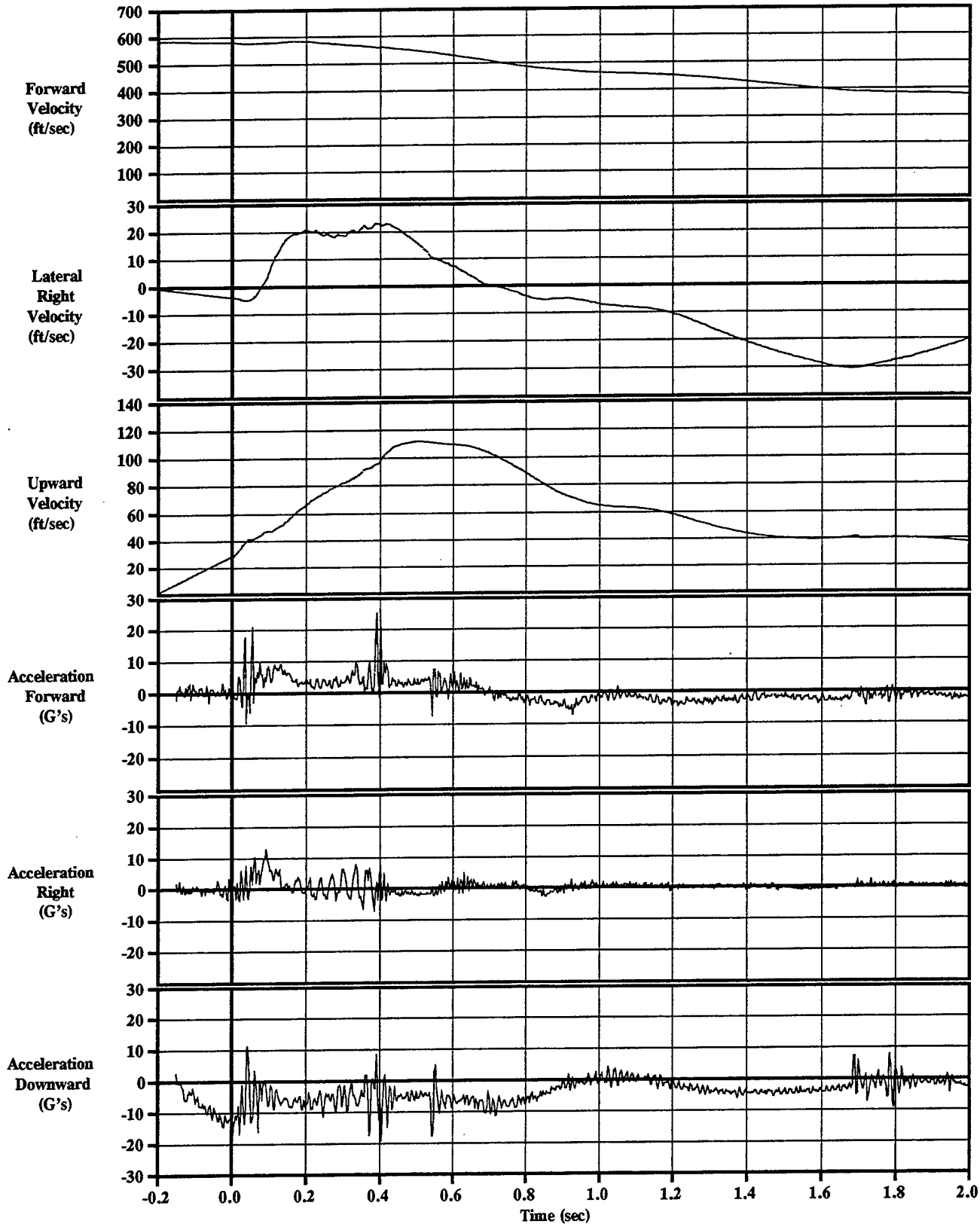

Figure C-6-2 IMU Velocities & Accelerations
Sled Test=6, Over-pressure KEAS=325, 5th%, Yaw=20

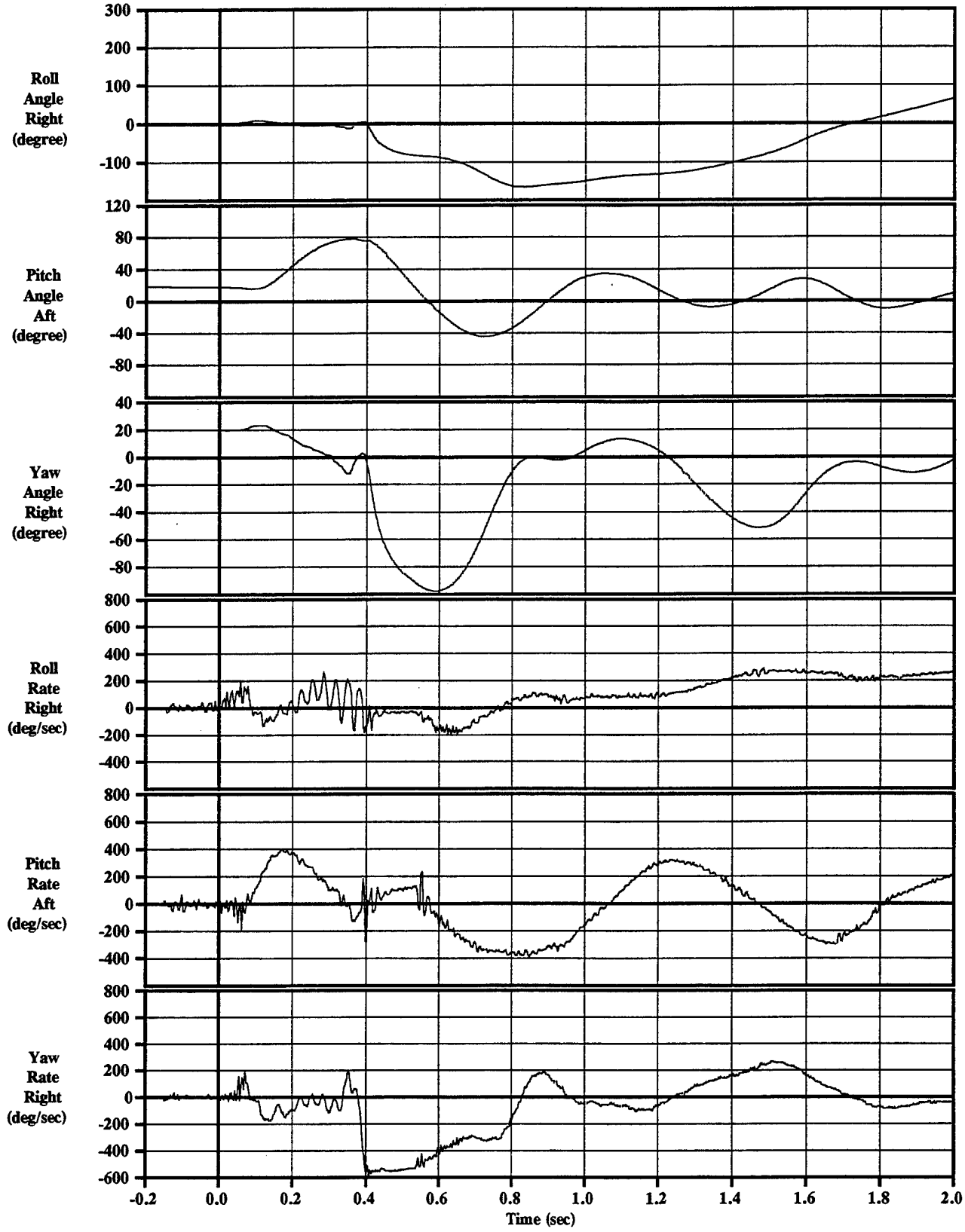

Figure C-6-3 IMU Rotation Angles & Rates
Sled Test=6, Over-pressure KEAS=325, 5th%, Yaw=20

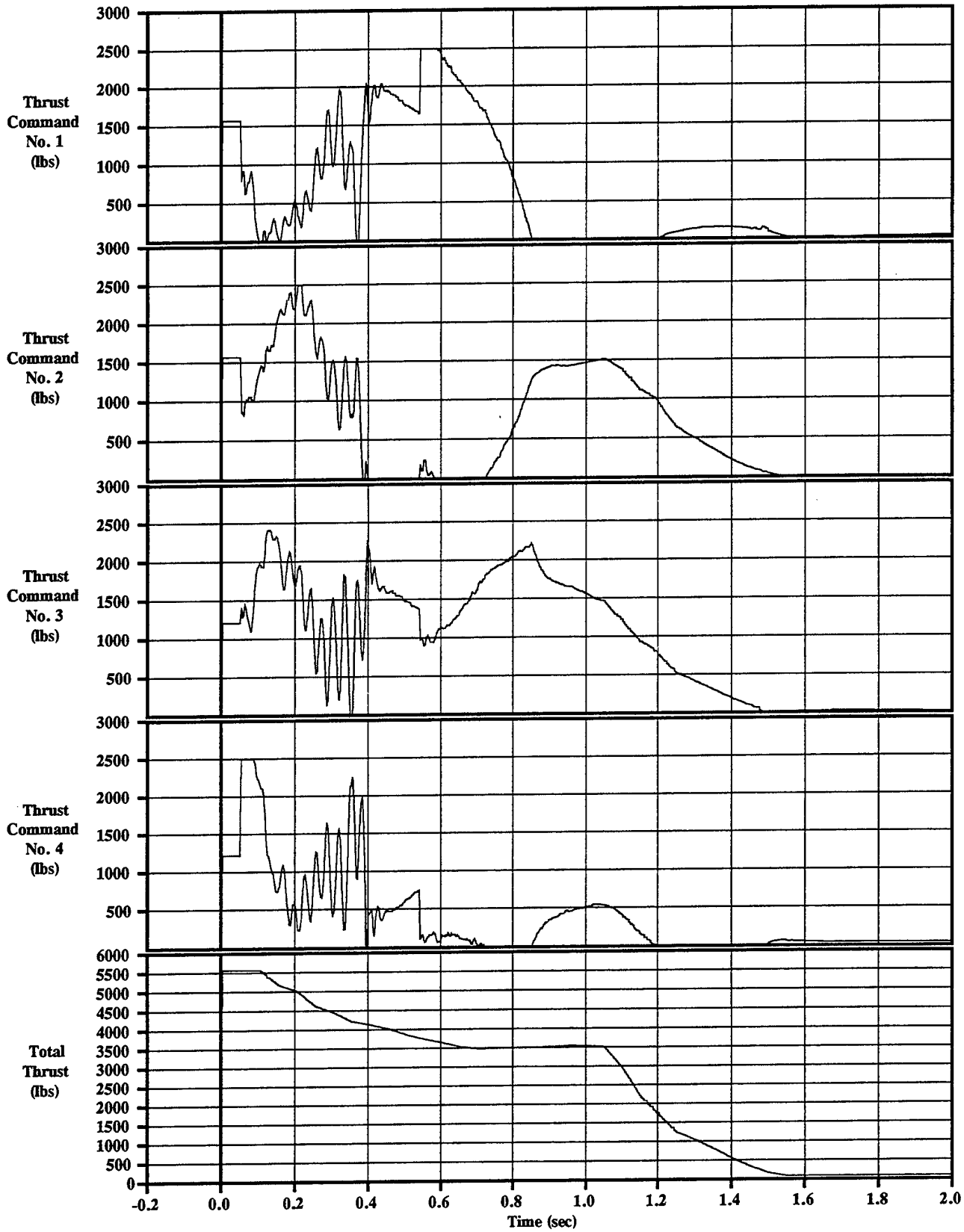

Figure C-6-4 Thrust Commands
Sled Test=6, Over-pressure KEAS=325, 5th%, Yaw=20

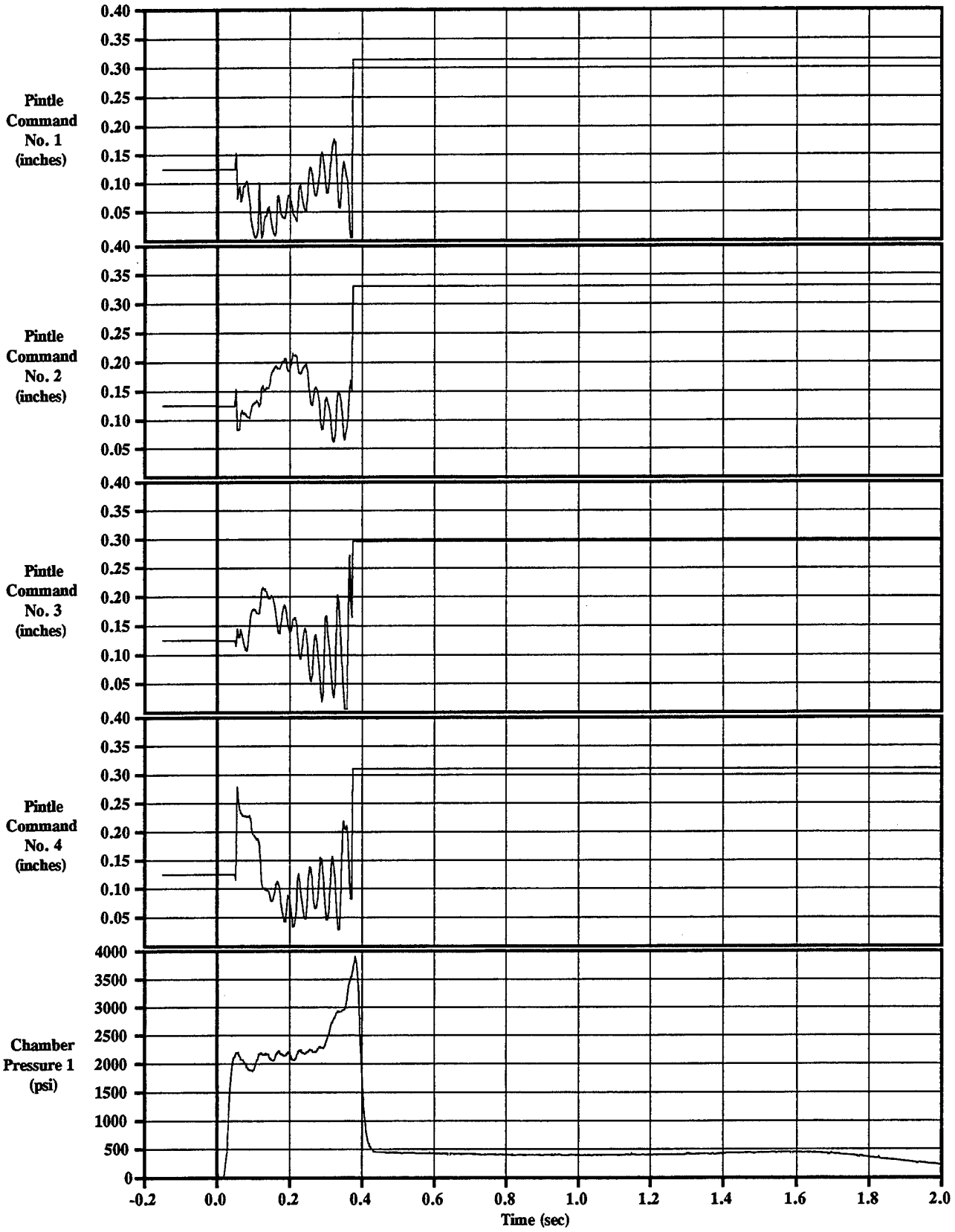

Figure C-6-5 Pintle Commands & Chamber Pressure
Sled Test=6, Over-pressure KEAS=325, 5th%, Yaw=20

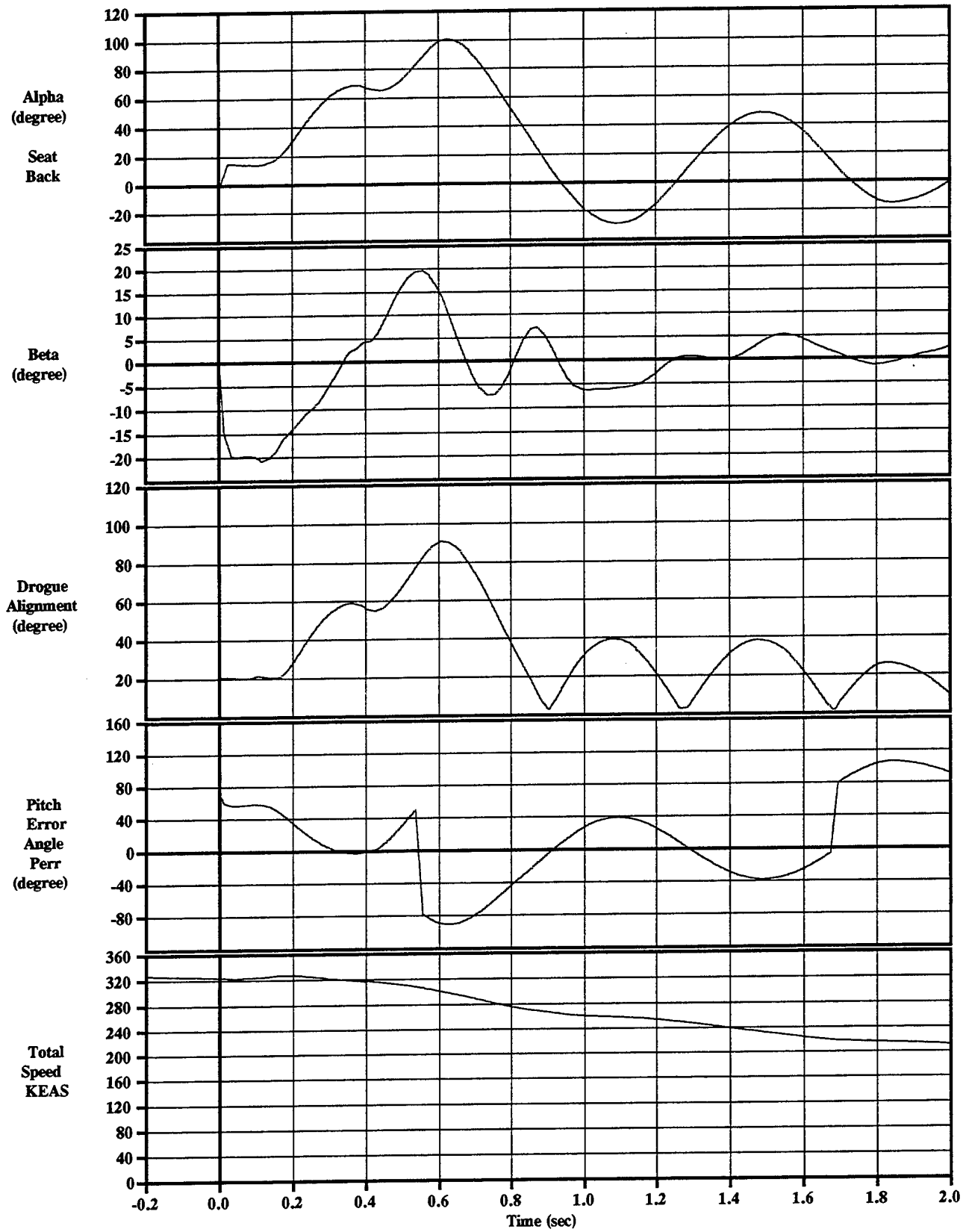

Figure C-6-6 IMU Control Angles and Total Velocity
Sled Test=6, Over-pressure KEAS=325, 5th%, Yaw=20

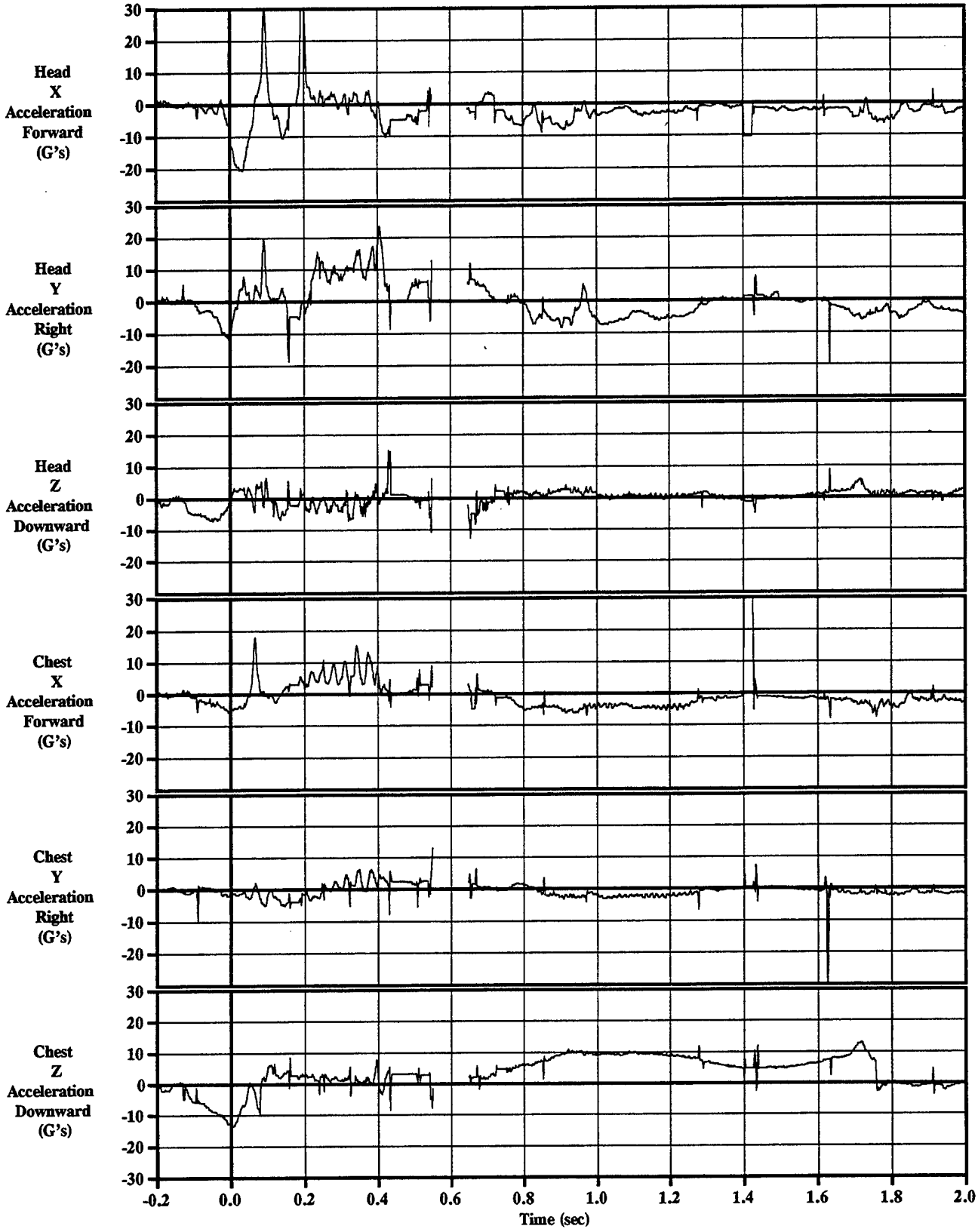

Figure C-6-7 Manikin Head & Chest Accelerations
Test=6, KEAS=325, 5th%, Yaw=20

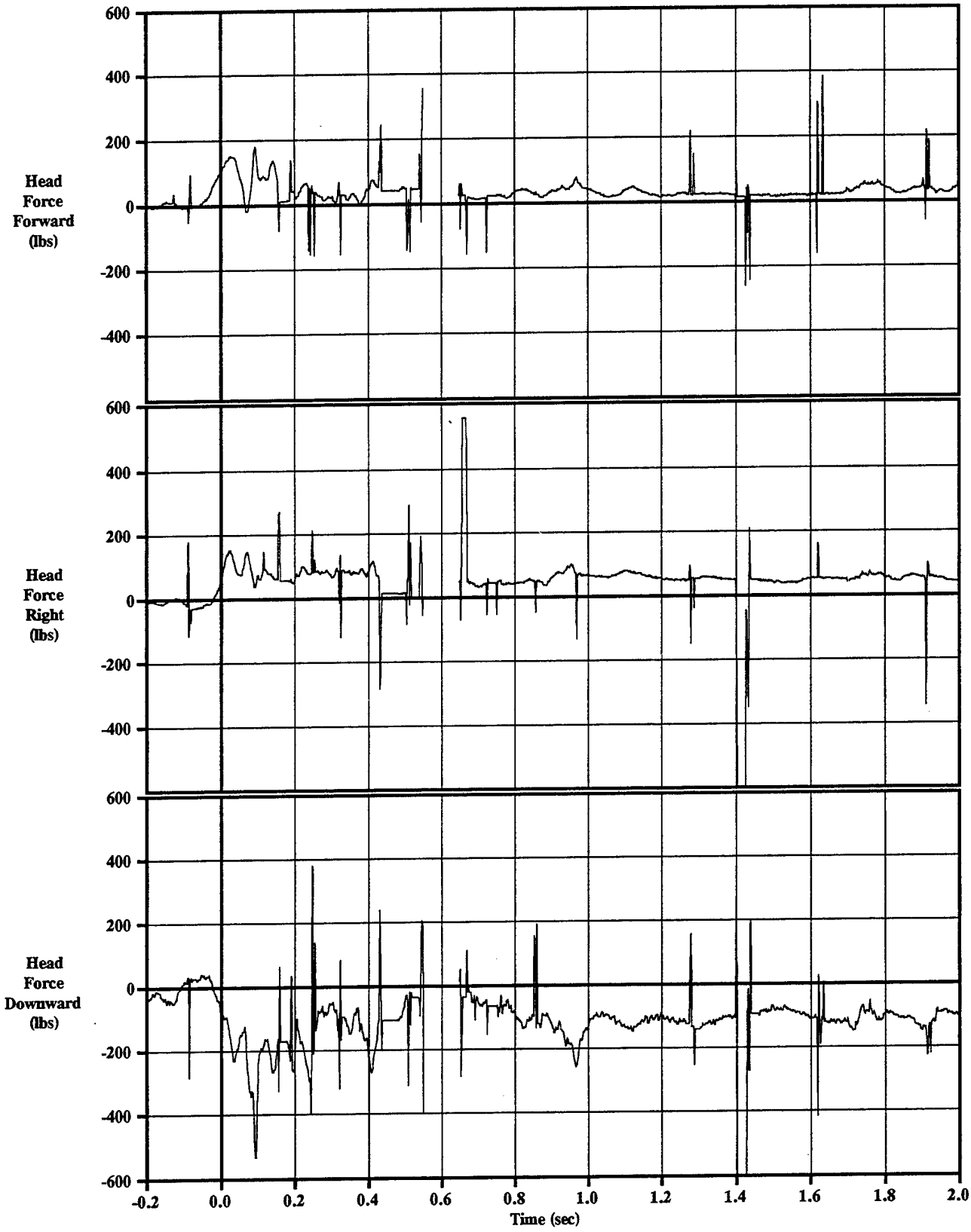

Figure C-6-8 Manikin Head Force
Test=6, KEAS=325, 5th%, Yaw=20

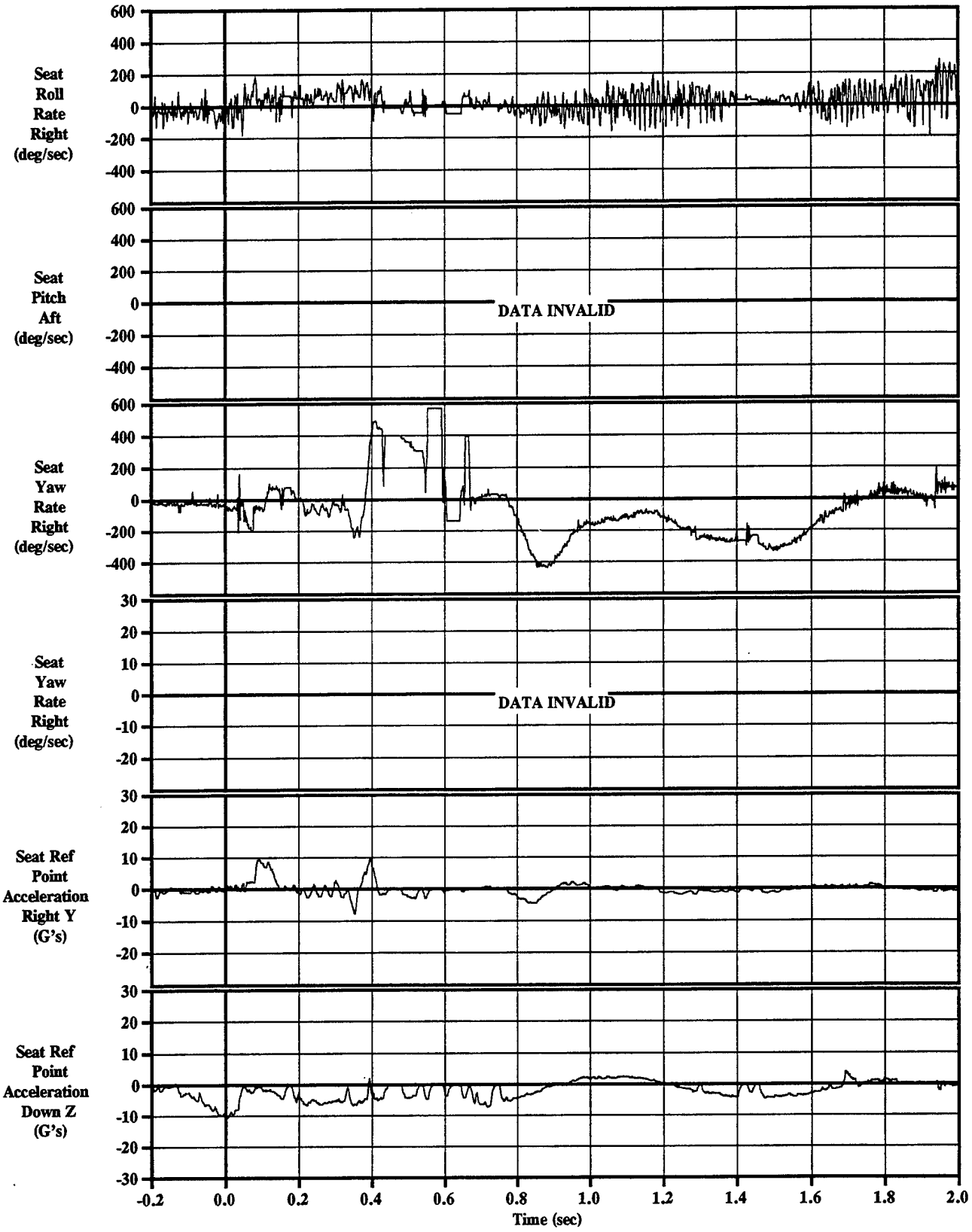

Figure C-6-9 Seat Angular Rates & Seat Pan Acceleration (80 Hz filter)
Test=6, KEAS=325, 5th%, Yaw=20

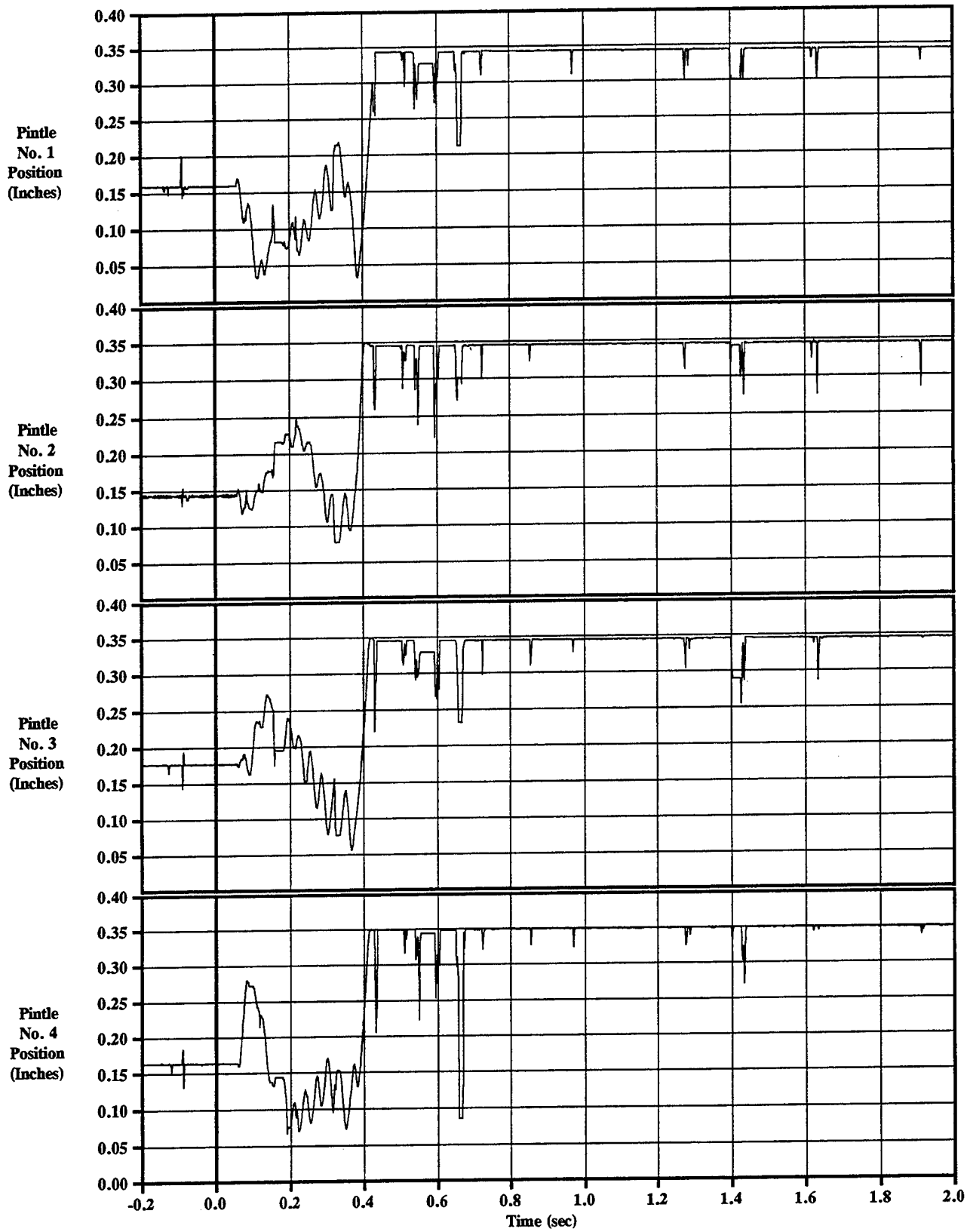

Figure C-6-11 Pintle Positions
Test=6, KEAS=325, 5th%, Yaw=20

Appendix C-7: Test #7

TEST SUMMARY

Objective

The objective of this test was to demonstrate the flight controls and controllable propulsion system of the 4th Generation Escape System in a 325 KEAS, 20° yaw flight condition.

Test Conditions

	Run Number	85E-D3A
	Test Date	13 August 1997
	System Launch Time	10:31 AM MDT 225:16:31:00.0 IRIG
	Sled Launch Point	TS 2903
	Seat Eject Point	TS 6998 @ 10.55993 sec
	Temperature	77 deg F
	Relative Humidity	59%
(1)	Wind	2.3 KTS from 275° (W)
	Barometric Pressure	12.662 lb/in^2
	Velocity	320 KEAS (592 fps)
	Sled Gx at Catapult Init	-1.23 G
	Roll	0 deg
	Pitch	0 deg
	Yaw	20 deg
	Hybrid III Manikin Size	Small

(1) 0° angle is a head wind. Positive to the right (clockwise).

Summary And Conclusions

The seventh system sled test of the 4th Generation Escape System program was conducted on Wednesday, 13 August at Holloman AFB, NM. The seat system successfully performed the full sequence of operations required for recovery from these ejection conditions. After separation from the guide rails, the seat system performed a yaw maneuver to correct the initial sideslip attitude, and then a pitchup maneuver to climb up for altitude recovery. At ~0.9 seconds after motor initiation, the system reoriented for drogue deployment which occurred ~0.2 seconds later. The parachute was then deployed when the system velocity fell to below 220 KEAS. Both the seat and manikin were successfully recovered by parachute. All avionics and propulsion hardware appeared normal during posttest inspection and testing.

The only configuration change from test 6 to this test was the removal of the CGU shock mounts. As demonstrated in this test, the CGU can withstand the shock and

vibration environment at the mounting location. Prior analysis based on shock and vibration data measured at other locations on the seat indicated the need for the GCU shock mounts. While the shock mounts did provide additional mechanical protection for the GCU, they also introduced undesirable characteristics into the control system. Based on the results of this test, it is planned to fly the remaining tests with the GCU hard mounted to the seat structure.

Data.

The primary data obtained from the IMU are presented in Figures C-7-1 through C-7-6.

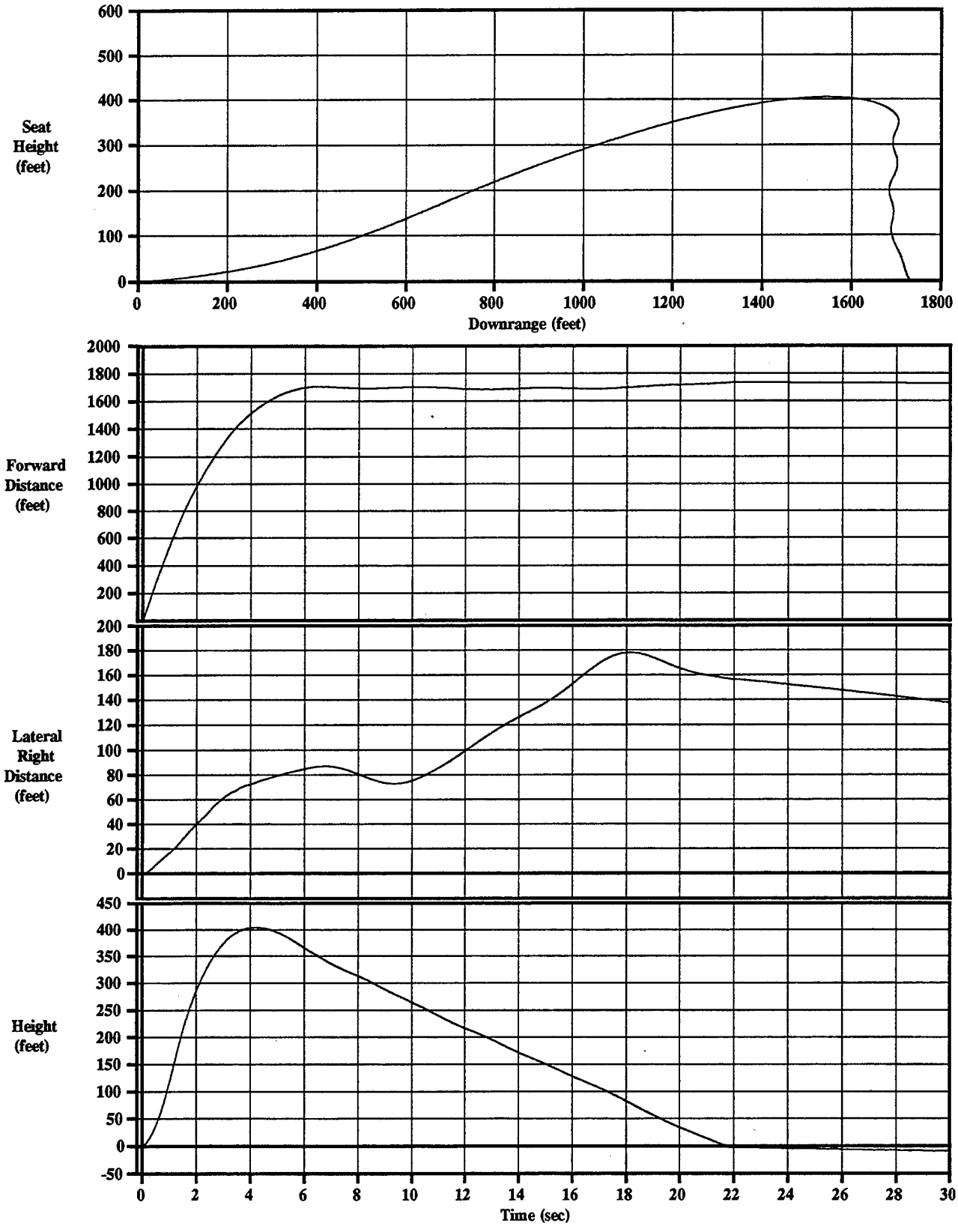

Figure C-7-1 IMU Displacements
Sled Test=7, KEAS=320, 5th%, Yaw=20

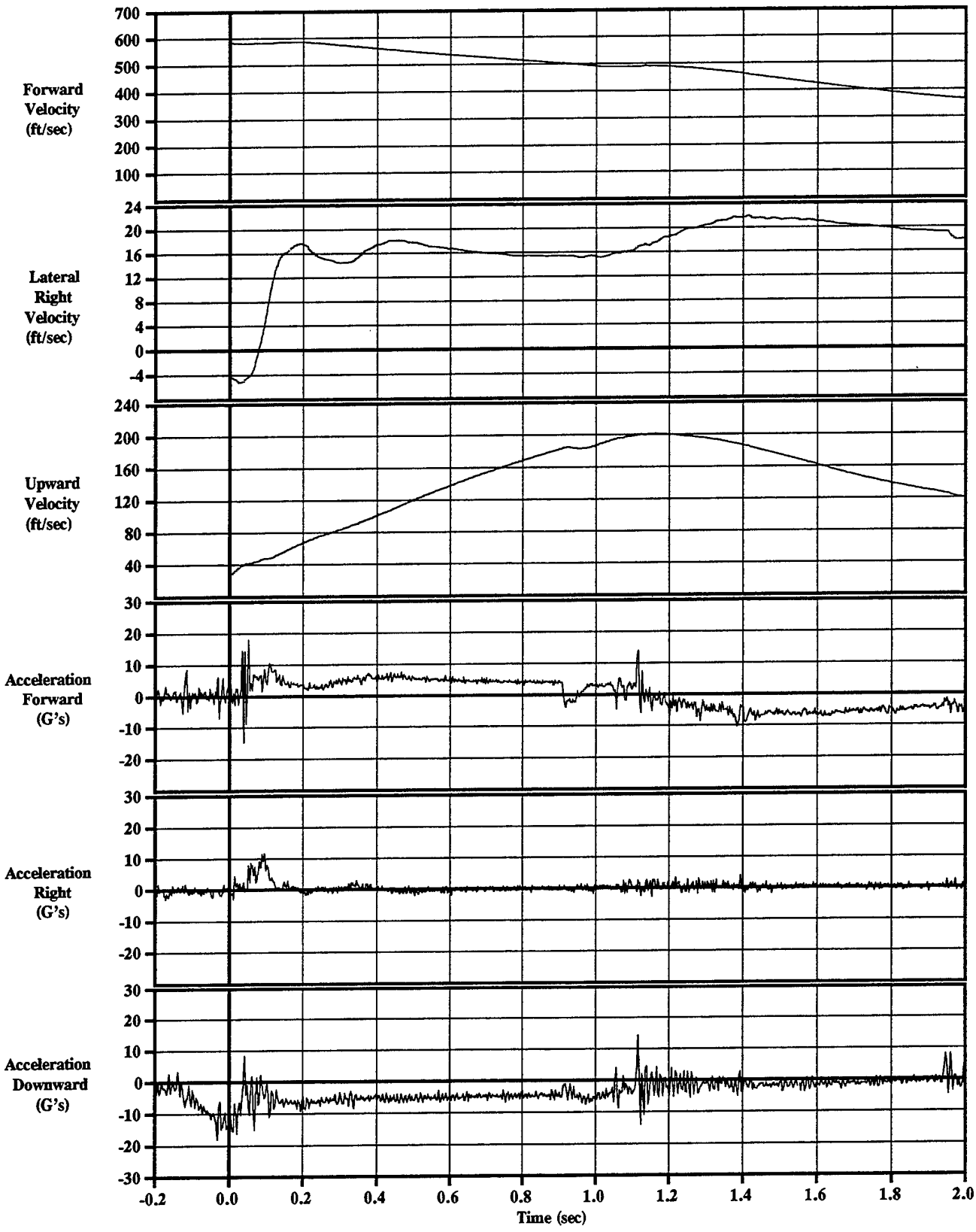

Figure C-7-2 IMU Velocities & Accelerations
Sled Test=7, KEAS=320, 5th%, Yaw=20

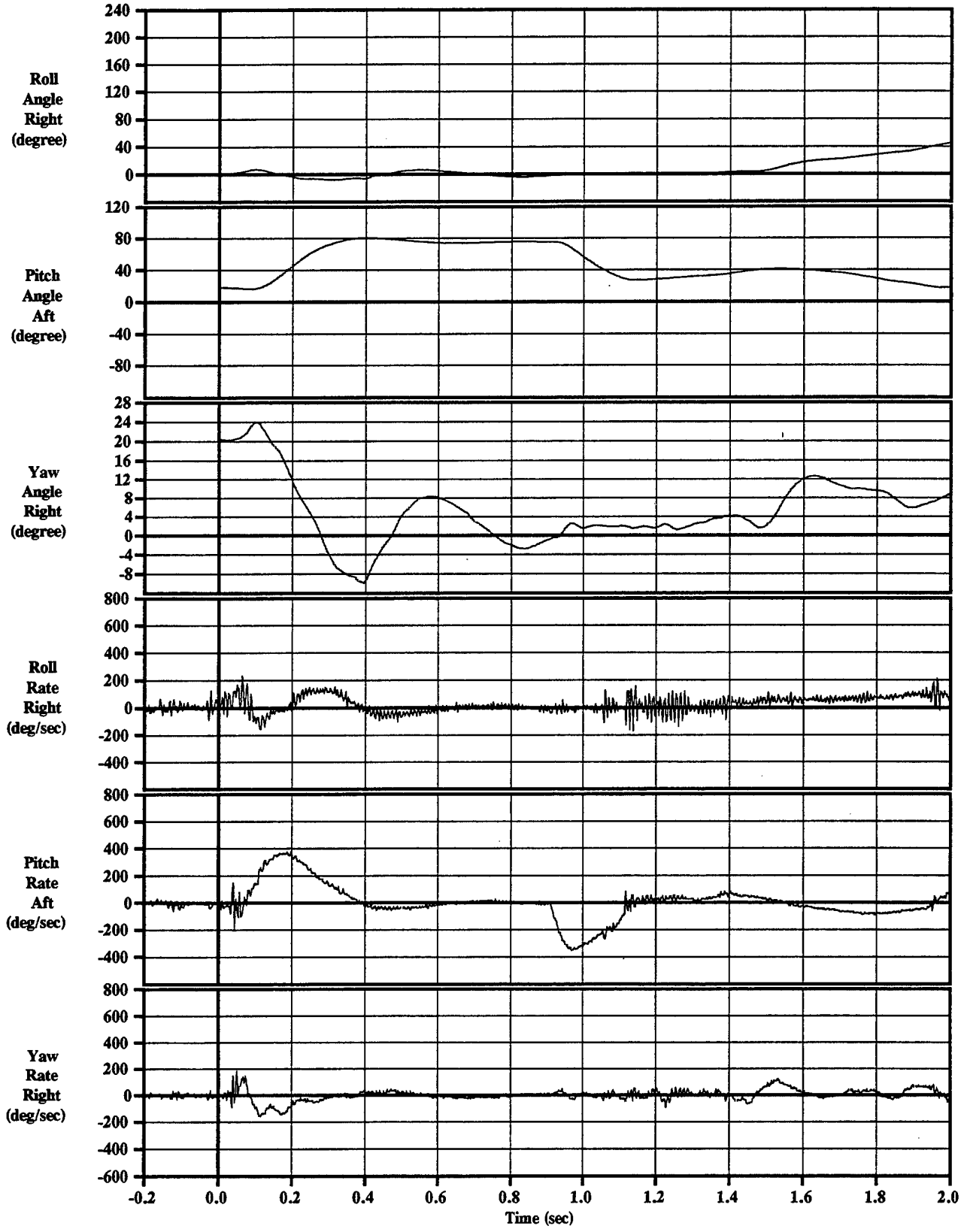

Figure C-7-3 IMU Rotation Angles & Rates
Sled Test=7, KEAS=320, 5th%, Yaw=20

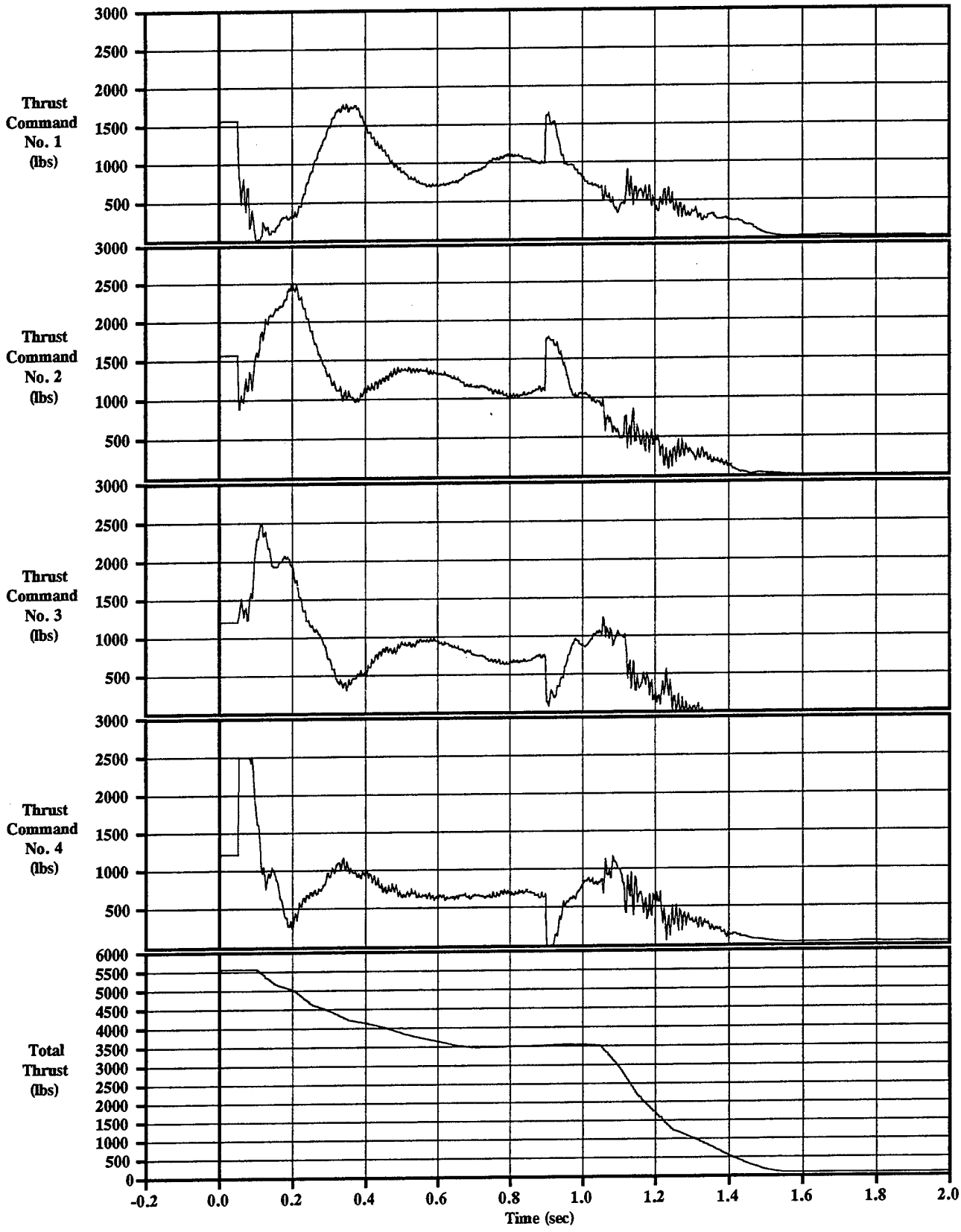

Figure C-7-4 Thrust Commands
Sled Test=7, KEAS=320, 5th%, Yaw=20

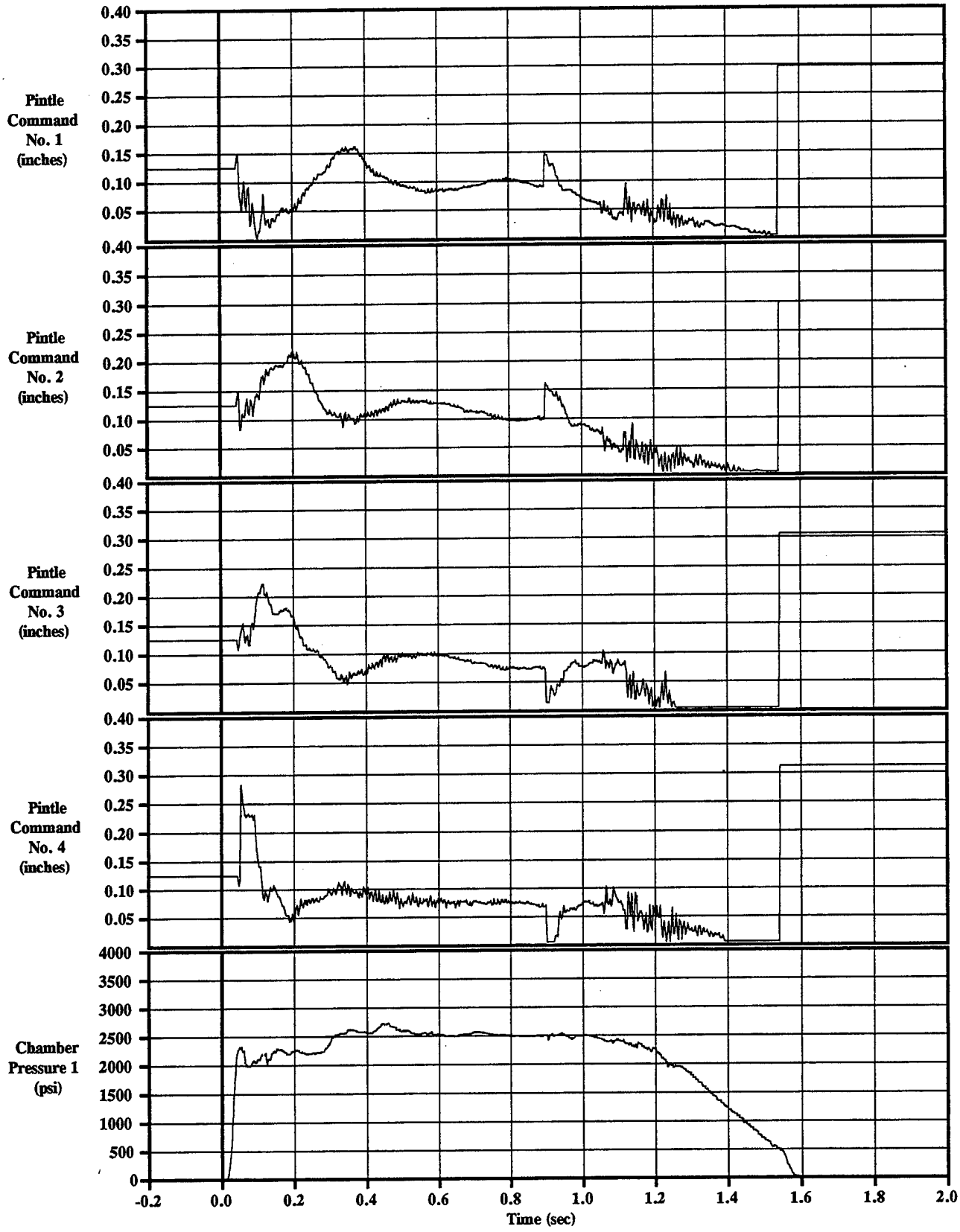

Figure C-7-5 Pintle Commands & Chamber Pressure
Sled Test=7, KEAS=320, 5th%, Yaw=20

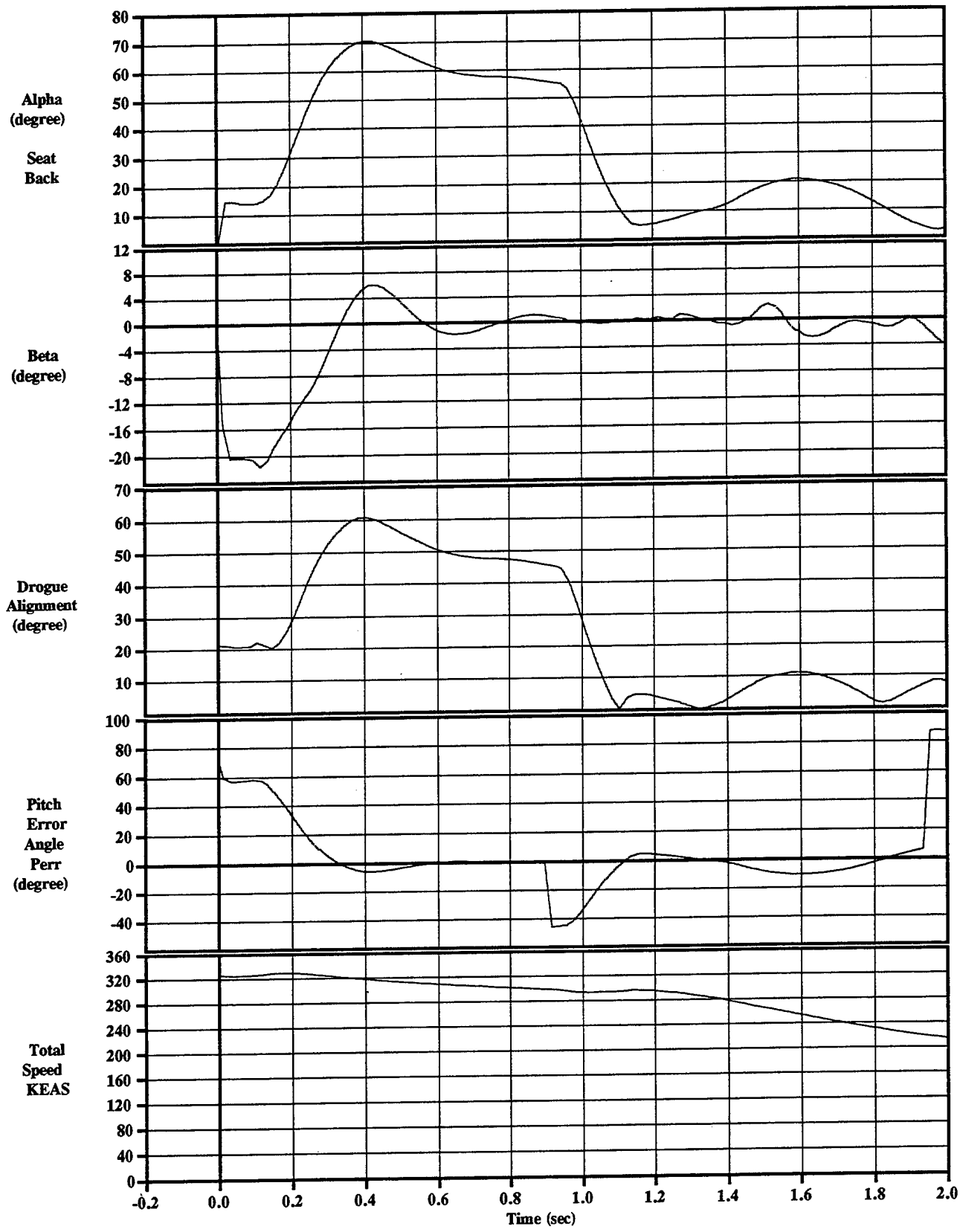

Figure C-7-6 IMU Control Angles and Total Velocity
Sled Test=7, KEAS=320, 5th%, Yaw=20

Appendix C-8: Test #8

TEST SUMMARY

Objective

The objective of this test was to demonstrate the flight controls and controllable propulsion system of the 4th Generation Escape System in a 450 KEAS, 20° yaw flight condition.

Test Conditions

	Run Number	85E-E1
	Test Date	4 September 1997
	System Launch Time	9:00 AM MDT 247:15:00:00.0 IRIG
	Sled Launch Point	TS 3787
	Seat Eject Point	TS 6998 @ 7.355138 sec
	Temperature	71 deg F
	Relative Humidity	68%
(1)	Wind	calm
	Barometric Pressure	12.807 lb/in^2
	Velocity	437 KEAS (799 fps)
	Sled Gx at Catapult Init	-0.5 G (estimated from IMU)
	Roll	0 deg
	Pitch	0 deg
	Yaw	20 deg
	ADAM Manikin Size	Small

(1) 0° angle is a head wind. Positive to the right (clockwise).

Summary And Conclusions

The eighth system sled test of the 4th Generation Escape System program was conducted on Thursday, 4 September at Holloman AFB, NM. The seat system successfully performed the full sequence of operations required for recovery from these ejection conditions. After separation from the guide rails, the seat system performed a yaw maneuver to correct the initial sideslip attitude, and then a pitch-up maneuver to climb up for altitude recovery. At ~0.9 seconds after motor initiation, the system reoriented for drogue deployment which occurred ~0.2 seconds later. The parachute was then deployed when the system velocity fell to below 220 KEAS. Both the seat and manikin were successfully recovered by parachute. All avionics and propulsion hardware appeared normal during posttest inspection and testing.

The MDRC for this test was 0.97 medium risk based on the IMU accelerations being transferred to the critical point. The neck normal force was 299 lbs and the side force was 60 lbs.

In order to address the pintle chatter problem seen on sled test 5, 6 and 7, we attempted to measure the avionics bus and actuator battery voltages after sled test 8. The avionics bus was accessible and the voltage was measured at 6.82 V approximately 9 minutes after firing the avionics thermal battery. The actuator batteries were not accessible. The avionics bus voltage is consistent with our theory that the GCU is off and the actuator controllers are driving the pintles into the throat. Given the limited data, no additional conclusions can be drawn.

As shown in Section 3, the actual and predicted performance matched very well. This indicates that the modeling changes for the lateral aerodynamic force, and the aerodynamic modeling in general are good at 450 KEAS.

Data.

The primary data obtained from the IMU and ADAM are presented in Figures C-8-1 through C-8-12.

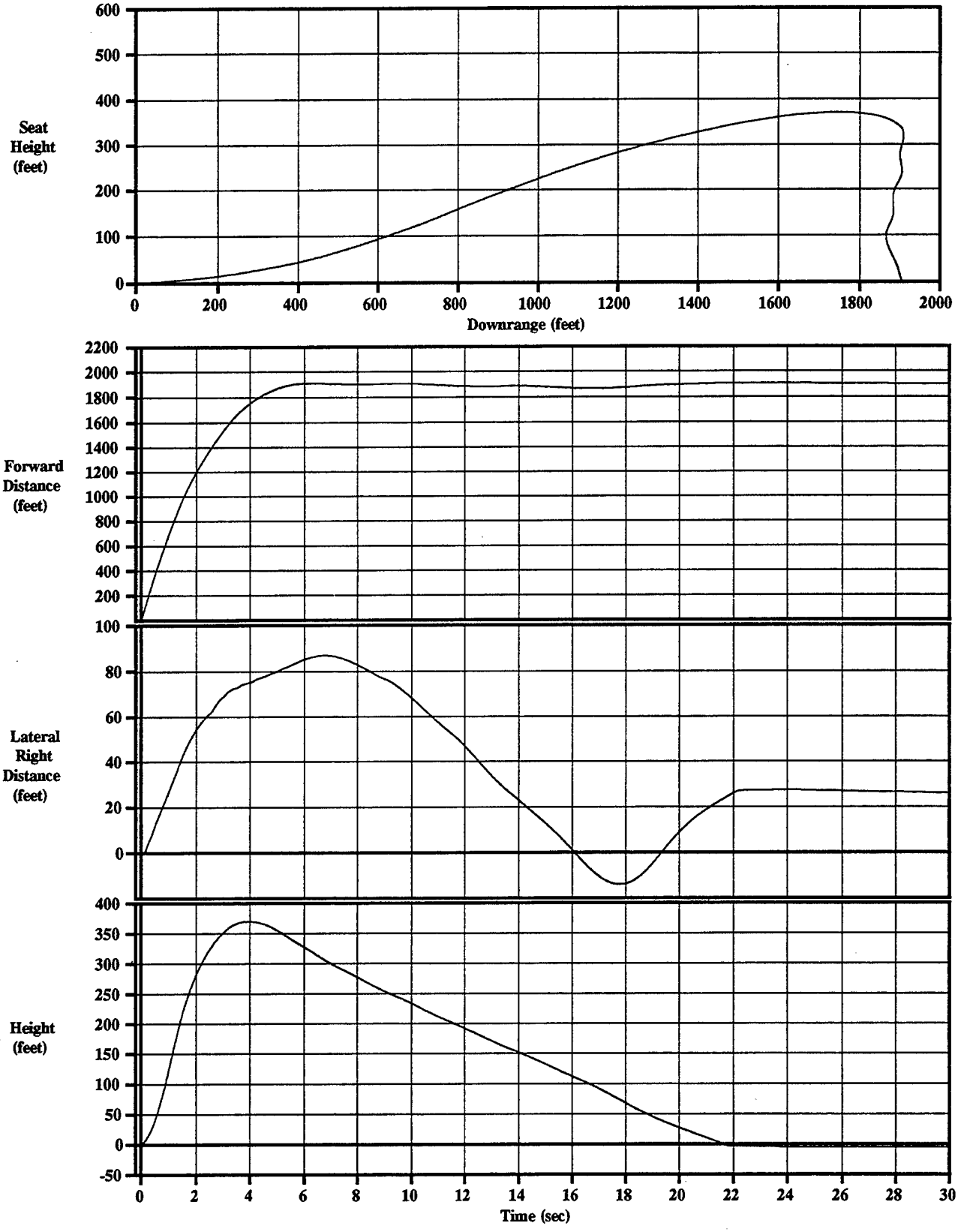

Figure C-8-1 IMU Displacements
Sled Test=8, KEAS=438, 5th%, Yaw=20

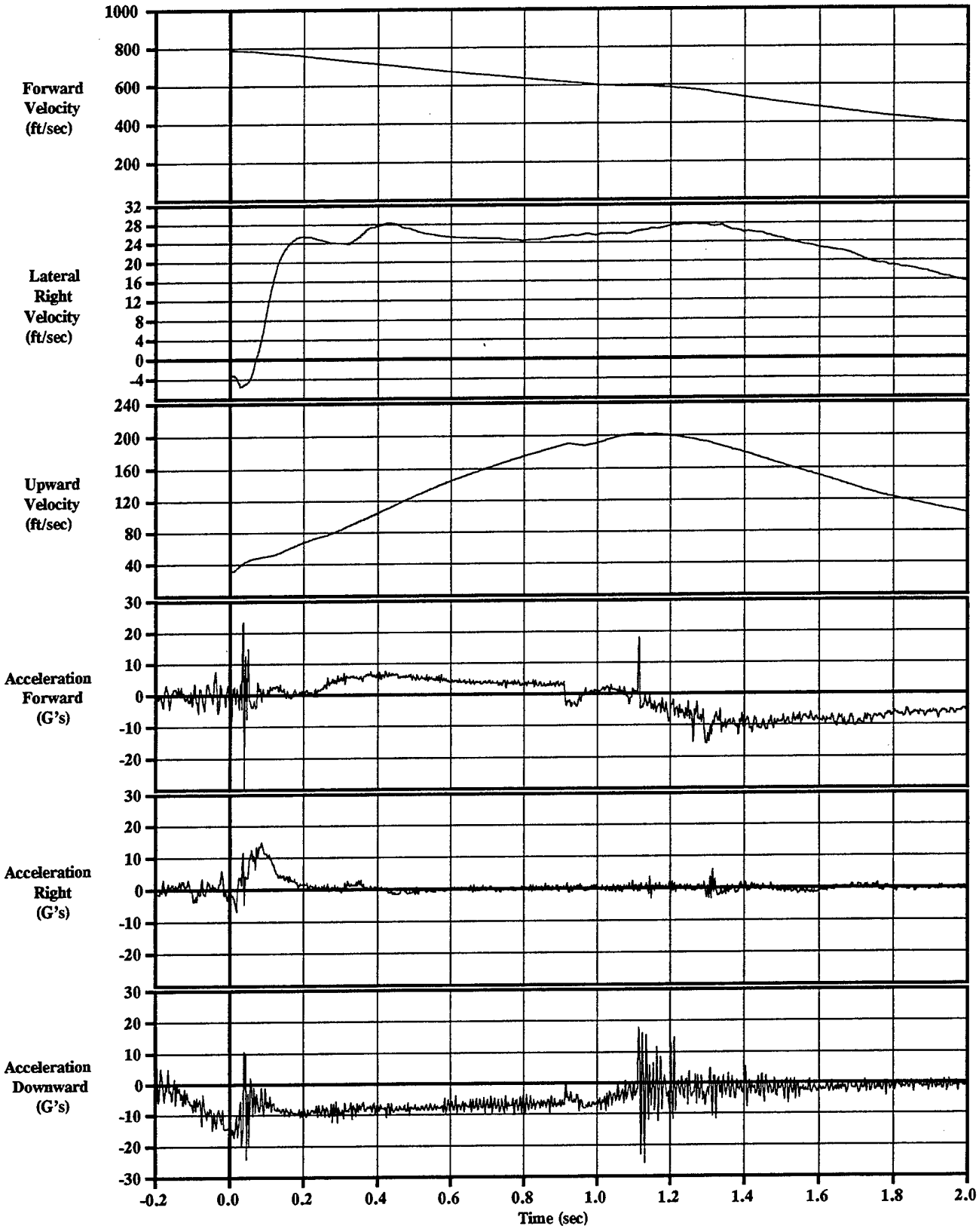

Figure C-8-2 IMU Velocities & Accelerations
Sled Test=8, KEAS=438, 5th%, Yaw=20

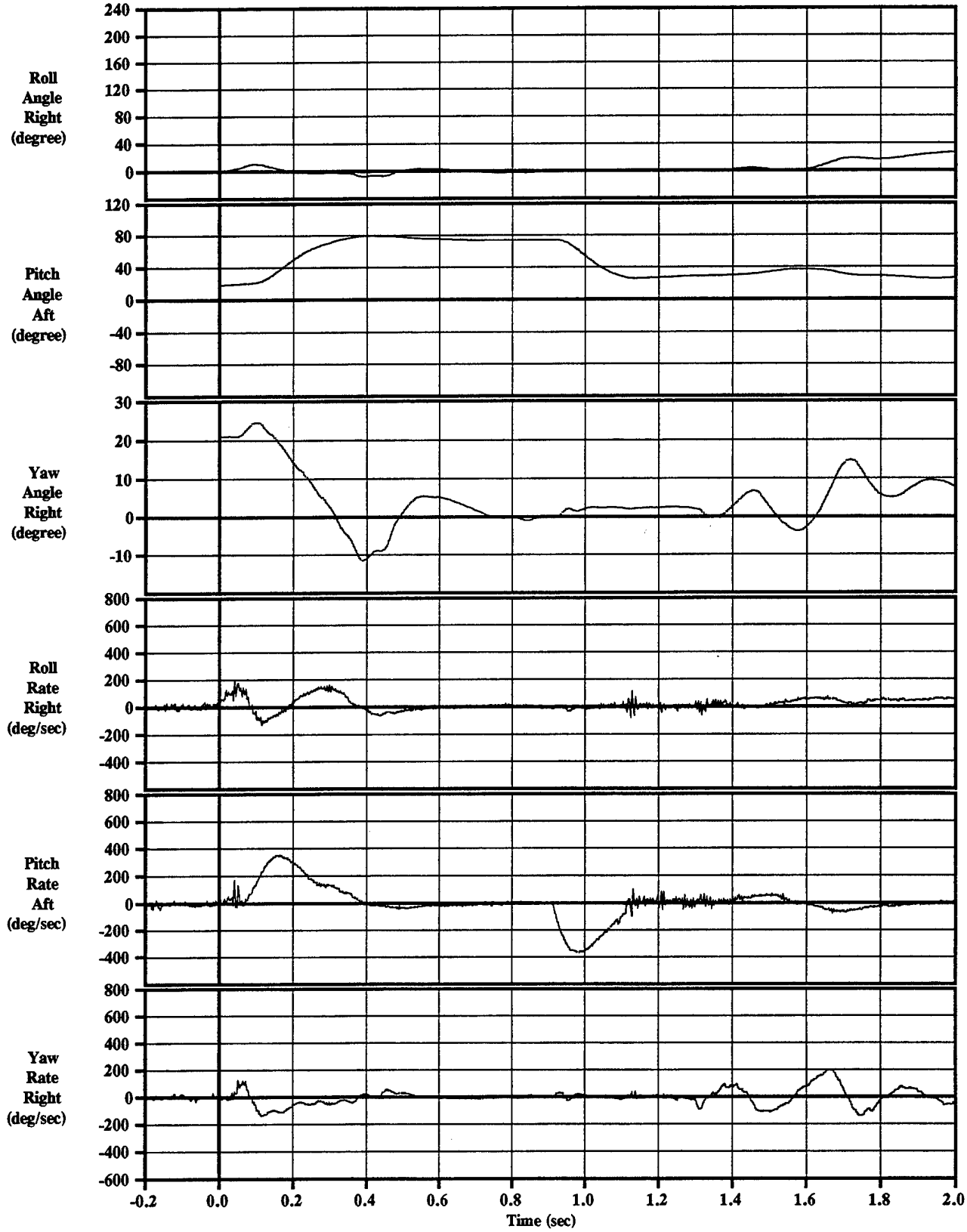

Figure C-8-3 IMU Rotation Angles & Rates
Sled Test=8, KEAS=438, 5th%, Yaw=20

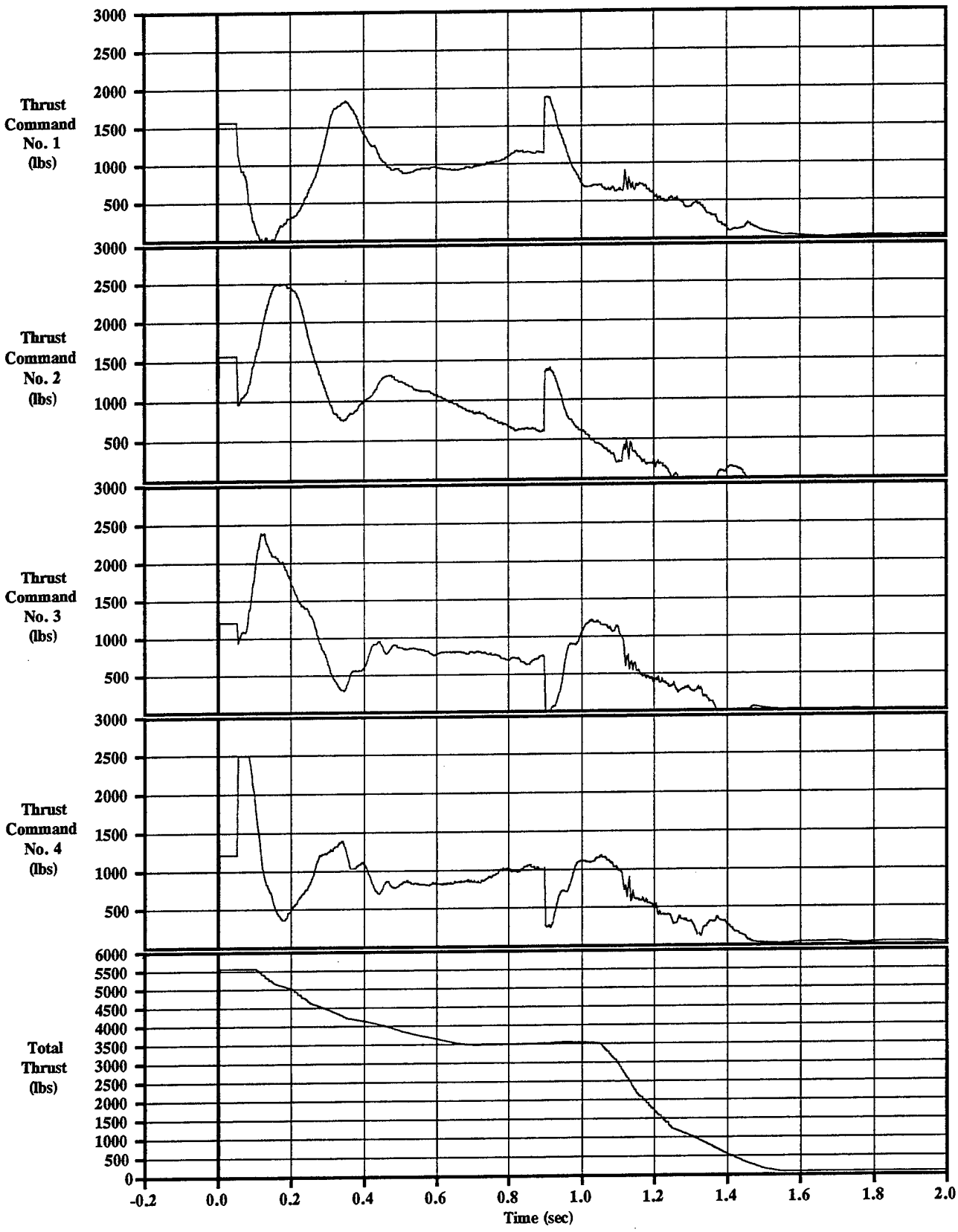

Figure C-8-4 Thrust Commands
Sled Test=8, KEAS=438, 5th%, Yaw=20

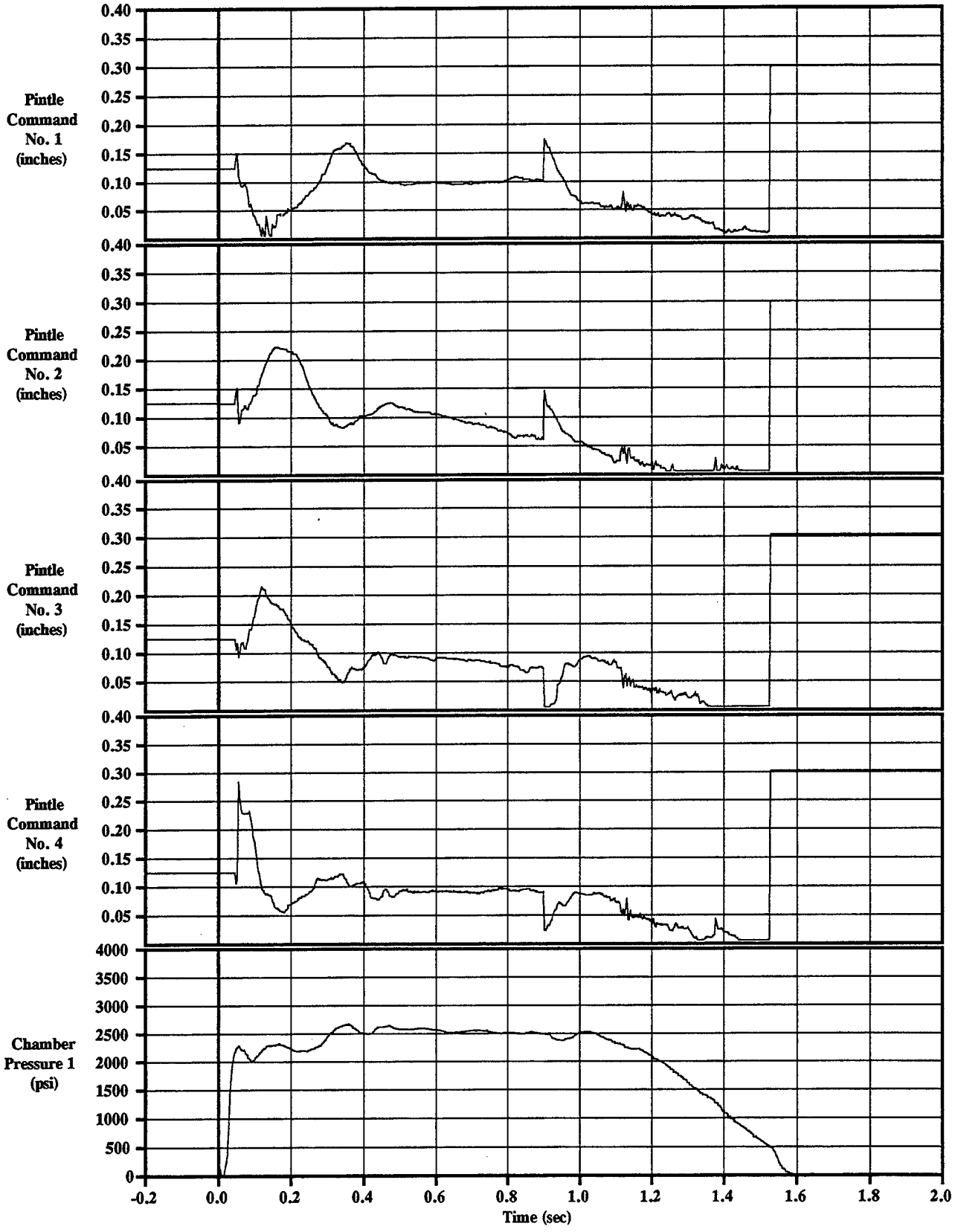

Figure C-8-5 Pintle Commands & Chamber Pressure
Sled Test=8, KEAS=438, 5th%, Yaw=20

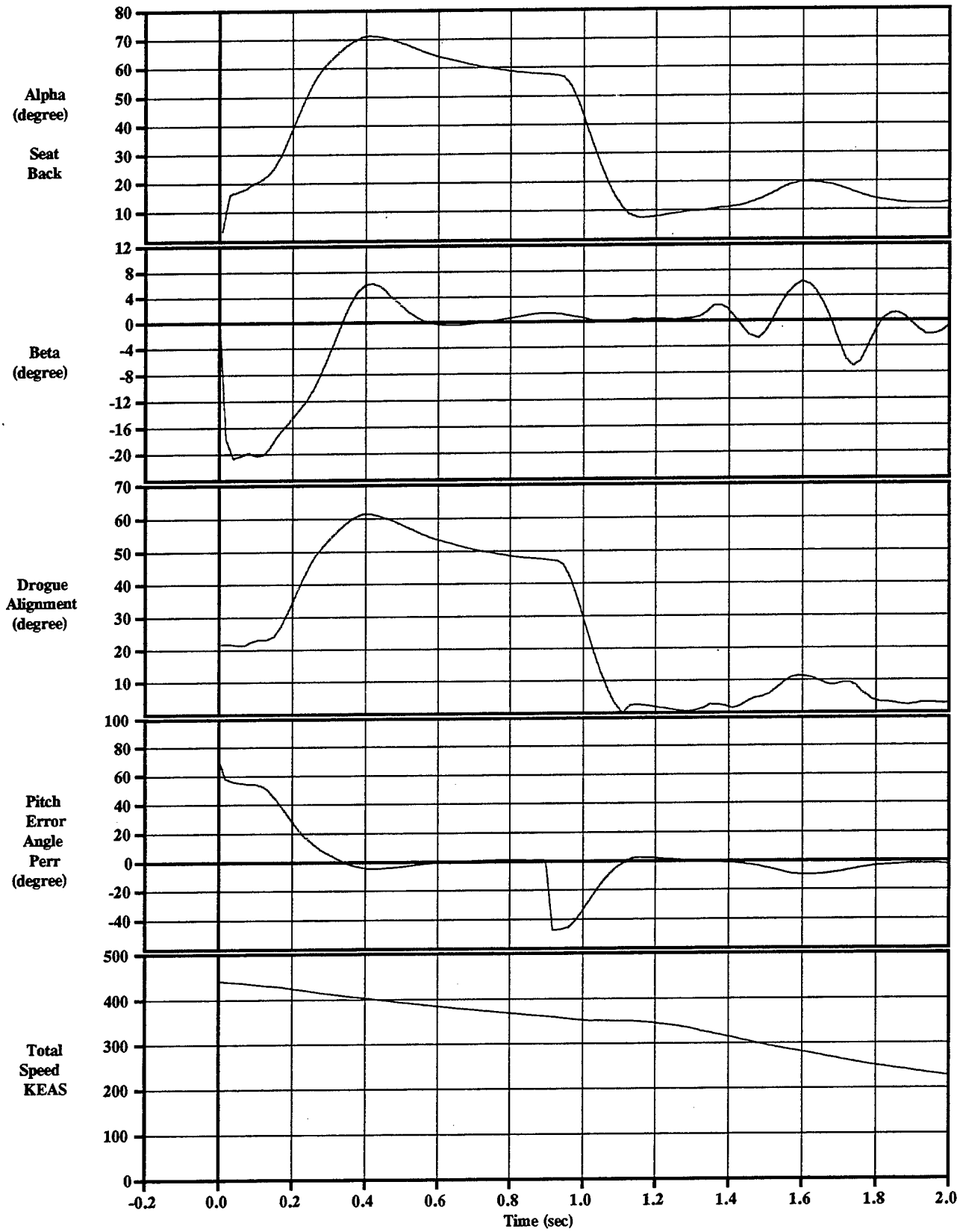

Figure C-8-6 IMU Control Angles and Total Velocity
Sled Test=8, KEAS=438, 5th%, Yaw=20

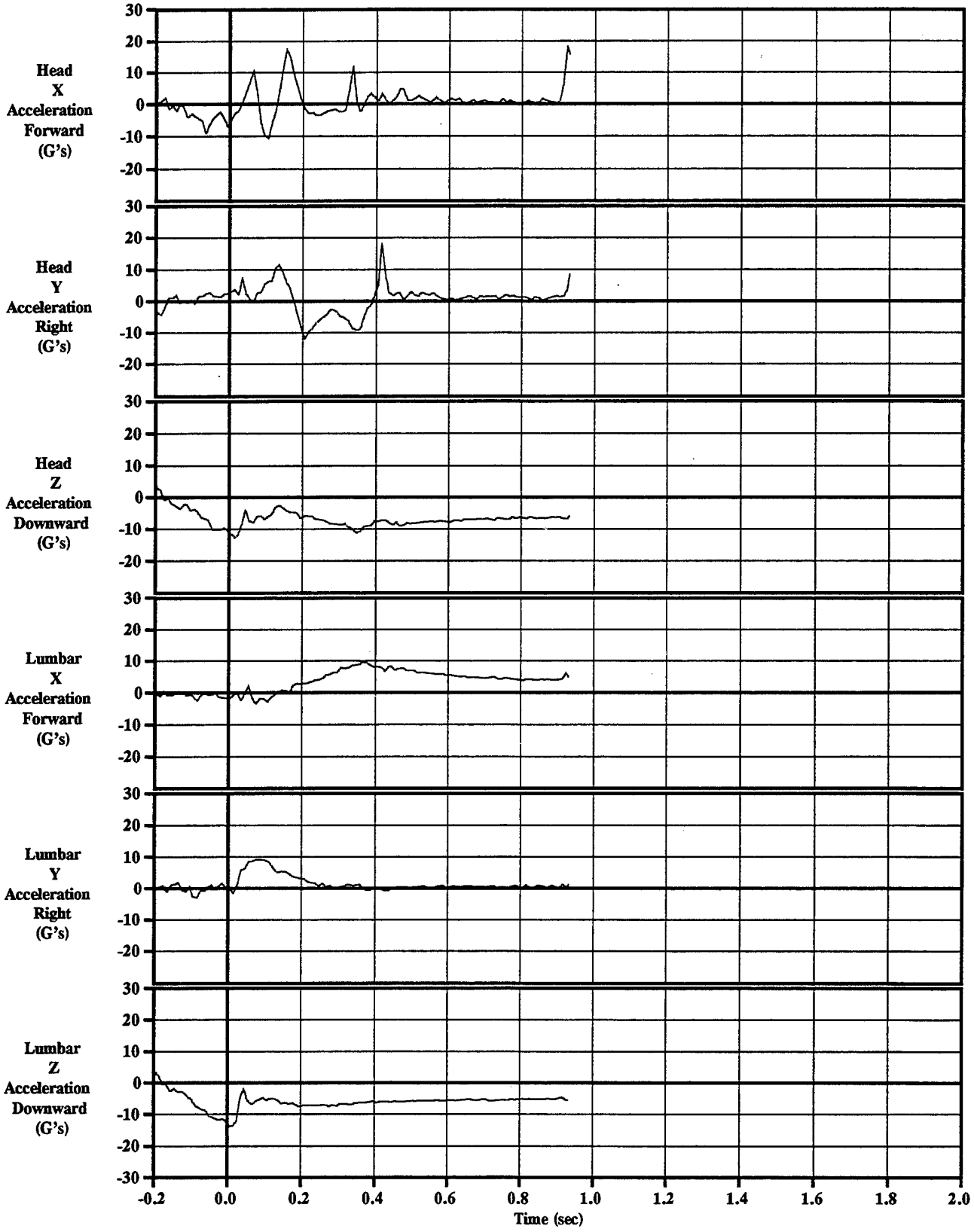

Figure C-8-7 ADAM Head & Lumbar Accelerations
Sled Test=8, KEAS=438, 5th%, Yaw=20

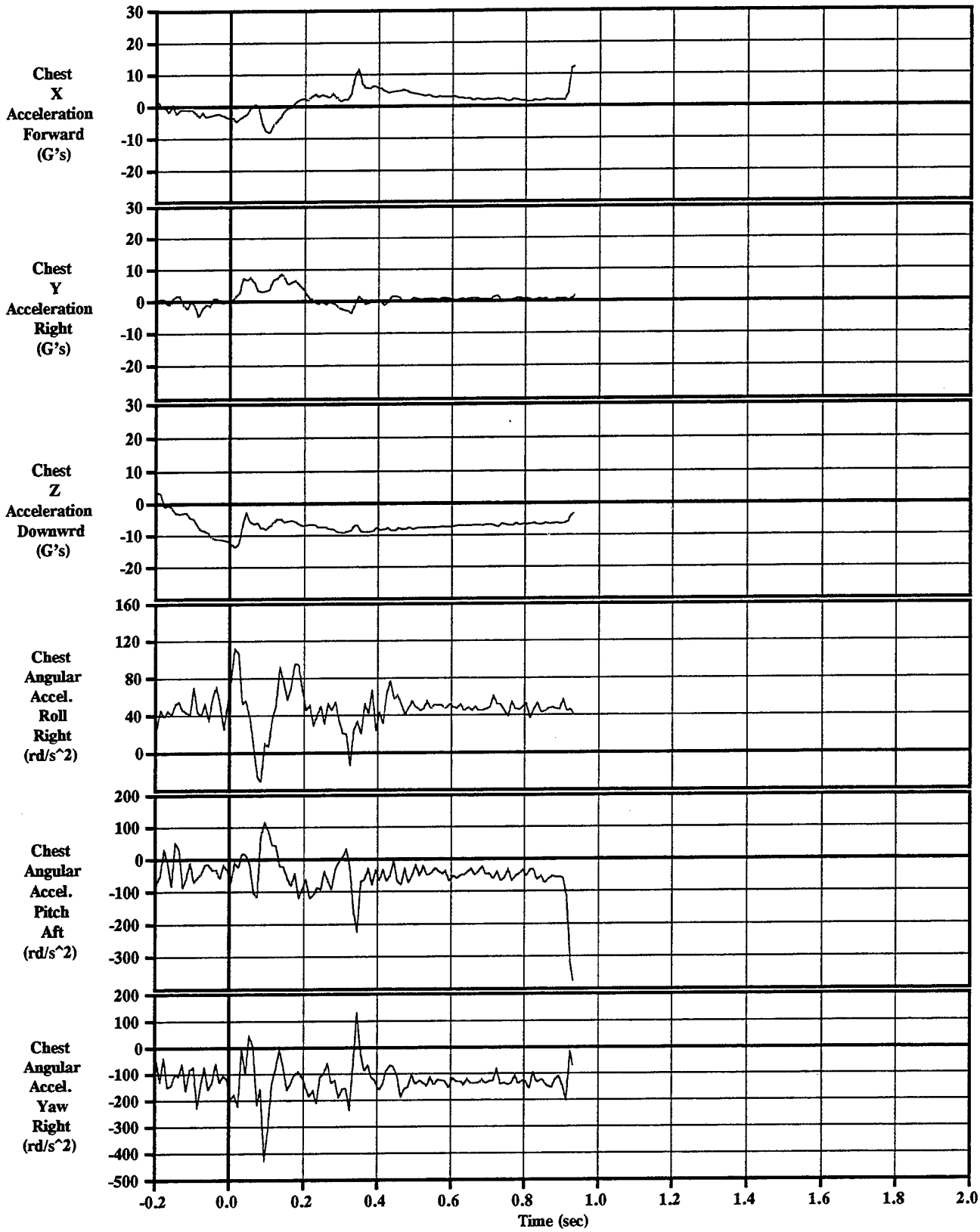

Figure C-8-8 ADAM Chest Linear & Angular Accelerations
Sled Test=8, KEAS=438, 5th%, Yaw=20

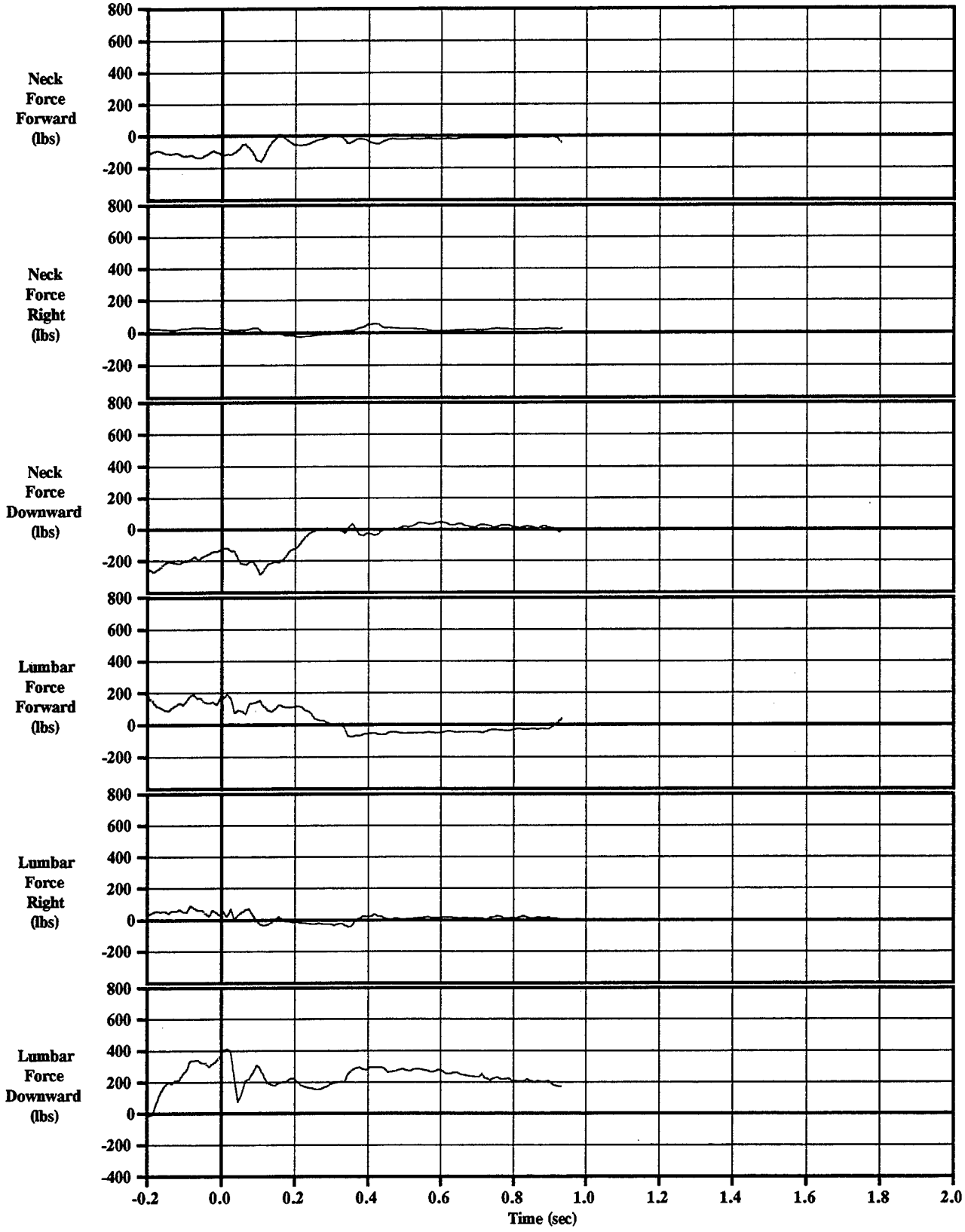

Figure C-8-9 ADAM Neck & Lumbar Forces
Sled Test=8, KEAS=438, 5th%, Yaw=20

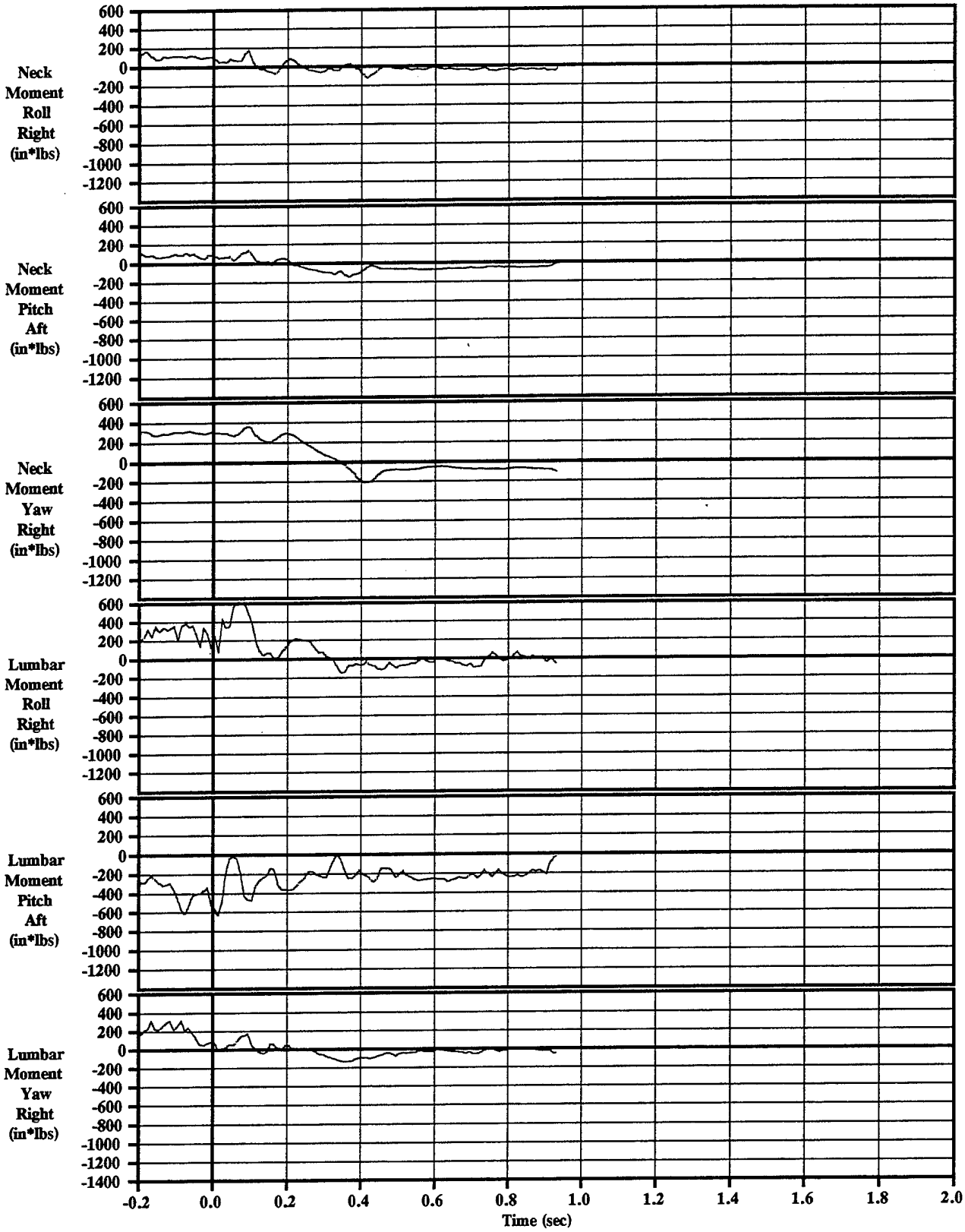

Figure C-8-10 ADAM Neck & Lumbar Moments
Sled Test=8, KEAS=438, 5th%, Yaw=20

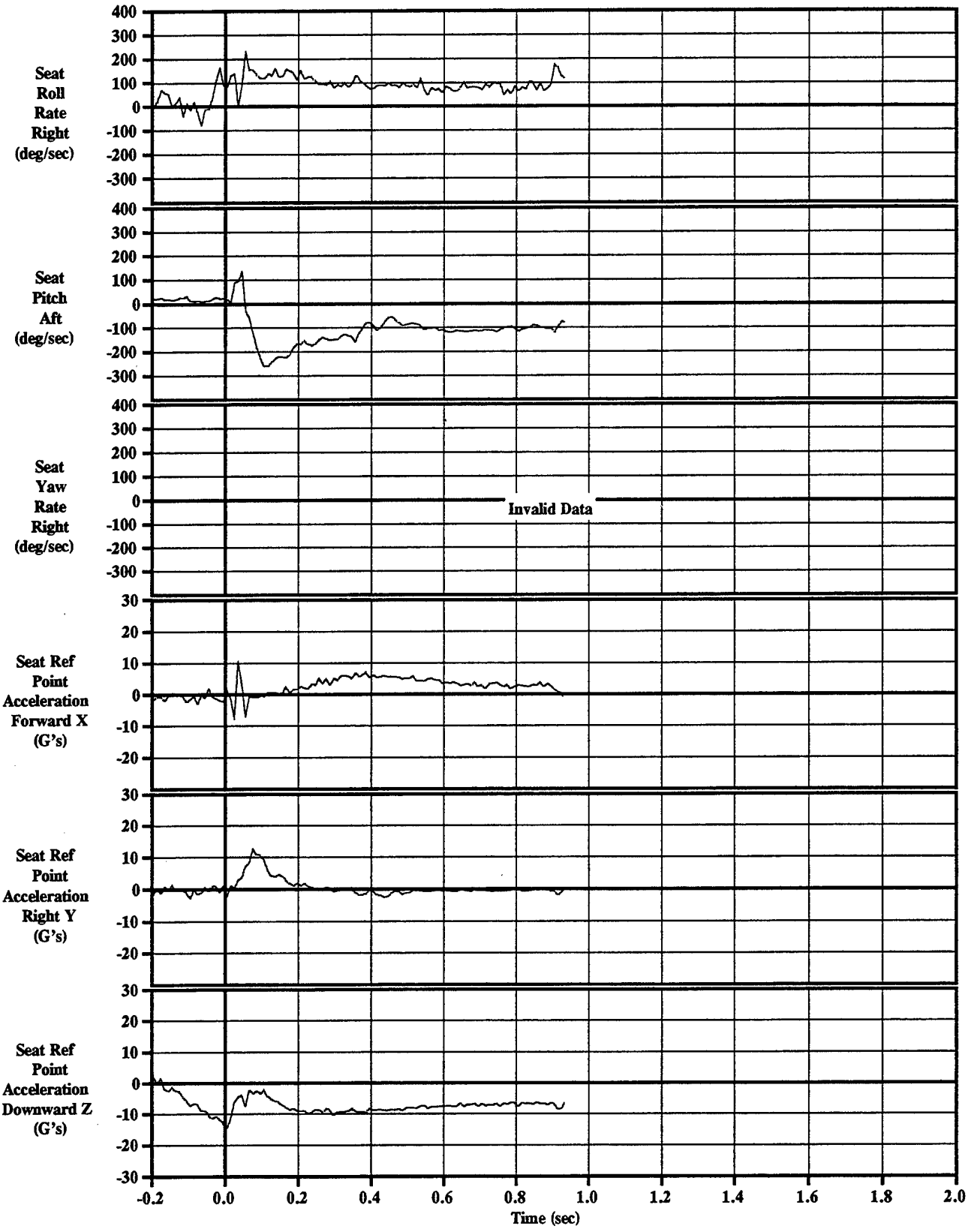

Figure C-8-11 ADAM Recorded Seat Rotation Rates and Accelerations
Sled Test=8, KEAS=438, 5th%, Yaw=20

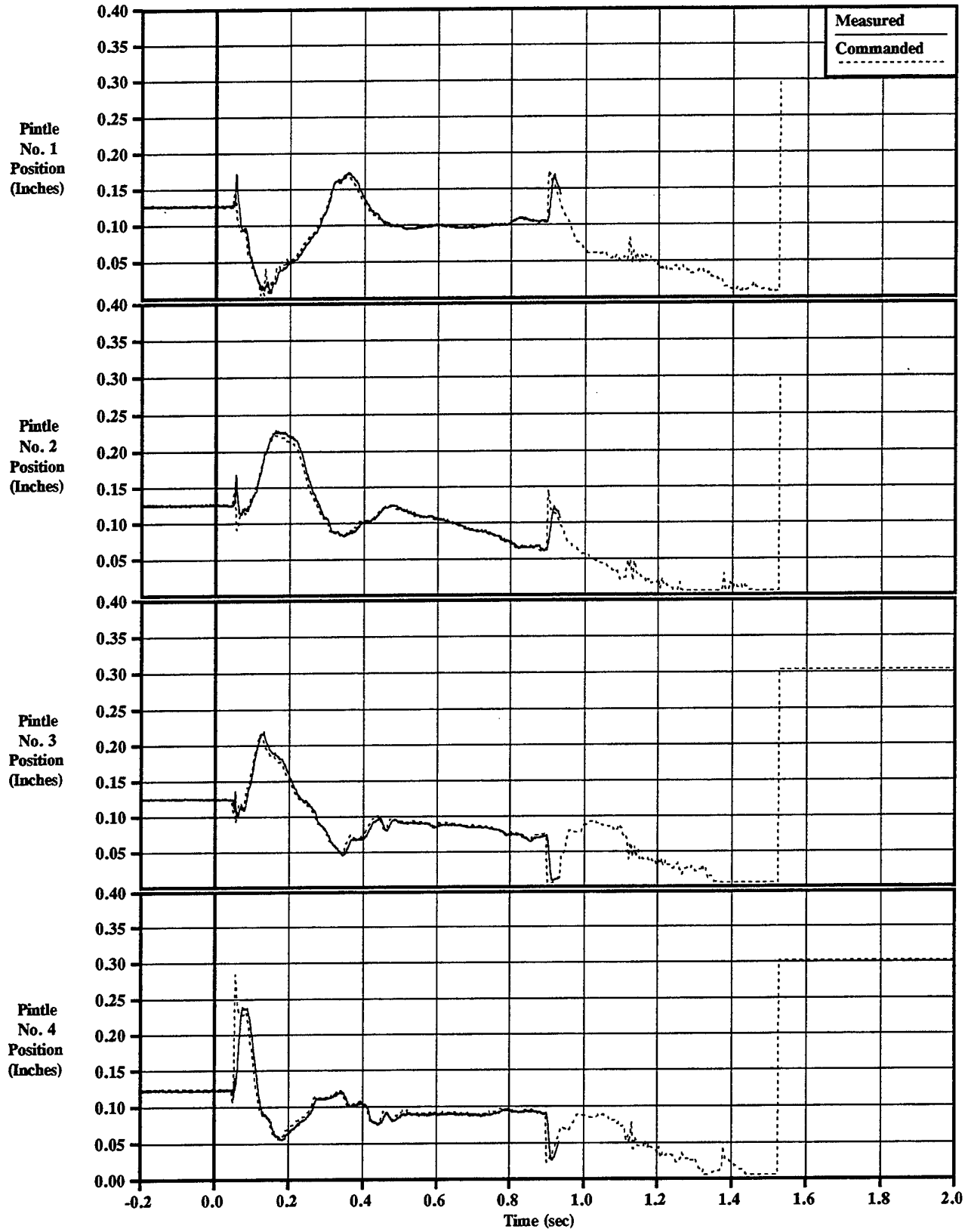

Figure C-8-12 Pintle Positions & Commands
Sled Test=8, KEAS=438, 5th%, Yaw=20

Appendix C-9: Test #9

TEST SUMMARY

Objective

The objective of this test was to demonstrate the flight controls and controllable propulsion system of the 4th Generation Escape System in a 600 KEAS, level flight condition.

Test Conditions

	Run Number	85E-F1
	Test Date	15 October 1997
	System Launch Time	11:49 AM MDT 288:17:49:00.0 IRIG
	Sled Launch Point	TS 873
	Seat Eject Point	TS 6998 @ 9.985815 sec
	Temperature	59 deg F
	Relative Humidity	46%
(1)	Wind	5.5 knots at 281°
	Barometric Pressure	12.851 lb/in^2
	Velocity	589.2 KEAS (1071.4 fps)
	Sled Gx at Catapult Init	-3.5 G
	Roll	0 deg
	Pitch	0 deg
	Yaw	0 deg
	ADAM Manikin Size	Small

(1) 0° angle is a head wind. Positive to the right (clockwise).

Summary And Conclusions

The ninth system sled test of the 4th Generation Escape System program was conducted on Wednesday, 15 October at Holloman AFB, NM. This test successfully demonstrated the ability of the controllable propulsion system to stabilize the escape system during a high speed ejection. After separation from the guide rails, the seat was pitched back at 80° to 60° angle of attack (AoA). This AoA was slightly higher than the planned AoA of ~70° and is being evaluated. At ~0.9 seconds after motor initiation, the system reoriented for drogue deployment which occurred ~0.2 seconds later. The parachute was then deployed when the system velocity fell to below 220 KEAS. Both the seat and manikin were successfully recovered by parachute.

The MDRC for this test was 0.83 medium risk based on the IMU accelerations being transferred to the critical point. The maximum neck normal force was 413 lbs and the side force was 92 lbs. The higher than expected neck load appears to be the result of

the brim being approximately 4" inches from the helmet instead of the planned 1.9". This increase is distance is due to a combination of manikin slump and brim billowing. Future tests will revise the brim rigging to prevent excessive billowing in order to maintain the desired brim-helmet separation distance.

Control angle overshoots of ~10° in alpha, and ~4° in beta at were observed at ~0.4 seconds on this test. Analysis of has determined that the overshoot was most likely caused by two primary effects:

- Impingement loads from the rocket plume on the seat structure
- Aerodynamic effects of the rocket plumes on the total body coefficients

The impingement load of the plume was modeled as a reaction thrust acting on the seat sides at the upper thrusters and the aerodynamic effect as a change to the Cx and Cz coefficients. With these changes good correlation with the test data was obtained. The effect of the plume impingement is to reduce the control moment authority of the system, resulting in reduced control margins. During Phase I off this program the plume impingement issue was addressed and at that time determined to be a negligible effect. Analysis of this test has indicated that the impingement force is not negligible and must be modeled in the simulation

Data.
The primary data obtained from the IMU and ADAM are presented in Figures C-9-1 through C-9-12.

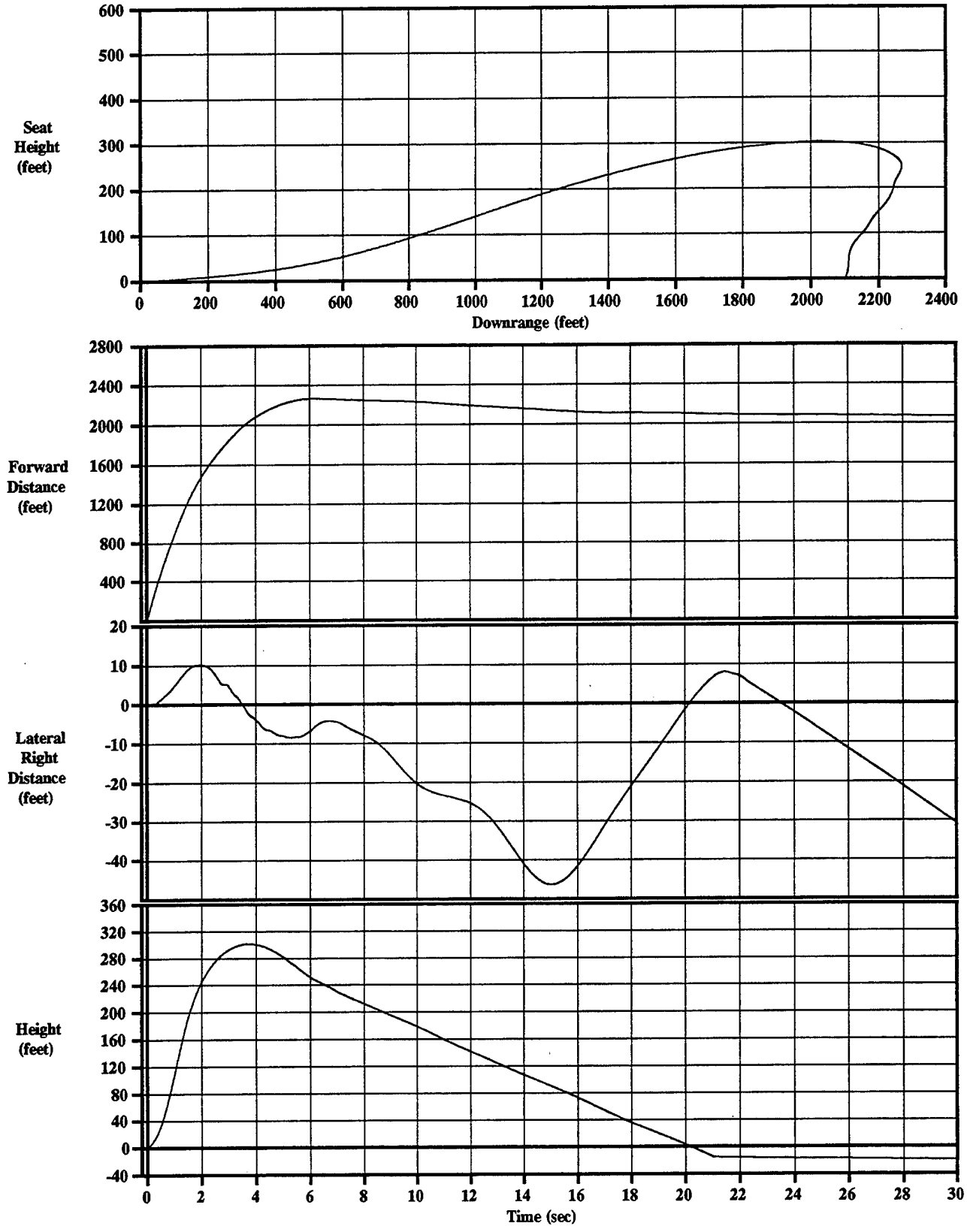

Figure C-9-1 IMU Displacements
Sled Test=9, KEAS=589, 5th%

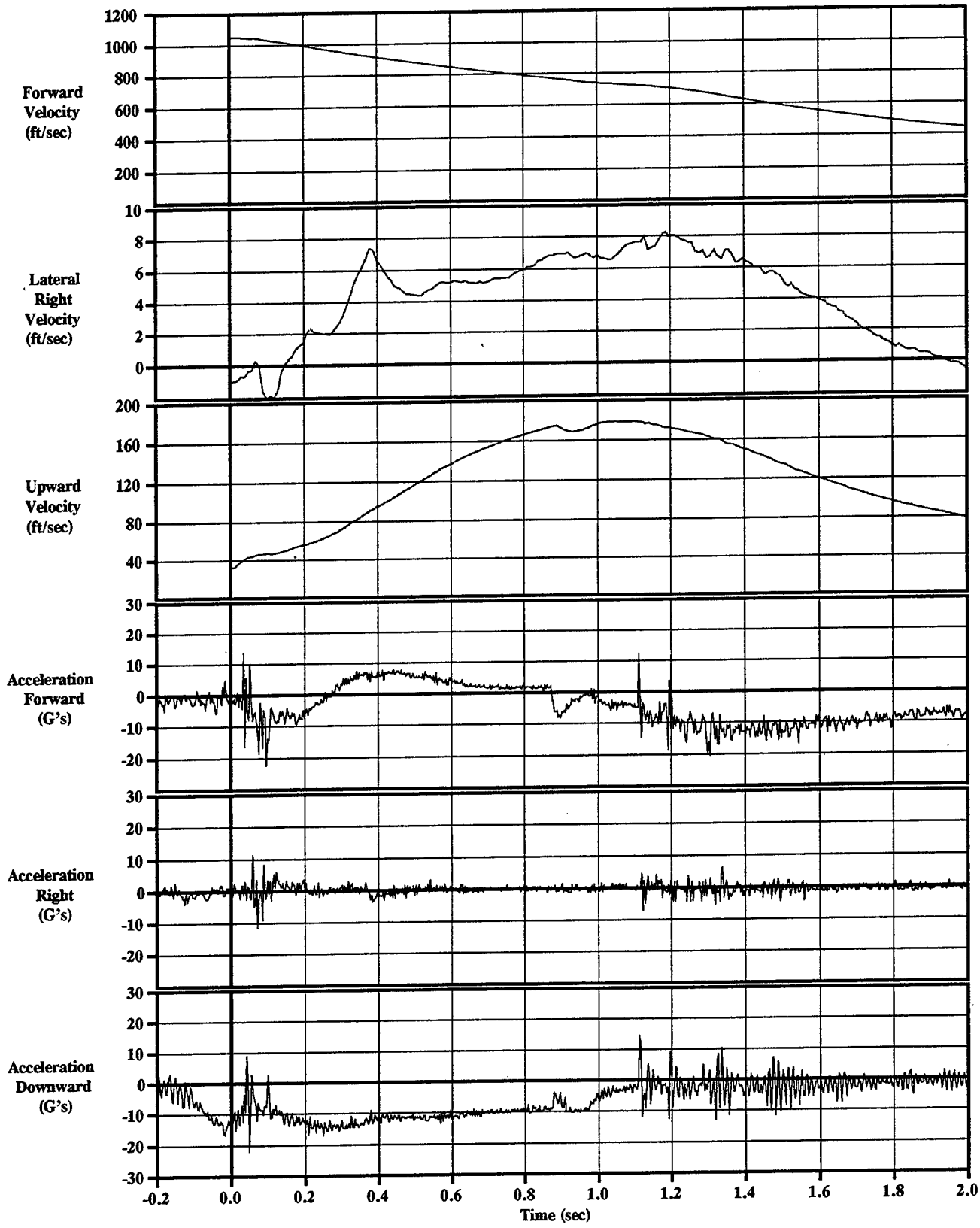

Figure C-9-2 IMU Velocities & Accelerations
Sled Test=9, KEAS=589, 5th%

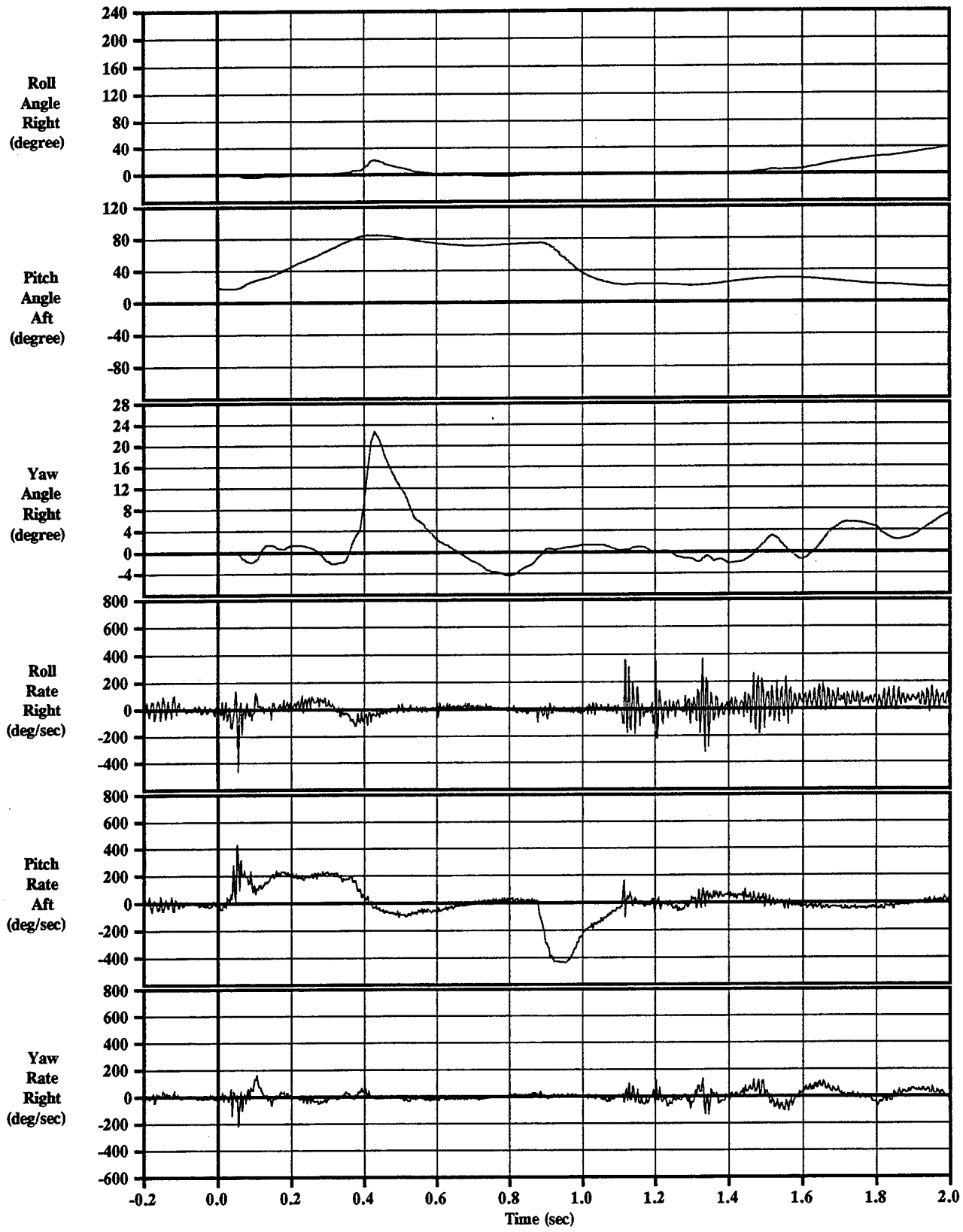

Figure C-9-3 IMU Rotation Angles & Rates
Sled Test=9, KEAS=589, 5th%

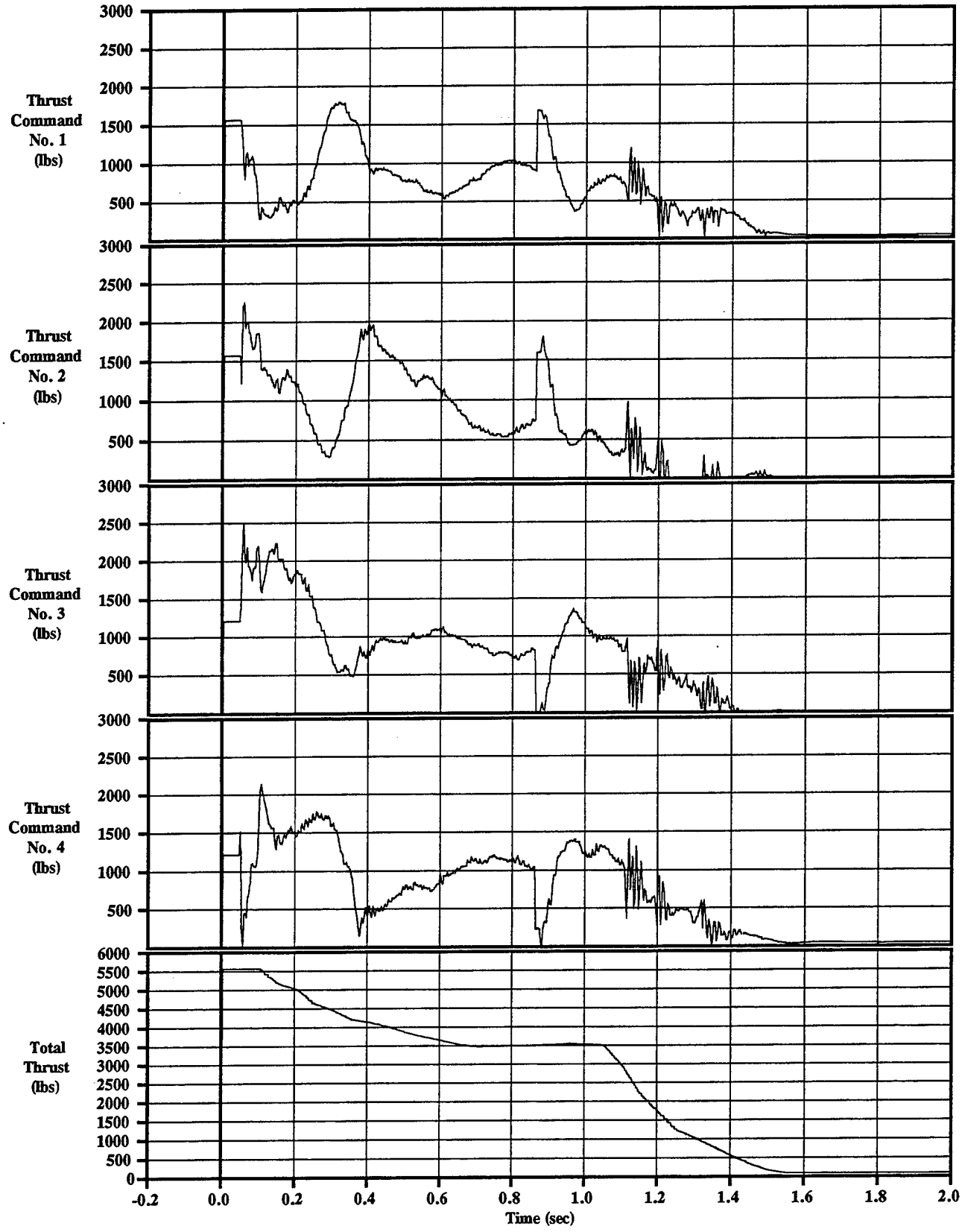

Figure C-9-4 Thrust Commands
Sled Test=9, KEAS=589, 5th%

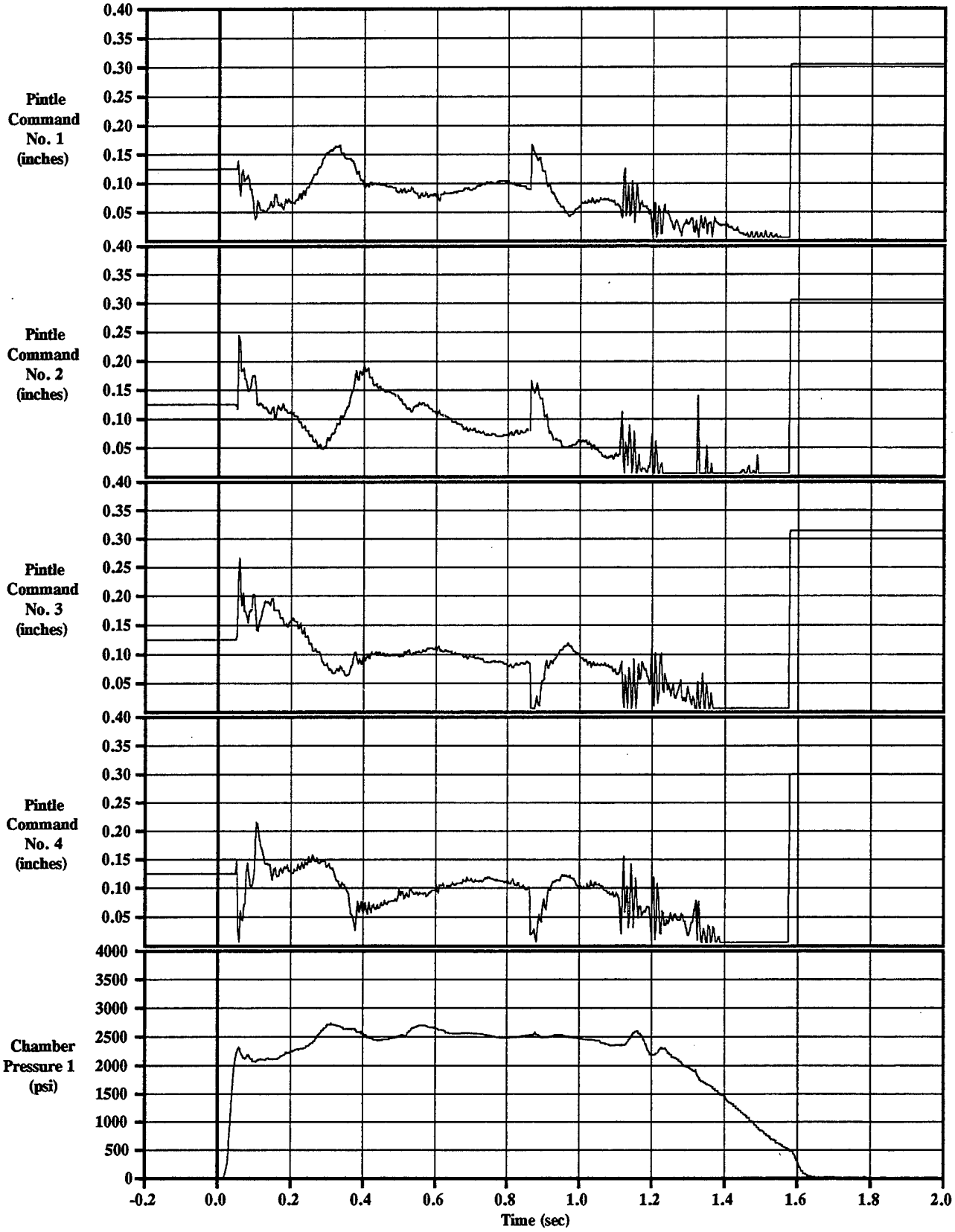

Figure C-9-5 Pintle Commands & Chamber Pressure
Sled Test=9, KEAS=589, 5th%

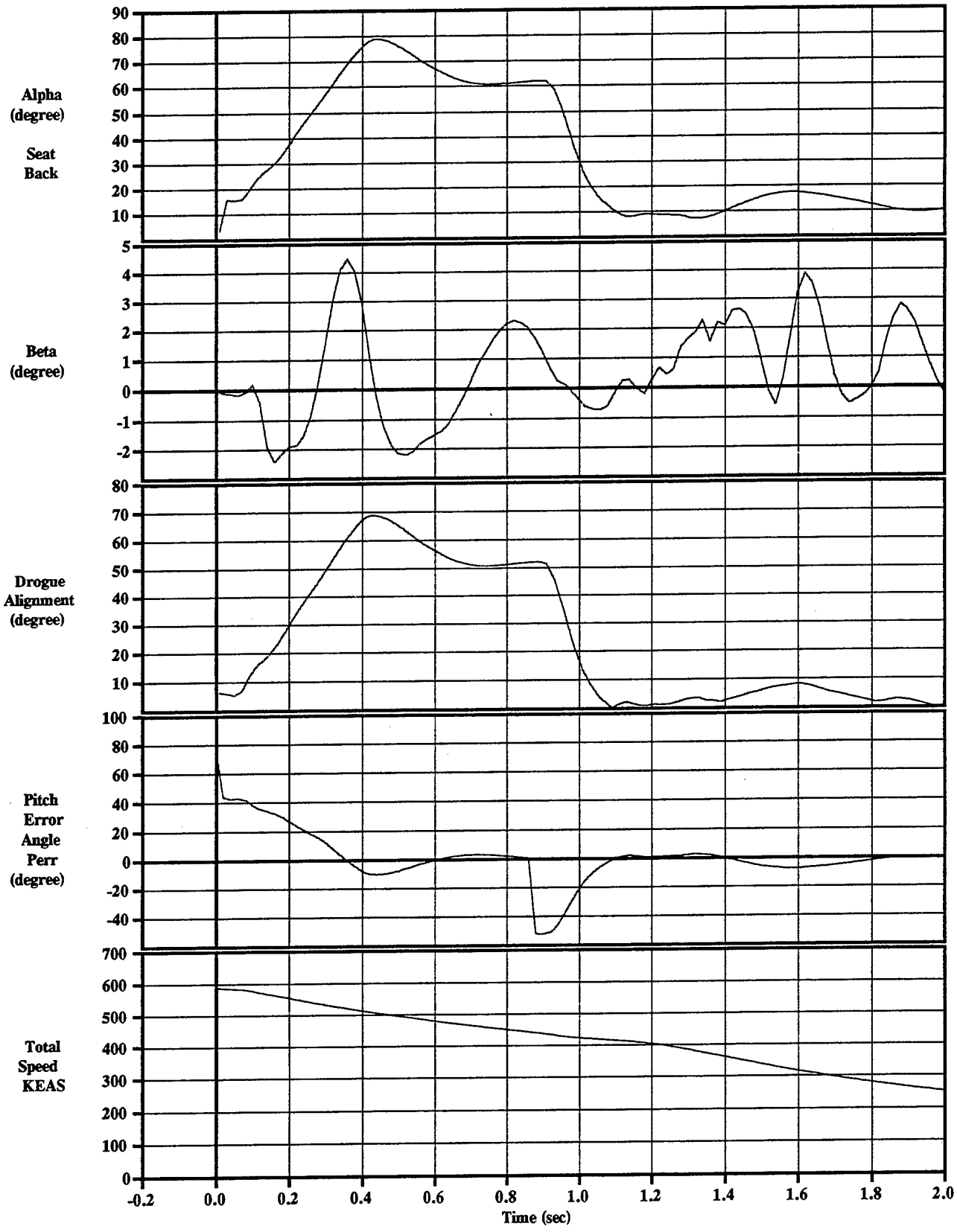

Figure C-9-6 IMU Control Angles and Total Velocity
Sled Test=9, KEAS=589, 5th%

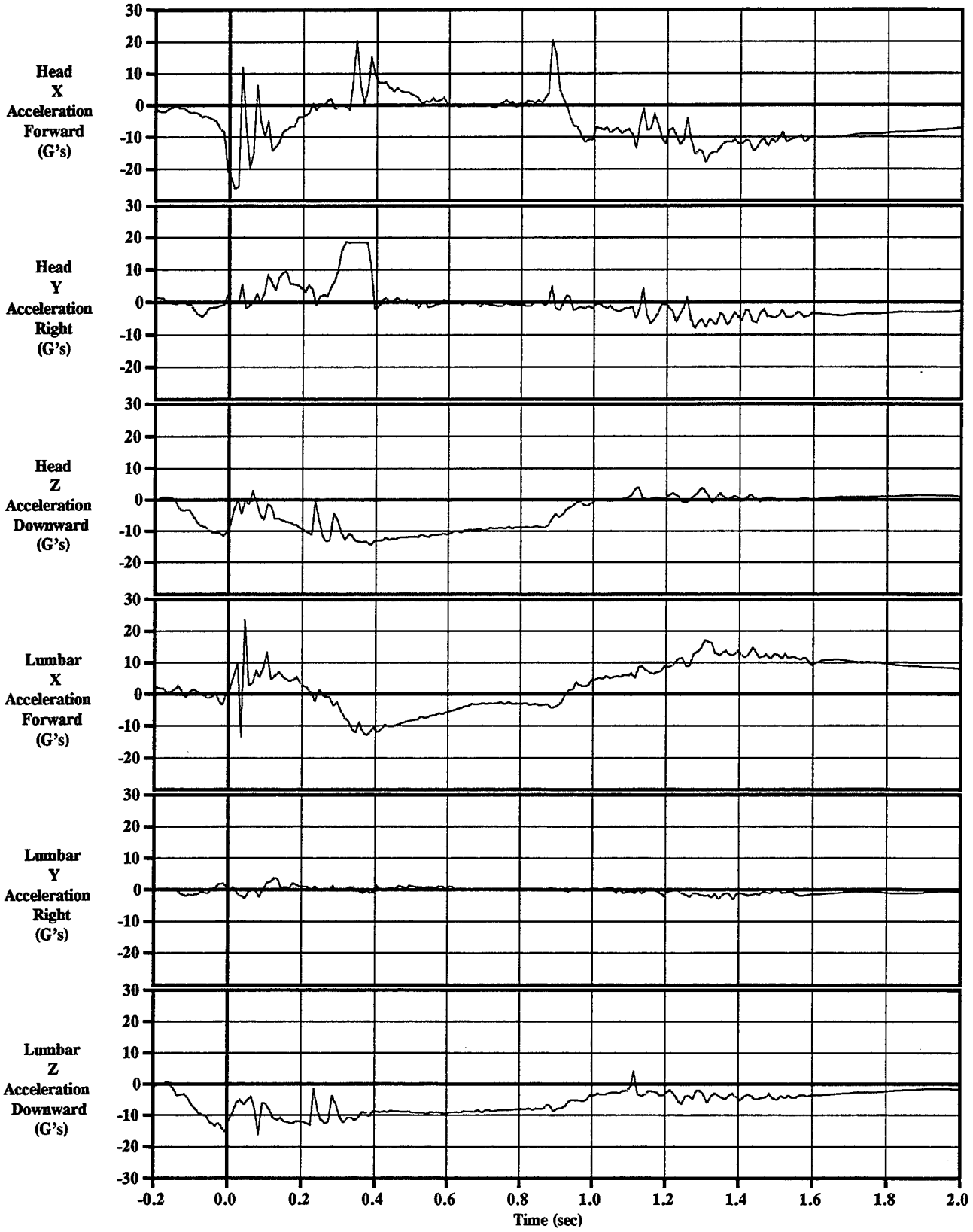

Figure C-9-7 ADAM Head & Lumbar Accelerations
Sled Test=9, KEAS=589, 5th%

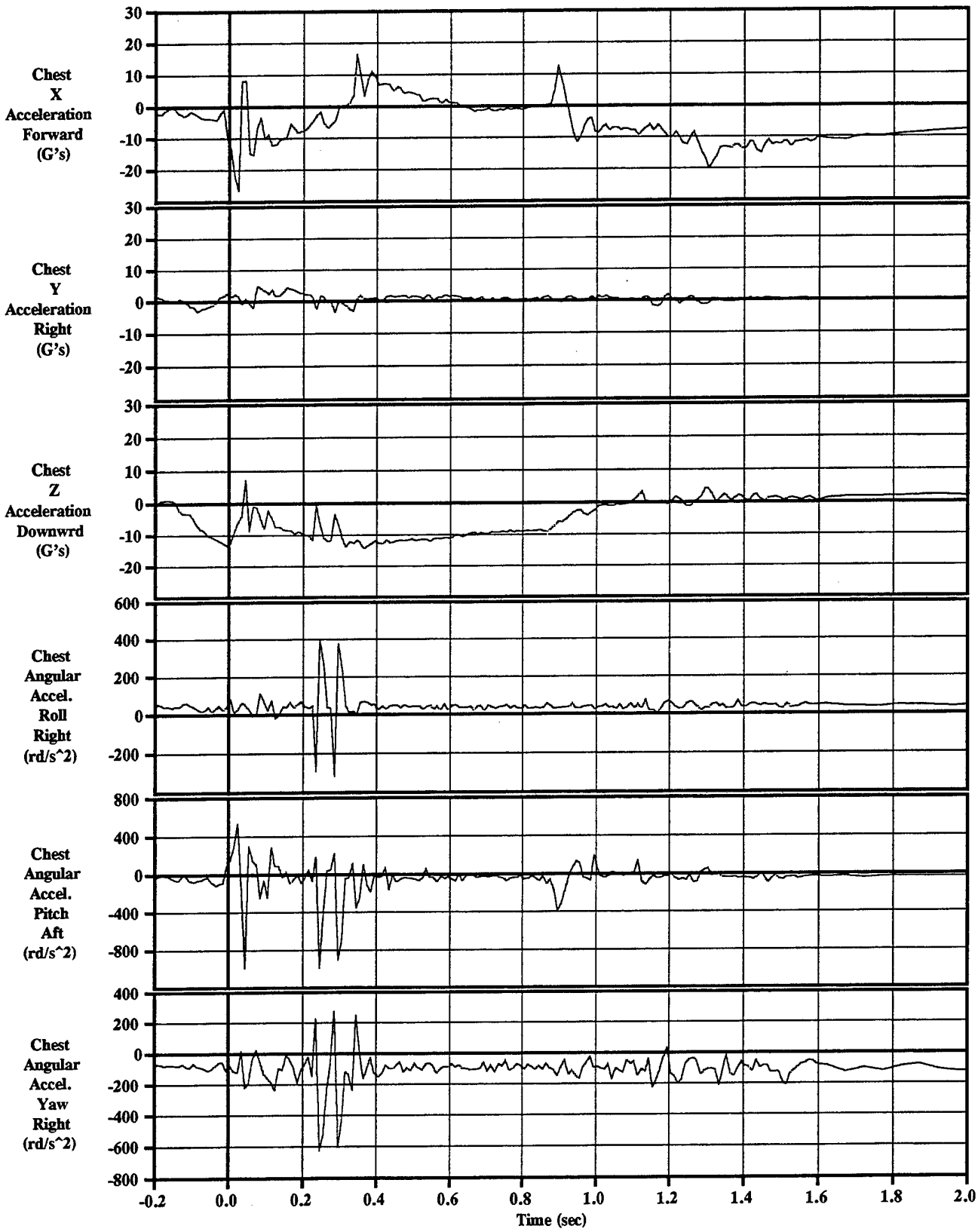

Figure C-9-8 ADAM Chest Linear & Angular Accelerations
Sled Test=9, KEAS=589, 5th%

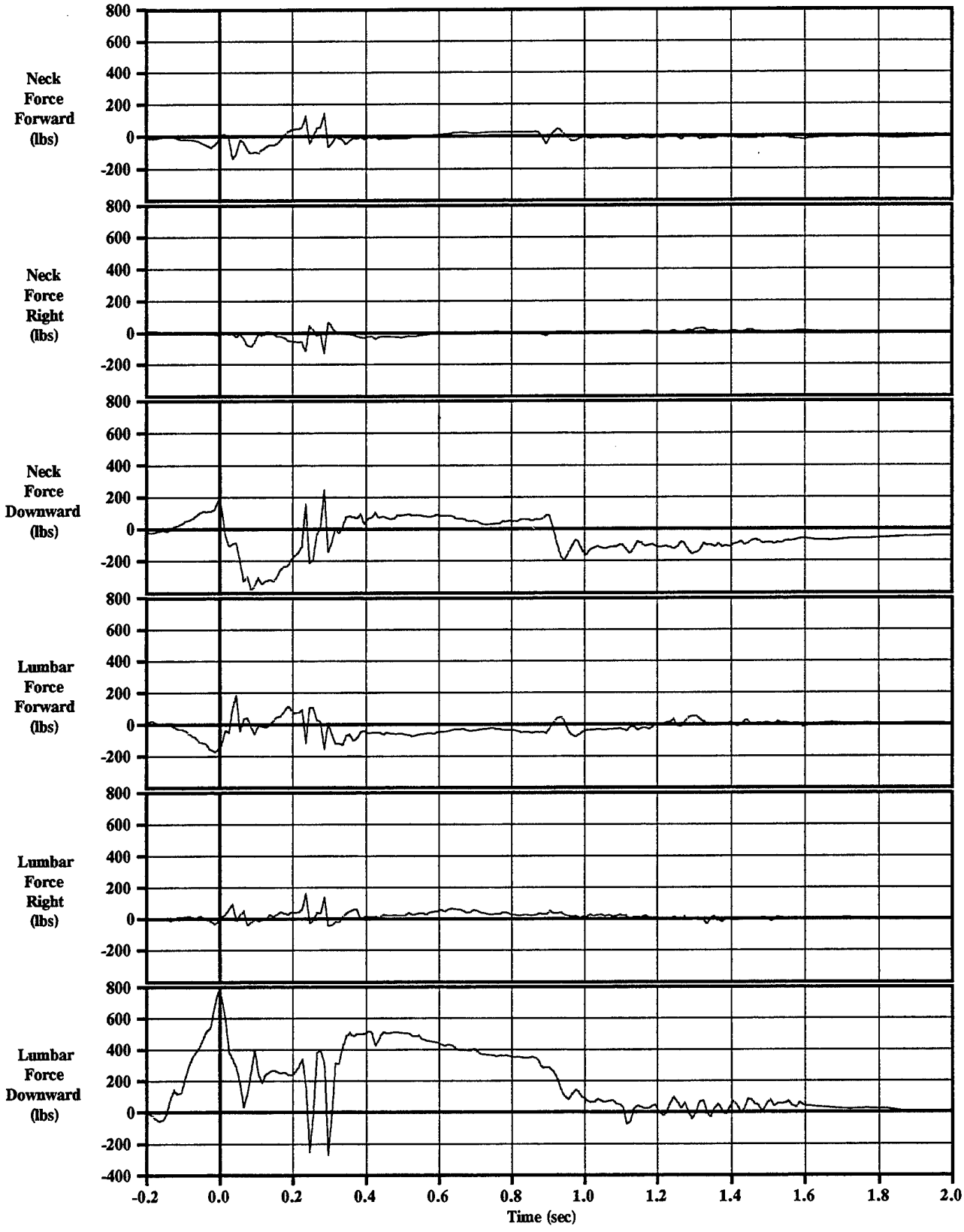

Figure C-9-9 ADAM Neck & Lumbar Forces
Sled Test=9, KEAS=589, 5th%

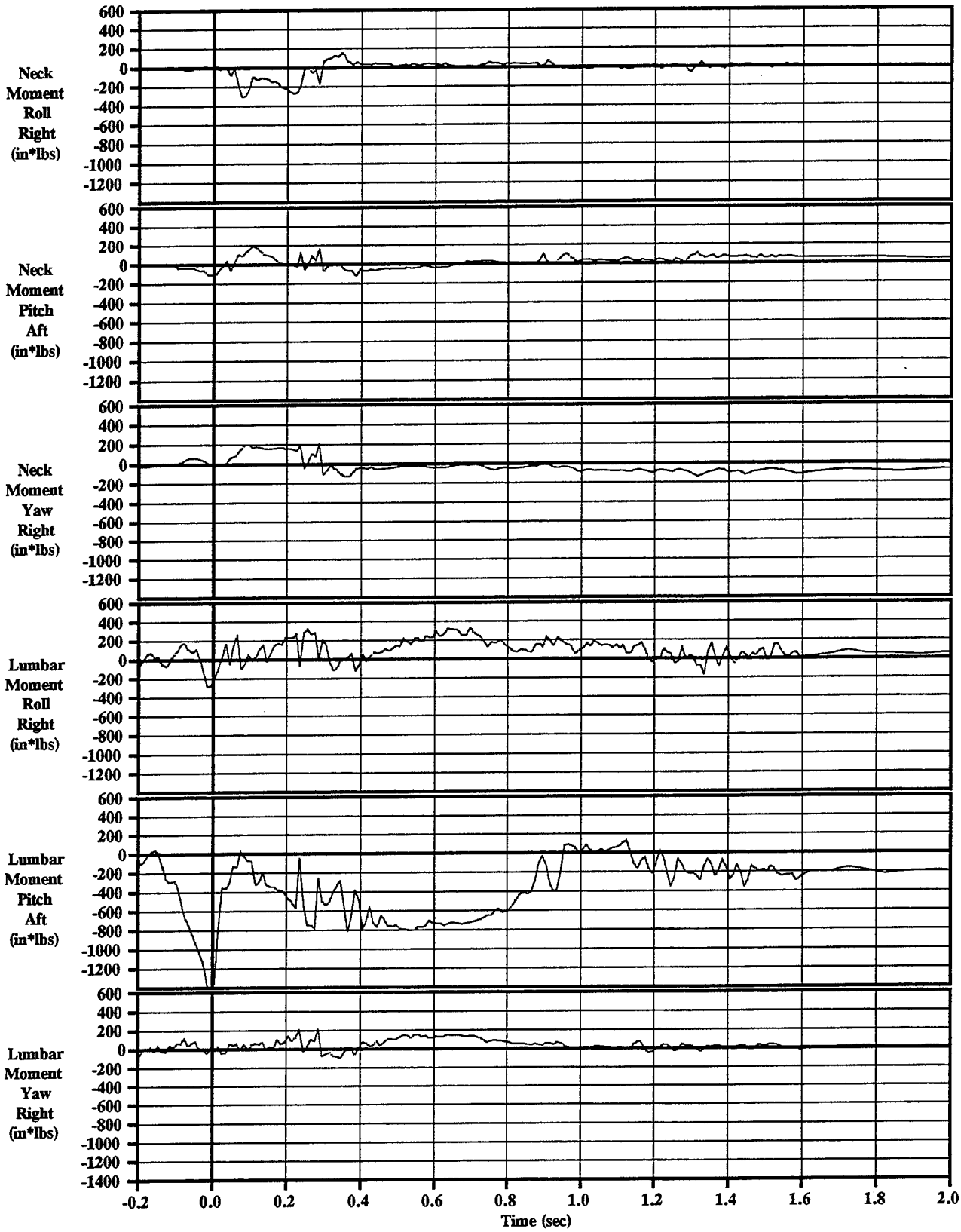

Figure C-9-10 ADAM Neck & Lumbar Moments
Sled Test=9, KEAS=589, 5th%

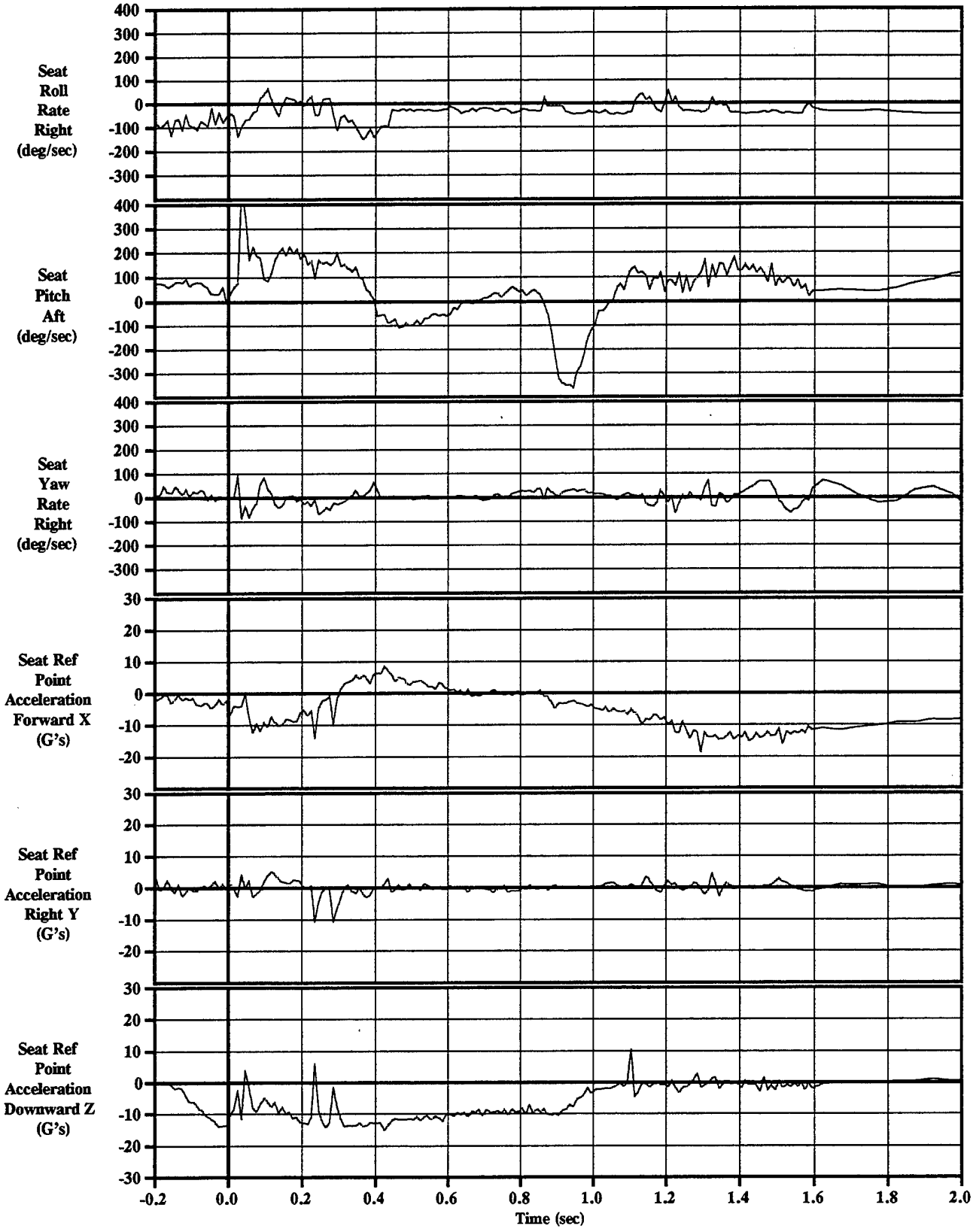

Figure C-9-11 ADAM Recorded Seat Rotation Rates and Accelerations
Sled Test=9, KEAS=589, 5th%

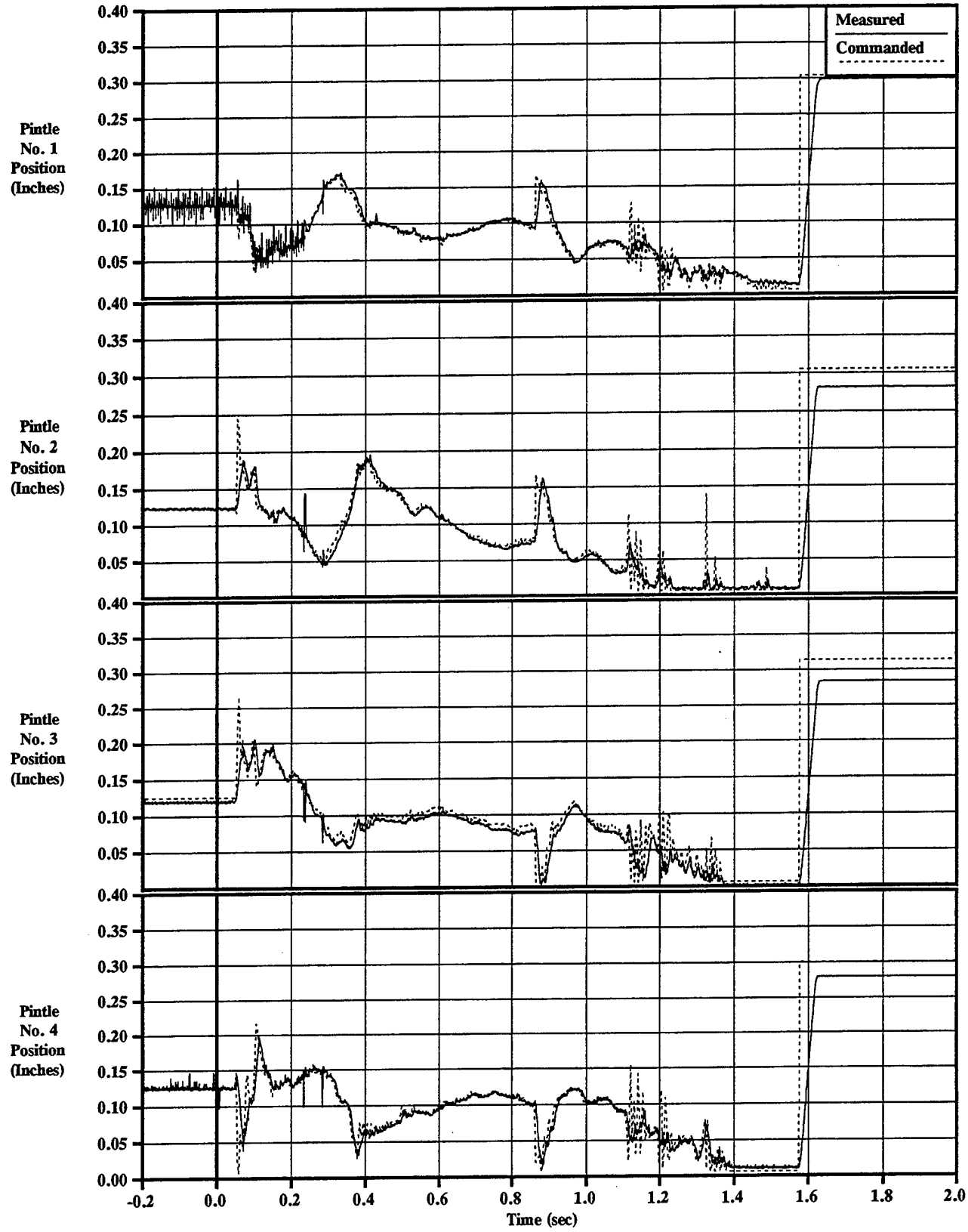

Figure C-9-12 Pintle Positions & Commands
Sled Test=9, KEAS=589, 5th%

Appendix C-10: test #10

TEST SUMMARY

Objective

The objective of this test was to demonstrate the flight controls system and high speed protection devices of the 4th Generation Escape System in an ejection at 700 KEAS, in level flight conditions.

Test Conditions

	Run Number	85E-G2
	Test Date	10 November 1997
	System Launch Time	10:30 AM MDT 314:17:30:00.0 IRIG
	Sled Launch Point	TS 249
	Seat Eject Point	TS 7417 @ 10.83093 sec
	Temperature	43 deg F
	Relative Humidity	64.2%
(1)	Wind	4.4 knots at 239°
	Barometric Pressure	12.774 lb/in^2
	Velocity	708.5 KEAS (1267 fps)
	Sled Gx at Catapult Init	~ 0 G
	Roll	0 deg
	Pitch	0 deg
	Yaw	0 deg
	ADAM Manikin Size	Small

(1) 0° angle is a head wind. Positive to the right (clockwise).

Summary And Conclusions

The tenth system sled test of the 4th Generation Escape System program was conducted on Monday, 10 November, at Holloman AFB, NM. This test successfully demonstrated the ability of the controllable propulsion system to stabilize the escape system during a high speed ejection. After separation from the guide rails, the seat pitched back to the intended 70° angle of attack (AoA) At ~0.9 seconds after motor initiation, the system reoriented for drogue deployment which occurred ~0.2 seconds later. The parachute was deployed when the system velocity fell below 220 KEAS. Both the seat and manikin were successfully recovered by parachute.

The MDRC for this test was 1.03, medium risk, based on the IMU accelerations being transferred to the critical point. The maximum neck normal force was 427 lbs and the side force was 91 lbs. The higher than expected neck load appears to be the result of

the brim being approximately 4.5 inches above the helmet instead of the planned 1.9 inches. This increase in distance is apparently due to a combination of manikin slump and brim billowing.

Data.

The primary data obtained from the IMU and ADAM are presented in Figures C-10-1 through C-10-12.

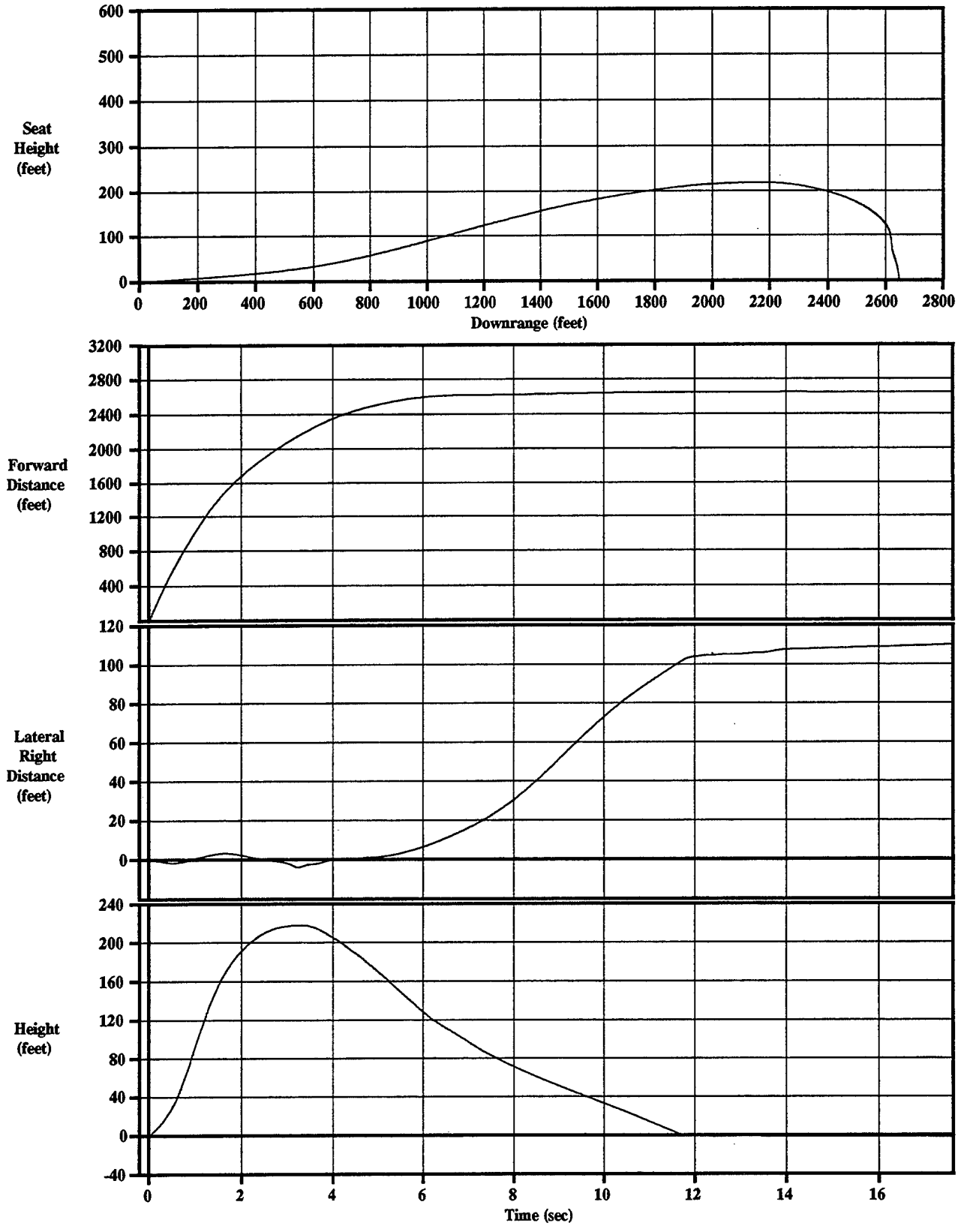

Figure C-10-1 IMU Displacements
Sled Test=10, KEAS=700, 5th%

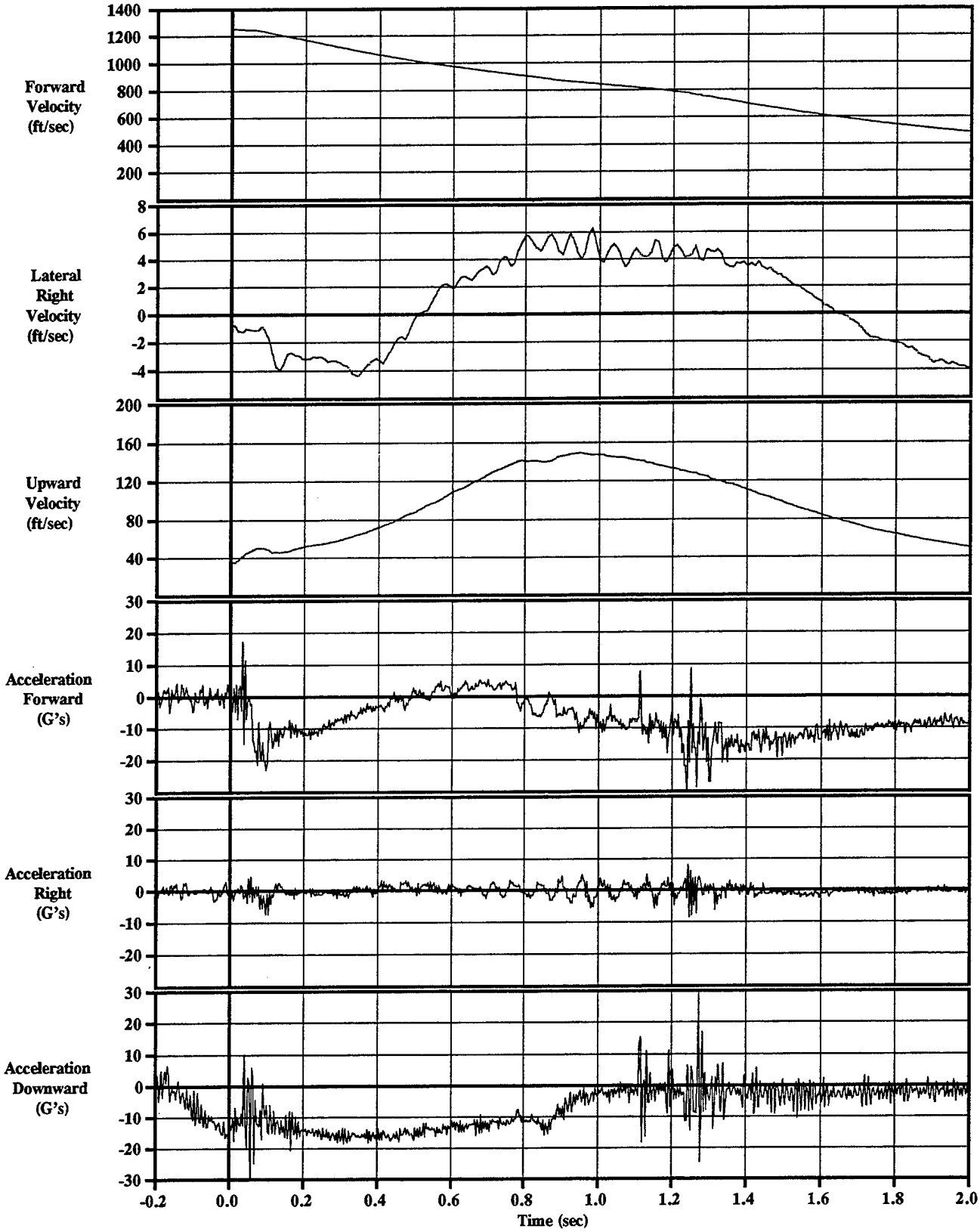

Figure C-10-2 IMU Velocities & Accelerations
Sled Test=10, KEAS=700, 5th%

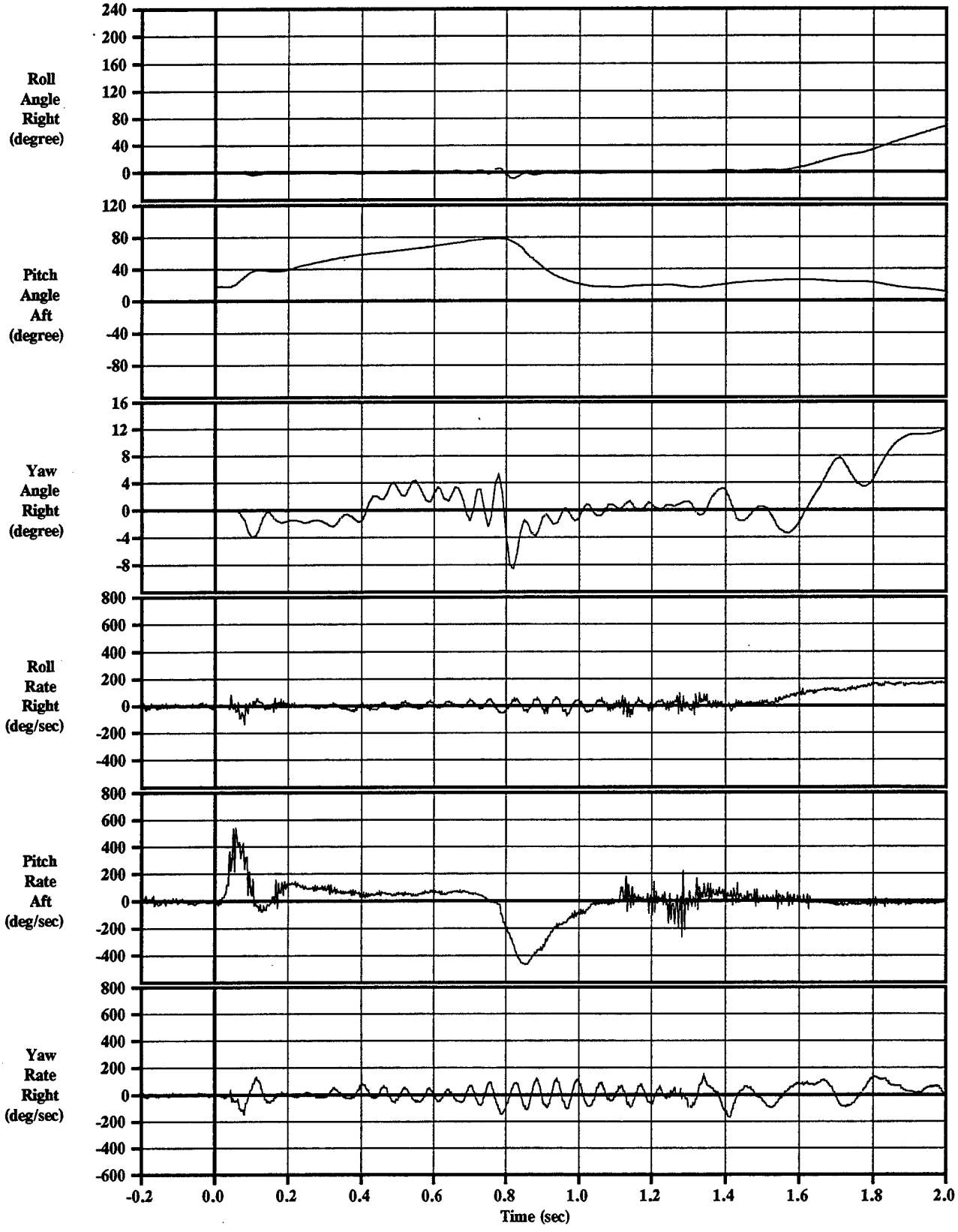

Figure C-10-3 IMU Rotation Angles & Rates
Sled Test=10, KEAS=700, 5th%

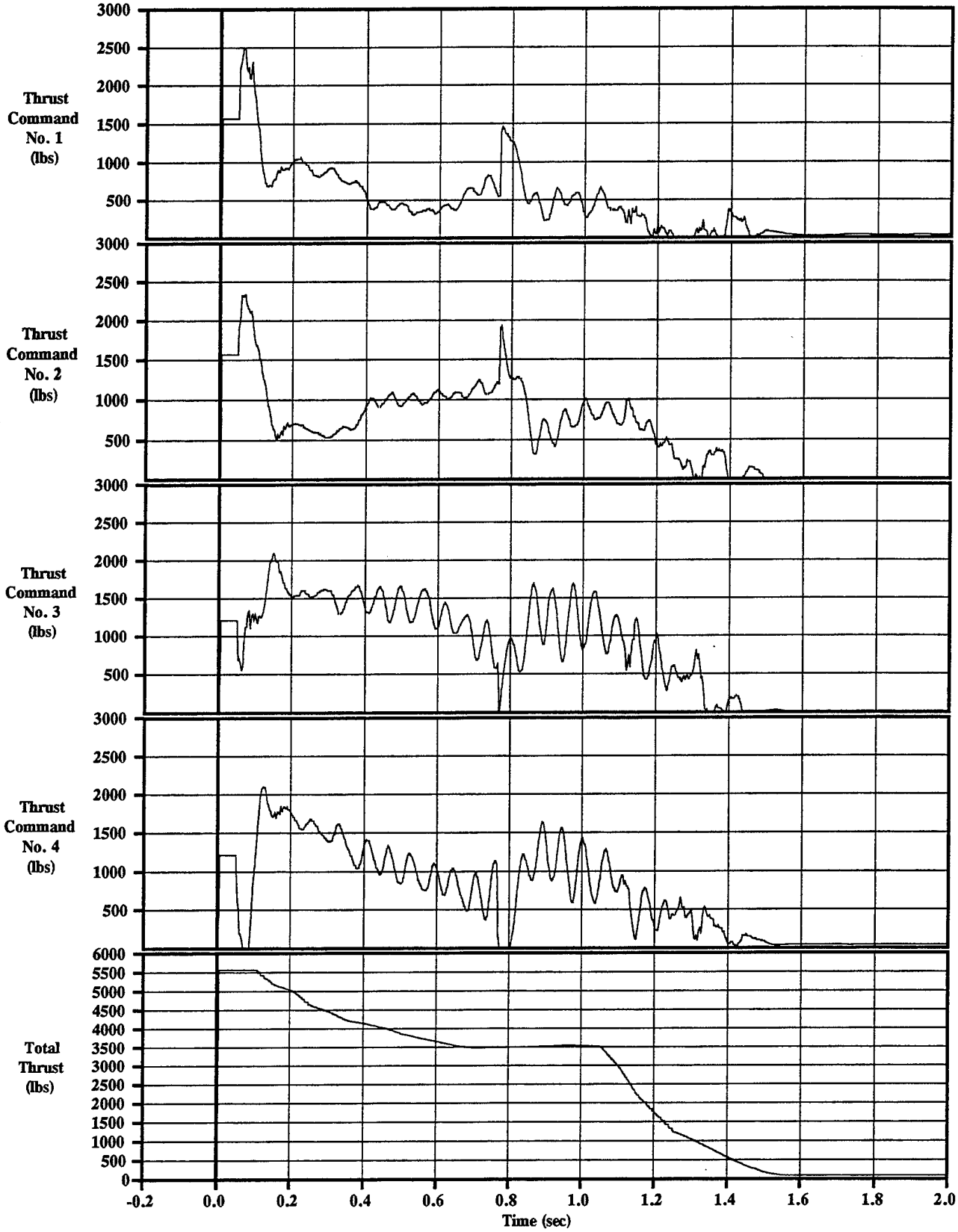

Figure C-10-4 Thrust Commands
Sled Test=10, KEAS=700, 5th%

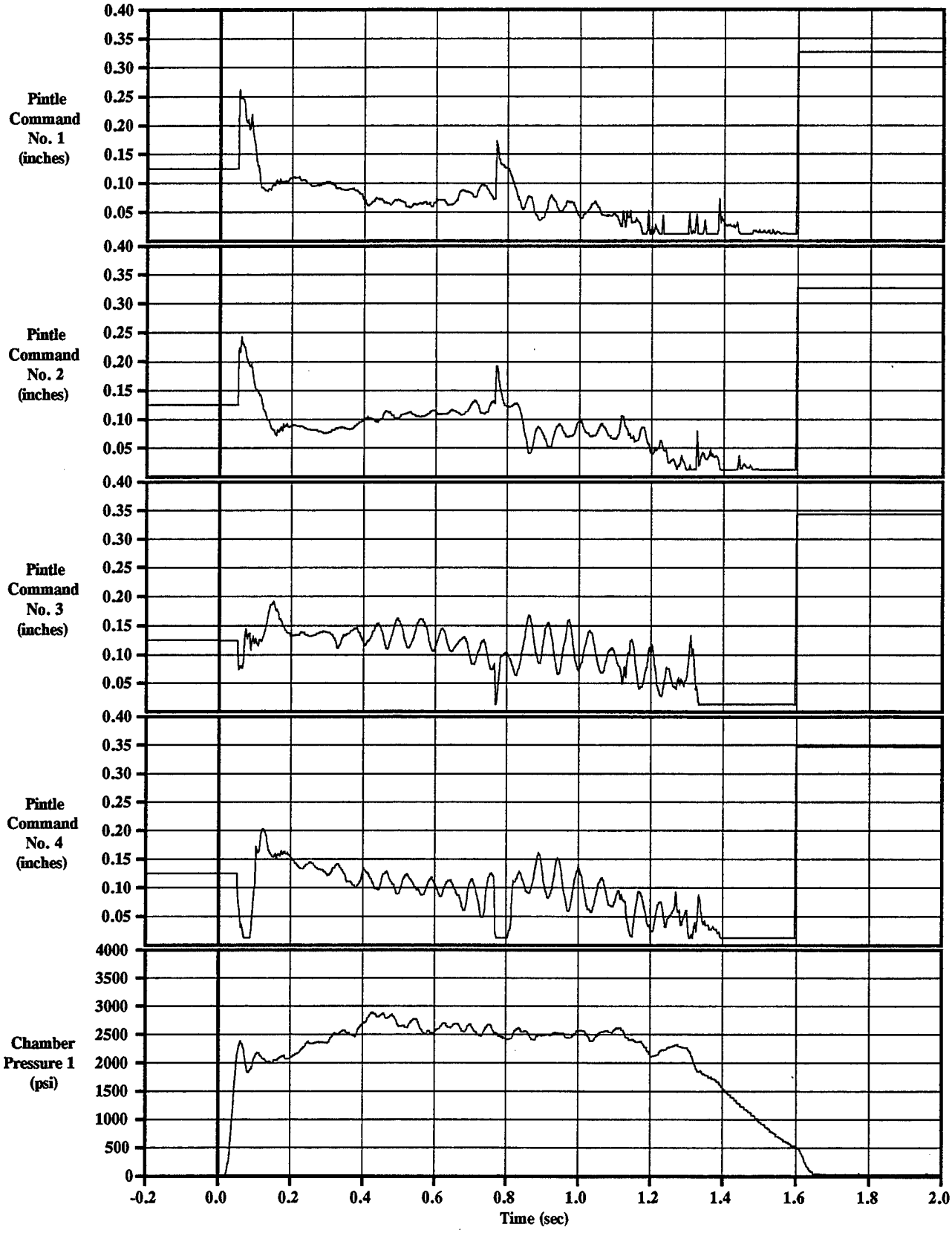

Figure C-10-5 Pintle Commands & Chamber Pressure
Sled Test=10, KEAS=700, 5th%

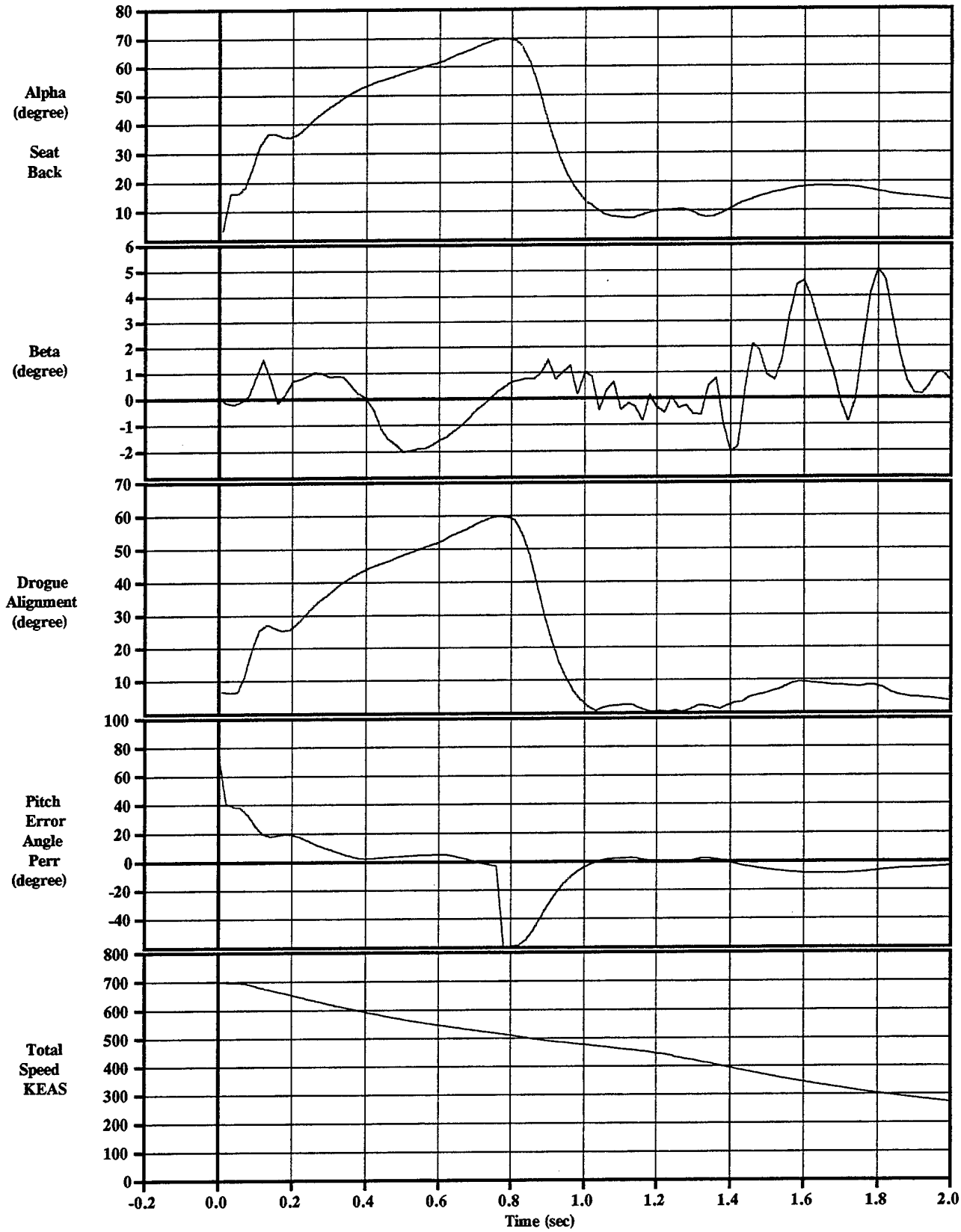

Figure C-10-6 IMU Control Angles and Total Velocity
Sled Test=10, KEAS=700, 5th%

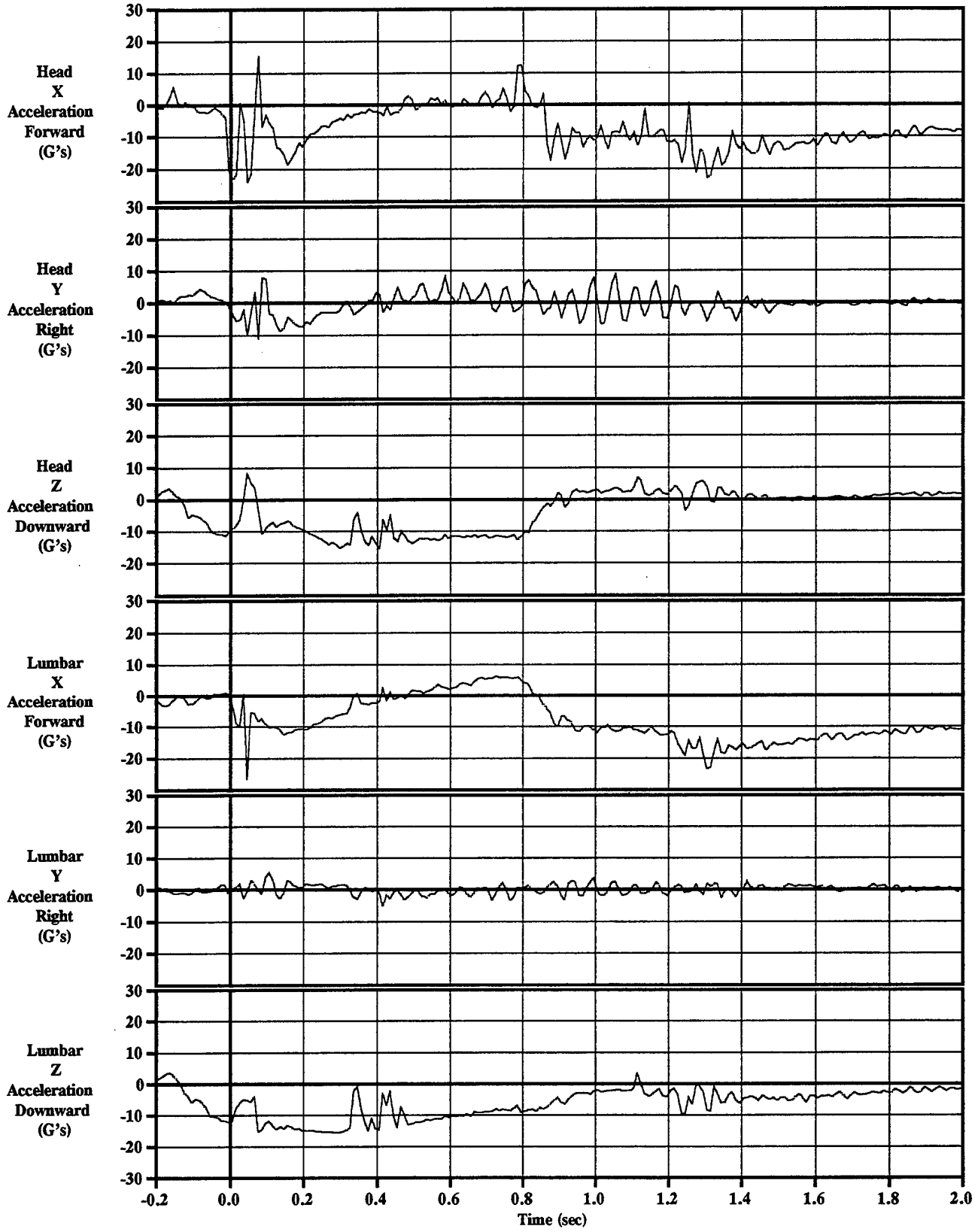

Figure C-10-7 ADAM Head & Lumbar Accelerations
Sled Test=10, KEAS=700, 5th%

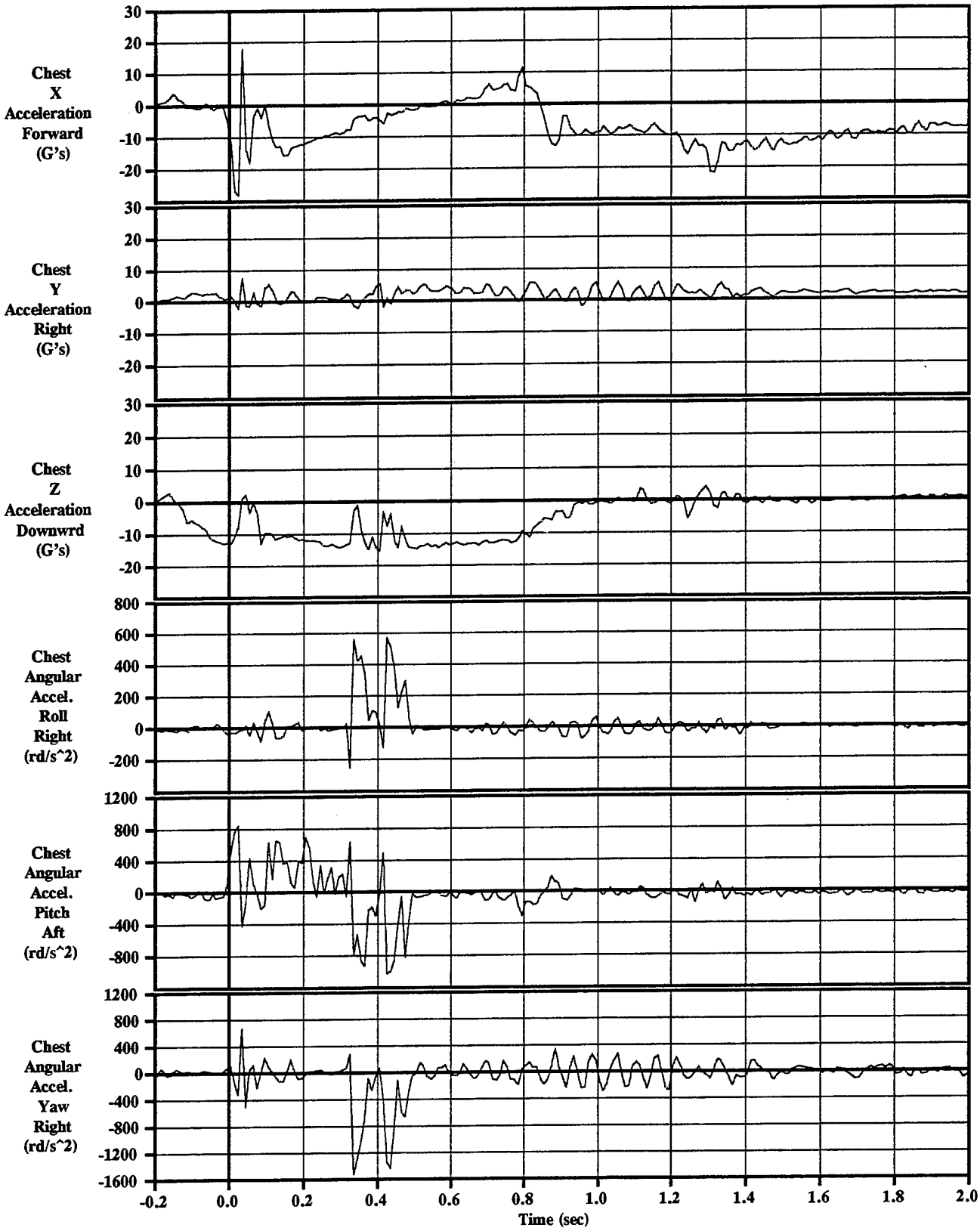

Figure C-10-8 ADAM Chest Linear & Angular Accelerations
Sled Test=10, KEAS=700, 5th%

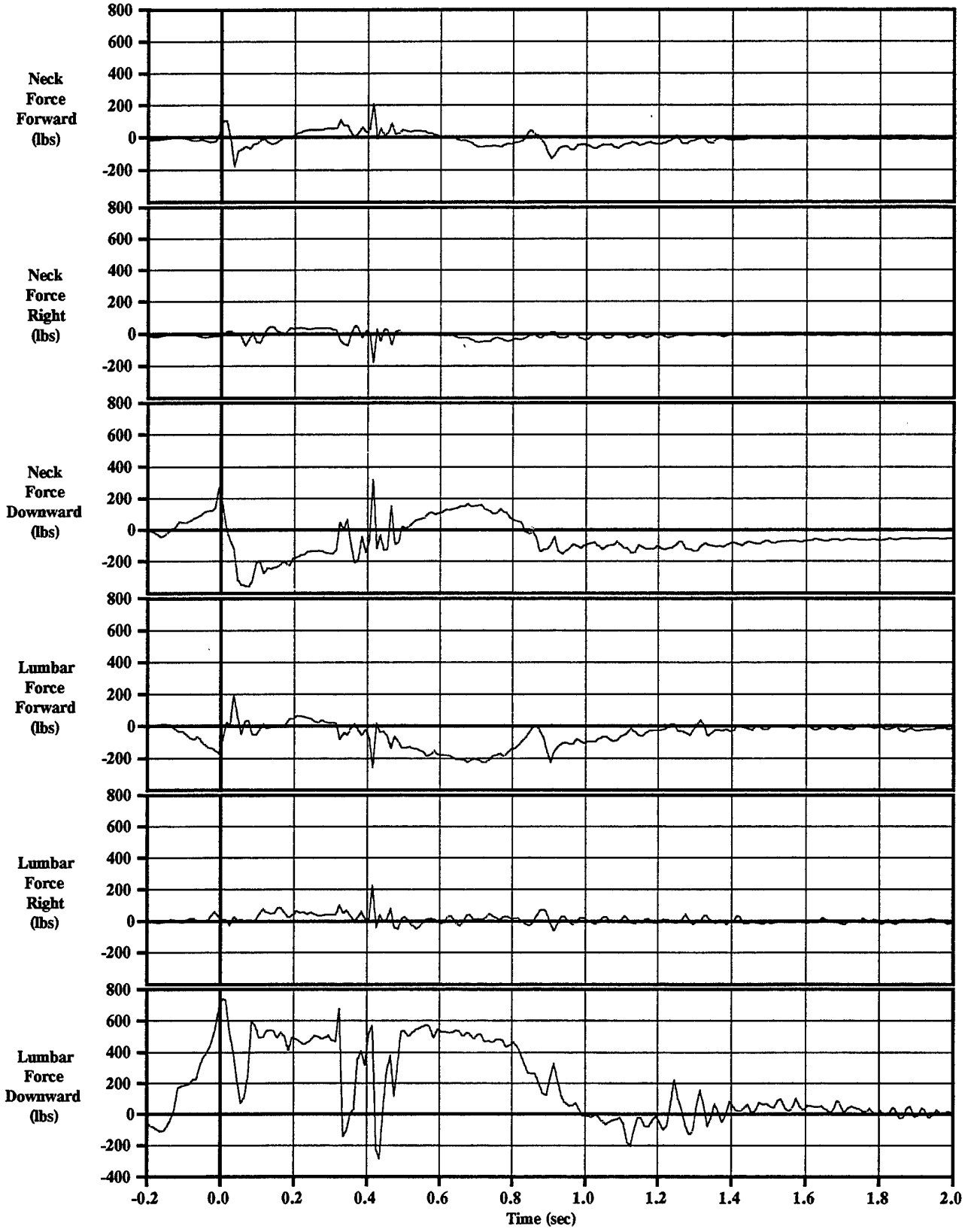

Figure C-10-9 ADAM Neck & Lumbar Forces
Sled Test=10, KEAS=700, 5th%

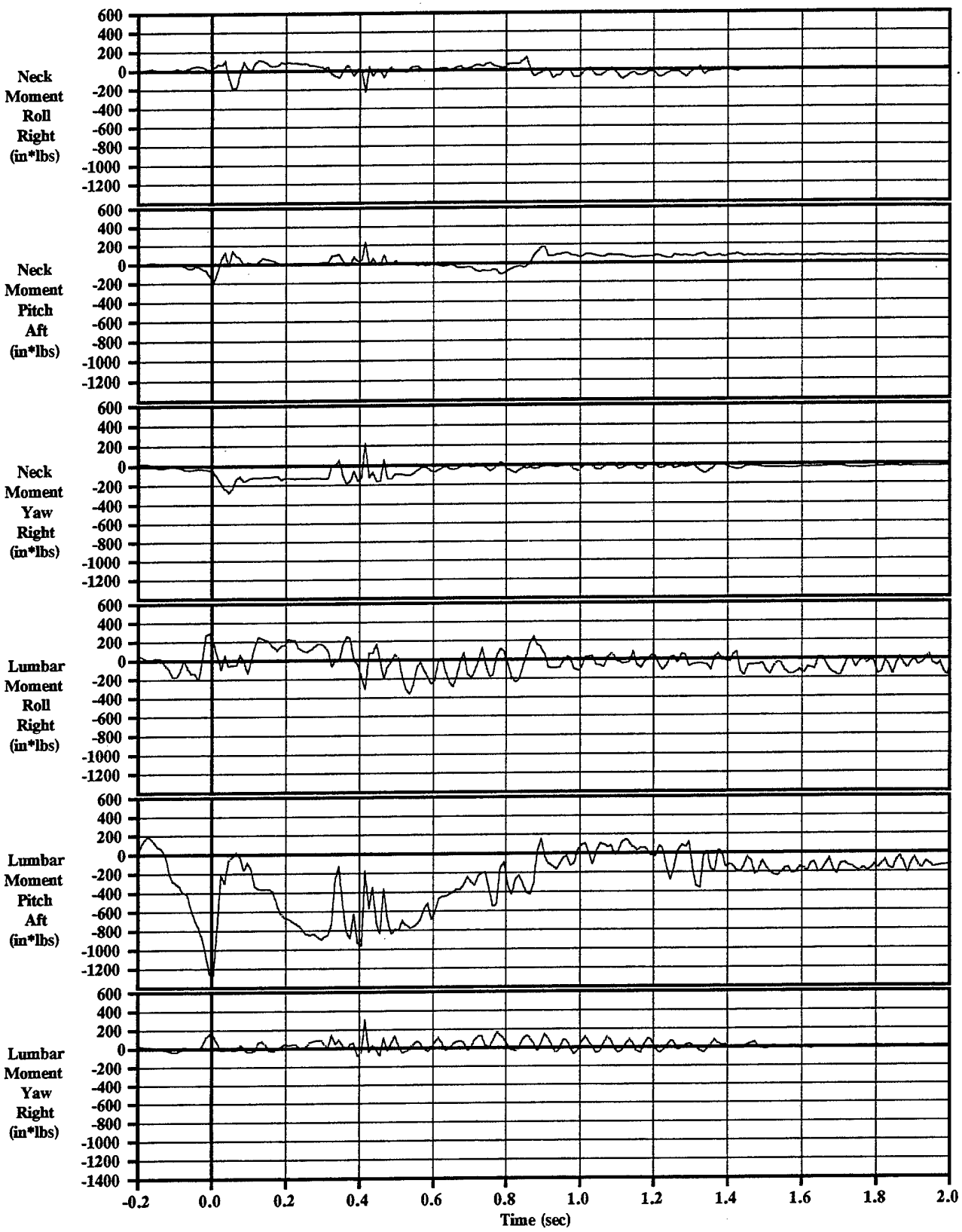

Figure C-10-10 ADAM Neck & Lumbar Moments
Sled Test=10, KEAS=700, 5th%

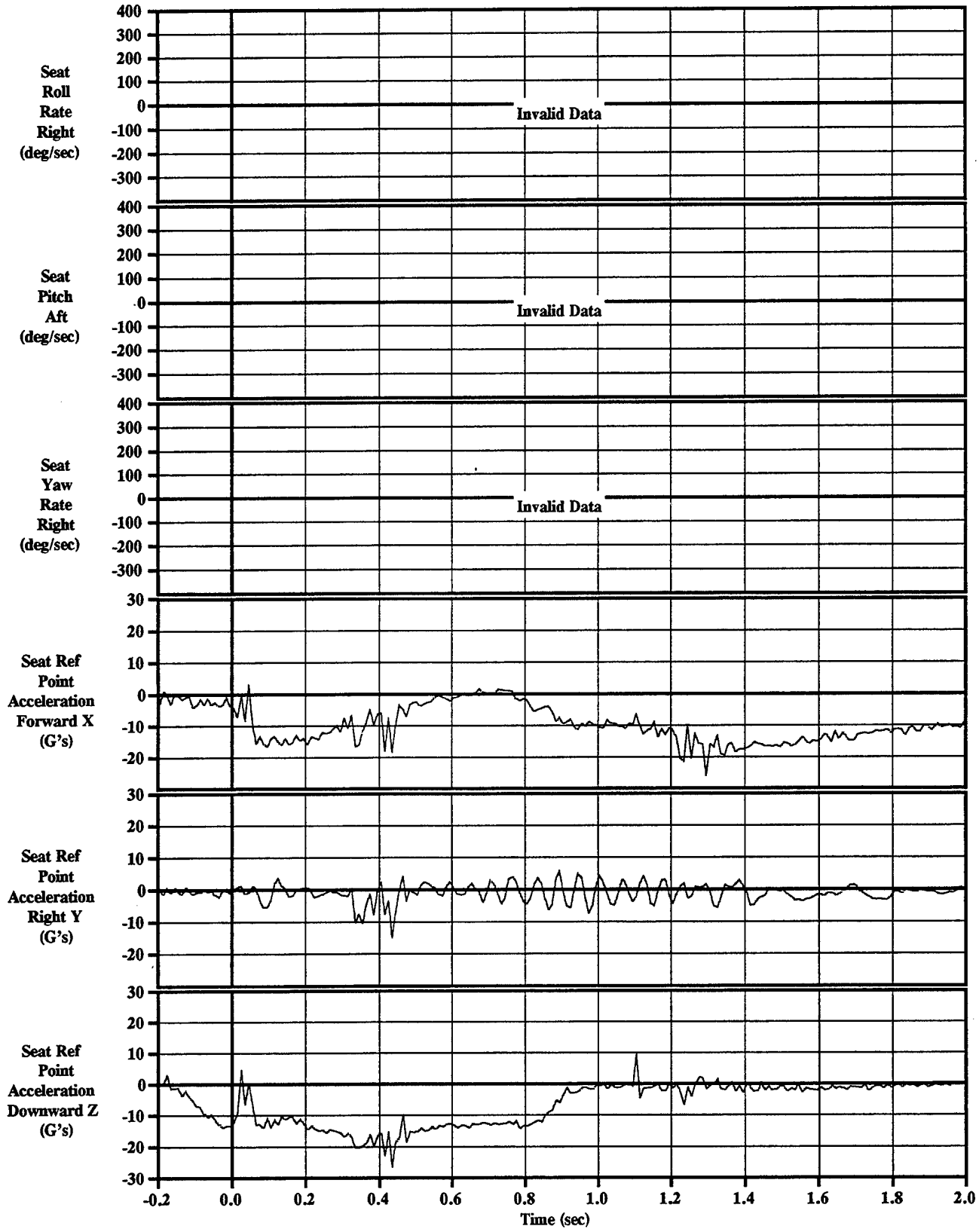

Figure C-10-11 ADAM Recorded Seat Rotation Rates and Accelerations Sled Test=10, KEAS=700, 5th%

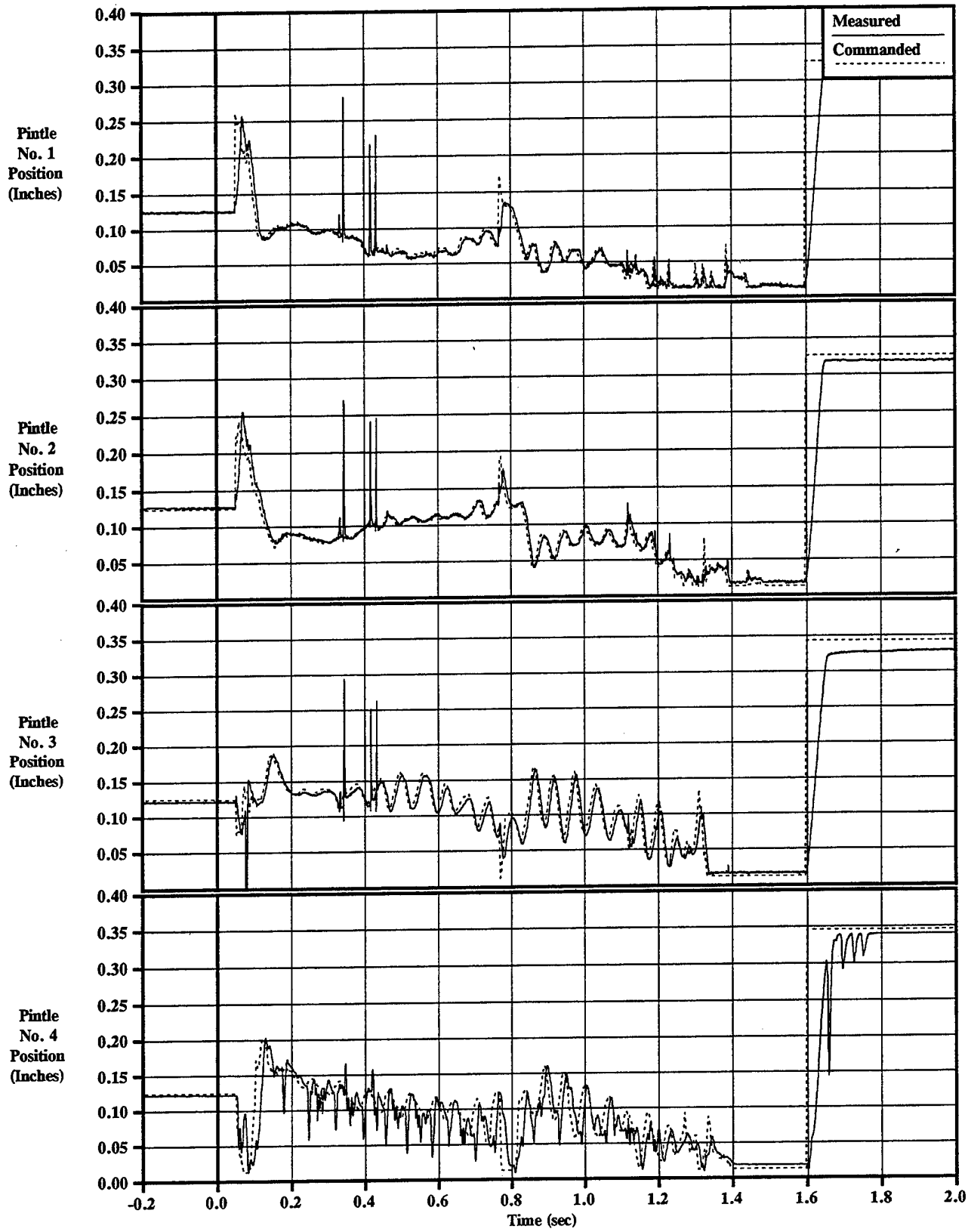

Figure C-10-12 Pintle Positions & Commands
Sled Test=10, KEAS=700, 5th%